

AD-A278 050



4

AD



# SNOWMELT FORECASTING - FURTHER COLD REGIONS DEVELOPMENT OF OPERATIONAL HYDROLOGICAL FORECASTING

Volume 1

by

K.M.Sambles and M.G.Anderson

March 1994

DTIC  
SELECTED  
APR 13 1994  
S B D

European Research Office

U.S. Corps of Engineers

London England

DISTRIBUTION STATEMENT A

Approved for public release  
Distribution Unlimited

CONTRACT NUMBER DAJA45-89-C-0028

Professor M.G.Anderson

DTIC QUALITY INSPECTED #

Approved for Public Release : Distribution Unlimited

# DISCLAIMER NOTICE



THIS DOCUMENT IS BEST QUALITY AVAILABLE. THE COPY FURNISHED TO DTIC CONTAINED A SIGNIFICANT NUMBER OF COLOR PAGES WHICH DO NOT REPRODUCE LEGIBLY ON BLACK AND WHITE MICROFICHE.

6194-EN-01

VOLUME 1

350 PY 94-11250  


DTIC QUALITY INSPECTED 3

94 4 12 1 69

## PREFACE

This report considers the development of an original physically-based distributed model of snowcover dynamics which is able to simulate the pattern of snowcover and snowdepth distribution during the melt season.

Model originality involves:

- (1) The application of physically-based equations to calculate snowmelt rate, and hence snowcover distribution, over an area.
- (2) The use of an original automated method that utilizes a Geographical Information System and a clustering routine to subdivide the catchment into homogeneous areas. These areas are used as the computational and spatial basis of the model. Each area is homogeneous with respect to slope angle, aspect, elevation and vegetation cover.
- (3) The use of an original logic structure that allows modelling of the changes in the physical structure of the snowpack throughout the melt season.

The validation and sensitivity analysis of the model raise modelling issues that are specific to the model developed. These are concerned with the specific assumptions that the model makes and problems that arise during the model development process. General conceptual issues can also be identified from the modelling development process. These are concerned with the relationship between the design of a field programme and the role that the model takes in this, model validation, sensitivity analysis of the model and data availability.

**ACKNOWLEDGEMENTS**

We would like to thank Dr. Timothy Pangburn and Hugh Greenan (CRREL) and Bill Roberts (University of Vermont) for their collaboration and support with the fieldwork, Dr. Randy Scoggins (WES) for his help in the early stages of the programming and Dr. Andrew Harrison (University of Bristol) for his collaboration with the development of the GIS based algorithm.

<b>Accession For</b>	
NTIS GRA&I	<input checked="" type="checkbox"/>
DTIC TAB	<input type="checkbox"/>
Unannounced	<input type="checkbox"/>
Justification	
By _____	
Distribution/	
Availability Codes	
Dist	Avail and/or Special
A-1	

**SUMMARY OF CONTENTS**

	<b>PAGE</b>
<b>Preface</b>	i
<b>Acknowledgements</b>	ii
<b>Summary of contents</b>	iii
<b>Detailed contents</b>	iv
<b>List of tables</b>	ix
<b>List of figures</b>	xiii
<b>List of photographs</b>	xix
<b>List of symbols</b>	xx
<b>Chapter 1. A review of snowcover modelling</b>	1
<b>Chapter 2. Snowcover dynamics</b>	32
<b>Chapter 3. Modelling strategy and model design</b>	49
<b>Chapter 4. Model structure I: Mathematics at a point</b>	62
<b>Chapter 5. Model structure II: Spatial distribution</b>	107
<b>Chapter 6. Model validation I: Data requirements and field design</b>	138
<b>Chapter 7. Model validation II: Results and discussion</b>	175
<b>Chapter 8. Model sensitivity analysis I: Point sensitivity</b>	230
<b>Chapter 9. Model sensitivity analysis II: Spatial sensitivity</b>	255
<b>Chapter 10. General and specific modelling issues arising from the model development</b>	286
<b>Bibliography</b>	298
<b>Appendix A</b>	308

**DETAILED CONTENTS**

	<b>PAGE</b>
Preface	1
Acknowledgements	ii
Summary of contents	iii
Detailed summary of contents	iv
List of tables	ix
List of figures	xiii
List of photographs	xix
List of symbols	xx
<b>Chapter 1. A review of snowcover modelling</b>	<b>1</b>
1.1. Introduction	1
1.2. Snowcover models	4
1.3. Index models	8
1.3.1. Single-variable index models	8
1.3.2. Multi-variable, energy budget index models	14
1.4. Physically-based models	18
1.5. The snow environment-model design relationship	25
1.6. Research objectives	28
<b>Chapter 2. Snowcover dynamics</b>	<b>32</b>
2.1. Introduction	32
2.2. Snowpack energy budget	32
2.3. Snowcover and snowdepth distribution patterns	35
2.4. Snowmelt discharge	39
2.5. The affect of vegetation cover	40
2.6. Summary	46
<b>Chapter 3. Modelling strategy and model design</b>	<b>49</b>
3.1. Modelling strategy	49
3.2. Model design	49
3.3. Comparison between WATBAL and the proposed model SNOMO	57

	PAGE
<b>Chapter 4. Model structure I: Mathematics at a point</b>	62
4.1. Introduction	62
4.2. The calculation of the snowpack energy budget components as derived from TSTM	64
4.2.1. Calculation of the direct incoming shortwave radiation, $S$ and $K_{\downarrow}$	66
4.2.2. Calculation of the reflected shortwave radiation, $K_{\uparrow}$	72
4.2.3. Calculation of the incoming longwave radiation, $L_{\downarrow}$	74
4.2.4. Calculation of the reflected longwave radiation, $L_{\uparrow}$	74
4.2.5. Calculation of the sensible heat flux, $Q_c$ , and the latent heat flux, $Q_e$	75
4.2.6. Calculation of the surface temperature and the solution of the heat flow equations	77
4.2.6.1. Solution within a layer	77
4.2.6.2. Solution at the interface of two layers	78
4.2.6.3. Solution at the upper boundary	80
4.2.6.4. Solution at the bottom boundary	82
4.3. The calculation of the energy budget components of a snowpack beneath a vegetation canopy as derived from the VEGIE submodel	84
4.3.1. Calculation of the foliage energy budget, $F_f$	84
4.3.2. Calculation of the ground energy budget, $F_g$	87
4.3.3. The root-finding algorithm	88
4.3.4. Calculation of the effective temperature	90
4.3.5. Mixed emissivities	90
4.4. The calculation of melt	92
4.4.1. Calculation of the energy introduced into the snowpack by rainfall, $Q_p$	92
4.4.2. Calculation of the snowpack internal energy change, $\Delta Q_s$	93
4.4.3. Calculation of the meltrate, $\Delta r$	94
4.5. The snowpack control programme	95
4.5.1. Snowpack characteristics and structure	95
4.5.2. The input file	99

	PAGE
4.6. Discussion	104
<b>Chapter 5. Model structure II: Spatial distribution</b>	<b>107</b>
5.1. Catchment discretization in distributed models	107
5.1.1. Consideration of catchment discretization approaches available	108
5.1.2. Proposed catchment discretization	114
5.1.3. The use of GIS in hydrology	115
5.2. The catchment discretization routine	122
5.3. Discussion	132
<b>Chapter 6. Model validation I: Data requirements and field design</b>	<b>138</b>
6.1. Introduction	138
6.1.1. The validation process	138
6.2. Data requirements	140
6.2.1. Operational data requirements	140
6.2.2. Validation data requirements	141
6.2.3. Choice of initial validation catchment	143
6.3. Catchment description: W3, Sleepers River Research Watershed, Danville, Vermont, USA	145
6.4. Field programme	161
6.4.1. 1988 field programme	161
6.4.2. 1989 field programme	166
6.5. Discussion	167
<b>Chapter 7. Model validation II: Results and discussion</b>	<b>175</b>
7.1. Introduction	175
7.2. Snowcover and snowdepth distribution data	175
7.2.1. Point data results	176
7.2.2. Spatial data results	184
7.3. SNOMO validation results	191
7.3.1. Point validation	191
7.3.2. Spatial validation	198

	<b>PAGE</b>
<b>7.4. Investigation into the point validation results</b>	<b>206</b>
7.4.1. Introduction	206
7.4.2. Results: 1988	209
7.4.3. Results: 1989	217
7.4.4. Discussion	219
<b>7.5. Discussion</b>	<b>224</b>
<b>Chapter 8. Model sensitivity analysis I: Point sensitivity</b>	<b>230</b>
8.1. Sensitivity analysis	230
8.2. The point sensitivity analysis of SNOMO	232
8.3. Deterministic point sensitivity analysis	233
8.3.1. Introduction	233
8.3.2. Results	239
8.3.3. Discussion	239
8.4. Stochastic point sensitivity analysis	247
8.4.1. Introduction	247
8.4.2. Results	250
8.5. Discussion	253
<b>Chapter 9. Model sensitivity analysis II: Spatial sensitivity</b>	<b>255</b>
9.1. Introduction	255
9.2. Spatial sensitivity results	261
9.2.1. Initial snowdepth	261
9.2.2. Elevation change	266
9.2.3. Slope angle	266
9.2.4. Aspect	269
9.2.5. Vegetation cover	269
9.2.5.1. Uniform vegetation cover, coniferous	269
9.2.5.2. Uniform vegetation cover, open	275
9.2.5.3. Vegetation cover configurations	276
9.3. Discussion	282
<b>Chapter 10. General and specific modelling issues arising from the model development</b>	<b>286</b>

	PAGE
10.1. Specific model development issues	286
10.1.1. Fulfilment of modelling objective and aims	286
10.1.2. Suggested future modifications to SNOMO	287
10.1.3. Suggested future modelling strategies	289
10.2. General modelling development issues	291
10.2.1. Validation problems	292
10.2.2. Sensitivity analysis problems	293
10.2.3. Field programme-model relationship	293
10.2.4. The development of multi-model, catchment management models	294
10.3. Discussion	296
 Bibliography	 298
Appendix A      Derivation of energy budget terms used in VEGIE	308

## LIST OF TABLES

	PAGE
Table 1.1. Examples of index models and their country of application.	9
Table 1.2. Degree-day calculations.	10
Table 1.3. Examples of physically-based snowmelt models and their scale of operation.	20
Table 1.4. Examples of process specific models.	26
Table 1.5. Relative contributions of different components of the energy budget of the snowpack to snowmelt (adapted from Kuusisto, 1986)	27
Table 1.6. Examples of snow environments and their related models	29
Table 2.1. Daily energy totals for the energy components and the derived term $\Delta r$ for figure 2.1, Oke (1987).	34
Table 2.2. Selected daily energy flux transfers ( $\text{MJm}^{-2}$ ) during a melt period in the absence of vegetation (Bad Lake, Saskatchewan), Male & Gray (1981).	34
Table 2.3. Daily melt totals attributable to the energy fluxes $Q^*$ , $Q_c$ and $Q_e$ (Price, 1988).	42
Table 2.4. Snowdepths under 3 vegetation cover types, W3, Danville, Vermont.	42
Table 3.1. Summary of the major differences between the proposed model SNOMO and WATBAL.	58
Table 4.1. Cloud genera and cloud type indices, Balick <u>et.al.</u> (1981a).	69
Table 4.2. Coefficients used in the TSTM and SNOMO energy budget calculations, Balick <u>et.al.</u> (1981a).	70
Table 4.3. Values of $\sigma_f$ for different vegetation types, Deardorff (1978) and Geiger (1965).	86

	PAGE
Table 4.4. Values used in SNOMO for the physical characteristics of SNOMO.	96
Table 4.5. SNOMO operational data requirements.	100
Table 4.6. Vegetation values for the New England environment, used in SNOMO.	103
Table 5.1. Summary of some of the hydrological applications of GIS.	118
Table 5.2. Terrain classes: Means and standard deviations.	125
Table 5.3. Terrain cells and associated terrain classes.	127
Table 5.4. Terrain cells and associated vegetation cover classes.	128
Table 5.5. Calculated catchment cells and their associated attributes.	129
Table 6.1. Remaining operational data requirements.	142
Table 6.2. Validation data requirements.	142
Table 6.3. Existing data coverage for W3.	153
Table 6.4. Summary of the data available at the Townline meteorological station, Danville, Vermont.	153
Table 6.5. Frost-tube site characteristics.	157
Table 6.6. Snowcourse locations and characteristics used in 1988 and 1989.	163
Table 7.1. Comparison between the calculated and observed snowdepths (centimetres) for points over the catchment W3, 1988.	193
Table 7.2. Comparison between the calculated and observed snowdepths (centimetres) for points over the catchment W3, 1989.	195
Table 7.3. Calculated snowdepths, W3 1988.	199
Table 7.4. Calculated snowdepths, W3 1989.	200

	PAGE
Table 7.5. Results for W3 (1988) arranged in melt day order to show the cell attributes.	203
Table 7.6. Results for W3 (1989) arranged in melt day order to show the cell attributes.	204
Table 8.1. Parameters and values used in the deterministic point sensitivity analysis of SNOMO.	234
Table 8.2. Relative sensitivity of TSTM parameters, Balick <i>et.al.</i> (1981a).	238
Table 8.3. Deterministic point sensitivity analysis: Melt date results for slope and aspect.	240
Table 8.4. Deterministic point sensitivity analysis: Melt date results for elevation.	240
Table 8.5. Deterministic point sensitivity analysis: Melt date results for initial snow temperature.	241
Table 8.6. Deterministic point sensitivity analysis: Melt date results for vegetation parameters.	241
Table 8.7. Deterministic point sensitivity analysis: Melt date results for snow albedo and emissivity.	242
Table 8.8. Deterministic point sensitivity analysis: results summary.	245
Table 8.9. Stochastic point sensitivity parameters and associated measurement errors or probability distributions.	248
Table 8.10. Stochastic point sensitivity analysis results.	251
Table 8.11. Stochastic point sensitivity analysis: results summary.	252
Table 9.1. Calculation of the number of potential variable combinations for the spatial sensitivity analysis of SNOMO.	257
Table 9.2. Variables used in the spatial sensitivity analysis of SNOMO.	259
Table 9.3. Distribution of cells in figure 9.1 on the basis of aspect, elevation and vegetation cover.	263

	PAGE
Table 9.4. Cells arranged in order of melt, for figure 9.3.	265
Table 9.5. Cells arranged in order of melt, for figure 9.4.	268
Table 9.6. Cells arranged in order of melt, for figure 9.5.	268
Table 9.7. Cells arranged in order of melt, for figure 9.6.	272
Table 9.8. Cells arranged in order of melt, for figure 9.7.	272
Table 9.9. Cells arranged in order of melt, for figure 9.8.	272
Table 9.10. Cells arranged in order of melt, for figure 9.9	274
Table 9.11. Cells arranged in order of melt, for figure 9.10	274
Table 9.12. Cells arranged in order of melt, for figure 9.11	279
Table 9.13. Cells arranged in order of melt, for figure 9.12	279
Table 9.14. Cells arranged in order of melt, for figure 9.13	280
Table 9.15. Cells arranged in order of melt, for figure 9.14	280

## LIST OF FIGURES

	PAGE
Figure 1.1. Areal and vertical changes in the snowpack occurring throughout the snow season (adapted from Rau & Herrmann, 1982).	2
Figure 1.2. Snowcover in relation to streamflow, Garstka <i>et.al.</i> (1958).	3
Figure 1.3. Components of a generalised snowmelt model, Ferguson & Morris (1987).	6
Figure 1.4. Calculation of degree-days above 0°C at the snow-line, Ferguson (1984).	11
Figure 1.5. A comparison of some of the different degree-day models available, Kuusisto (1978).	13
Figure 1.6. Comparison of the SNOW-17 and degree-day models simulated values with the lysimeter daily outflow, Roberge <i>et.al.</i> (1988).	17
Figure 1.7. Comparison of energy balance (energy budget) and temperature index models during the 1971 and 1972 melt seasons, Anderson (1976).	24
Figure 1.8. Identification of the vacant model niche.	30
Figure 2.1. Energy budget components for a melting snowcover at Bad Lake, Saskatchewan (51°N), on 10 April 1978, Oke (1987).	33
Figure 2.2. Distribution of the snowcover on a hillside at noon each day during the melt period of March 1967, Dunne & Black (1971).	37
Figure 2.3. 1976 and 1977 mean snowdepth and density for various terrain types, and percentage distribution of various types of terrain in the study basins, Woo & Marsh (1978).	38
Figure 2.4. Daily energy balance (energy budget) in dense forest during active snowmelt, US Army Corps of Engineers (1956).	41
Figure 2.5. Variation of maximum frost depth under 4 cover types, W3 catchment, Danville, Vermont.	43

	PAGE
Figure 2.6. Variation of albedo with vegetation cover, 6 January 1971, O'Neill & Gray (1972).	45
Figure 2.7. Energy exchanges and environmental factors operating in an idealised snow environment at the start of the melt season.	47
Figure 2.8. The idealised snow environment towards the end of the melt season.	47
Figure 3.1. Model development strategy and related report chapters.	50
Figure 3.2. The choice of alternative submodels and modelling pathways and the generation of uncertainty within the model design process, Anderson & Sambles (1988).	52
Figure 3.3. Basic design structure of the proposed model.	53
Figure 3.4. Proposed model originality and related report chapters.	56
Figure 4.1. Simplified logic structure of SNOMO and related report chapters.	63
Figure 4.2. Energy exchanges modelled by the Terrain Surface Temperature Model, Balick <i>et al.</i> (1981a).	65
Figure 4.3. Geometrical relationships between the Earth and the solar beam, Oke (1987).	71
Figure 4.4. Geometry for solar beam irradiance of a sloping plane, Oke (1987).	73
Figure 4.5. Finite difference grid used by TSTM and SNOMO, adapted from Balick <i>et al.</i> (1981a).	79
Figure 4.6. Schematic representation of the root-finding algorithm ( <i>regula falsi</i> ), Balick <i>et al.</i> (1981b).	89
Figure 4.7. Modelling scenarios demonstrating compaction by SNOMO.	97
Figure 5.1. The division of a catchment using the hillslope plane method, VSAS2 (Bernier, 1982).	109

	PAGE
Figure 5.2. The structure of the SHE model, showing the division of a catchment using the grid method, Beven & O'Connell (1982).	111
Figure 5.3. The basic modules of a geographical information system, Burrough (1986).	116
Figure 5.4. Input data required for the ANSWERS model, de Roo <i>et.al.</i> (1989).	119
Figure 5.5. Summary of the catchment discretization procedure developed for SNOMO.	123
Figure 5.6. Final catchment subdivision and cell numbers.	130
Figure 5.7. A comparison of the results of three different methods of catchment discretization.	135
Figure 6.1. Location of the W3 catchment.	146
Figure 6.2. Topographic map of the W3 catchment, Anderson <i>et.al.</i> (1977).	147
Figure 6.3. Area-elevation curve for the W3 catchment, Anderson <i>et.al.</i> (1977).	148
Figure 6.4. Vegetation cover, W3, 1988.	149
Figure 6.5. Distribution of soils, W3.	151
Figure 6.6. Location of frost-tube sites, meteorological stations and transect sites.	155
Figure 6.7. Seasonal precipitation-elevation relationships for the W3 watersheds (based on the period from 10/59 to 9/74; winter is November-March and summer is April-October), Anderson <i>et.al.</i> (1977).	160
Figure 6.8. Locations of the snowcourses established in 1988 and 1989.	162
Figure 6.9. Snowdepths, transect 1, 23/3 to 3/4/88.	168
Figure 6.10. Snowdepths, transect 2, 23/3 to 3/4/88.	169
Figure 6.11. Snowdepths, transect 3, 23/3 to 3/4/88.	170
Figure 6.12. Snowdepths, transect 4, 23/3 to 3/4/88.	171

	PAGE
Figure 7.1. Variation in snowdepth with vegetation cover, W3, 1989.	177
Figure 7.2. Snowdepths at snowcourse sites 1 and 2, 21/3 to 4/4/89.	178
Figure 7.3. Snowdepths at frost-tubes 22-26 and clear-cut site CC8, 21/3 to 4/4/89.	178
Figure 7.4. Variation in snowdepth with elevation, W3, 1989.	180
Figure 7.5. Snowdepth at 5 adjacent frost-tube sites.	182
Figure 7.6. % bare ground visible, W3, 30/3/88 (Julian day 90).	185
Figure 7.7. % bare ground visible, W3, 3/4/88 (Julian day 94).	186
Figure 7.8. % bare ground visible, W3, 6/4/88 (Julian day 97).	187
Figure 7.9. Measured snowdepths, W3, 21-23/3/89 (Julian days 80-82).	188
Figure 7.10. Measured snowdepths, W3, 28/3/89 (Julian day 87).	189
Figure 7.11. Measured snowdepths, W3, 4/4/89 (Julian day 94).	190
Figure 7.12. Observed and predicted snowdepths, Townline, 1988.	194
Figure 7.13. Observed and predicted snowdepths, Townline, 1989.	197
Figure 7.14. W3 melt day prediction, 1988.	201
Figure 7.15. W3 melt day prediction, 1989.	202
Figure 7.16. Affect of mass conservation on calculated snowdepths, 1988.	210
Figure 7.17. Affect of compaction on calculated snowdepths, 1988.	210
Figure 7.18. Affect of variable start date on calculated snowdepths, 1988.	212

	PAGE
Figure 7.19. Calculated average daily $K\downarrow$ , Townline, 1988.	212
Figure 7.20. Calculated average daily $K\uparrow$ , Townline, 1988.	214
Figure 7.21. Calculated average daily $L\downarrow$ , Townline, 1988.	214
Figure 7.22. Calculated average daily $L\uparrow$ , Townline, 1988.	215
Figure 7.23. Daily input cloud cover values, 1988.	215
Figure 7.24. Affect of cloud cover on calculated snowdepths, 1988.	216
Figure 7.25. Affect of cloud cover values of 10 tenths for days 84-89 on calculated snowdepths, 1988.	216
Figure 7.26. Affect of mass conservation on calculated snowdepths, 1989.	218
Figure 7.27. Affect of compaction on calculated snowdepths, 1989.	218
Figure 7.28. Affect of variable start date on calculated snowdepths, 1989.	220
Figure 7.29. Calculated average daily $K\downarrow$ , Townline, 1989.	221
Figure 7.30. Calculated average daily $K\uparrow$ , Townline, 1989.	221
Figure 7.31. Calculated average daily $L\downarrow$ , Townline, 1989.	222
Figure 7.32. Calculated average daily $L\uparrow$ , Townline, 1989.	222
Figure 7.33. Daily input cloud cover values, 1989.	223
Figure 7.34. Affect of cloud cover on calculated snowdepths, 1989.	223
Figure 7.35. Relationship between SNOMO, the catchment subdivision and the field programme.	228
Figure 8.1. Affect of variation of the snow albedo on snowdepth.	243
Figure 9.1. 1988 validation result.	262
Figure 9.2. Vegetation cover, W3, 1988.	262

	<b>PAGE</b>
<b>Figure 9.3. Spatial sensitivity analysis results: Initial snowdepth.</b>	<b>264</b>
<b>Figure 9.4. Spatial sensitivity analysis results: Elevation change.</b>	<b>267</b>
<b>Figure 9.5. Spatial sensitivity analysis results: Slope angle.</b>	<b>267</b>
<b>Figure 9.6. Spatial sensitivity analysis results: +90° aspect.</b>	<b>270</b>
<b>Figure 9.7. Spatial sensitivity analysis results: +180° aspect.</b>	<b>270</b>
<b>Figure 9.8. Spatial sensitivity analysis results: +270° aspect.</b>	<b>271</b>
<b>Figure 9.9. Spatial sensitivity analysis results: uniform vegetation cover, coniferous.</b>	<b>273</b>
<b>Figure 9.10. Spatial sensitivity analysis results: uniform vegetation cover, open.</b>	<b>273</b>
<b>Figure 9.11. Spatial sensitivity analysis results: vegetation configuration 1.</b>	<b>277</b>
<b>Figure 9.12. Spatial sensitivity analysis results: vegetation configuration 2.</b>	<b>277</b>
<b>Figure 9.13. Spatial sensitivity analysis results: vegetation configuration 3.</b>	<b>278</b>
<b>Figure 9.14. Spatial sensitivity analysis results: vegetation configuration 4.</b>	<b>278</b>
<b>Figure 10.1. The inclusion of SNOMO into a catchment eco/hydro-system mode</b>	<b>295</b>

## LIST OF PHOTOGRAPHS

	PAGE
Photograph 1. Regional snowcover distribution. Snowcover is concentrated in drainage channels and is absent from remaining terrain (Hamelin & Cook, 1967).	35
Photograph 2. W3 catchment: Digital Elevation Map (DEM).	123
Photograph 3. W3 catchment: aspect, derived from the DEM.	123
Photograph 4. W3 catchment: slope angle, derived from the DEM. Pixel colour decreases as slope angle increases.	124
Photograph 5. W3 catchment: elevation, superimposition of catchment mask and elevation classes.	124
Photograph 6. W3 catchment: aspect, superimposition of catchment mask and slope angle classes.	124
Photograph 7. W3 catchment, slope angle, superimposition of catchment mask and slope angle classes.	124
Photograph 8. W3 catchment, distribution of terrain cells with catchment mask superimposed.	126
Photograph 9. W3 catchment, vegetation cover.	126
Photograph 10. W3 catchment, 7 April 1988, vegetation control over snowcover distribution.	180
Photograph 11. W3 catchment, 6 April 1988, slope angle and aspect control over snowcover distribution.	180
Photograph 12. W3 catchment, transect 1 and SC6A, 25 March 1988.	182
Photograph 13. W3 catchment, transect 1 and SC6A, 31 March 1988.	182
Photograph 14. W3 catchment, transect 1 and SC6A, 3 April 1988.	182

## LIST OF SYMBOLS

This report uses both the Système Internationale (S.I.) and c.g.s (centimetre, gram, second) system of units. Where possible the SI system is used. The c.g.s. system units are used for variables that are associated with certain calculations that are taken from a source in c.g.s units and where it is unnecessary to convert these to S.I. units. This is explained in the relevant section of the text. This report uses some material from American sources, which uses either metric or imperial units. Where difficulties would arise in the conversion of imperial to metric units the material is left in its original units. All the symbols used in the equations in the text are explained and the units are given immediately following the equations. This list is intended as a quick reference list and because of the mixture of units used the units are not given. The list explains the symbols used in the major physically-based equations used in the text, with the exception of the equations in appendix A, which are explained in appendix A.

Roman capital letters.

$A(u^*, z)$	Mugge-Möller absorption function.
CA	cloud adjustment factor.
CC	visual cloud cover.
CIR	coefficient dependent on cloud type.
$C_p$	specific heat of dry air at a constant pressure.
$C_{p_i}$	specific heat of ice.
$C_{p_w}$	specific heat of water.
D	constant heat flux at bottom boundary.
$D_o$	value of D obtained by using previous estimate of $T_g$ .
$D_N$	value of D obtained by using latest estimate of $T_g$ .
$E_f$	foliage latent heat loss to atmosphere.

$E_g$	latent heat loss to atmosphere at ground (snow) surface.
$F_f$	foliage energy-budget.
$F_g$	ground (snow) energy-budget.
$G$	energy flux into a ground (snow) surface from the ground or snow surface below.
$H_f$	foliage sensible heat flux.
$H_g$	sensible heat flux at ground (snow) surface.
$K^*$	net shortwave radiation.
$K_{\downarrow}$	incoming shortwave radiation.
$K_{\uparrow}$	reflected incoming shortwave radiation.
$K_{ab}$	amount of incoming shortwave radiation absorbed at the surface.
$L^*$	net longwave radiation.
$L_{\downarrow}$	incoming longwave radiation.
$L_{\downarrow}(o)$	incoming longwave radiation with clear skies.
$L_{\uparrow}$	reflected longwave radiation.
$L_f$	latent heat of fusion.
$L_v$	latent heat of vaporisation.
$P$	air pressure.
	precipitation rate.
$Q^*$	net radiation flux.
$Q_c$	sensible heat flux.
$Q_e$	latent heat flux.
$Q_g$	heat flux across ground/snow interface.
$Q_p$	energy introduced into the pack by rainfall.
$R_{\downarrow}$	radiative energy loss through bottom boundary.
$R_{\uparrow}$	radiative energy from constant temperature radiating surface below bottom boundary.
$R_{g\downarrow}$	downward directed longwave radiation flux at ground (snow) surface.
$R_{g\uparrow}$	upward directed longwave radiation flux at ground (snow) surface.
$RH$	relative humidity.
$Ri$	Richardson's Number.

$R_n$	combined net thermal IR term for the interaction between the foliage, ground and their loss to the sky.
$R_{gl}$	incoming longwave radiation from the sky.
$S$	incoming shortwave radiation (allowing for slope, cloud cover and optical air mass number).
$S_c$	shortwave radiation on a horizontal surface amended for the affects of cloud and optical air mass.
SCF	dimensionless stability function for momentum and heat.
SF	slope factor.
$S_o$	shortwave radiation incident at top of atmosphere.
$S_h$	direct beam shortwave radiation on a horizontal surface (excluding the affects of clouds and optical air mass).
$T$	temperature.
$T_a$	air temperature at instrument height.
$T_B$	temperature of bottom surface.
$T_d$	dewpoint temperature.
$T_g$	surface temperature.
$T_p$	temperature of rain.
$T_R$	under surface temperature.
$T_{sn}$	temperature of snow.
$U$	horizontal wind speed with respect to height $z$ .
$W$	relative saturation of top surface.
$W_t$	longwave radiation emitted from a surface composed of foliage and ground (snow).

**Roman small letters.**

$a$	extinction coefficient.
$b_{kB}$	bottom geometric shape factor.
$b_{kR}$	under surface geometric shape factor.
$d$	depth of snowpack.
$e_a$	water vapour pressure.
$g$	acceleration due to gravity.

h	hour angle.
k	von Karman's constant. thermal conductivity.
$k_i$	thermal conductivity of air.
m	optical air mass number.
t	apparent solar time. time.
z	zenith angle of the sun as a function of the time of the day and the time of the year. instrument height.
$u^*$	effective water vapour content of atmosphere.

## Greek capital letters.

$\Delta Q_m$	net latent heat storage due to melting or freezing.
$\Delta Q_s$	snowpack internal energy change.
$\Delta r_{sn}$	meltrate, centimetres of snow.
$\Delta r_w$	meltrate, millimetres of water equivalent.
$\hat{\theta}$	slope factor.
$\Phi_M \Phi_H$	dimensionless stability functions for momentum and heat.
$\Omega$	solar azimuth angle.
$\hat{\Omega}$	slope azimuth angle.

## Greek small letters.

$\alpha$	albedo.
$\alpha_f$	foliage albedo.
$\alpha_g$	ground (snow) albedo.
$\bar{\alpha}_g$	area average ground (snow) albedo.
$\alpha_o$	atmospheric albedo for Rayleigh scattering.
$\hat{\beta}$	slope angle.
$\delta$	solar declination.

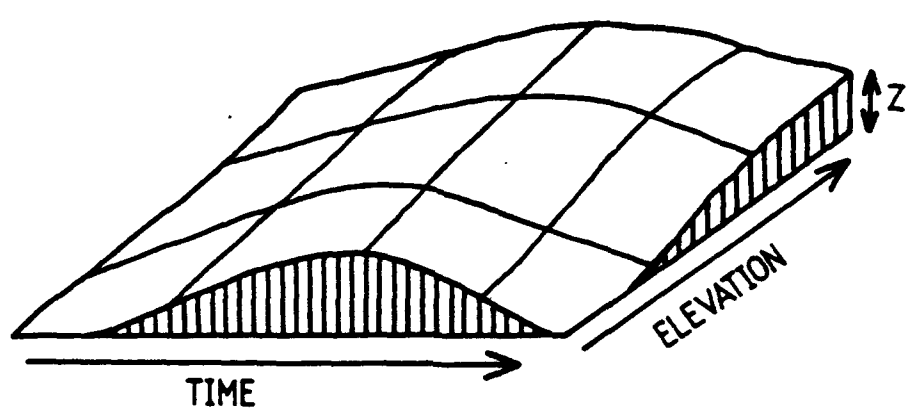
$\epsilon$	emissivity.
$\epsilon_B$	bottom boundary thermal IR emissivity.
$\epsilon_f$	foliage emissivity.
$\epsilon_g$	ground (snow) emissivity.
$\epsilon_R$	under surface thermal IR emissivity.
$\theta$	potential temperature.
$\bar{\theta}$	average potential temperature between surface and height $z$ .
$\kappa$	thermal diffusivity.
$\rho$	air density.
$\rho_i$	density of ice.
$\rho_0$	1000mb.
$\rho_s$	surface pressure.
$\rho_{sn}$	density of snow.
$\rho_w$	density of water.
$\sigma$	Stefan-Boltzmann constant.
$\sigma_f$	foliage cover fraction.
$r$	coefficient dependent on time of year.
$\theta$	latitude of location.
$x$	state of vegetation.

## CHAPTER 1: A REVIEW OF SNOWCOVER MODELLING

### 1.1 Introduction.

Snow hydrology is a temporally and areally complex and variable subsystem within the hydrological cycle. The term *snowcover dynamics* encompasses the areal and vertical changes in the snowpack (the snowcover and snowdepth distribution patterns) that occur due to the processes of accumulation and melt (figure 1.1). Associated with the changes in snowcover and snowdepth are changes in the physical characteristics of the snowpack and, during melt, a volume of meltwater runoff (figure 1.2).

Snowcover is an important factor in the hydrological cycle of many parts of the world. For example, in North America the mean maximum length of snowcover duration is eight and a half months (September 15-June 1) and the mean minimum duration is two weeks (January 15-February 1) with only seven USA states experiencing more than one in three years without snowcover (McKay & Gray, 1981). Snowfall and snowcover can be of economic importance (The Independent, 1989) with possible economic hardships resulting from badly timed snowfall/snowmelt in relation to harvesting/planting or from abnormally high or low snowfalls. The area affected by snowfall in the Northern Hemisphere extends over many different climatic zones each with a characteristic topography and vegetation, for example, tundra, prairie, high mountain and desert. These with their accompanying differences in snowcover duration, result in characteristic snow environments. There is a correspondingly large range of processes that are associated with the snow environments. A detailed knowledge and ability to simulate the processes occurring in



Z Snowdepth

Figure 1.1. Areal and vertical changes in the snowpack occurring throughout the snow season (adapted from Rau & Herrmann, 1982).

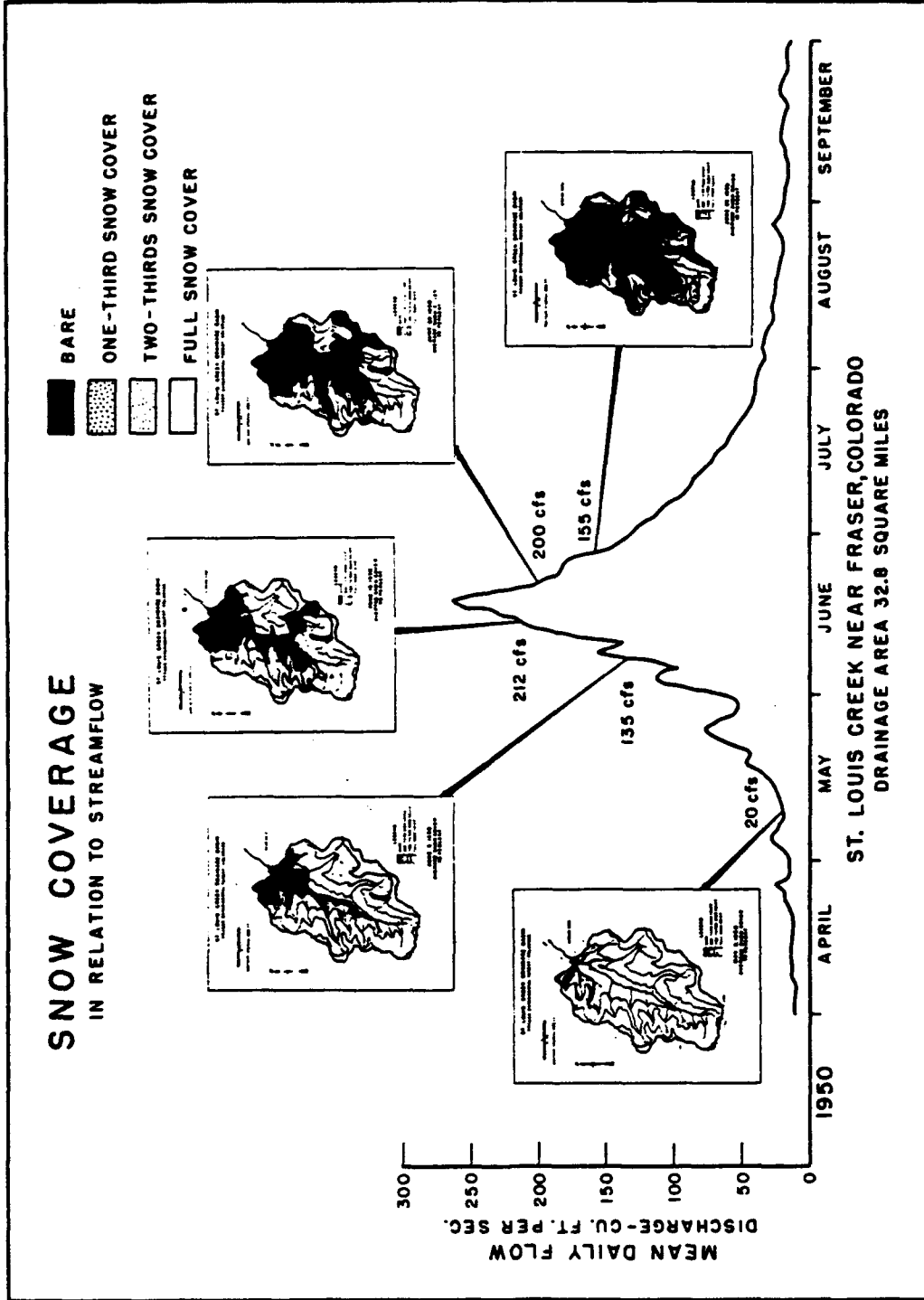


Figure 1.2. Snowcover in relation to streamflow, Garstka et.al. (1958).

these snow environments is specifically required for:

- (1) Prediction of streamflows. Predictions are either short-term (one day or one week) concerned with flood flows, or long-term concerned with seasonal water yield for domestic, agricultural and energy supply purposes. Many crop irrigation schemes in arid regions bordered by high mountains (for example, India and Iran) rely upon snowmelt runoff as their primary water source.
- (2) Assessment of the impact of landuse changes. These can be caused by, for example, silvicultural changes (Swanson, 1972, Berris & Harr, 1987 and DeWalle et.al., 1977) and leisure related activities, Simons (1988).
- (3) An understanding of the action of snow and snowmelt as a pollutant carrier and concentrator, for example the acid snow flushes reported by Goodison et.al. (1986).
- (4) A research tool for use in hydrology, botany, zoology, ecology, geomorphology, agricultural studies and as a consideration in the context of possible global climatic change.

## 1.2 Snowcover models.

Snow hydrology models, and therefore models concerned with snowcover dynamics and the processes of snowcover dynamics, are found in the literature as specific process models or under the blanket term *snowmelt model*. The term snowmelt model is a slight misnomer as most snowmelt models include a snow accumulation routine (however simple) most are however restricted to the snowmelt period. Historically, snowmelt models have concentrated on the prediction of the snowmelt hydrograph, this was in direct response to the need to predict snowmelt flood flows and to utilize the snowmelt water resource. Research interest has now broadened to investigate, for example, snowpack metamorphosis, meltwater pathways and snow distribution patterns. However, prediction of the snowmelt hydrograph remains the primary aim of many snowmelt models.

The development of snowmelt models has paralleled that of non-snow hydrology models. There has been an increase in model complexity from simple statistical models to complex physically-based models (Anderson & Sambles, 1988). This has resulted in the range of modelling methodologies that are available today. Statistical models (Hendrick & DeAngelis, 1976) are now largely redundant and the two main methodologies available today are the *index* and *physically-based* approaches. Snowmelt models, whatever their methodology, operate at two spatial scales, the *catchment-scale* and the *point-scale*. Catchment-scale models simulate snowmelt over a catchment, point-scale models at a point. Ferguson & Morris (1987) describe the structure of a generalised snowmelt model (figure 1.3). There are four subunits to this structure:

- (1) A meteorological submodel. In a catchment-scale snowmelt model the meteorological submodel is responsible for the manipulation of the available meteorological data, so that the data is representative of the meteorology at the snowpack. This usually involves extrapolation of meteorological data from distant point sources, for example, the use of lapse rates to calculate air temperatures, or the extrapolation of precipitation totals, wind speeds and evaporation (Reiners et al., 1984). For more complex models the term 'meteorological submodel' should be changed to 'input data handling submodel'. This would enable the inclusion of data other than meteorological data, for example, vegetation cover input data.
- (2) A snowmelt submodel. This calculates the volume of meltwater reaching the ground. The volume of meltwater is calculated using either an index approach or a physically-based approach. The choice of submodel is affected by many factors and both this and the two modelling methodologies are discussed in detail in the following sections.
- (3) A transformation submodel. This routes the estimated meltwater to the outflow stream. Transformation submodels vary in complexity, reflecting the variation in current hillslope runoff modelling techniques. Physically-based or lumped approaches can be taken.

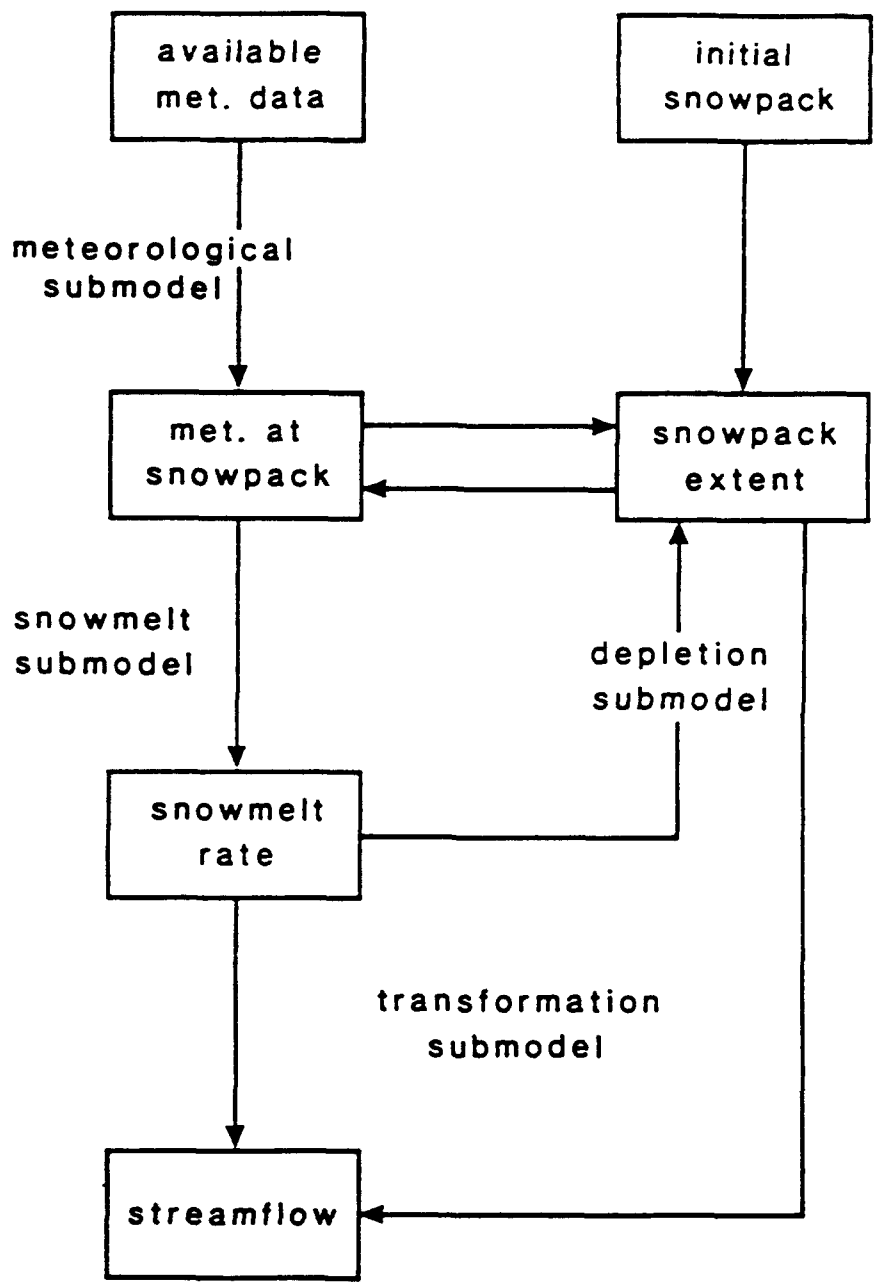


Figure 1.3. Components of a generalised snowmelt model, Ferguson & Morris (1987).

Some transformation submodels are included with the snowmelt submodel and the meltwater movement through the snowpack and the hillslope are considered together (Dunne et.al., 1976).

(4) A depletion submodel. This calculates the depletion of the snowpack. The areal depletion of the snowpack is calculated if modelling is at the catchment-level and the point snowdepth depletion is calculated if modelling is at the point-level. Again these submodels vary in complexity, the majority are simple volume or depth subtractions (Moussavi et.al., 1989) but there are some more complex models (Buttle & McDonnell, 1987). The initial snowpack extent is important at both the point and the catchment-level. Errors in the estimation of initial snowpack extent can manifest themselves in the depletion submodel rendering the melt output, however accurately calculated by the snowmelt submodel, inaccurate. If the initial snowpack extent is zero an accumulation model is required in addition to a snowmelt model. Initial snowpack extent can be estimated from mountain snow-lines, using remote sensing methods or measured in the field.

The relative importance of each submodel is dependent upon the quality of the data, the level of accuracy required and the objective of the model. There are many varying subdivisions of snowmelt models depending upon the methodology, scale or environment of the model. This chapter examines snowmelt models in terms of the two main methodologies that are available (index and physically-based) and the environment that the model is simulating.

### 1.3 Index models.

Index models express melt rate as a function of one or more variables and are concerned with the manipulation of these index variables to produce a melt volume, which is the primary output. The melt process and the catchment are treated in a lumped manner and no attempt is made to simulate the physical processes occurring during melt. Index models are usually calibrated using calibration factors (commonly called melt factors) which ensure the correct calculation of the melt volume. The most commonly used index variable is air temperature, but other variables such as vegetation and incident solar radiation are also used (Male & Gray, 1981 and Martinec & Rango, 1986). Index models vary in complexity from simple single-variable models to complex multi-variable models based on the energy budget of the snowpack. Table 1.1 shows examples of currently available index models and their country of application.

#### 1.3.1 Single-variable index models.

These relate one index variable, usually air temperature to melt rate. If air temperature is used it is usually in the form of a degree-day index. Garstka *et al.* (1958) define a degree-day as a departure of 1°C per day in the mean daily temperature from an adopted reference temperature. The reference temperature is usually 0°C. The mean of the daily maximum and minimum air temperatures is often used as the daily mean temperature. Despite this definition the calculation of the degree-day and its meaning vary considerably in the literature. Table 1.2 shows the calculation of three degree-day indices. The calculation of examples 1 and 2 varies. Example 3 demonstrates another calculation variation and the confusing terminology that can occur in the literature. Kuusisto (1978) calculates melt using a 'degree-day formula', equation 1.3, which involves the use of a degree-day factor (KM). KM is also confusingly called a melt factor and is essentially a calibration factor. KM

**Table 1.1. Examples of index models and their country of application.**

**(1) Single-index**

Moussavi <u>et.al.</u> (1989)	Iran
Ferguson (1984)	Scotland
Roberge <u>et.al.</u> (1988)	S.E. Canada
Martinec & Rango (1986)	24 basins worldwide
Pangburn (1987)	USA.
Kuusisto (1978)	Finland

**(2) Multi-index, energy budget**

Anderson (1973)	New England, USA.
Roberge <u>et.al.</u> (1988)	S.E. Canada
Moussavi <u>et.al.</u> (1989)	Iran.

Table 1.2. Degree-day calculations.

(1) Moussavi et al. (1989).

$$C = a(t_{\max*} - t_{\min*}) + f \quad (1.1)$$

where,

- C degree-day factor,  $\text{mmtime unit}^{-1} \cdot \text{C}^{-1}$ .  
 a slope of variation of the degree-day,  $\text{mmday}^{-1} \cdot \text{C}^{-1}$ .  
 $t_{\max*}$  mean daily maximum temperature above freezing point in a given month, °C.  
 $t_{\min*}$  mean daily minimum temperature above freezing point in a given month, °C.  
 f minimum degree-day at the start of the melt season,  $\text{mmday}^{-1} \cdot \text{C}^{-1}$ .

(2) Ferguson (1984).

$$D_i = \frac{\max^2(0,y) - \max^2(0,x)}{4(y-x)} + \frac{\max^2(0,y) - \max^2(0,z)}{4(y-z)} \quad (1.2)$$

where,

- $D_i$  degree-days above snowline (degree-day index).  
 x minimum air temperature in the 24 hours to 0900 GMT on day i.  
 y maximum air temperature in the next 24 hours.  
 z minimum air temperature in the next 24 hours.  
 (see figure 1.4).

(3) Kuusisto (1978).

$$M = KM(T - KT) \quad (1.3)$$

where,

- M amount of melt,  $\text{mmday}^{-1}$ .  
 KM degree-day factor,  $\text{mm} \cdot \text{C}^{-1} \cdot \text{day}^{-1}$  (kept constant or increased linearly with date of season or with the decrease in water equivalent).  
 T temperature, °C (either daily mean or the mean of the daily maximum and minimum).  
 KT threshold temperature, °C.

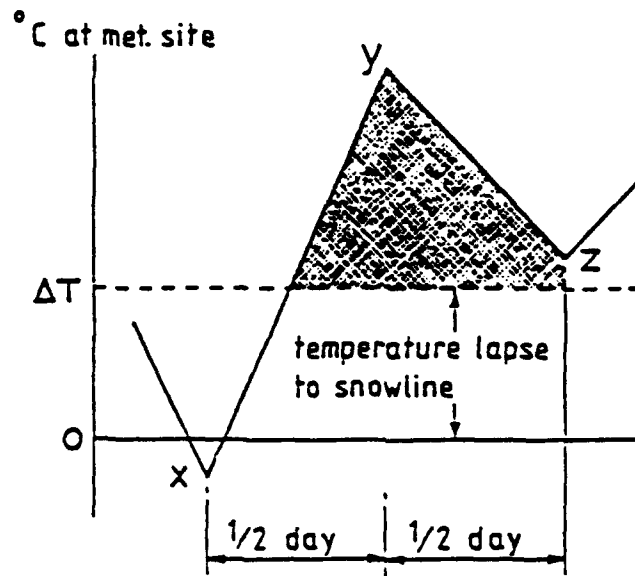


Figure 1.4. Calculation of degree-days above 0°C at the snow-line, Ferguson (1984).

remains constant and the determination of KM is not given although a range of values for KM are given in order for optimization to occur. In a more sophisticated version of equation 1.3 KM is varied with the date of the season or with the decrease in water equivalent. However, usually the degree-day index is a manipulation of the maximum and minimum current and previous air temperatures and is separate from the melt factor (which is a constant used in calibration). An example of a typical index model (using only one index) is the model by Ferguson (1984) to calculate the snowmelt over a catchment in the Cairngorm Mountains (Scotland). The melt volume is calculated by:

$$V_i = A_i D_i M \quad (1.4)$$

where,

$V_i$  melt volume,  $10^3 \text{m}^3$ .

$A_i$  snowpack area,  $\text{km}^2$ .

$D_i$  degree-days above snow-line (degree-day index, table 1.2).

$M$  constant,  $\text{mm}^\circ\text{C}^{-1}\text{day}^{-1}$ .

$A_i$  is calculated using the areal feedback equation:

$$A_{i+1} = (A_i^2 - V_i A_o / W_o)^{1/2} \quad (1.5)$$

where,

$A_o$  initial snowpack area,  $\text{km}^2$ .

$W_o$  initial mean water equivalent depth,  $\text{mm}$ .

Kuusisto (1978) investigates various index models. He starts with a degree-day model and gradually increases the complexity (figure 1.5) The most complex model is an index approach to the calculation of the snowpack energy budget. This demonstrates a continuum between the single-index and the energy budget based index snowmelt models.

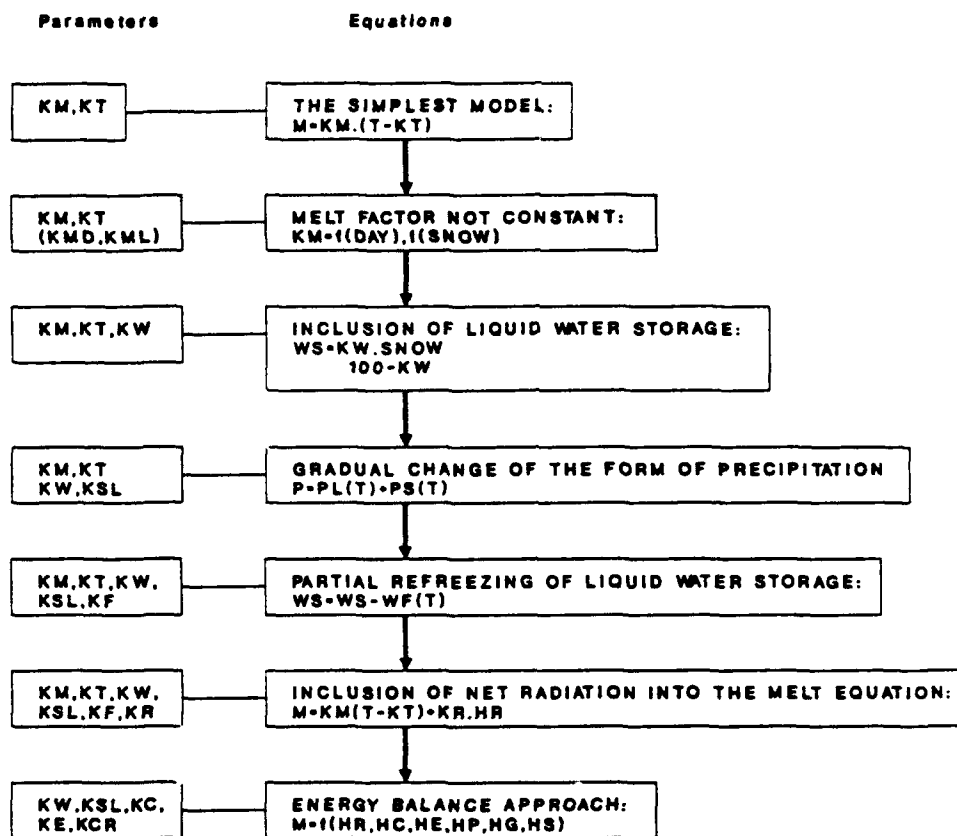


Figure 1.5. A comparison of some of the different degree-day models available, Kuusisto (1978).

### 1.3.2 Multi-variable, energy budget based index models.

The most sophisticated index models calculate the various components of the snowpack energy budget equation (often using a simplified version of this equation) using indices (Anderson, 1973 and Moussavi et.al., 1989). Air temperature is again the most commonly used index variable. These models are conceptual models in that their basis is the energy budget of the snowpack and they represent the processes occurring more accurately and in more detail than do the single-index models. However they are still index models and in reality most are manipulating the same index, air temperature, but in a more sophisticated manner. An example of this is Moussavi et.al. (1989):

The simplified energy balance is:

$$M = M_{Ra} + M_R + M_C + M_1 \quad (1.6)$$

where,

M total meltrate.

$M_{Ra}$  meltrate due to net radiation.

$M_R$  meltrate originated by heat transfer of rainfall.

$M_C$  meltrate induced by convective heat transfer from a warm air mass.

$M_1$  latent heat transfer associated with evaporation from or condensation to the snowpack.

Units: mm per time unit.

Each of the terms in the energy balance are calculated using the index method, for example:

$$M_C = m_f t_{max} \quad (1.7)$$

where,

$M_c$  meltrate caused by convective heat transfer,  $\text{mmday}^{-1}$ .

$m_f$  melt factor,  $\text{mmday}^{-1}\cdot\text{C}^{-1}$ .

$t_{\text{max}}$  average daily maximum temperature above freezing point in a given month,  $^{\circ}\text{C}$ .

and

$$M_{\text{nr}} = \zeta R_s \quad (1.8)$$

where,

$M_{\text{nr}}$  meltrate caused by net solar radiation.

$\zeta$  dimensionless coefficient indicating the amount of radiant energy contributing to snowmelt.

$R_s$  mean solar incoming radiation expressed in melt equivalent water depth per time unit,  $\text{mmday}^{-1}$ .

$R_s$  is calculated by:

$$R_s = K_{rs} R_a T_d^{\frac{1}{2}} \quad (1.9)$$

where,

$R_a$  mean extra-terrestrial radiation in equivalent water depth,  $\text{mmday}^{-1}$ .

$T_d$  average daily temperature range in a given month,  $^{\circ}\text{C}$ .

$K_{rs}$  coefficient,  $^{\circ}\text{C}^{-\frac{1}{2}}$ .

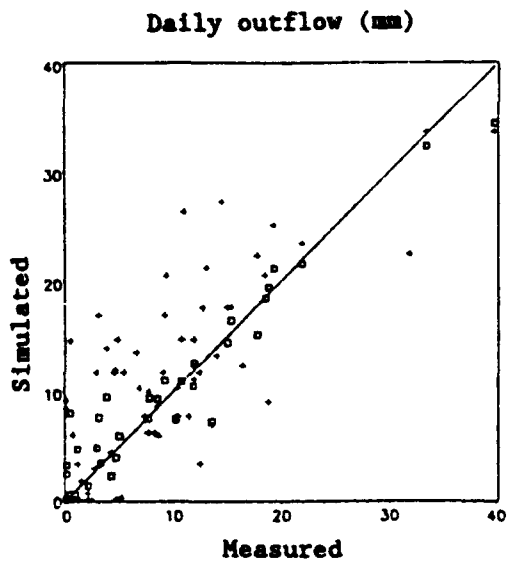
Models of this type, as the example shows, include more calibration factors than the simpler index models. Index models can operate at both the catchment and the point scale. The melt calculation is usually performed at a point and then multiplied by the catchment area to achieve a catchment snowmelt volume. Initial snowcover can be determined from aerial photography, satellite remote sensing (Rango, 1988) or by ground survey methods. Index models are widely used in operational streamflow forecasting models. For example, SNOW-17 (Anderson, 1973) an energy budget based index model has been incorporated into the NWSRFS (National Weather Service River Forecasting System) and is used for streamflow prediction in seven

River Forecast Centres across the USA and has operated satisfactorily under a wide variety of climatic conditions (Roberge et.al., 1988).

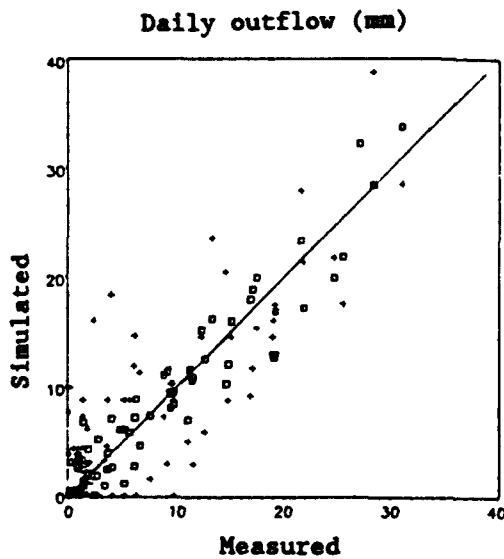
Index models are most commonly used as the snow 'box' in the larger hydrological models. For example, Pangburn (1987) uses a degree-day index model for a cold regions modification to the large hydrological model MILHY (MILitary HYdrological model). Several papers Roberge et.al. (1988), Moussavi et.al. (1989) and Kuusisto (1978) compare the performance of degree-day models against the energy budget index models. All three papers agree that an index model that is more complex than a degree-day model performs better than a degree-day model. Kuusisto (1978) found that a temperature based model using liquid water storage and parameters removing discontinuities in the form of precipitation and refreezing as a function of temperature gave a better performance than a degree-day model and an energy budget based index model. The failure of the energy budget based model was thought to be due to time-averaging problems, errors in parameterization and net radiation measurement errors. Moussavi et.al. (1989) tested two models (an energy budget based index model and a complex degree-day model) against a simple degree-day model and concluded that both model performances were superior to the degree-day model, however it was not specified whether the performance of the energy budget based model was superior to that of the complex degree-day model. Roberge et.al. (1988) tested SNOW-17 against a degree-day model that had been previously calibrated at the test site (boreal fir forest at Lac Laflamme, Quebec, Canada). A selection of their results is shown in figure 1.6. They concluded:

- (1) That the results from SNOW-17 stayed consistently better than those provided by the degree-day model.
- (2) That SNOW-17 is an efficient snowmelt model especially adequate for the boreal forest environment of eastern Canada.
- (3) That SNOW-17 because it is based on the energy budget gives a greater scope and range of information, in addition to melt flows, than the degree-day model.

(a) Years of calibration (1982 & 1984).



(b) Years of validation (1981, 1983 & 1985).



SNOW-17

+ Degree-day

Figure 1.6. Comparison of the SNOW-17 and degree-day models simulated values with the lysimeter daily outflow, Roberge *et al.* (1988).

They also state that the results given by SNOW-17 when incorporated into the NWSRFS for the New England river basins were unsatisfactory when:

- (a) ice lenses disrupted water movement through the snow.
- (b) air temperature was a bad indicator of the snowpack energy-budget.

Anderson (1978) states that air temperature is an inadequate index of melt during the following conditions:

- (1) very warm temperatures and little wind, melt is overestimated.
- (2) high dew-points and strong winds, melt is underestimated.
- (3) under clear skies and abnormally cool temperatures during melt and when the pack is ripe, melt is underestimated.

The more complex the index model the more input data, for example radiation, or the more parameterization or calibration is required. The advantage of index models generally and of degree-day models in particular is that they require very basic input data. Air temperature and precipitation are commonly measured at meteorological stations. However as these models are calibrated there is uncertainty in their application to ungauged catchments. Index models operating at the catchment-scale use simple areal feedback equations to calculate areal snowcover (Ferguson, 1984) and rely heavily upon initial snowcover estimates. Catchment subdivision, if it occurs, is usually on the basis of elevation (Moussavi *et.al.*, 1989) and is correlated with snow-lines.

#### 1.4 Physically-based models.

Physically-based snowmelt models calculate the components of the full energy budget using physically-based equations, that is equations that represent as close as is possible the process that is being modelled.

The full energy budget of a snowpack is:

$$\Delta Q_s + \Delta Q_m = Q^* + Q_c + Q_e + Q_g + Q_p \quad (1.10)$$

where,

- $\Delta Q_s$  snowpack internal energy change.
- $\Delta Q_m$  latent heat storage change due to melting or freezing.
- $Q^*$  net radiation flux.
- $Q_c$  sensible heat flux.
- $Q_e$  latent heat flux.
- $Q_g$  heat flux across ground/snow interface.
- $Q_p$  energy introduced into the pack by rainfall.

Units:  $\text{MJm}^{-2}\text{day}^{-1}$ .

The meltrate is derived from  $\Delta Q_m$ . The components of equation 1.10 are calculated using physically-based equations, for example Anderson (1976) calculates  $Q^*$  as:

$$Q^* = K\downarrow - K\uparrow + \epsilon L\downarrow - \Delta t \epsilon \sigma T_o^4 \quad (1.11)$$

where,

- $K\downarrow$  incoming shortwave radiation,  $\text{calcm}^{-2}$ .
- $K\uparrow$  reflected shortwave radiation,  $\text{calcm}^{-2}$ .
- $\epsilon$  emissivity, 0.99.
- $L\downarrow$  incoming longwave radiation,  $\text{calcm}^{-2}$ .
- $\sigma$  Stefan-Boltzmann constant,  $\text{calcm}^{-2}\cdot\text{K}^{-4}$ .
- $\Delta t$  computational time interval, sec.
- $T_o$  snow surface temperature, °K.

Table 1.3 lists some examples of current physically-based snowmelt models and the scale at which they operate. These models can also be divided into fully physically-based models and quasi-physical models. Anderson (1976) identifies a group of models which, although based on the snowpack energy budget, use separate equations to calculate the change in the snowpack internal energy change ( $\Delta Q_s$ )

**Table 1.3. Examples of physically-based snowmelt models and their scale of operation.**

**(1) Quasi-physical**

Leaf & Brink (1973a & b)	Catchment-scale
Rachner & Matthäus (1986)	Catchment-scale
Sosedko & Kochelaba (1986)	Catchment-scale
Anderson (1968)	Catchment-scale

**(2) Fully physically-based**

Anderson (1976)	Point-scale
Price & Dunne (1976)	Point-scale
Jordan <u>et.al.</u> (1986)	Point-scale
Obled & Rosse (1977)	Point-scale
Morris (1987)	Point-scale
Kelly <u>et.al.</u> (1986)	Point-scale
Kuchment <u>et.al.</u> (1986)	Catchment-scale
Motovliov (1986)	Point-scale

and the snowmelt. Snowpack metamorphism is also not calculated or is treated in a simplified manner, as is the calculation of the snowpack internal temperatures. These are defined here as quasi-physical models. Some quasi-physical models also use a simplified energy budget and use a mixture of index and physically-based equations. Fully physically-based models use no index methods and use equations that are as physically-based as possible, i.e. calibration factors are kept to a minimum. The snowpack heat deficit is calculated as part of the snowpack energy budget equation.

Table 1.3 also shows the predominance of point-scale fully physically-based models as opposed to catchment-scale. One model, Kuchment et.al. (1986) was found in the literature that appears to be a distributed fully physically-based model. The remaining distributed models are all quasi-physical. Morris (1985) notes the lack of fully physically-based distributed models. It is concluded that there are very few fully physically-based distributed snowmelt models available at present (only one example has been found in the literature)

The term 'energy budget' or 'energy balance' model is used widely in the literature. This has various interpretations depending upon the author. Morris (1985) labels any model which uses the energy budget of a snowpack as the basis of the melt calculation as an energy budget model. Therefore, she includes index, fully physically-based and quasi-physical model types in this category. Anderson (1976) uses a much stricter definition which is that only fully physically-based models can be referred to as energy budget models. This variation in the definition of energy budget models is important when reviewing the literature that compares index methods with energy budget methods. This literature is not always a comparison between index and physically-based methods, but is often one between degree-day and energy budget based index models (Roberge et.al., 1988 and Moussavi et.al., 1989). The distinction is important. This report will take the term 'energy budget' model as referring to fully physically-based and quasi-physical models of

snowmelt, as defined above.

Energy budget models, because they are physically-based are more flexible in their output than index models. For example, radiation totals and snowpack temperatures can be obtained as output in addition to melt volume. Therefore energy budget models are much more flexible and adaptable as research tools than temperature index models. They can be adapted for use in chemical and ecological studies (Roberge *et al.*, 1988) and give a much greater insight into the processes operating within the snow subsystem. However, they require more input data in order to operate. Anderson (1976) lists four minimum data requirements for an energy budget model. These are solar radiation (estimated or measured) and measurements of air temperature, vapour pressure and wind speed. Anderson (1978) states that energy budget models will operate better than temperature index models, that is they will give an improved melt volume calculation, when the meteorological conditions are such that air temperature is not such a good index of melt volume, these conditions were stated in section 1.3.

Anderson (1978) discusses the relative merits of temperature index and energy budget models and gives the following reasons why, for practical forecasting, an energy budget model is possibly not as good as a temperature index model:

- (1) The extrapolation of wind data and incoming solar radiation from low to high elevations is difficult in mountainous areas.
- (2) Incoming longwave radiation and snow albedo are not regularly measured variables and therefore have to be estimated from other information.
- (3) The methods used to estimate radiation exchange in forests are approximate and require vegetation cover data which is not available on a wide scale.
- (4) Turbulent transfer over irregular terrain, with some vegetation cover and a dynamic snow surface, is not completely understood.

Anderson (1978) concludes that because of modelling

simplifications and data inadequacies an energy budget method of computing energy exchange may contain as much overall error as a temperature index method. However, he also concludes that energy budget models have an advantage over temperature index models for forecasting and design purposes because of their ability to simulate extreme events.

Anderson (1976) summarised the relative merits of temperature index and energy budget models by a comparison between his SNOW-17 temperature index model (Anderson, 1973) and his fully physically-based energy budget model (Anderson, 1976). Figure 1.7 shows the results from some of his comparative simulations. He concluded that:

- (1) The minimum data required for the operation of an energy budget model are a good estimation of incoming solar radiation and measurements of air, wind speed and vapour pressure.
- (2) Energy budget models perform better when applied to open areas because of the greater ability of energy budget models to operate under variable meteorological conditions.
- (3) Under the stable conditions of the forest floor index models give similar results to those of energy budget models.
- (4) Physiographic factors, for example topography, vegetation cover and climatic factors, should be considered when choosing between energy budget and index models. Generally the more varied the physiography and the climate the better the performance of the energy budget model when compared to the index model.
- (5) When extreme conditions need to be modelled, energy budget models should be used.

To summarize, the following main points should be considered if a choice between the two modelling methodologies is required:

- (1) Operation and calibration data availability.
- (2) Expected physiographic and climatic conditions.
- (3) Detail and type of results required.
- (4) Probability of extreme events.

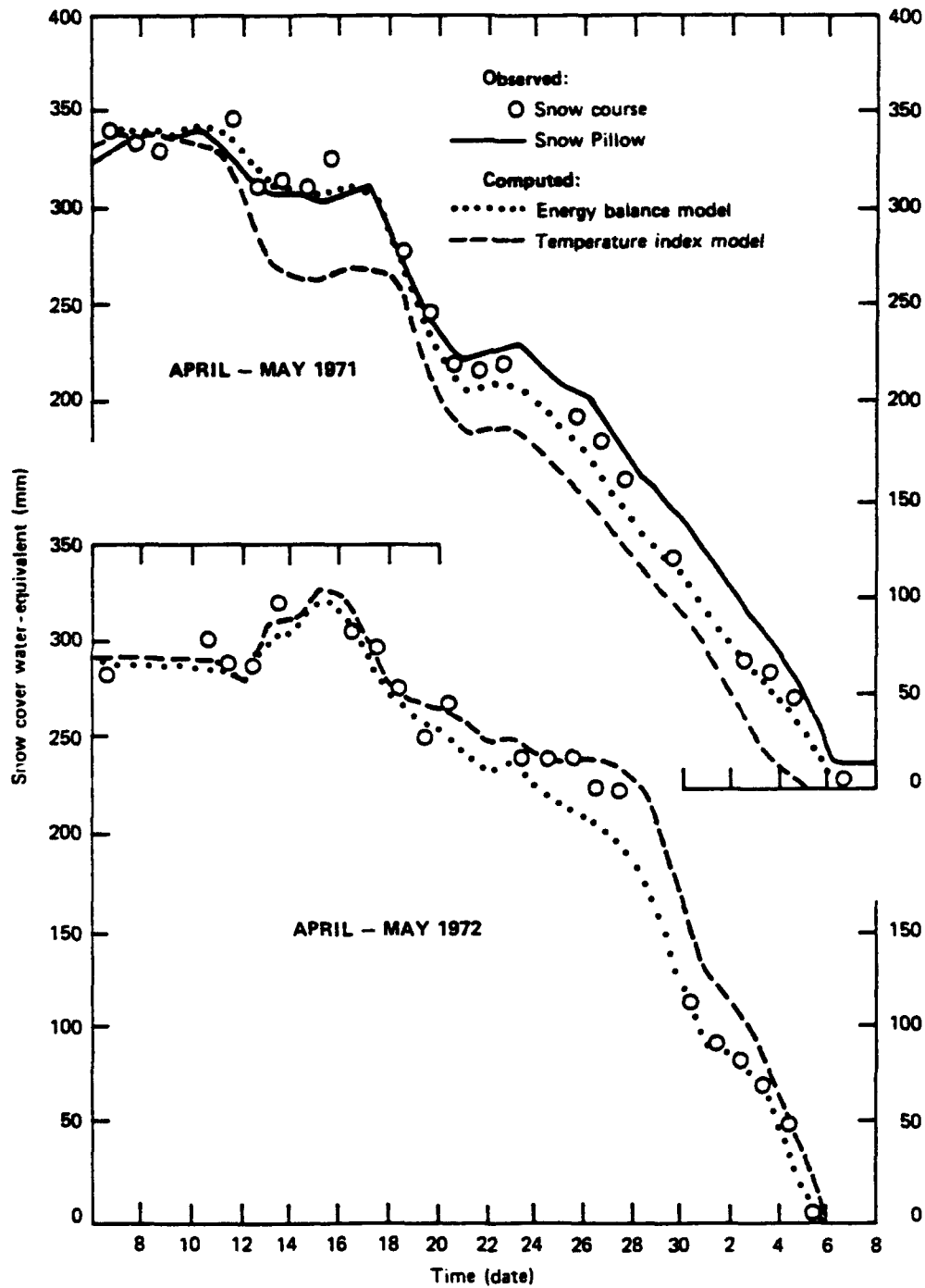


**Figure 1.7.** Comparison of energy balance (energy budget) and temperature index models during the 1971 and 1972 melt seasons at the Townline meteorological station, Sleepers River Research Watershed, Vermont, USA (Anderson, 1976).

There is a second group of physically-based models, these are the process-specific models. These are models of individual or groups of processes that comprise the melt process, they do not however, include the whole process of melt (table 1.4). There are some non-physically-based process-specific models, for example Woo & Steer (1986) (Monte-Carlo simulation of forest snow depth) and Buttle & McDonnell (1987) (snowpack depletion). Process specific models do not attempt to integrate the specific process modelled with other melt processes. These models are often validated using laboratory or small-scale field experimental data.

#### 1.5 The snow environment-model design relationship.

There is a relationship between model design and the snow environment for which it is designed. There are a large range of snow environments some of which have unique processes, for example avalanching (high mountain areas, Brugnot & Pochat, 1981) and Chinook evaporation (Eastern Canadian Rockies, Golding, 1978). Aside from these unique processes the snowmelt process can always be described using the energy budget equation (equation 1.8). The relative dominance and importance of the components of this equation will vary according to the snow environment and the specific combination of topography, climate and vegetation that is present. For example, prairie snowmelt is often characterised as occurring over a short time and resulting in flooding (Hendrick *et al.*, 1971). This is due to the uniformity of the terrain, absence of relief, shallow snowpacks and absence of forest cover. These are all topographic, climatic and vegetational controls. This situation is very different from a mountainous, forested basin with a deep snowpack. Here the melt period will be extended and the risk of snowmelt flooding infrequent. Table 1.5 is taken from Kuusisto (1986) and shows a selection of different environments and the relative contributions of

**Table 1.4. Examples of process specific models.**

<b>Author</b>	<b>Process</b>
Roberge & Plamondon (1987)	Pipe-flow
de Quervain (1972)	Intergranular melt
Powers <u>et.al.</u> (1985)	Thermal convection in snow
Granberg (1988)	Forest shading
Woo & Steer (1986)	Forest snowdepth
Swift (1976)	Mountain solar radiation
Buttle & McDonnell (1987)	Snowpack depletion
Colbeck (1974)	Capillary percolation
Colbeck (1977)	Thermodynamic deformation of wet snow
Stephenson & Freeze (1974)	Subsurface flow and snowmelt runoff

Table 1.5. Relative contributions of different components of the snowpack energy-budget to snowmelt (adapted from Kuusisto, 1986).

Reference	Site	Elevation (m)	Observation period	Average melt (mmday <sup>-1</sup> )	Percentage contribution of the component		
					Q <sup>a</sup>	Q <sub>c</sub>	Q <sub>p</sub> Q <sub>g</sub>
Treidl (1970)	Open field (Michigan), 46°N		Jan 23, 1969	15	17	47	36
Dewalle & Melman (1971)	Forest opening (Colorado), 39°N	3260	June 1968	50	56	44	-3 0
de la Casinière (1974)	Open field in mountains (France), 46°N	3550	July 1968	16	85	15	-15
Weller & Holmgren (1974)	Open field (Alaska), 71°N	10	June 1971		100	-19	-10 -22
Granger & Male (1978)	Open field in prairies (Canada), 51°N		Melt season 1974 Melt season 1975	8 5	59 95	41 5	-10 -29 -1
Hendrie & Price (1979)	Deciduous forest (Ontario), 46°N		April 1978	10	100	0	0
Chauré (1982)	Open tundra (Canada, N.W.T.), 79°N	200	Melt seasons 1969-70		100	-90	-77 -45
Moore & Owens (1984)	Open field in mountains (New Zealand), 43°S	1450	Melt season 1982	31	16	57	25 2
Vehviläinen (1986)	Small basin, 82% forest (Finland), 64°N	120	Melt seasons 1971-81	5	86	15	-13 <1

different components of the energy budget of the snowpack to snowmelt in these environments.

Models developed in one environment may not be easily transferable to different environments. The Leaf & Brink (1973a & b) model, developed for the Colorado subalpine environment, is an example of this. In the Colorado subalpine environment 95-98% of annual streamflow is generated by snowmelt (Garstka *et al.*, 1958). This factor plays a major part in the design of the model. The validity of transferring the model to, for example, the New England environment (where the percentage of annual streamflow generated by snowmelt is much lower) is therefore questionable and may involve extensive calibration and modification of the model. Additionally if a model is to be used in varying environments, for example as SNOW-17 is used in the NWSRFS, for comparative purposes the model does not want to be too environment specific. If the model used has to be radically altered to adjust to each different environment problems will arise in the comparison of the results produced from the different environments. This will be because of the different parameters selected and modifications made. Table 1.6 shows some snow environments and their related models.

The common areal subdivision of index models at the catchment-scale relies upon elevation and snow-lines. This method is therefore bias towards the mountain, high-relief environment as opposed to the prairie, low-relief environment.

#### 1.6 Research objectives.

There is therefore the need for a physically-based distributed snowcover model, a model of snowcover dynamics, at the level of operational complexity that maximises the advantages of being physically-based, but minimises the disadvantages and still remains flexible in terms of data input and operation. This model niche is demonstrated in figure 1.8.

Table 1.6. Snow environments and related models.

SNOW ENVIRONMENT TYPE	PACK DEPTH	VEGETATION COVER TYPE	MELT	EXAMPLE
Prairie/Steppe	Shallow	Grassland Arable	Rapid	Male & Gray (1975) Kuz'min (1961)
High Mountain	Deep plus alpine permafrost	Forest Tundra	Prolonged	Leaf & Brink (1973a & b)
Temperate Lowlands	Deep	Mixed/deciduous forest, pasture, cultivated mix	Prolonged	Dunne & Black (1971)
Tundra	Shallow plus permafrost	Tundra	Rapid	Everett & Ostendorf (1988)

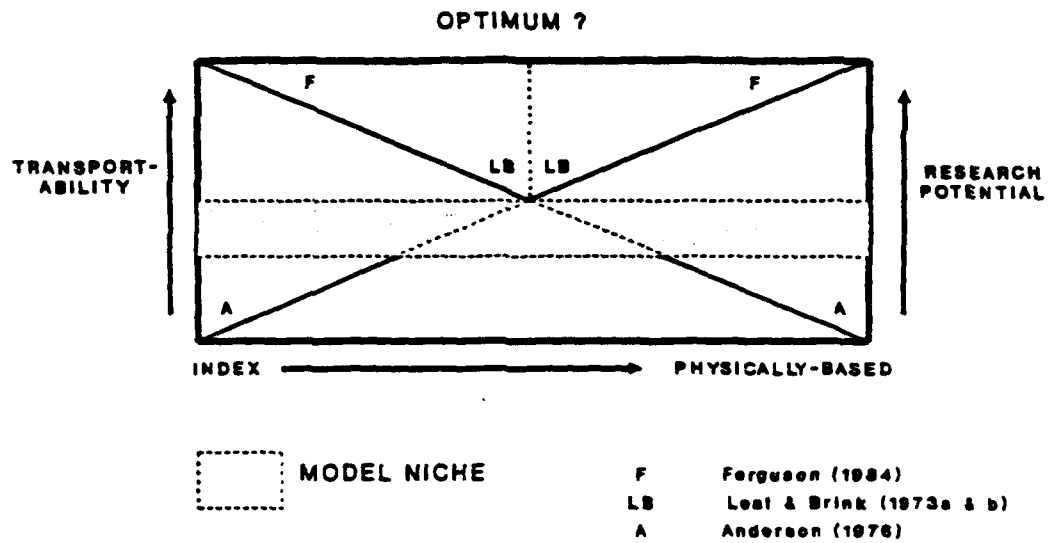


Figure 1.8. Identification of the vacant model niche.

Therefore, the objective of this research is the development of a physically-based distributed snowcover model.

The aims of the model are to:

- (1) Model the spatial and temporal variations of hydrological, meteorological and energy budget parameters in a cold regions watershed.
- (2) Model the spatial pattern of snowcover throughout the snow season.
- (3) Predict the impact of landuse change on cold regions watershed hydrology.
- (4) Provide the model code and an operational manual for the code in order to facilitate future use of the model.

## CHAPTER 2: SNOWCOVER DYNAMICS.

### 2.1 Introduction.

Chapter 1 has identified the need for a distributed physically-based model of snowcover dynamics and has proposed the development of such a model. The process that the proposed model is to simulate must be examined in order to formulate the basic design requirements of the model. This chapter briefly examines the process of snowcover dynamics in terms of four basic components:

- (1) The energy budget of the snowpack.
- (2) The snowcover and snowdepth distribution patterns.
- (3) The snowmelt discharge.
- (4) The affect of vegetation cover.

### 2.2 Snowpack energy budget.

The energy budget of a melting snowpack is described by equation 1.10 (chapter 1). Meltrate per unit area is derived from this equation by:

$$\Delta r_w = \frac{\Delta Q_m}{L_f \rho_w} \quad (2.1)$$

where,

- $\Delta r_w$  meltrate, millimetres water equivalent day<sup>-1</sup>.  
 $L_f$  latent heat of fusion, MJkg<sup>-1</sup>.  
 $\rho_w$  density of water, kgm<sup>-3</sup>.

Figure 2.1 shows the variation in the energy budget components throughout a 24 hour period and in the absence of rain. Table 2.1

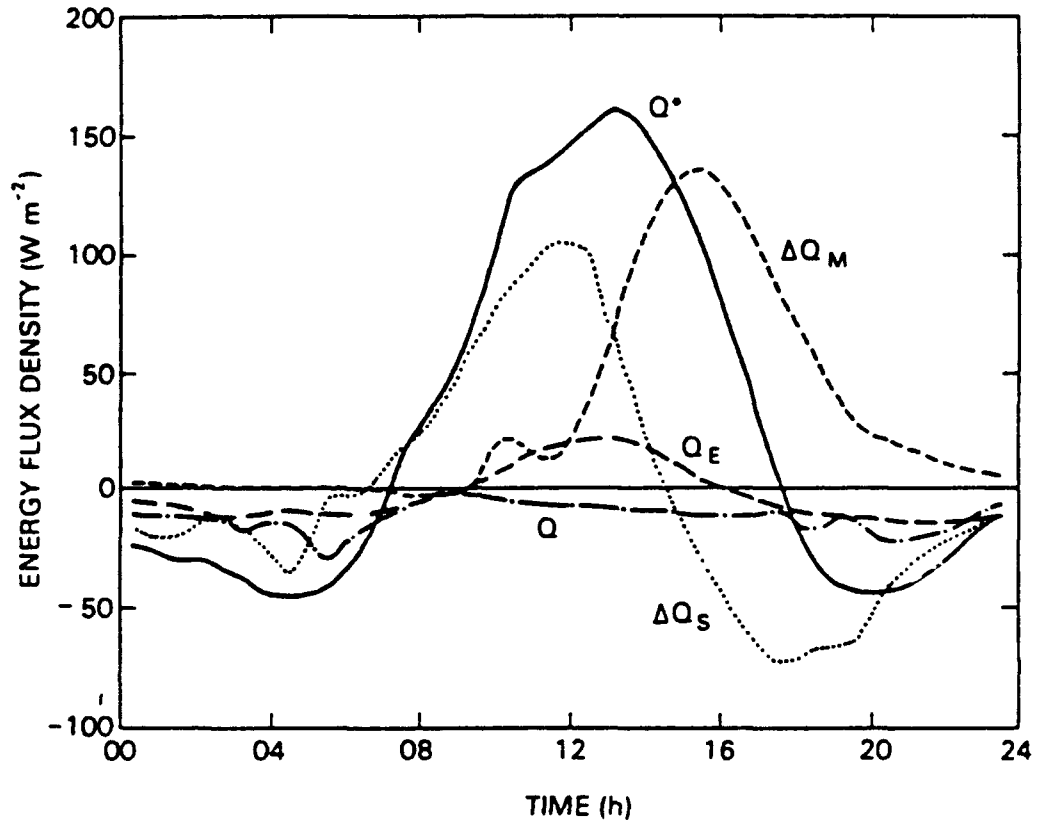


Figure 2.1. Energy budget components for a melting snowcover at Bad Lake, Saskatchewan (51°N), on 10 April 1978, Oke (1987).

Table 2.1. Daily energy totals for the energy components and the derived term  $\Delta r$  for figure 2.1, Oke (1987).

Energy component	$\text{MJm}^{-2}\text{day}^{-1}$
$Q^*$	2.02
$\Delta Q_H$	2.97
$\Delta Q_s$	-0.11
$Q_c$	-0.84
$Q_e$	-0.07
$Q_p$	0.11

$$\Delta r = 8.92 \text{mmhr}^{-1}$$

Table 2.2. Selected daily energy flux transfers ( $\text{MJm}^{-2}$ )<sup>a</sup> during the melt period in the absence of vegetation (Bad Lake, Saskatchewan), Male & Gray (1981).

Date	$K^*$	$L^*$	$Q^{*b}$	$Q_c$	$Q_e$	$Q_g$
11/4/75	8.09	-6.32	1.77	0.186	-0.855	-0.045
12/4/75	9.62	-8.48	1.14	0.782	-0.026	-0.022
14/4/75	12.29	-9.43	2.86	0.013	-0.396	-0.004
17/3/76	4.63	-4.50	0.13	1.830	-0.555	0.064
27/3/76	7.20	-7.72	-0.52	1.517	-0.208	-0.237
28/3/76	7.79	-7.12	0.67	0.070	-0.201	-0.111
29/3/76	9.07	-7.66	1.41	0.532	-0.060	-0.180
30/3/76	9.29	-6.04	3.25	0.827	0.140	-0.270

<sup>a</sup> positive values indicate an energy gain by the snow.  
<sup>b</sup> the daily net radiation flux transfer:  $Q^* = K^* + L^*$

gives the daily energy totals for the energy budget components in figure 2.1 and calculates  $\Delta r$  for that 24 hour period. Table 2.2 shows some comparable results for other years at the same station (Bad Lake, Saskatchewan). Detailed discussions of the energy budget of a melting snowpack and the associated changes in the physical characteristics of the snowpack can be found in Oke (1987), Male & Gray (1981), Price (1977) and Male & Granger (1978).

### 2.3 Snowcover and snowdepth distribution patterns.

Snowpack area and depth varies due to the accumulation pattern of the snowpack (itself dependent upon factors such as drifting and topography) and the variation of the energy budget components which leads to differential melt rates and different dates for the initiation of melt. The pattern of snowcover retreat is dependent upon the scale of the area over which melt is occurring. Steppuhn & Dyck (1974) give three scales:

(1) Regional. (1-1,000,000 km<sup>2</sup>), eg. Rango (1988).

The snowpack retreat pattern is due to climatic differences in, for example, precipitation, radiation and air temperature. This involves regional meteorological patterns, for example, localized precipitation and major elevation changes, usually correlated to snow lines. Snowcover is usually categorised as 0% or 100% cover. The scale range is very large and at the lower end (1-10 km<sup>2</sup>) snowmelt patterns will relate to major topographic features, see photograph 1, major valley orientations and major vegetation changes.

(2) Local. (1000-5m<sup>2</sup>), eg. Leaf & Brink (1973a & b).

Snowmelt patterns relate to local, within-field terrain variables (elevation, aspect and slope angle), vegetation distribution and vegetation variables (canopy density, tree species) and landuse or forest management practices.



Photograph 1. Regional snowcover distribution. Snowcover is concentrated in drainage channels and is absent from remaining terrain (Hamelin & Cook, 1967).

(3) Micro. ( $<5m^2$ ), eg. Dunne & Black (1971), figure 2.2

Snowmelt patterns relate to differences that occur within a few square meters of hillslope in, for example, surface roughness variation, variations in depth hoar development, individual objects (telegraph poles, isolated trees), field boundaries (drifting and shading) and micro-topographic features (depressions, hillocks). Figure 2.2 shows the patchy nature of snowcover retreat due to micro-topographic variations.

Therefore, in the development of a spatial snowmelt model the resolution that is required for the modelling of the residual snowcover is very important. The proposed model of snowcover dynamics will concentrate on the simulation of residual snowcover patterns at the local scale. Woo & Marsh (1977 and 1978) investigate the relationship between topography and snowcover pattern at the local scale. They divided the study watershed ( $33km^2$ ) into 4 nested basins of  $33km^2$ ,  $21km^2$ ,  $10km^2$  and  $0.5km^2$  each. The basin topography was divided into 6 terrain types and snowdepth and density data collected for all 4 basins. Figure 2.3 shows some of their results and that there is a definite relationship between terrain type and snowdepth distribution, the relationship is less clear between aspect and the snowdepth distribution.

There is relatively little literature on snowdepth distribution patterns and even less on models of snowmelt distribution patterns. This reflects the previously discussed (chapter 1) emphasis on meltflow prediction. Buttle & McDonnell (1987) discuss five models of snowpack depletion the majority of which were originally suggested by Ferguson (1984). The models were applied at the local scale to a discretized watershed, divided into homogeneous units on the basis of aspect and vegetation cover. They conclude that the choice of model is dependent upon the nature of the environment that the model is to be applied to. A model which assumes that melt occurs at the snowpack margins is more suited to predict snowmelt for well-exposed areas with shallow discontinuous snowpacks and a model which assumes uniform melt is more suited to predict melt in regions of deep,

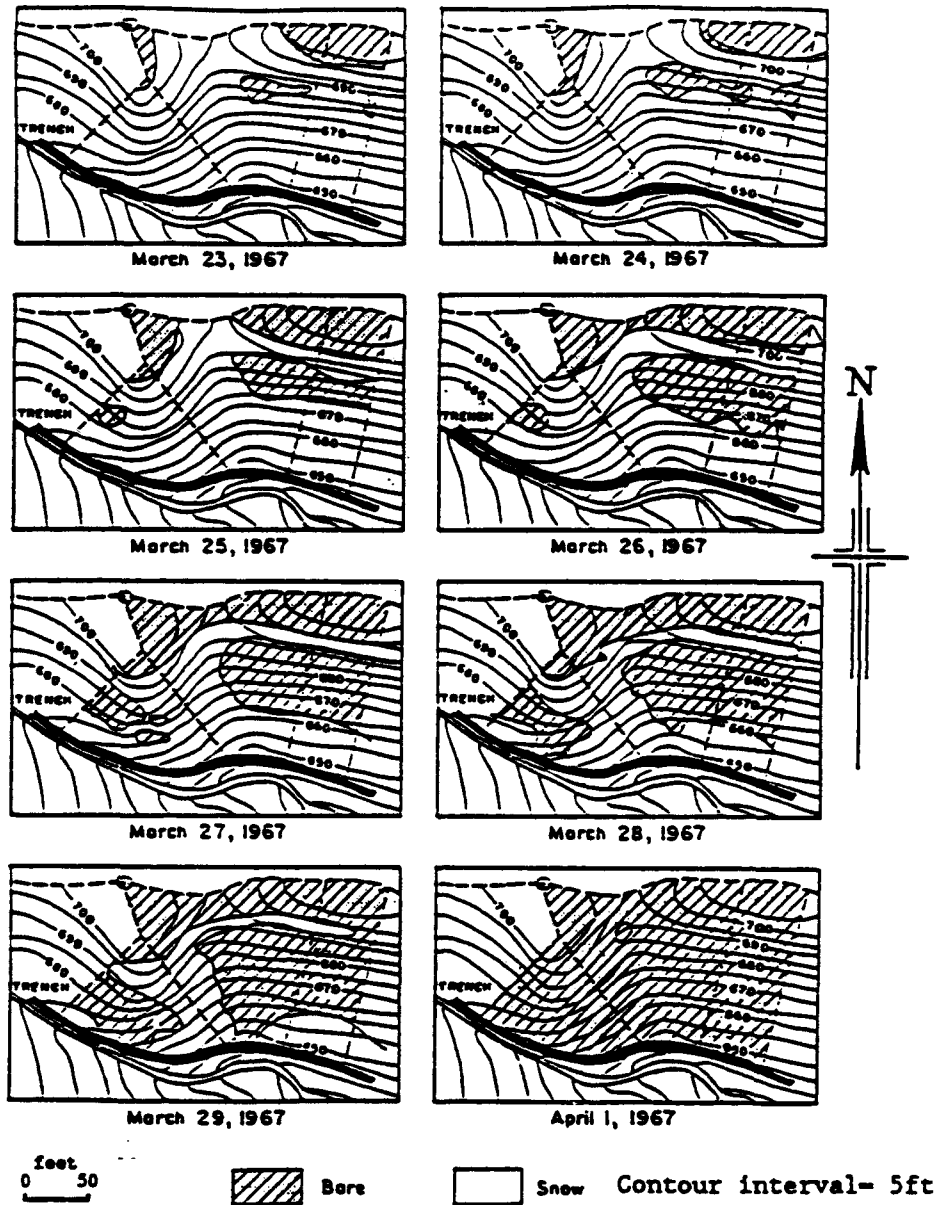


Figure 2.2. Distribution of the snowcover on 3 small hillside plots at noon each day during the melt period of March 1967, Sleepers River Research Watershed, Vermont, USA (Dunne Black, 1971).

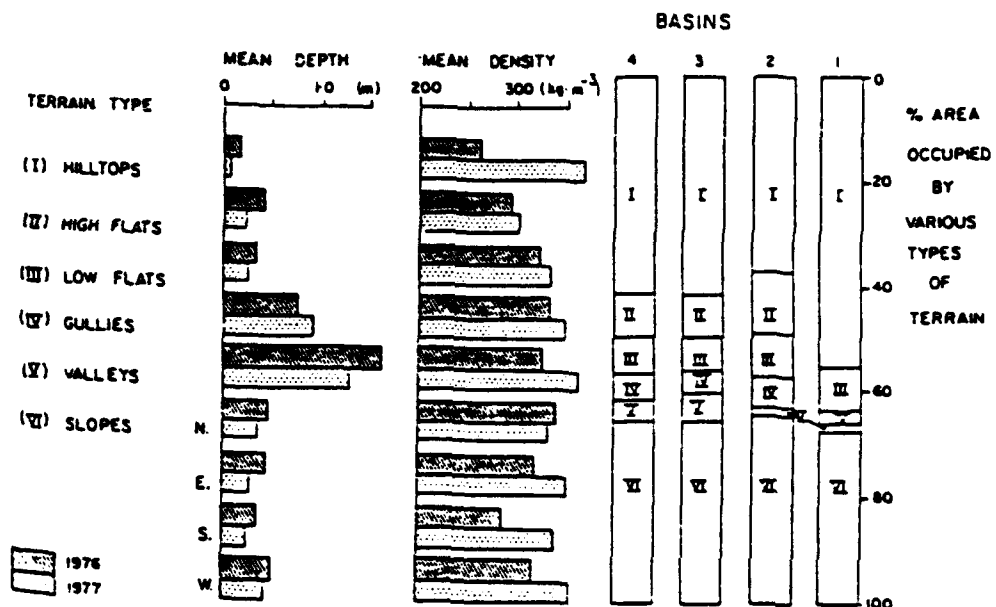


Figure 2.3. 1976 and 1977 mean snowdepth and density for various terrain types and percentage distribution of various types of terrain in the study basins, Woo & Marsh (1978).

continuous snowcover.

The studies by Woo & Marsh (1977 and 1978) and Buttle & McDonnell (1987) both involve a subdivision of the catchment into local-scale units on the basis of topography and vegetation cover. The methods for observing snowcover (ground and aerial reconnaissance and photography) and the factors influencing snowcover depletion patterns (aspect, slope angle, elevation and forest cover) are discussed in US. Army Corps of Engineers (1956). They also observe that the greater the diversity of the terrain and vegetation cover the more protracted the snowmelt period.

Snowcover and snowdepth distribution patterns therefore depend upon the scale at which the pattern is viewed, the initial accumulation pattern and (at the local scale) the variable melt due to differences in topographic, vegetation and meteorological factors.

#### 2.4 Snowmelt discharge.

This follows a diurnal pattern reflecting the decrease or cessation of meltflows during the night. Snowmelt is facilitated by rain. Rain during melt is more common in some snow environments, for example in the Pacific Northwest USA., Oregon (Berris & Harr, 1987) than in others, for example, the Prairies (Male & Gray, 1975). Flooding during snowmelt is facilitated by rainfall, abnormally high air temperatures and the topographic and vegetational homogeneity of the catchment (Hendrick *et al.*, 1971). Meltflow occurs on the surface of the snowpack, within the snowpack and at the base of the snowpack. Meltwater will infiltrate the soil underlying or adjacent to the snowpack unless the soil is saturated, frozen or impermeable due to other factors. The presence of frozen soil acts as an impermeable layer and prevents infiltration. The melting of a frozen soil will also add to the total melt volume. Rapid melt releases large volumes of water within a short time and again can cause soil saturation and overland flow. Figure 1.2 (chapter 1) demonstrates

the close relationship between streamflow and the areal distribution and disappearance of the snowpack during melt.

### 2.5 The effect of vegetation cover.

Vegetation cover affects the snowpack energy budget, the internal characteristics of the snowpack, the snowcover and snowdepth distribution patterns and the snowmelt discharge. Various studies Hendrie & Price (1978), Lafleur & Adams (1986), Price (1988), Price & Petzold (1984), US. Army Corps of Engineers (1956) and Wilson & Petzold (1973) discuss the energy budget and radiation balance of deciduous and coniferous forests during snowmelt. Figure 2.4 summarizes the energy exchanges that occur in dense coniferous forest during active snowmelt. Some of the effects of vegetation cover on the snowpack energy budget have already been mentioned. The effect of the increase in  $L\downarrow$  due to canopy absorption of  $K\downarrow$  and subsequent increase in the temperature of the air in the canopy (Price & Petzold, 1984) has already been discussed. This increase in  $L\downarrow$  can lead to greater values of  $Q^*$  for forested areas when compared to adjacent open areas. Price (1988) demonstrates that  $Q^*$  can account for 90% of the observed melt and that the convective and latent heat fluxes ( $Q_c$  and  $Q_e$ ) are small due to low wind speeds near the forest floor and a damping of turbulent motion caused by the greater stability of the air over the snowpack. Table 2.3 shows the relative importance of  $Q^*$ ,  $Q_c$  and  $Q_e$  in a deciduous forest.  $Q_g$  is generally thought to be a negligible component of the forest snowpack energy budget (figure 2.4), however the daily melt totals attributable to  $Q^*$ ,  $Q_c$  and  $Q_e$  in table 2.3 do not account for all the daily observed runoff. This difference can be explained by measurement error or possibly by the contribution of  $Q_g$ . Field observations (figure 2.5) demonstrate the regular occurrence of frozen ground under coniferous forest and the variation in occurrence of frozen ground with varying vegetation cover.

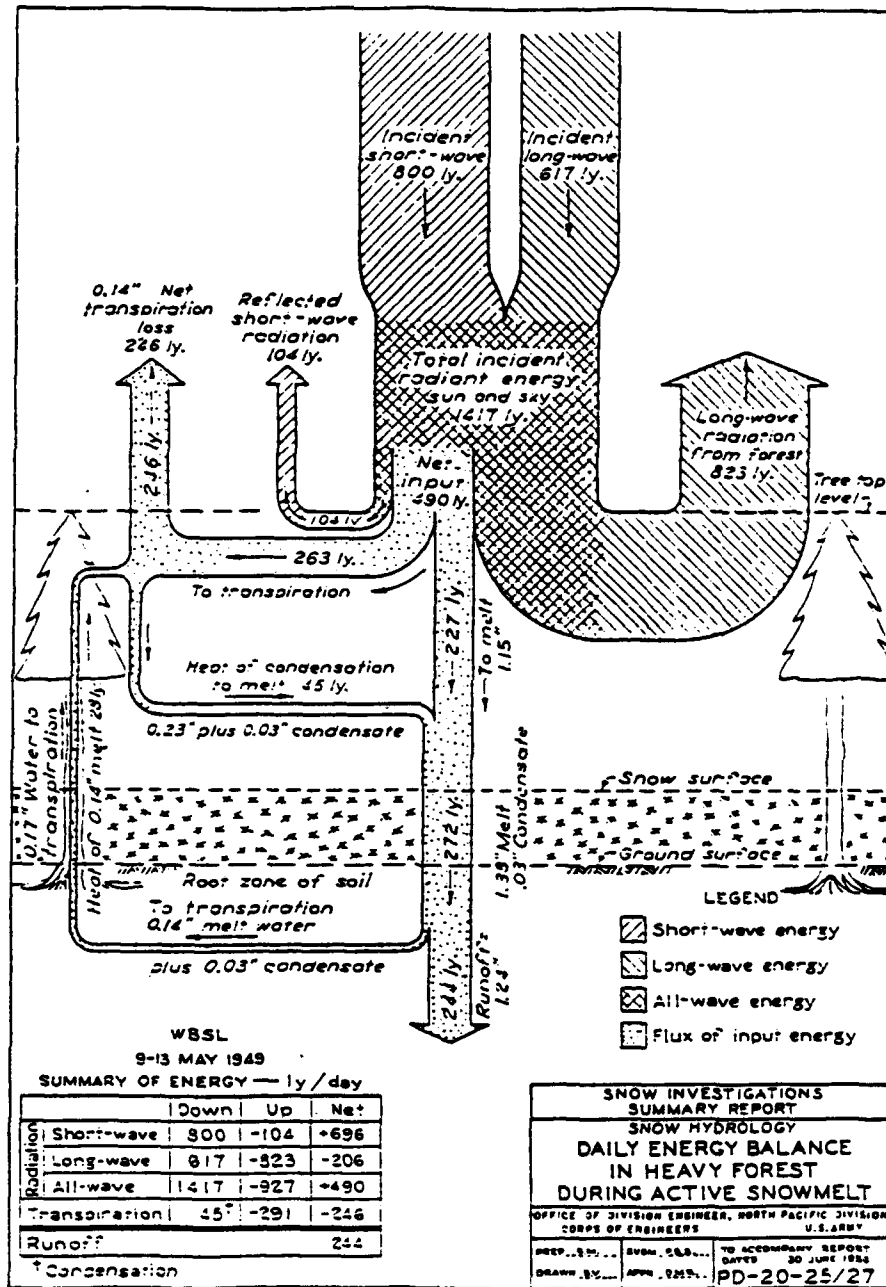


Figure 2.4. Daily energy balance (energy budget) in dense forest during active snowmelt, US Army Corps of Engineers (1956).

Table 2.3. Daily melt totals attributable to the energy fluxes  $Q^*$ ,  $Q_c$  and  $Q_e$ , (Price, 1988).

Date (04/78)	Observed snowmelt runoff	Melt from		
		$Q^*$	$Q_c$	$Q_e$
-----mm water-----				
10	0.9	0.1	0.00	0.08
11	1.8	1.8	0.34	0.21
12	8.5	8.1	1.01	0.17
13	7.8	5.6	0.56	0.22
14	8.2	9.1	0.64	0.00
15	6.8	7.4	0.58	0.02
16	13.0	12.2	0.26	0.05
17	14.4	13.1	0.26	0.03
18	14.5	14.9	0.89	0.05
19	5.2	3.6	0.40	0.00
20	5.6	4.0	0.17	0.11
Period totals	86.7	[79.9	+	5.11 + 0.99]

Table 2.4. Snowdepths under 3 vegetation cover types, W3, Danville, Vermont.

Date	Snowdepth (cm)		
	Deciduous	Coniferous	Open
2/3/88	77	68	64
8/3/88	74	63	62
16/3/88	73	64	59
23/3/88	73	63	56
30/3/88	49	45	32
6/4/88	13	24	0

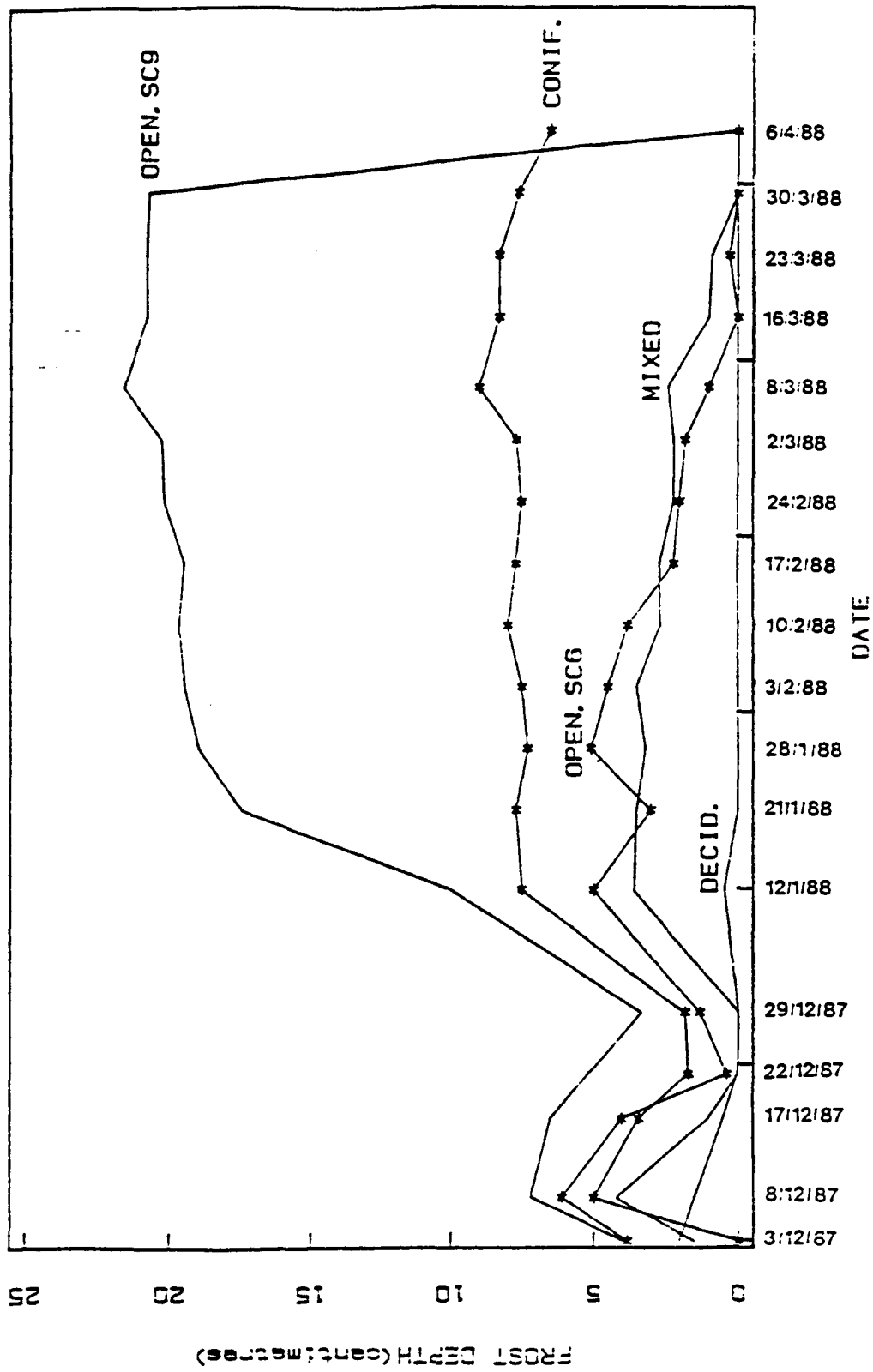


Figure 2.5. Variation of maximum frost depth under 4 cover types, W3 catchment, Danville, Vermont.

Figure 2.6 demonstrates the variation of albedo with vegetation cover. Here, the albedo of a snowcover in an open field area is much higher and is clearly distinguishable from the albedo of the tree-covered area. Price (1988) records overnight albedo changes from 0.40 to 0.90 at Perch lake, Ontario (Canada), due to a snowfall onto a deciduous forest. Canopy debris causes a reduction in albedo at the forest floor. Debris accumulation increases as the snow surface ages and is greater under a coniferous canopy than a deciduous. Field observation (table 2.4) indicates a variation of snowdepth with cover type. In the pre-melt period snowdepths are greatest under deciduous forest cover. As melt progresses bare ground appears first in open areas then under deciduous cover and lastly under coniferous cover. The retardation of melt in forested areas when compared to open areas if, as discussed above,  $Q^*$  values are greater in the forested areas is unexplained although it could be the result of larger  $Q_c$  and  $Q_e$  values in the open areas or density and depth variations between the snowpacks.

Forest clearings accumulate more snow than the surrounding forest (Swanson, 1972 and Anderson *et al.*, 1977). The pattern of snow accumulation in forested areas is affected by wind patterns as in open areas, but to a lesser degree. Drifting and scouring do however occur. The interception of snow by the canopy is an important factor when considering the total precipitation that reaches the forest floor. The US. Corps of Engineers (1956) estimates the interception of seasonal forest snowfall as between 13-27%. Interception is a temporary storage of the snowfall input and, if evaporation occurs, is a means by which the snowfall input reaching the forest floor is reduced.

DeWalle *et al.* (1977) and Harr (1986) discuss the affect of clear-cutting on the snowpack energy budget and the snowmelt runoff. Changes in vegetation cover due to clear-cutting, fire etc., affect the snowpack energy budget and the accumulation pattern of the snowcover and therefore change the volume of snowmelt runoff and the pattern of snowcover and snowdepth distribution. There are no fully

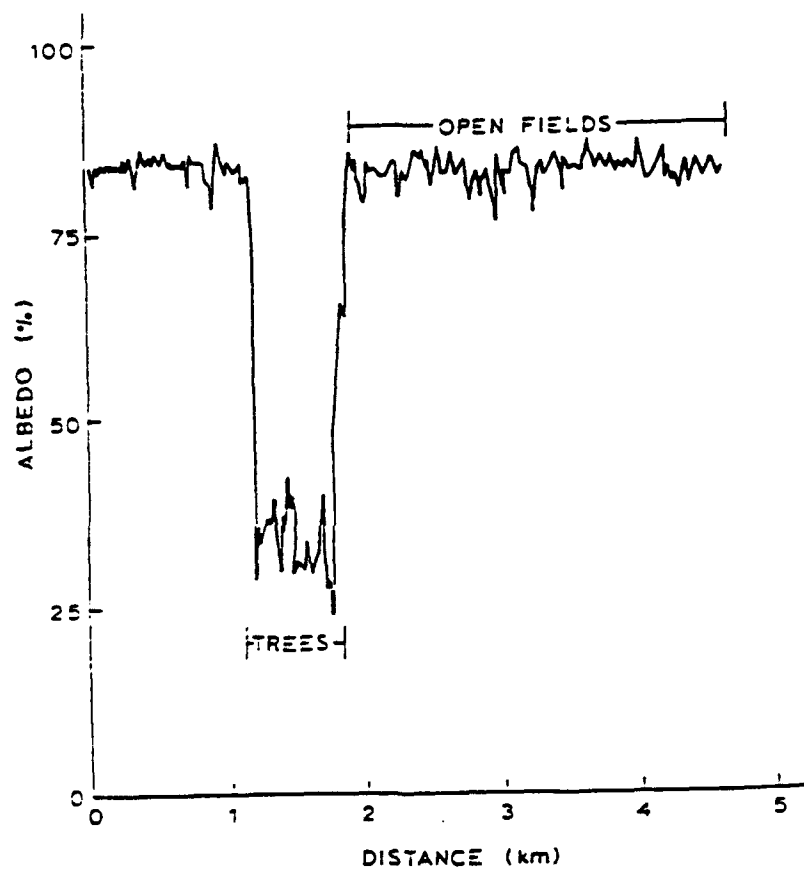


Figure 2.6. Variation of albedo with vegetation cover, 6 January 1971, O'Neill & Gray (1972).

distributed models of forest snowcover available in the literature at present.

## 2.6 Summary.

The four main components of snowcover dynamics and the affect of vegetation have been discussed. In reality these processes occur simultaneously. This can cause difficulties in the isolation or measurement of the specific interactions between the processes. Figures 2.7 and 2.8 demonstrate, albeit simplified, some of the complexity of the interactions between these component processes.

Figure 2.7 summarises the energy exchanges and environmental factors operating in an idealised snow environment during the start of the melt season. Precipitation falls as snow or rain with associated snow accumulation or melt enhancement. Snow accumulation is not areally homogeneous, drifting causing greater snow depths next to obstacles (the fence) and at the base of slopes. Snow accumulation will also be less under the forest, especially the conifers, than in the open. Snow interception also results in albedo variation. This and other factors result in the variation of the energy budget between the forested and the open area. The slope aspect and angle, cloudiness, wind speed and other factors affect the energy budget for the whole area. Snowpack internal properties, i.e. density, thermal conductivity, thermal diffusivity vary with the age of the pack, pack history, i.e. wind hardened layers, and pack depth. The pack can be multi-layered and contain ice layers and lenses. Melt results in snow surface flow, snow throughflow and soil throughflow.

The residual melt pattern at the small and local scales is shown in figure 2.8. Snowcover remains in areas where snow accumulation was greater (the base of the slope, surface hollows and beside the fence) and where the energy budget is less causing a retardation of melt (under the forest canopy and at the forest margin). This

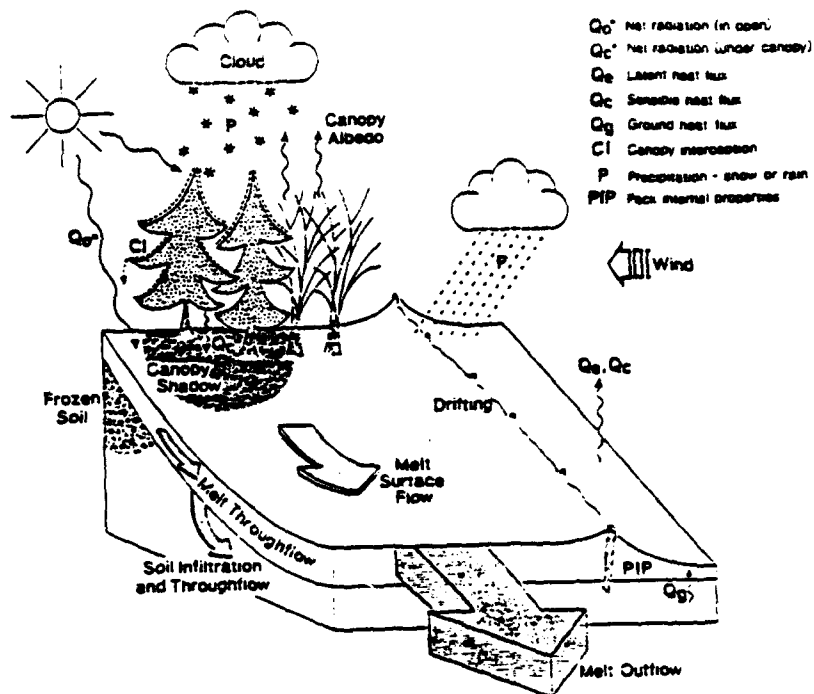


Figure 2.7. Energy exchanges and environmental factors operating in an idealised environment at the start of the melt season.

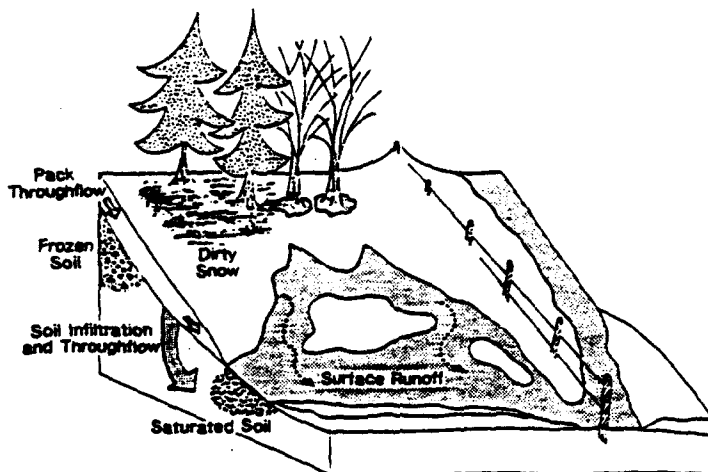


Figure 2.8. The idealised snow environment towards the end of the melt season.

diagram demonstrates the variation and hierarchy in the importance of various factors in influencing residual melt patterns. Melt will usually be initiated at the top of a slope as this is the most exposed to the sun. However, in this case, the upper part of the slope is forest covered and therefore the melt is retarded. Field observations (chapter 7) have shown that in this situation vegetation cover takes precedence over slope in determining the residual melt pattern. Under homogeneous vegetation cover, slope determines the pattern of melt and hence snowcover and snowdepth distribution (chapter 7). Under different snow environments, the prairies for example, other factors such as accumulation patterns may take precedence. Snowmelt flow is as the start of melt situation (figure 2.7) but as melt progresses the presence of bare ground and saturated soils may result in overland flow.

The snowmelt environment is therefore a complex interrelated system operating under variable ground, topographic, vegetation and meteorological conditions. The effects of the variance of these factors on the energy budget of the snowpack is known and when the melt occurs there is a corresponding distribution of the residual snowpack.

This chapter has briefly examined the complex process of snowcover dynamics. This process can be divided into simpler subprocesses, these can be considered as the basic process requirements of the proposed model. The model design (chapter 3) involves the development of a logic structure to represent the process and subprocess interactions and the utilization of relevant physically-based equations to model the subprocesses.

## CHAPTER 3: MODELLING STRATEGY AND MODEL DESIGN

### 3.1 Modelling strategy.

The development of a model in response to a research question involves a series of interrelated stages, figure 3.1. Initially the research objective(s) must be identified, the model design established and the design converted into an operational model. This model must then be validated against real-time data and the model interrelationships examined using sensitivity analysis. At each stage the assumptions that the model makes must be reviewed and finally the further applications of the model and future work must be considered as well as answering the question "has the research objective(s) been fulfilled?". Each stage in the strategy is interrelated and feedback occurs between the various stages. Figure 3.1 illustrates this strategy and relates it to the chapters of this report. The research objective has been formulated in chapter 1 and the objective and aims of the proposed model were identified. Chapter 2 provided an examination of the nature of the process that is to be modelled and enabled the identification of the basic design requirements of the proposed model.

### 3.2 Model design.

In order to fulfil the modelling objective and aims, and following the discussion of the components of snowcover dynamics, the basic model design requirements are:

- (1) To model the energy budget components of the snowpack over the catchment.

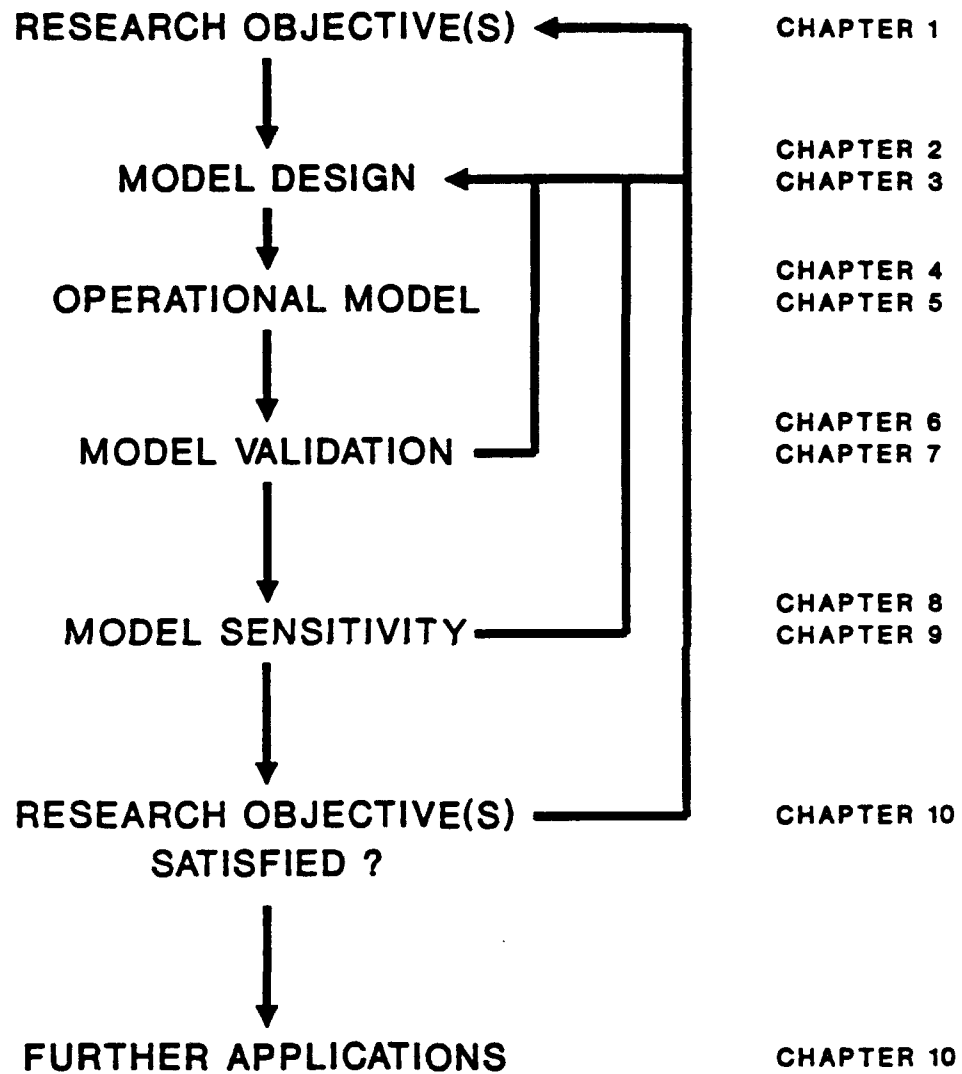


Figure 3.1. Model development strategy and related report chapters.

- (2) To model the affect of the spatial variance in vegetation cover and topography (aspect, slope angle and elevation) at a local scale on the components of the energy budget of the snowpack.
- (3) To model the physical characteristics of the snowpack.
- (4) To calculate the snowmelt volume.
- (5) To use physically-based equations when possible but to operate at an optimum complexity.

At each stage of model design there are choices of alternative submodels and modelling pathways, figure 3.2. Figure 3.2 also demonstrates the generation of conceptual uncertainty that occurs in the model development and design process due to the choice of modelling pathway, submodel type and degree of calibration. Each choice is made as a balance between the time, computing and data constraints that a more complex submodel may require and the loss of information and increased generalization that a less complex submodel would require. The prioritization of the model aims has important implications for the model design and structure. The primary aim is the generation of the pattern of snowcover and snowdepth distribution during the melt season. This means that submodels or algorithms which enhance the modelling of the pattern of snowcover and snowdepth distribution will be utilized to the possible detriment of the lesser model aims, such as the simulation of meltwater runoff. The runoff, for example, still remains to be calculated but the sophistication and physical basis of the modelling may not be as great as that used to model the pattern of snowcover and snowdepth distribution.

Figure 3.3 shows the basic design of the proposed model and is a modified version of the Ferguson & Morris (1987), figure 1.3 (chapter 1), basic structure of a catchment snowmelt model and is discussed below:

- (1) Meteorological submodel.

The meteorological submodel is expanded to include a Geographical Information System (GIS) and a method of subdividing the catchment into homogeneous units (cells). The subdivision (or

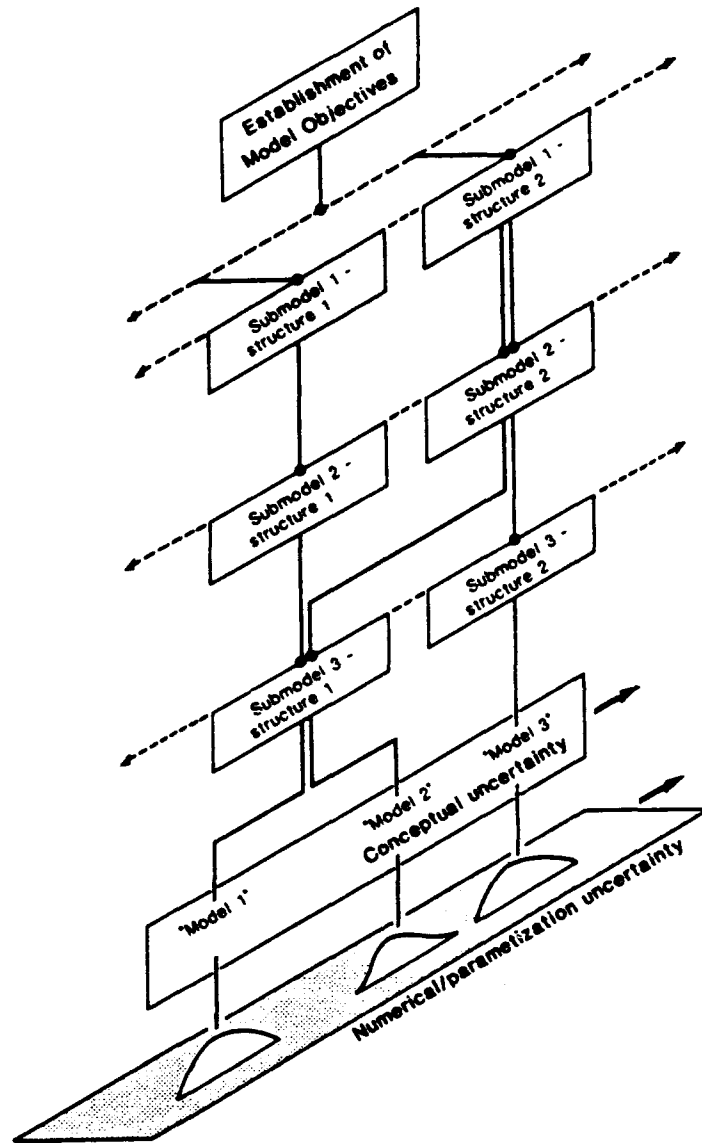


**Figure 3.2.** The choice of alternative submodels and modelling pathways and the generation of uncertainty within the model design process, Anderson & Sambles (1988).

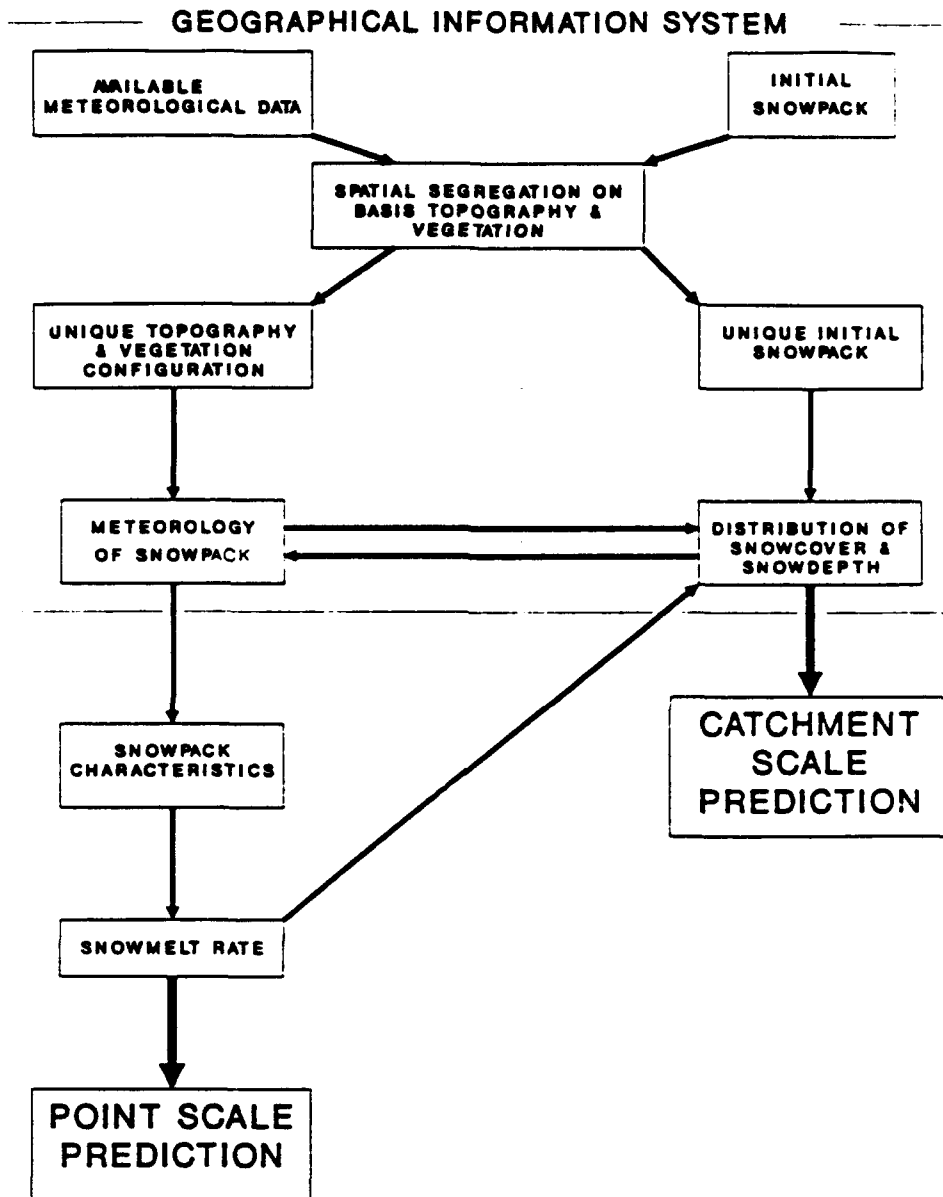


Figure 3.3. Basic design structure of the proposed model.

discretization) of the catchment is performed on the basis of slope angle, slope aspect, elevation and vegetation cover, these being the spatially variant factors that affect the energy budget of the snowpack and hence the pattern of snowcover and snowdepth distribution (chapter 2). Each cell therefore has a certain combination of slope angle, aspect, elevation and vegetation cover. The effects of slope angle, aspect and vegetation are incorporated directly into the energy budget calculations and the effect of elevation on the air temperature is calculated using a lapse rate term, the modified air temperature is then used in the energy budget calculations (chapter 4). To facilitate the subdivision of the catchment and in order to handle the output in a spatial manner a GIS is used. The GIS is a tool to enable easier handling of the spatial variables of topography and vegetation cover. The spatial data is digitized and handled by a computer which makes it much more flexible to change in, for example, vegetation cover and input and output demands. An algorithm to subdivide the catchment into cells is used in conjunction with the GIS which is much more objective and flexible than 'by-hand' methods. The GIS and the subdivision algorithm are discussed in detail in chapter 5 and are crucial to the spatial nature of the proposed model.

(2) Snowmelt submodel.

This calculates the snowmelt and hence the snowdepth at the mid-point of the cell. No attempt is made to model inter-cell interactions, that is, lateral heat and melt flows. Each cell is modelled as a separate section of the total snowpack. This 'point' model substructure is discussed fully in chapter 4. The snowmelt submodel uses a detailed series of physically-based energy budget and melt calculations and treats the snowpack characteristics in a quasi-physical, more lumped manner. These calculations are taken from various existing sources and are adapted to the snowcover dynamics situation. They are linked together in a series of original logic structures and control algorithms and have an original spatial basis.

(3) Transformation submodel.

The simulation of meltwater runoff is not a priority requirement of the proposed model. Choice of submodel complexity varies between a simple volume calculation for each cell, a recession coefficient calculation to simulate streamflow discharge or a complex physically-based scheme again to simulate streamflow discharge. The simple volume calculation is used.

(4) Depletion submodel.

The depletion of the snowpack is calculated for each cell. The results for each cell are then placed in their spatial context, using the GIS, to obtain the pattern of snowcover and snowdepth over the melt period.

Figure 3.4 shows the originality of the proposed model and the report chapters that deal with the model input, calculation and output. The proposed model is named SNOMO (SNOW Model) and will be referred to as such for the remainder of the report. The originality of the objective and aims of SNOMO were discussed in chapter 1. The originality in the design of SNOMO is the balance between complexity and simplicity that is dependent upon the model requirements and the spatial nature of the modelling structure.

The originality of SNOMO both in design and objective is reinforced by a comparison between SNOMO and an existing model, if available, that is simulating a similar situation. The structure and methodology of the Leaf & Brink (1973a & b) model, WATBAL, is therefore compared with that of the proposed model SNOMO. The comparison will:

- (1) Aid the identification and confirmation of the originality of SNOMO.
- (2) Identify any features in WATBAL that may be incorporated into SNOMO to improve the proposed design or structure of the model.

WATBAL was chosen for comparative purposes as it is the model currently available in the literature that most closely resembles SNOMO in terms of the spatial basis of the modelling. The spatial

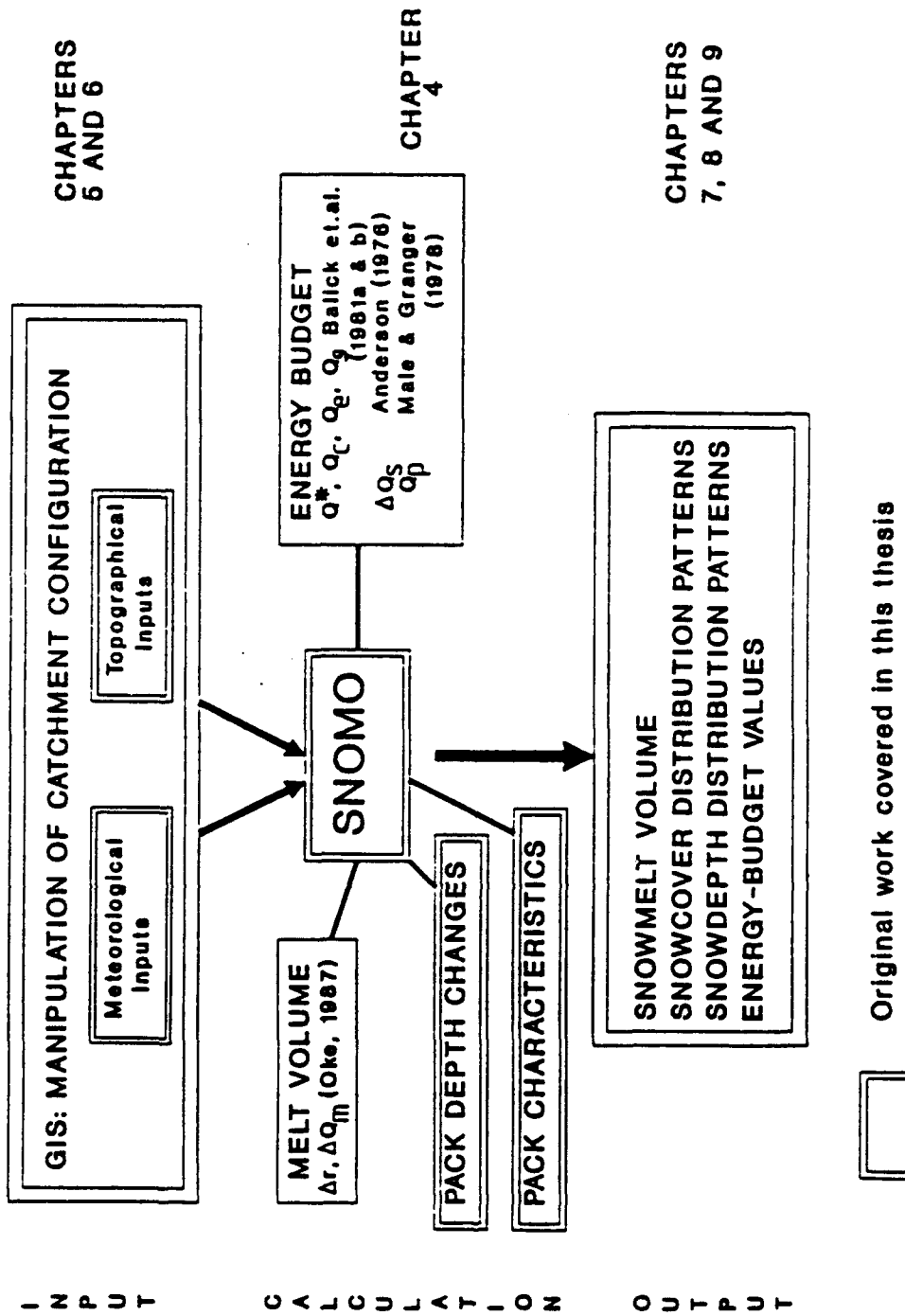


Figure 3.4. Proposed model originality and related report chapters.

basis of the model was the primary factor in the choice of WATBAL as the comparative model. This is because the primary aim of SNOMO is the simulation of the patterns of snowcover and snowdepth distribution.

### 3.3 Comparison between WATBAL and the proposed model SNOMO.

Table 3.1 shows some of the major points that differentiate between the proposed model SNOMO and WATBAL. The proposed model SNOMO and WATBAL are broadly similar in that they both possess a spatial basis that is similar (the subdivision criteria of slope angle, aspect, elevation and vegetation cover are identical) and they both utilise the energy budget and the temperature of the snowpack in order to calculate the melt. However, the proposed model SNOMO differs from WATBAL in the following major ways:

- (1) SNOMO will calculate the energy available for snowmelt using the full energy budget of the snowpack throughout both the pre-melt and the melt period. The elements comprising the energy budget of the snowpack are derived from physically-based equations. In contrast WATBAL calculates the energy available for melt from a modified snowpack energy budget only when the snowpack heat deficit has been eliminated and the pack is isothermal. The heat deficit and temperature of the snowpack are derived from the air temperature above the pack, not the energy budget of the snowpack. The elements comprising the modified energy budget of the snowpack are derived from air temperature, available tables and semi physically-based equations.
- (2) The proposed subdivision of the catchment by SNOMO is computerised, the subdivision of the catchment by WATBAL is performed manually. The relative merits of these two approaches are discussed (chapter 5).
- (3) SNOMO will calculate incoming solar radiation using physically-

**Table 3.1. Summary of the major differences between the proposed model SNOMO and WATBAL.**

WATBAL	SNOMO
Calibrated	Uncalibrated
Uses degree-days to calculate calculate $K\downarrow$ and uses tables to calculate affect of slope and aspect on $K\downarrow$ .	Uses solar geometry to calculate affect of slope and aspect. Uses physically-based (PB) equations to calculate $K\downarrow$ .
Manual subdivision.	Computerised subdivision.
Snowpack energy-budget (EB) only calculated during melt.	Snowpack EB calculated throughout simulation.
$\Delta Q_s$ 'calculated' using the heat deficit approach.	$\Delta Q_s$ calculated using PB equations.
$Q_p$ calculated using 'cold content' or semi-PB equations.	$Q_p$ calculated using PB equations.
$Q_c$ not calculated, allowed for in DIFMOD, nowhere in RADBAL.	$Q_c$ calculated using PB equations.
$Q_e$ calculated by calculation of ET, semi-PB equations, C coefficient.	$Q_e$ calculated using PB equations.
The affect of the vegetation canopy is calculated using semi-PB equations.	The affect of the vegetation canopy is calculated using PB equations.
Response unit has to border a stream channel.	Response unit does not have to border a stream channel.
Main aim is prediction of streamflow, then ET.	Main aim is prediction of the pattern of snowcover and snowdepth distribution.
Pack depth is modelled in inches of water equivalent.	Pack depth is modelled in centimetres of snow.
Predicts streamflow.	Does not predict streamflow.

based equations. This value will then be modified for slope angle and aspect using spherical trigonometry. In contrast WATBAL calculates incoming solar radiation using a degree-day method and modifies this value for slope angle and aspect using values from the Frank & Lee (1966) tables.

- (4) The main aim of SNOMO is the prediction of the pattern of snowcover and snowdepth distribution. In contrast, the main aim of WATBAL is the prediction of streamflow.
- (5) SNOMO will be an uncalibrated model, WATBAL is calibrated.
- (6) SNOMO will model the variation in pack characteristics with depth and through time by modelling either a two-layer or one-layered snowpack. Each layer will have individual characteristics which are designated at the appropriate time and depth. In contrast, WATBAL models the snowpack as a single layer with albedo, density and thermal diffusivity varying through time.

The comparison between the proposed model SNOMO and WATBAL has demonstrated several useful points in the consideration of model development:

- (1) The influence of environment on model design.

WATBAL was designed for the Colorado subalpine forest environment. Here 95-98% of the annual runoff is generated by the spring snowmelt, no melt usually occurs until spring once the snowpack has begun to accumulate. The water equivalent on 1 April is also an accurate measurement of the peak water equivalent. These factors influence the design of WATBAL and therefore create problems when WATBAL is applied to dissimilar environments, such as the Northwest or Northeast mountain environments of the USA. These problems do not negate the utility of SNOMO but are simply a product of the application of WATBAL to an environment for which it was not designed.

(2) The influence of model aim on model design.

The importance of the influence of model aim on model design is obvious but must be remembered when comparing the two models. One of the reasons WATBAL does not predict the patterns of snowcover and snowdepth distribution is because it was not designed to do this, it was designed to predict streamflow. The absence of the prediction of the pattern of snowcover and snowdepth distribution must therefore be seen not as a shortcoming of the model but as a result of the aim of the model, much as the absence of streamflow prediction in SNOMO is a conscious decision and does not detract from the model performance. Until SNOMO predicts streamflow or WATBAL predicts the pattern of snowcover and snowdepth distribution direct comparison between the two model results is difficult.

WATBAL has been incorporated (C.Troendle pers. comm.) into a Colorado mountain forest management and ecosystem model, MMARM (Multi-Resource Management Response Model). This incorporates WATBAL with, for example, insect population models, forest growth models and nutrient models and aims at the modelling of the forest ecosystem and the effects of forest management practices on this. MMARM is a menu-driven user-friendly system that allows a choice of data and model at the relevant stages of the investigation. The idea of incorporating the model into a much larger management framework is an idea that could be adapted successfully by the proposed model SNOMO. The proposed model SNOMO, like WATBAL, has the potential for inclusion into a management model for planners, foresters, agronomists, hydrologists and civil engineers. The inclusion of the proposed model SNOMO into this type of structure is possible and is discussed further in chapter 10.

The comparisons made in this chapter have highlighted the significant and important differences between the two models, the originality of the proposed model SNOMO, some of the problems that occur when designing a model such as the influence of the environment on model design, identified a possible future structure for the

proposed model SNOMO and have reinforced the model niche that SNOMO is to fill.

## CHAPTER 4: MODEL STRUCTURE I: MATHEMATICS AT A POINT

### 4.1 Introduction.

The basic operational structure of SNOMO has been discussed in chapter 3, that is the division of the catchment into homogeneous units (cells) and the subsequent calculation of the snowpack characteristics, energy budget and melt at the mid-points of these cells. This chapter considers the energy budget, snowpack characteristics and melt calculations that are performed at the mid-point of a cell (figure 4.1). Chapter 5 considers the spatial basis of SNOMO and the algorithms used to achieve the spatial subdivision of SNOMO and to handle the initial input data.

The main logic structure of SNOMO can be described as broadly consisting of two sections:

(1) Control programme.

This is responsible for the determination of the type of precipitation (section 4.4), the calculation of melt (section 4.4), the calculation of the effect of rain-on-snow (section 4.4), the calculation of the heat flux across the ground/snow interface ( $Q_g$ , section 4.4), various operational markers (section 4.5), the calculation of the depth of the snowpack and the physical characteristics of the snowpack (section 4.5) and the input and output of the model (section 4.5 and chapter 5).

(2) Algorithm to calculate the majority of the components of the snowpack energy budget.

This algorithm is responsible for the calculation of the snowpack energy budget components  $K\downarrow$ ,  $K\uparrow$ ,  $L\downarrow$ ,  $L\uparrow$ ,  $Q_c$  and  $Q_e$ , and the snowpack surface and internal temperatures. The algorithm is adapted from the US Corps of Engineers Terrain Surface Temperature Model (TSTM) as developed by Balick *et al.* (1981a & b). The basic equations used by the original TSTM remain the same as in the

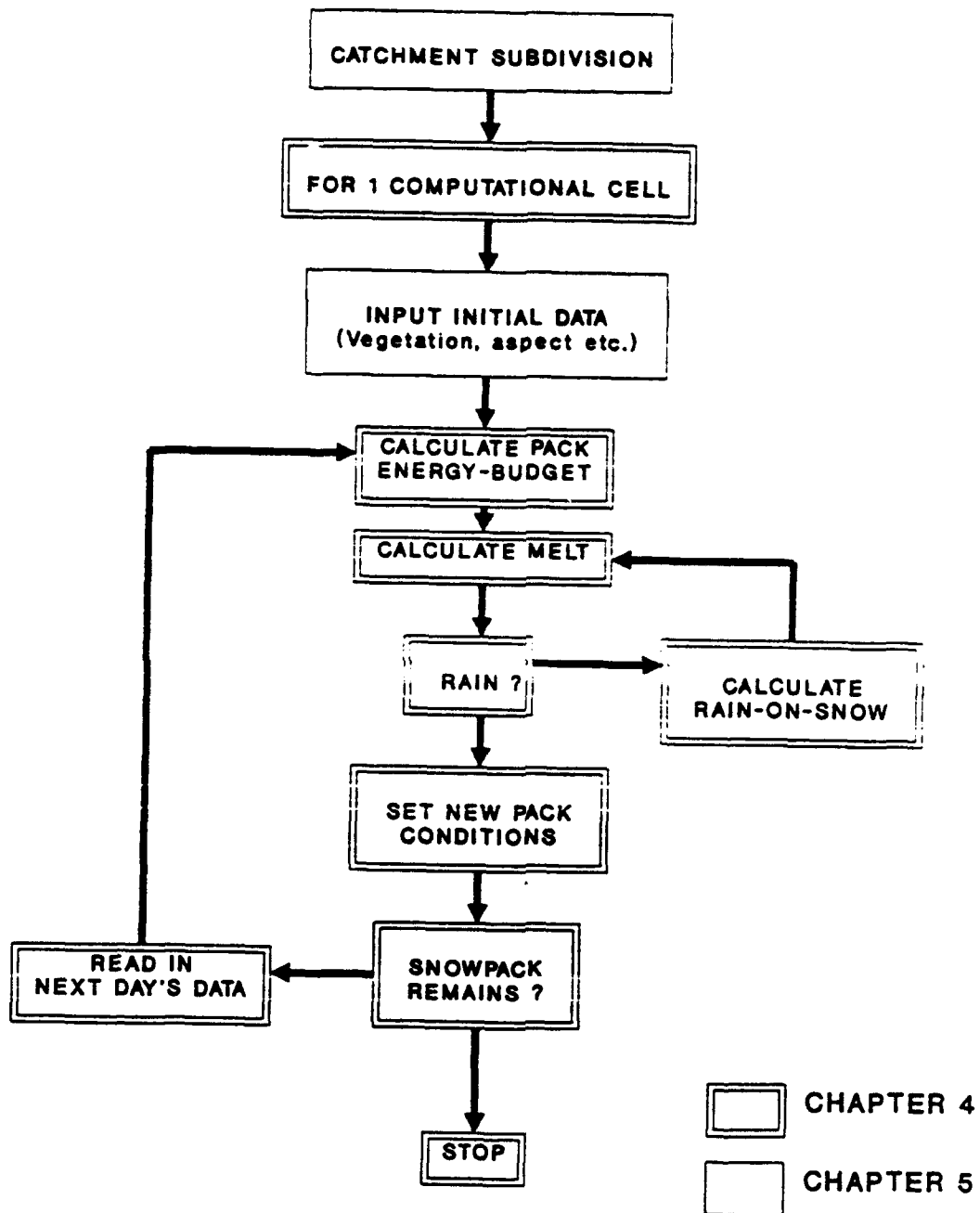


Figure 4.1. Simplified logic structure of SNOMO and related report chapters.

modified TSTM. The data and operational controls of TSTM have been radically modified to enable continuous daily modelling over time periods greater than a month, a decrease in input data requirements and a presentation of the required outputs at the required time intervals. TSTM can operate with or without a vegetation cover, modelled using the vegetation component VEGIE. TSTM and VEGIE are documented in Balick et.al. (1981a & b).

The equations used in SNOMO have been taken from existing literature and have been formulated into an original logic structure (as discussed in chapter 3, figures 3.3 and 3.4). TSTM has been heavily modified from its original state as presented in Balick et.al. (1981a & b) and has also been incorporated into the logic structure of SNOMO. The following chapter therefore discusses the calculation of snowmelt, that is handled by the TSTM equations and other equations taken from the literature (sections 4.1 to 4.4), the calculation of the snowpack characteristics and structure and the model input and output that are handled by the control programme (section 4.5). The equations and logic structures presented in this chapter are translated into FORTRAN-77 code. Volume 2 of this report contains the resultant computer programme, demonstration input and output files and a detailed presentation of the programme logic.

#### 4.2 The calculation of the snowpack energy budget components as derived from TSTM.

Figure 4.2 shows the TSTM concept in diagrammatic form. TSTM predicts surface temperatures for a multi-layered (in SNOMO 2 layers maximum) system by determining energy transfer in and out of the system. TSTM assumes that the layers and the environment above them are horizontally uniform and therefore that the most significant heat fluxes are vertical. The temperature behaviour in the layer can be described by the one-dimensional heat flow equation:



$$\frac{\partial T(z,t)}{\partial t} = \kappa(z) \frac{\partial^2 T(z,t)}{\partial z^2} \quad (4.1)$$

where,

T      temperature  
z      distance into the material system  
t      time  
κ      thermal diffusivity

The boundary condition across the earth's surface is the surface heat balance equation:

$$K^* + L^* + Q_c + Q_e + G = 0 \quad (4.2)$$

TSTM calculates using units from the c.g.s. (centimetre, gram and second) system and outputs in  $Wm^{-2}$  and °C. In SNOMO the output units have been changed to langley and  $MJm^{-2}day^{-1}$  but the internal calculations remain in the c.g.s. system. The modified TSTM calculates the components of equation 4.2 for a snow surface.

#### 4.2.1 Calculation of the direct incoming shortwave radiation, S, and K↓.

TSTM calculates only the direct incoming shortwave radiation, S, ie. if it is found that the sun is not shining directly onto the surface then it is assumed that there is no shortwave radiation. The shortwave radiation incident at the top of the atmosphere, the solar constant, is modified by:

- (1) Optical air mass number, m. This is the ratio of the slant path taken by the beam to the zenith angle, z, so that  $m=1/\cos z = \sec z$ .
- (2) Atmospheric transmissivity. This is the concentration of gases and water vapour in the atmosphere.
- (3) Cloud cover and type.
- (4) Latitude, slope angle and slope aspect.

The equation to calculate  $S_h$ , the direct beam shortwave radiation on a horizontal surface (excluding the effects of clouds and optical air mass number) is taken from Khale(1977):

$$S_h = (1-\alpha_g) [1-A(u^*)] (0.349)S_o \cos z + (1-\alpha_g) [(1-\alpha_o)/(1-\alpha_o\bar{\alpha}_g)] (0.651)S_o \cos z \quad (4.3)$$

where,

- $\alpha_g$  surface albedo, decimal.
- $A(u^*, z)$  Mugge-Möller absorption function, equal to  $0.271(u^* \sec z)^{0.303}$ .
- $u^*$  effective water vapour content of the atmosphere,  $\text{gcm}^{-2}$ .
- $(0.349)S_o$  amount of shortwave radiation of wavelength greater than  $0.9\mu\text{m}$ ,  $\text{calcm}^{-2}\text{min}^{-1}$ .
- $S_o$  shortwave radiation incident at the top of the atmosphere,  $\text{calcm}^{-2}\text{min}^{-1}$ .
- $z$  zenith angle of the sun as a function of the time of the day and the time of the year.
- $\alpha_o$  atmospheric albedo for Rayleigh scattering, equal to  $0.085-0.247\log_{10}[(\rho_s/\rho_o)\cos z]$ , decimal.
- $\rho_s$  surface pressure, mb.
- $\rho_o$  1000mb.
- $\bar{\alpha}_g$  area average ground albedo, decimal.
- $(0.651)S_o$  amount of shortwave radiation of wavelength less than  $0.9\mu\text{m}$ ,  $\text{calcm}^{-2}\text{min}^{-1}$ .

The effective water vapour content,  $u^*$ , is the total precipitable water excluding clouds. Precipitable water is estimated from surface air temperature and relative humidity:

$$u^* = \exp(0.07074T_d + r) \quad (4.4)$$

where,

$T_d$  dewpoint temperature, °C.

$r$      -0.02290   April-June  
           0.02023   July-March.

The value of  $S_h$  once modified for cloud cover, cloud type and optical air mass number is  $S_c$  and is calculated in two stages. First a cloud adjustment factor, CA, is calculated which is dependent upon cloud type and the optical air mass number. This is then modified for cloud cover to result in  $S_c$ .

$$CA = (a/94.4) \exp[-m(b-0.059)] \quad (4.5)$$

where,

$a$  and  $b$      empirical coefficients dependent upon cloud type  
                   (tables 4.1 and 4.2).

$m$             optical air mass number.

$$S_c = S_h - ([S_h - (S_h CA)] CC^2) \quad (4.6)$$

where,

CC     visual cloud cover, tenths.

$S_c$  is then modified for latitude, slope angle and slope aspect by using a slope factor SF.

$$K\downarrow = S_c \times SF \quad (4.7)$$

SF is calculated from spherical trigonometry and the geometry of a slope, from figure 4.3 (Oke, 1987)

$$\cos\hat{\theta} = \cos\hat{\beta}\cos z + \sin\hat{\beta}\sin z\cos(\Omega - \hat{\eta}) \quad (4.8)$$

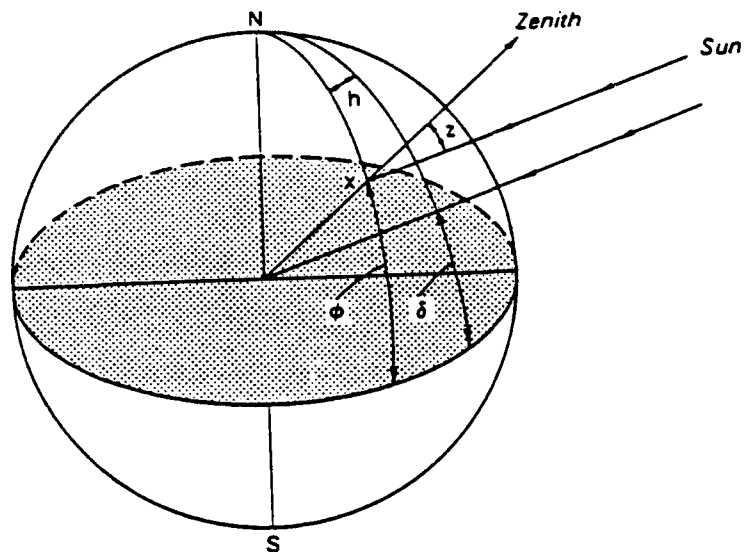
Table 4.1. Cloud Genera and Cloud Type Indices\*, Balick *et al.* (1981a).

Cloud Genera	Abbreviation	Index value	Comments
Cirrus	Ci	1	High clouds composed of white delicate filaments, patches of narrow bands, elements often curved or slanted and smaller than Cs, never overcast or precipitating.
Cirrostratus	Cs	2	High clouds appearing as whitish veil usually fibrous, often produces halo phenomena, thinner than As, does not appear to move, nonprecipitating.
Altostratus	As	3	Midlevel clouds, patches, usually broken, lee wave clouds, elements smaller than Sc, nonprecipitating.
Altostratus	As	4	Midlevel grey sheet or layer of striated, fibrous or uniform appearance, large horizontal extent; thicker than Cs, thinner than Ns, precipitation generally light and continuous (if any).
Stratocumulus	Sc	5	Grey and/or whitish layer or patch, nearly always has dark spots and is nonfibrous; elements larger than Ac, nonprecipitating.
Stratus	St	6	Grey rather uniform base, patches ragged if present, precipitation unusual but light and continuous if present, lower and more uniform than Sc, less dense and less 'wet' than Ns.
Nimbostratus	Ns	7	Grey often dark, diffuse, large horizontal and vertical extent, thicker than As, more uniform than Sc, often precipitating, precipitation continuous.
Fog	FG	8	

\* Cloud genera; Cumulus (Cu), Cirrocumulus (Cc) and Cumulonimbus (Cb) are not treated here. At low cloud covers (0.3) Cu and Cc may be approximated with Ac.

Table 4.2. Coefficients used in the TSTM and SNOMO energy budget calculations, Balick et.al (1981a).

CLOUD TYPE	COEFFICIENT		
	a	b	CIR
Cirrus	82.2	0.079	0.04
Cirrostratus	87.1	0.148	0.08
Altostratus	52.5	0.112	0.17
Altostratus	39.0	0.063	0.20
Stratocumulus	34.7	0.104	0.22
Stratus	23.8	0.159	0.24
Nimbostratus	11.2	-0.167	0.24
Fog	15.4	0.028	0.25



$z$  Solar zenith angle  
 $\phi$  Latitude of location  
 $\delta$  Solar declination  
 $\Omega$  Solar azimuth angle  
 $h$  hour angle

**Figure 4.3.** Geometrical relationships between the Earth and the solar beam. The angles are defined with reference to the equatorial plane (shaded) and the point of interest (X), Oke (1987).

where,

$\theta$  slope factor (angle of incidence between the sun and the normal to the slope).

$\hat{\beta}$  slope angle.

$z$  solar zenith angle.

$\Omega$  solar azimuth angle.

$\hat{\Omega}$  slope azimuth angle.

Some of the variables used in equation 4.8 are derived from spherical trigonometry, figure 4.4, Oke(1987):

$$\cos z = \sin \theta \sin \delta + \cos \theta \cos \delta \cos h \quad (4.9)$$

$$\cos \Omega = (\sin \delta \cos \theta - \cos \delta \sin \theta \cos h) / \sin z, t < 12 \quad (4.10)$$

$$= 360^\circ (\sin \delta \cos \theta - \cos \delta \sin \theta \cos h) / \sin z, t > 12 \quad (4.11)$$

where,

$\theta$  latitude of location.

$\delta$  solar declination.

$h$  hour angle.

$t$  local apparent solar time.

#### 4.2.2 Calculation of the reflected shortwave radiation, $K_{\uparrow}$ .

TSTM calculates the amount of direct incoming shortwave radiation,  $K_{\downarrow}$ , that is absorbed at the surface,  $K_{ab}$ .

$$K_{ab} = K_{\downarrow}(1 - \alpha_g) \quad (4.12)$$

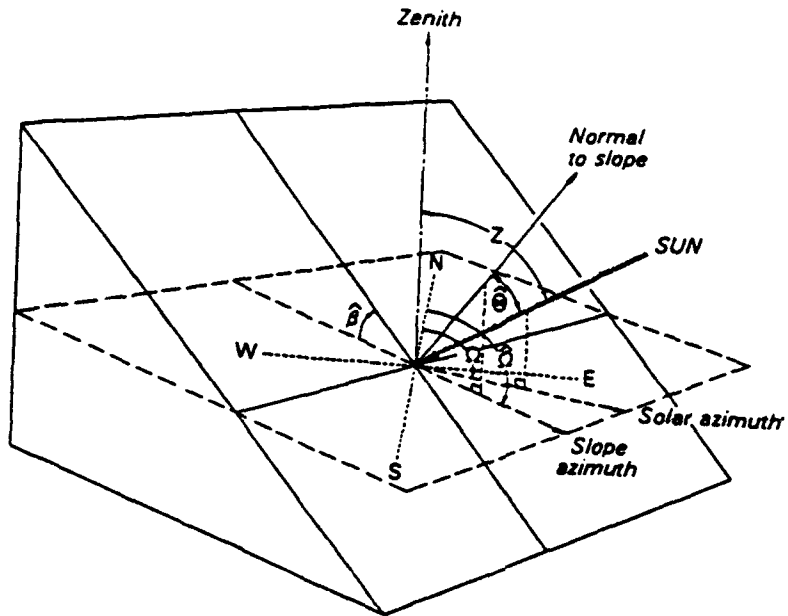
where,

$\alpha_g$  surface albedo, decimal.

$(1 - \alpha_g)$  absorptivity of the surface, decimal.

The reflected shortwave radiation,  $K_{\uparrow}$ , is therefore calculated:

$$K_{\uparrow} = K_{\downarrow} - K_{ab} \quad (4.13)$$



- $Z$  Solar zenith angle  
 $\beta$  Slope angle  
 $\Omega$  Solar azimuth angle  
 $\theta$  Angle of incidence (between the sun and the normal to the slope).

Figure 4.4. Geometry for solar beam irradiance of a sloping plane, Oke (1987).

#### 4.2.3 Calculation of the incoming longwave radiation, $L\downarrow$ .

The equation used to calculate incoming longwave radiation with clear skies,  $L\downarrow_{(o)}$ , is:

$$L\downarrow_{(o)} = \epsilon \sigma T_a^4 (c + b e_a^{0.5}) \quad (4.14)$$

where,

- $\epsilon$  emissivity, taken as 1.
- $\sigma$  Stefan-Boltzmann constant,  $0.813 \times 10^{-10}$ ,  $\text{cal cm}^{-2} \text{min}^{-1} \cdot \text{K}^4$
- $T_a$  shelter air temperature,  $^{\circ}\text{K}$
- b and c empirical constants,  $c=0.61$ ,  $b=0.05$ . These are the values calculated by Budyko as referenced by Sellers (1965) and are the most commonly used.
- $e_a$  water vapour pressure, millibars.

The value of  $e_a$  is obtained from Tetten's equation:

$$e_a = \text{RH} \times 6.108 \times \exp(AT_a) / (T_a + 273.15 - B) \quad (4.15)$$

where,

- RH relative humidity, decimal.
- A 17.269.
- B 35.86.

$L\downarrow_{(o)}$  is then modified for cloudy skies:

$$L\downarrow = L\downarrow_{(o)} (1 + \text{CIR} \times \text{CC}^2) \quad (4.16)$$

where,

- CIR coefficient dependent upon cloud type, see table 4.2.

#### 4.2.4 Calculation of the reflected longwave radiation, $L\uparrow$ .

The surface is treated as a grey body emitter, such that:

$$L\uparrow = \epsilon_g \sigma (T_g)^4 \quad (4.17)$$

where,

- $\epsilon_g$  emissivity of the ground.  
 $T_g$  current surface temperature as predicted by the model.

#### 4.2.5 Calculation of the sensible heat flux, $Q_c$ , and the latent heat flux, $Q_e$ .

The calculation of  $Q_c$  and  $Q_e$  follows the aerodynamic profile, sometimes called the flux-gradient, method which infers the fluxes on the basis of average profiles of atmospheric properties and the degree of turbulent activity.

Sensible heat flux,  $Q_c$ , is calculated using an equation slightly modified from Oke (1978):

$$Q_c = -\rho C_p k^2 z^2 \left( \frac{\Delta U \Delta \theta}{\Delta z \Delta z} \right) (\Phi_M \Phi_H)^{-1} \quad (4.18)$$

where,

- $\rho$  air density,  $\text{kgm}^{-3}$ .  
 $C_p$  specific heat of dry air at constant pressure,  $\text{Jkg}^{-1}\cdot\text{K}^{-1}$ .  
 $k$  von Karman's constant, 0.40.  
 $z$  observation height, m.  
 $U$  horizontal wind speed with respect to height  $z$ .  
 $\theta$  potential temperature,  $^{\circ}\text{K}$ .  
 $\Delta U/\Delta z$  partial derivative of wind speed with respect to height  $z$ .  
 $\Delta \theta/\Delta z$  partial derivative of potential temperature with respect to height  $z$ .  
 $\Phi_M \Phi_H$  dimensionless stability functions for momentum and heat, SCF.

Potential temperature,  $\theta$ , is defined by:

$$\theta = \frac{T_a(1000)^{0.286}}{P} \quad (4.19)$$

where,

$T_a$  air temperature, °K.  
 $P$  air pressure, mb.

Atmospheric stability is categorized using the Richardson Number,  $Ri$ . This is then used to determine SCF:

$$Ri = \frac{g}{\theta} \cdot \left( \frac{\Delta\theta}{\Delta z} \right) / \left( \frac{\Delta U}{\Delta z} \right)^2 \quad (4.20)$$

where,

$g$  acceleration due to gravity,  $ms^{-1}$ .  
 $\theta$  average potential temperature between the surface and height  $z$ , °K.

If  $Ri \leq 0$ ,  $SCF = 1.175(1 - 15Ri)^{0.75}$

If  $0 < Ri \leq 0.2$ ,  $SCF = (1.5Ri)^2$

If  $Ri > 0.2$ ,  $SCF = 0$ .

In TSTM  $\Delta\theta/\Delta z$  and  $\Delta U/\Delta z$  are approximated by first order differences and it is assumed that the air temperature at the surface equals the temperature of the surface and that the wind velocity at the surface is zero.

The latent heat flux,  $Q_e$ , is calculated using a similar equation based on Oke (1978):

$$Q_e = -\rho L_v k^2 z^2 \left( \frac{W \Delta q \Delta U}{\Delta z \Delta z} \right) SCF \quad (4.21)$$

where,

$L_v$  latent heat of vaporization,  $597.3 \text{ calg}^{-1}$ .  
 $W$  relative saturation of the top surface, decimal.  
 $q$  specific humidity,  $gg^{-1}$ .

The Richardson Number is used in the determination of SCF, as is the

calculation of  $Q_c$ .

#### 4.2.6 Calculation of the surface temperature and the solution of the heat flow equations.

The complicated nonlinear boundary conditions require that the heat conduction equation be solved numerically:

$$\frac{\partial T(z,t)}{\partial t} = \kappa(z) \frac{\partial^2 T(z,t)}{\partial z^2} \quad (4.22)$$

where,

- T      temperature, °K.
- z      depth, cm.
- t      time, min.
- $\kappa$       thermal diffusivity,  $\text{cm}^2\text{min}^{-1}$ .

Each layer is assumed to be homogeneous and it is assumed that the thermal characteristics, specifically the thermal conductivity and diffusivity, are constant.

##### 4.2.6.1 Solution within a layer.

An explicit scheme is employed within each layer to solve the one-dimensional heat equation. The temperature at time  $t+\Delta t$  given the temperature profile at time  $t$  at the node  $z$  is given by:

$$T(t+\Delta t, z) = T(t, z) + \kappa(\Delta t/\Delta z^2) [T(t, z+\Delta z) - 2T(t, z) + T(t, z-\Delta z)] \quad (4.23)$$

where,

- $\Delta t$       time increment.
- $\Delta z$       spatial increment.

Numerical stability requires that  $\kappa\Delta t/\Delta z^2 < 1/4$ . The problem of numerical stability is important for thin, highly conductive layers.

#### 4.2.6.2 Solution at the interface of two layers.

This is achieved by solving an explicit finite difference scheme which handles the interface between layers. It is assumed that there is perfect thermal contact at the interface i.e. continuity of the heat flux and temperatures at the interfaces. With reference to figure 4.5, let layer 1 have thermal conductivity  $k_1$ , and thermal diffusivity  $\kappa_1$ , and layer 2 have thermal conductivity and diffusivity  $k_2$  and  $\kappa_2$  respectively. Knowing the temperatures  $T_{i-1}$ ,  $T_i$  and  $T_{i+1}$  at time  $t$  and at the node points  $i-1$ ,  $i$  and  $i+1$ , the problem is to calculate the new temperature  $T(i,t+1)$ , or  $T'_i$ , at the interface.  $T_{i-1}$  is approximated by the truncated Taylor Series,

$$T_{i-1} = T_i - \Delta z_1 \left( \frac{\partial T}{\partial z} \right)_{i1} + \frac{\Delta z_1^2}{2} \left( \frac{\partial^2 T}{\partial z^2} \right)_{i1} \quad (4.24)$$

where,

$i1$  partial derivative in layer 1 at the interface.

Therefore,

$$\left( \frac{\partial^2 T}{\partial z^2} \right)_{i1} = \frac{2}{\Delta z_1^2} \left[ T_{i-1} - T_i + \Delta z_1 \left( \frac{\partial T}{\partial z} \right)_{i1} \right] \quad (4.25)$$

The first order approximation to  $\partial T / \partial t$  is given by:

$$\frac{\partial T}{\partial t} \Big|_{i1} = \frac{T'_i - T_i}{\Delta t} \quad (4.26)$$

Since  $\partial T / \partial t = \kappa_1 (\partial^2 T / \partial z^2)$ , by substituting into equation 4.26:

$$\frac{T'_i - T_i}{\Delta t} = \frac{2\kappa_1}{\Delta z_1^2} \left[ T_{i-1} - T_i + \Delta z_1 \left( \frac{\partial T}{\partial z} \right)_{i1} \right] \quad (4.27)$$

Equation 4.27 assumes  $k_1$  of unity and if multiplied by  $k_1$ , and divided by  $\Delta z_1$  results in:

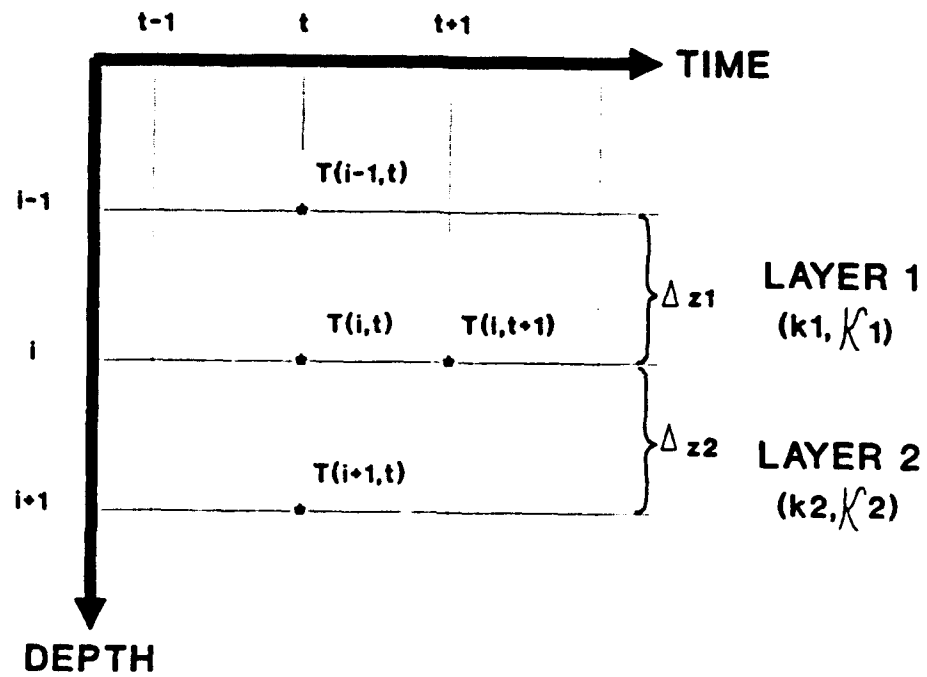


Figure 4.5. Finite difference grid used by TSTM and SNOMO, adapted from Balick *et al.* (1981a).

$$\frac{k_1 \Delta z_1^2}{2\kappa_1 \Delta z_1} \left[ \frac{T'_i - T_i}{\Delta t} \right] - \frac{k_1 T_{i-1}}{\Delta z_1} + \frac{k_1 T_i}{\Delta z_1} = k_1 \left( \frac{\partial T}{\partial z} \right)_{i1} \quad (4.28)$$

Equation 4.28 rearranged results in:

$$k_1 \left( \frac{\partial T}{\partial z} \right)_{i1} = \frac{k_1}{2\Delta z_1 \kappa_1 (\Delta t / \Delta z_1^2)} (T'_i - T_i) - \frac{k_1 T_{i-1}}{\Delta z_1} + \frac{k_1 T_i}{\Delta z_1} \quad (4.29)$$

Similarly for layer 2:

$$k_2 \left( \frac{\partial T}{\partial z} \right)_{i2} = \frac{-k_2}{2\Delta z_2 \kappa_2 (\Delta t / \Delta z_2^2)} (T'_i - T_i) + \frac{k_2 T_{i+1}}{\Delta z_2} - \frac{k_2 T_i}{\Delta z_2} \quad (4.30)$$

Continuity of the heat flux implies that equation 4.29 = 4.30.

Therefore after simplification the final equation used to calculate  $T'_i$  is:

$$\left[ \frac{k_1}{2\Delta z_1 \kappa_1 (\Delta t / \Delta z_1^2)} + \frac{k_2}{2\Delta z_2 \kappa_2 (\Delta t / \Delta z_2^2)} \right] T'_i = \left[ \frac{k_1}{2\Delta z_1 \kappa_1 (\Delta t / \Delta z_1^2)} \right. \\ \left. + \frac{k_2}{2\Delta z_2 \kappa_2 (\Delta t / \Delta z_2^2)} \right] T_i + \frac{k_1}{\Delta z_1} T_{i-1} - \left( \frac{k_1}{\Delta z_1} + \frac{k_2}{\Delta z_2} \right) T_i + \frac{k_2}{\Delta z_2} T_{i+1} \quad (4.31)$$

#### 4.2.6.3 Solution at the upper boundary.

The new or updated value of the surface temperature  $T(t+\Delta t, 0)$  is calculated by solving the surface heat balance equation for the surface temperature  $T_g$ . The heat balance equation is:

$$K^* + L^* + Q_c + Q_e + G = 0 \quad (4.34)$$

where,

G heat flux into the surface from below the surface.

$$G = k(\partial T / \partial z) \quad (4.35)$$

where,

$k$  thermal conductivity of the surface layer.

$G$  is approximated by:

$$G = k \left( \frac{T_1 - T_g}{\Delta z} \right) \quad (4.36)$$

where,

$T_1$  temperature at the present time for the first node point below the surface.

Letting  $D = K^* + L\downarrow + Q_c + Q_e$  the heat balance equation becomes:

$$-\epsilon\sigma T_g^4 + k \left( \frac{T_1 - T_g}{\Delta z} \right) + D = 0 \quad (4.37)$$

or upon rewriting,

$$T_g^4 - \frac{kT_1}{\epsilon\sigma\Delta z} + \frac{kT_g}{\epsilon\sigma\Delta z} - \frac{D}{\epsilon\sigma} = 0 \quad (4.38)$$

The function  $F$  is defined by:

$$F(T_g) = T_g^4 + \frac{k}{\epsilon\sigma\Delta z} T_g - \left( \frac{kT_1 + D\Delta z}{\epsilon\sigma\Delta z} \right) \quad (4.39)$$

The updated surface temperature is a root of  $F$ . The Newton-Raphson algorithm has been employed to locate a value of  $T_g$  such that  $F$  vanishes. The derivative of  $F$  with respect to  $T_g$  is needed to employ the Newton-Raphson scheme:

$$\frac{dF(T_g)}{dT_g} = 4T_g^3 + \frac{k}{\epsilon\sigma\Delta z} - \frac{dD/dT_g}{\epsilon\sigma} \quad (4.40)$$

$dD/dT_g$  is approximated by:

$$\frac{dD}{dT_g} = \frac{(D_N - D_0)}{-\Delta T} \quad (4.41)$$

where,

- $D_N$  value of D using the latest estimate of  $T_g$ .  
 $D_0$  value of D obtained by using the previous estimate of  $T_g$ .  
 $\Delta T$  change in temperature.

The starting value for the scheme is taken to be the surface temperature at the previous time step. It appears that three to five iterations yield satisfactory convergence to the new surface temperature.

#### 4.2.6.4 Solution at the bottom boundary.

The bottom boundary condition is the heat flux through the bottom of the lowest layer. TSTM allows for one of the following three options:

- Option 1: A constant temperature at the bottom boundary.  
 Option 2: A constant heat flux at the bottom boundary.  
 Option 3: A constant heat flux at the bottom boundary and an additional constant temperature radiating surface below the bottom boundary.

Option 3 requires additional input data: (i) bottom boundary thermal IR emissivity, (ii) bottom boundary geometric shape factor, (iii) under surface thermal IR emissivity, (iv) under surface geometric shape factor; and (v) under surface temperature. The bottom boundary condition is kept constant in time regardless of the option chosen. Option 1 results in a straightforward boundary condition, but for options 2 and 3 it is required that the following equation be satisfied:

$$R\downarrow - G - R\uparrow - D = 0 \quad (4.42)$$

where,

- R<sub>↓</sub>** radiative energy loss through bottom boundary.  
**G** heat flux into lower surface.  
**R<sub>↑</sub>** radiative energy from constant temperature radiating surface below the bottom boundary.  
**D** constant heat flux at the bottom boundary.

G is given by:

$$G = k \left( \frac{\partial T}{\partial x} \right) \quad (4.43)$$

where,

**k** thermal conductivity of the bottom layer.

and is approximated by:

$$G = k \left( \frac{T_B - T_1}{\Delta z} \right) \quad (4.44)$$

where,

**T<sub>B</sub>** temperature of the bottom surface.

**T<sub>1</sub>** temperature of the first node point above the bottom surface.

Substitution into equation 4.42 results in:

$$\epsilon_B \sigma b_{kB} T_B^4 - k \left( \frac{T_B - T_1}{\Delta z} \right) - \epsilon_R \sigma b_{kR} T_R^4 - D = 0 \quad (4.45)$$

where,

**ε<sub>B</sub>** bottom boundary thermal IR emissivity.

**b<sub>kB</sub>** bottom geometric shape factor.

**ε<sub>R</sub>** under surface thermal IR emissivity.

**b<sub>kR</sub>** under surface geometric shape factor.

**T<sub>R</sub>** under surface temperature.

Equation 4.45 is solved by employing the Newton-Raphson iterative scheme.

**4.3 The calculation of the energy budget components of a snowpack beneath a vegetation canopy as derived from the VEGIE submodel.**

VEGIE, the vegetation submodel of the TSTM, is used in SNOMO to calculate the energy budget components of a snowpack at the forest floor and the surface and internal temperatures of that pack. VEGIE, Balick *et al.* (1981b) is an adaptation of work by Deardorff (Deardorff, 1978). The foliage and ground energy budget equations, treatment of the foliage cover, sensible and latent heat transfer equations and techniques for solving and interpolating parameters according to the degree of vegetative cover are taken directly from Deardorff (1978). The derivation of the primary equations is given below. The derivation of some of the components of these equations is complex and for the purposes of clarity these are contained in appendix A.

**4.3.1 Calculation of the foliage energy budget,  $F_f$ .**

The equation to calculate the foliage energy budget,  $F_f$ , is taken directly from Deardorff (1978):

$$F_f = \sigma_f \{ [(1 - \alpha_f)S] + \epsilon_f R_{st} + R_n \} - H_f - E_f \quad (4.46)$$

where,

- $\sigma_f$  foliage cover fraction, decimal.
- $\alpha_f$  foliage albedo, decimal.
- $\epsilon_f$  foliage emissivity, decimal.
- $R_n$  combined net thermal IR term for the interaction between the foliage, ground and their loss to the sky,  $\text{cal cm}^{-2} \text{min}^{-1}$ .
- $R_{st}$  incoming longwave radiation from the sky ( $L\downarrow$ ),  $\text{cal cm}^{-2} \text{min}^{-1}$ .
- $S$  incoming solar radiation ( $K\downarrow$ ),  $\text{cal cm}^{-2} \text{min}^{-1}$ .
- $H_f$  foliage sensible heat flux,  $\text{cal cm}^{-2} \text{min}^{-1}$ .

$E_f$  foliage latent heat loss to atmosphere,  $\text{cal cm}^{-2} \text{min}^{-1}$ .

$R_n$  is a function of the foliage and ground emissivities ( $\epsilon_f$ ,  $\epsilon_g$ ) and temperatures ( $T_f$ ,  $T_g$ ). The parameters  $\alpha_f$ ,  $\sigma_f$ ,  $\epsilon_f$ ,  $\epsilon_g$  are inputs to the model.  $S$  and  $R_g \downarrow$  are calculated by the TSTM.  $T_g$  is the ground temperature estimate from the previous time step and  $T_f$  is determined by the root-finding algorithm. Sensible heat transfers from the foliage are primarily functions of temperature, wind speed and vapour pressure differences between the foliage or the air adjacent to it and the air at the instrument shelter height. Energy storage and conduction by the foliage are neglected.

Five foliage input parameters are required for VEGIE:

- (1) Foliage cover fraction,  $\sigma_f$ , (0-1).

This describes the density of the vegetation cover and is an area average shielding factor associated with the degree to which the foliage prevents shortwave radiation from reaching the ground.  $\sigma_f=0$  represents no foliage, no shielding and  $\sigma_f=1$  represents complete radiative blocking. Table 4.3 shows various limiting values of  $\sigma_f$  taken from Geiger (1965) and Deardorff (1978) for various vegetation covers. Table 4.3 shows only limiting values between which  $\sigma_f$  will vary, because the individual composition of each stand will affect the value of  $\sigma_f$ .  $\sigma_f=0.16$  is the threshold value for forest-floor plant growth. If less than 16% of the outside light is able to penetrate the canopy the forest floor will remain dead, mosses can colonize at  $\sigma_f$  values of 0.16-0.18. It is assumed that  $\sigma_f$  does not vary with the sun zenith or azimuth angle.  $\sigma_f$  can be roughly related to the Leaf Area Index (LAI) for ground vegetation by:

$$\sigma_f = \text{LAI} + 7 \quad (4.47)$$

- (2) State of vegetation,  $\chi$ , (1-1000).

$\chi$  is used as a multiplier of the stomatal resistance function

in VEGIE. A summer value, when the vegetation is healthy and active, is 1, a winter and therefore dormant or dead vegetation cover value is 1000. Other values can be chosen to adjust stomatal resistance for moisture stress, senescence or other factors.

- (3) Foliage emissivity,  $\epsilon_f$ , (0-1).
- (4) Foliage albedo,  $\alpha_f$ , (0-1).
- (5) Foliage height,  $z_f$ , (cm).

All of the radiant energy terms of the foliage energy budget, equation 4.46, are weighted by  $\sigma_f$ . The turbulent transfer terms  $H_f$  and  $E_f$  are not weighted but are calculated for a unit of ground area (the one exception is in the determination of the value for the canopy resistance to water vapour diffusion for the  $\epsilon_f$  term, appendix AIII, which assumes that the exchange takes place directly between the foliage and the air above it). Equation 4.46 is solved for the value of  $T_f$  that makes  $F_f=0$ .

#### 4.3.2 Calculation of the ground energy budget, $F_g$ .

The equation to calculate the ground energy budget,  $F_g$ , is:

$$F_g = (1-\sigma_f)[(1-\alpha_g)S] + R_{g\downarrow} - R_{g\uparrow} - H_g - E_g - G \quad (4.48)$$

where,

- $\alpha_g$  albedo of the surface material (snow), decimal.
- $R_{g\downarrow}$  downward longwave radiation flux at the snow surface,  $\text{calcm}^{-2}\text{min}^{-1}$ .
- $R_{g\uparrow}$  Upward directed longwave radiation flux at the snow surface,  $\text{calcm}^{-2}\text{min}^{-1}$ .
- $H_g$  sensible heat flux at the snow surface,  $\text{calcm}^{-2}\text{min}^{-1}$ .
- $E_g$  latent heat loss to the atmosphere at the snow surface,  $\text{calcm}^{-2}\text{min}^{-1}$ .
- $G$  conduction of heat in top soil layer,  $\text{calcm}^{-2}\text{min}^{-1}$ .

The energy budget components, with the exception of  $G$ , are adjusted for foliage density. Insolation is simply multiplied by  $(1 - \sigma_f)$ , the adjustments for the remaining components are more complex and are contained in appendix A. Terms for the incoming and outgoing longwave radiation,  $R_g^\downarrow$  and  $R_g^\uparrow$ , are functions of  $T_g$ ,  $T_f$ ,  $\epsilon_g$ ,  $\epsilon_f$  and  $R_s^\downarrow$ , the terms include reflection. The turbulent transfer at the ground is calculated per unit area but is buffered by the layer of vegetation and is therefore a function of  $\sigma_f$ . The turbulent transfer also occurs between the ground and the air within the foliage layer which is an arbitrary mixture of conditions at the ground, foliage, and air at shelter height. Conduction,  $G$ , is calculated as in the TSTM. The root-finding algorithm is used to find the value of  $T_s$  that makes  $F_s=0$ .

#### 4.3.3 The root-finding algorithm.

The root-finding algorithm is used to find the temperatures  $T_f$  or  $T_g$ , for which the sum of the energy budget components is zero (or within a specified range from zero). When solved for temperature the energy budgets are fourth order equations, however Balick *et al.* (1981b) showed that there was only one real and reasonable root given realistic conditions. Therefore, a very simple algorithm was adapted for VEGIE and is called the regula falsi technique.

Figure 4.6 illustrates the steps in the algorithm. An initial guess of temperature  $T$  is made which is unrealistically low,  $200^\circ\text{K}$  for example, such as point A, figure 4.6a. The energy budget,  $F=f(T)$ , is evaluated here and its sign determined.  $F$  is reevaluated at progressively higher temperatures at regular steps (say  $5^\circ\text{K}$ ) until the sign of  $F$  changes. Points A and B in figure 4.6b are determined. The intercept of a straight line between points  $f(A)$  and  $f(B)$  is found which is point C in figure 4.6c. Then  $f(A)$  becomes  $f(C)$ , a new line between  $f(A)$  and  $f(B)$  is determined, a new intercept is found (figure 4.6d) and so on until  $F$  is less than some assigned value ( $F \leq 0.001$  for VEGIE).

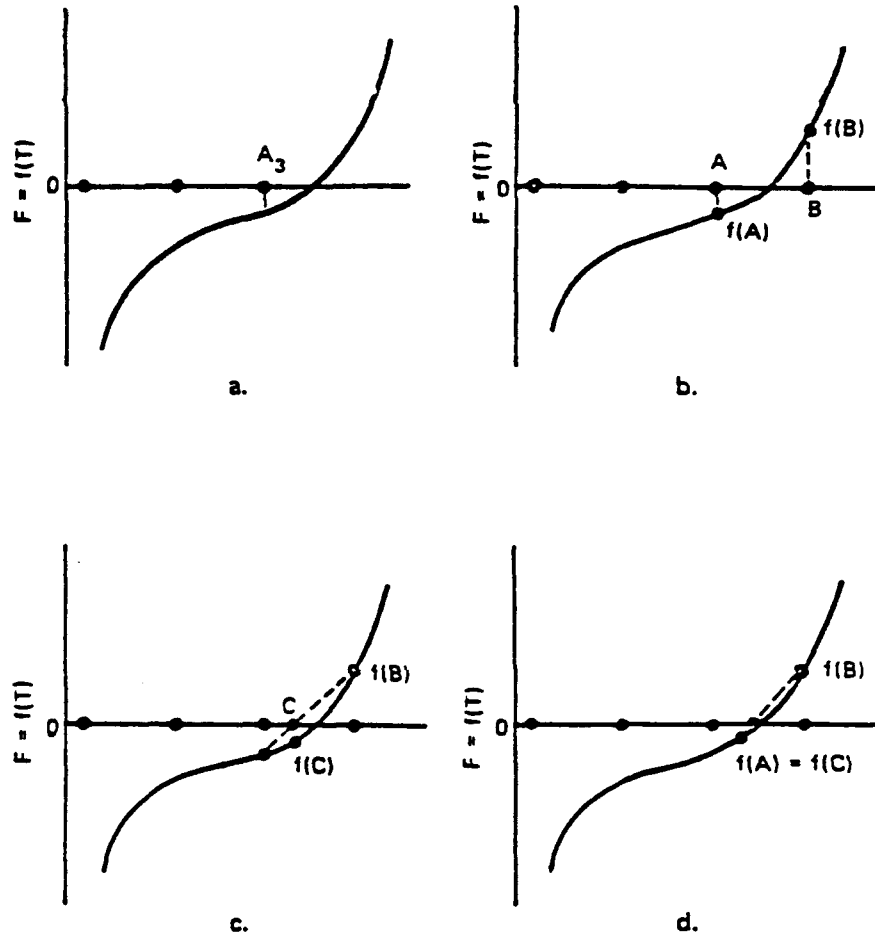


Figure 4.6. Schematic representation of the root-finding algorithm (*regula falsi*), Balick et.al. (1981b).

#### 4.3.4 Calculation of effective temperature.

The simplest method for combining ground and vegetation temperature would be a simple average weighted by the foliage cover:

$$T = \sigma_f T_f + (1 - \sigma_f) T_g \quad (4.49)$$

However, when temperatures are observed radiometrically, it is more appropriate to mix the radiant exitance from the two materials and solve for temperature as follows:

$$T = [\sigma_f \epsilon_f T_f^4 + (1 - \sigma_f) \epsilon_g T_g^4]^{0.25} \quad (4.50)$$

The report, Balick *et al.* (1981b), emphasises that effective temperature is the primary product of the TSTM/VEGIE system. In the adaptation of TSTM/VEGIE for SNOMO the energy budget components of the ground surface are the primary product followed by the effective temperatures of the ground surface.

#### 4.3.5 Mixed emissivities.

When a simple foliage layer partially covers a soil surface, a sensor receives longwave radiation emitted from both in proportion to the amount of cover, their emissivities and their temperatures. The sensor also receives longwave radiation reflected by the surface materials from the sky and the surroundings. Radiation from the sky and this reflection varies mainly with atmospheric temperature and water vapour and clouds and is then time-dependent. Varying mixtures of emissivity also effect energy fluxes and transformations to some extent. Therefore, the effects of emissivity mixtures within a scene element can be a critical issue on signature prediction and analysis. VEGIE deals with this in two ways. First, a single arbitrary case is presented where only foliage cover and ground emissivity are varied. Secondly VEGIE is used to examine the more complex case where

environmental conditions and energy budget changes are considered.

The longwave radiation emitted per unit time and area,  $W_t$ , for a surface composed of foliage and ground is:

$$W_t = \sigma_f \epsilon_f \sigma T_f^4 + (1 - \sigma_f) \epsilon_g \sigma T_g^4 \quad (4.51)$$

For a greybody near thermal equilibrium, longwave radiation reflectivity is  $(1 - \epsilon)$ . Therefore, a sensor pointed down at a grass/ground surface would receive emitted and reflected radiation from the surface. Ignoring multiple reflection and atmospheric, spectral and directional effects, this quantity is:

$$W_t = \sigma_f \epsilon_f \sigma T_f^4 + (1 - \sigma_f) \epsilon_g \sigma T_g^4 + (1 - \sigma_f)(1 - \epsilon_g) \epsilon_a \sigma T_a^4 + \sigma_f(1 - \epsilon_f) \epsilon_a \sigma T_a^4 \quad (4.52)$$

Here the subscript a indicates values for the atmosphere.  $W_t$ , from equations 4.51 and 4.52 can be converted to average temperature with:

$$T = \left( \frac{W_t}{\sigma} \right)^{0.25} \quad (4.53)$$

Tests performed on VEGIE demonstrated the importance of the inclusion of reflection. Effective temperatures as a function of foliage cover with different soil emissivities and with/without reflection were considered. If reflection was not considered, an uncertainty of 0.04 in  $\epsilon_g$  results in a 4°C error in T at  $\sigma_f=0$  and about 1.5°C at  $\sigma_f=0.5$  and is small above  $\sigma_f=0.8$ . Errors of emissivity affect the reflection terms in the opposite direction which greatly reduces the net effect. Errors caused by ignoring reflection in this case are greater than 5°C for  $\epsilon_g < 0.92$  at  $\sigma_f=0$ , greater than 3°C at  $\sigma_f=0.5$ , and always greater than 1°C. Treating bare ground as a blackbody ( $\epsilon_g=1$  and no reflection) results in an error of 8.5°C.

#### 4.4 The calculation of melt.

The calculation of melt utilizes the energy budget variables  $Q^*$ ,  $Q_c$ ,  $Q_e$  and  $Q_g$  that are calculated by the TSTM/VEGIE subroutine. In order to solve the snowpack energy budget (equation 1.10, chapter 1) for  $\Delta Q_m$  the energy budget variables for the energy introduced to the pack by the rain,  $Q_p$ , (Male & Granger, 1978) and the change in internal energy of the snowpack,  $\Delta Q_s$ , (Anderson, 1976) also have to be calculated. The melt rate is derived from  $\Delta Q_m$  and is calculated in snow and water equivalent units using an equation from Oke (1987). The ability to model  $Q_g$  by TSTM has been described in section 4.2.6.4. However, at present, SNOMO assumes that  $Q_g$  is zero. This is in order to simplify the modelling conditions.

##### 4.4.1 Calculation of the energy introduced into the snowpack by rainfall, $Q_p$ .

The heat transferred to the snow by rainwater is the difference between its energy content before falling on the snow and its energy upon reaching thermal equilibrium within the pack. The thermal state of the pack (at or below 0°C) determines whether the energy produced by the rain causes melt or an increase in pack temperature. The energy produced when rain falls onto a melting pack, where the rainwater does not freeze, is expressed by:

$$Q_p = \rho_w C_{p_w} (T_p - T_{sn}) P / 1000 \quad (4.54)$$

where,

- $Q_p$  energy introduced into the pack by rainfall,  $\text{kJm}^{-2}\text{day}^{-1}$ .
- $\rho_w$  density of water,  $\text{kgm}^{-3}$ .
- $C_{p_w}$  specific heat of water,  $\text{kJkg}^{-1}\cdot\text{C}^{-1}$ .
- $T_p$  temperature of the rain, °C.
- $T_{sn}$  temperature of the snow, °C.
- $P$  precipitation rate,  $\text{mmday}^{-1}$ .

The specific heat of water is  $4.18 \times 10^3 \text{ Jkg}^{-1} \cdot \text{C}^{-1}$ , Oke(1978). The temperature of the rain is assumed to be equal to the air temperature ( $T_p = T_a$ ) and the snowpack is melting therefore  $T_{sn} = 0^\circ\text{C}$ . The working equation for the calculation of  $Q_p$  ( $\text{MJm}^{-2}\text{day}^{-1}$ ) in SNOMO is therefore:

$$Q_p = [(\rho_w C_p T_a P) / 1000] / 1000 \quad (4.55)$$

Equation 4.55 is taken from Male & Granger (1978).

#### 4.4.2 Calculation of the snowpack internal energy change, $\Delta Q_s$ .

Snowpack internal energy change,  $\Delta Q_s$ , is calculated from Anderson (1976):

$$\Delta Q_s = (d \rho_{sn})_t [(C_{p_i} T_{sn})_{t+\Delta t} - (C_{p_i} T_{sn})_t] \quad (4.56)$$

where,

- $\Delta Q_s$  snowpack internal energy change,  $\text{MJm}^{-2}\text{day}^{-1}$ .
- $d$  depth of snowpack, m.
- $\rho_{sn}$  density of snow,  $\text{kgm}^{-3}$ .
- $C_{p_i}$  specific heat of ice,  $\text{MJkg}^{-1} \cdot \text{K}^{-1}$ .
- $T_{sn}$  snow temperature,  $^\circ\text{K}$ .
- $t$  time unit, one day.

The specific heat of ice is  $0.0021 \text{ MJkg}^{-1} \cdot \text{K}^{-1}$  and the density of water is  $1000 \text{ kgm}^{-3}$ . The average density of the snowpack is used and is calculated to allow for the varying proportions of different snow densities (this is discussed further in section 4.5).

#### 4.4.3 Calculation of the meltrate, $\Delta r$ .

The snowpack energy budget equation can now be solved for  $\Delta Q_m$ :

$$\Delta Q_m = Q^* + Q_c + Q_e + Q_p + Q_g - \Delta Q_s \quad (4.57)$$

The meltrate,  $\Delta r$ , can then be calculated either in snow ( $\Delta r_{sn}$ ) or water equivalent ( $\Delta r_w$ ) units, Oke (1987):

$$(1) \quad \Delta r_{sn} = \frac{\Delta Q_m}{L_f \rho_{sn}} \cdot 100 \quad (4.58a)$$

where,

$\Delta r_{sn}$  meltrate, cm snow day<sup>-1</sup>.

$\Delta Q_m$  net latent heat storage change due to melting or freezing, MJm<sup>-2</sup>day<sup>-1</sup>.

$L_f$  latent heat of fusion, MJkg<sup>-1</sup>.

$\rho_{sn}$  density of snow, kgm<sup>-3</sup>.

$$(2) \quad \Delta r_w = \frac{\Delta Q_m}{L_f \rho_w} \cdot 1000 \quad (4.58b)$$

where,

$\Delta r_w$  meltrate, mm water equivalent day<sup>-1</sup>.

$\rho_w$  density of water, kgm<sup>-3</sup>.

The volume of meltwater generated for each cell can be calculated by multiplying  $\Delta r_w$  by the cell area.

#### 4.5 The snowpack control programme.

The snowpack control programme is responsible for the modelling of snowpack dynamics at a point and ultimately spatially. The modelling of the snowpack dynamics at a point are discussed in this section. Chapter 5 discusses the modelling of snowpack dynamics over an area. The control programme is original to SNOMO.

##### 4.5.1 Snowpack characteristics and structure.

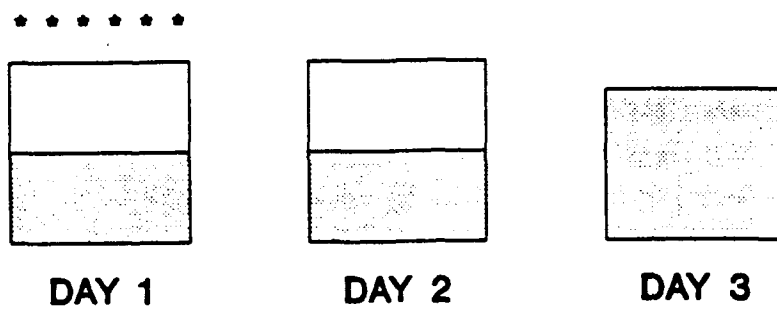
SNOMO simplifies the snowpack into either a two-layered or one-layered structure. The snow layers are composed of either 'old' or 'new' snow, with both the 'old' and 'new' snow possessing specific values of the physical characteristics of emissivity, albedo, density, thermal conductivity and thermal diffusivity, see table 4.4. The values shown in table 4.4 are extreme values, for example the albedo of freshly fallen, mid-winter snow in comparison to the albedo of spring snow on a forest floor. When the pack is two-layered and the snow density of the whole pack is required, for example in equations 4.58a & b the proportion of each density is calculated using the knowledge of the thickness of each layer. An average density is calculated from this. Therefore, for each day the total height of the snowpack, the depth, and the thickness of each layer has to be calculated. The depth of the snowpack will change due to snowfall, snowmelt, or density changes resulting in compacting of the pack. Snowfall or snowmelt is either addition to or subtraction from the pack. Compacting changes are modelled when snowfall patterns result in a conversion of a 'new' snow layer (low density) into an 'old' snow layer (high density). This is part of the process of snow metamorphosis. In SNOMO compacting of the snowpack is modelled on the day after a day with no snowfall. This is demonstrated by the two modelling scenarios shown in figure 4.7. In both figures 4.7a and 4.7b the initial pack structure is two-layered with the 'new' snow layer above the 'old' snow layer. In figure 4.7a no snow falls

Table 4.4. Values used in SNOMO for the physical characteristics of snow.

	NEW SNOW	OLD SNOW
DENSITY ( $\text{gcm}^{-3}$ )	0.10	0.48
ALBEDO (decimal)	0.95	0.40
EMISSIVITY (decimal)	0.82	0.99
THERMAL DIFFUSIVITY ( $\text{cm}^2\text{min}^{-1}$ )	0.06	0.24
HEAT CONDUCTIVITY ( $\text{calcm}^{-2}\text{min}^{-1}\cdot\text{K}^{-1}$ )	0.03	0.08

Sources: Oke (1987), Balick et. al. (1981a) and Grey & Male (1981)

(a)



(b)

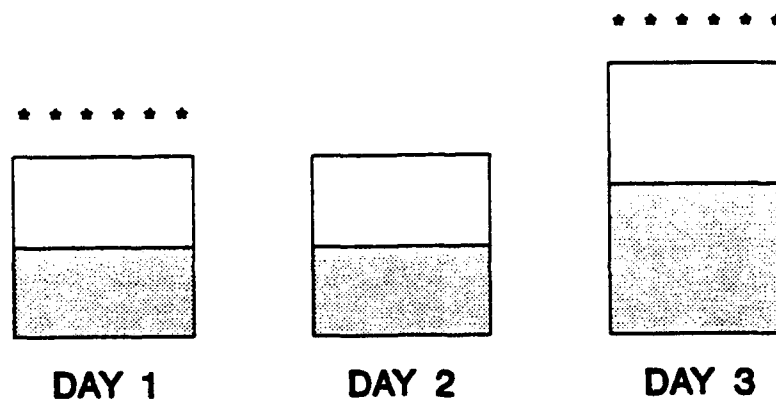
 OLD SNOW NEW SNOW

Figure 4.7. Modelling scenarios demonstrating compaction by SNOMO.

on day 2 and therefore the 'new' snow present on day 2 is compacted to form 'old' snow on day 3. There is no snowfall on day 3 and the resultant pack has a one-layered structure consisting of all 'old' snow. In figure 4.7b compaction on day 3 is identical to the situation in figure 4.7a. However, a snowfall on day 3 results in a two-layered pack structure with the freshly fallen snow as the upper 'new' snow layer.

Additions to snowdepth, by snowfall are modelled before any subtraction from the depth, by snowmelt. This is for ease of computation because over the season there are usually more days with snowfall than snowmelt. Addition and subtraction of snow from the pack causes changes in the pack depth and layering structure and therefore in pack density. The effect of these changes will vary depending on their timing. Snowfall on consecutive days is treated as the same snowfall event and therefore will form one 'new' snow layer. Snowmelt is subtracted from the surface down through the pack and uses snowmelt calculated in centimetres of snow. For example, in a two-layered pack with a 'new' snow layer thickness of 10cm and an 'old' snow layer thickness of 30cm the snowmelt is calculated (using an average density) as 5cm of snow. This 5cm is then subtracted from the surface of the pack reducing the thickness of the 'new' snow layer to 5cm. If the snowmelt depth was 15cm the resultant pack would have a one-layered 'old' snow structure and a depth of 25cm.

SNOMO requires an initial snowpack depth and structure with temperatures at the layer boundaries. The initial profile can be approximated if necessary, a simplification is required to produce a one- or two-layered pack in any case. The start conditions for SNOMO that are in use at present are a known depth. The pack is said to be two-layered with a 'new' snow layer 5cm thick, the remaining depth is 'old' snow. TSTM requires the temperatures at the layer boundaries. The temperatures at the surface and at the one/two-layer boundary are taken as equal to the air temperature and the base temperature is taken as  $-1^{\circ}\text{C}$  in the open and  $-10^{\circ}\text{C}$  under coniferous forest (these are premelt temperatures for the New England environment). Once

initiated TSTM calculates the subsequent temperatures. TSTM also requires the degree of saturation of the snow,  $W$ , expressed as a decimal. This is used in the calculation of  $Q_e$ . The use of  $W$  in SNOMO is simplified to 1 if melt is occurring and 0 if melt is not occurring.

To summarise, SNOMO calculates snow precipitation and adds this to the pack in the first iteration, then calculates the energy budget of the pack and any resultant melt, adds any snowfall to the pack or compresses the pack due to lack of snowfall, subtracts any snowmelt and makes the relevant structural and physical characteristic changes. SNOMO then returns and calculates the energy budget for the following day.

#### 4.5.2 The input file.

The input file consists of four groups of data. These are data describing the physical characteristics of the snowpack or soil, topographical data, meteorological data and a miscellaneous data group. An example of an input file is given in Volume 2 of this report. The input data required for the operation of SNOMO is shown in table 4.5 and is discussed in more detail below:

- (1) Data describing the physical characteristics of the snowpack or soil. This is, as discussed in section 4.5.1, physical data for both 'old' and 'new' snow. The characteristics are thermal conductivity, thermal diffusivity, emissivity, albedo and density. The characteristics for a sandy soil are also included and the depth of the soil profile. The soil characteristics are largely redundant and therefore their accuracy is not important (as long as reasonably realistic values are chosen from the literature). The depth of the soil profile is set to one metre. The initial snowdepth is also input. The derivation of the initial snowdepth is based on the relationship between snowdepth, vegetation cover type and

Table 4.5. SNOMO operational data requirements.

Instrument shelter height  
Latitude

For each cell:

Air pressure  
Air temperature (maximum and minimum)\*  
Cloud cover amount\*  
Cloud cover type  
Elevation  
Initial snowdepth  
Julian day  
Precipitation amount  
Relative humidity\*  
Slope angle  
Slope aspect  
Snow/soil density  
Snow/soil surface absorptivity  
Snow/soil surface emissivity  
Snow/soil heat conductivity  
Snow/soil thermal diffusivity  
Soil depth  
Wind speed\*

For a vegetated cell:

Foliage albedo  
Foliage cover fraction  
Foliage emissivity  
Foliage height  
State of vegetation

\* daily input data

elevation. This is discussed in chapter 7 and is a result of the field programme discussed in chapter 6. The initial temperature profile is also input, see section 4.5.1.

- (2) Topographic data. This is the latitude of the catchment, slope aspect, slope angle and area of the cell. Slope aspect is input as from the south, therefore south=0°, north=180°, east=-90° and west=+90°.
- (3) Meteorological data. The atmospheric pressure and the cloud type are input as constants. The air temperature (°C), relative humidity (%), cloud cover (tenths), wind speed ( $\text{ms}^{-1}$ ) and precipitation (mm water equivalent) are input as daily values with their corresponding Julian date and time of observation (usually 1100 hours). The daily values of air temperature, wind speed, relative humidity and cloud cover are interpolated over 24 hours to obtain a value at the desired computational interval (5 minutes). Air temperature is input as a daily maximum and minimum. The maximum temperature is assumed to occur at 1400 hours. This is to allow a more realistic interpolation of the temperatures over the 24 hour period.
- (4) Miscellaneous data. This is the Julian date of the first day modelled, observation height, cell number, simulation year, critical snowdepth (that is the depth of snow below which no snow is said to be present), the calling of the vegetation data file and the use of a lapse rate term on air temperatures.
- (5) Lapse rate option. If required the air temperatures can be amended to allow for the effects of elevation change on air temperatures. The amendment is performed within SNOMO using a given lapse rate term. A lapse rate is chosen relating to the environment SNOMO is modelling. The lapse rate that is currently in use is that for the New England environment.

SNOMO could be modified so that lapse rate could be input as a variable in the input file, this is at present not required and has therefore been omitted due to time constraints. The New England lapse rate in use is taken from Hendrick *et al.* (1971). Hendrick *et al.* (1971) divided the New England environment into four elevation zones:

- 660-1000 ft.
- 1000-1500 ft.
- 1500-2000 ft.
- 2000-2500 ft.

The daily air temperature decreased by 1.5°F and the maximum daily temperature decreased by 2°F with every change to a higher elevation zone. Therefore the daily minimum temperature decreases 1°F with every change to a higher elevation zone. An indicator of the relative elevation point in relation to the point data source (the meteorological station) is contained in the input file and this enables the corresponding increase or decrease in temperatures to be calculated.

- (6) Vegetation option. This activates VEGIE if the operator requires. Three vegetation types are currently available: open, coniferous woodland and deciduous woodland. A data file containing the vegetation parameters  $\sigma_f$ ,  $\chi$ ,  $\epsilon_f$ ,  $\alpha_f$  and  $z_f$  as discussed in section 4.3 is called. SNOMO is at present using values for the New England forests and environment, table 4.6. The values are median values as obviously  $\sigma_f$  and  $\alpha_f$  will vary with the individual tree and stand characteristics. 'Open' refers to pastureland and clear-cut and the forest types refer to New England species. The situation in, for example, the Rocky Mountains (Colorado) would be Alpine pasture, Ponderosa Pine and Aspen. Clear-cut that is less than five years old is, at present, modelled as 'open'. VEGIE is activated for the two forest types and the open situation is modelled without VEGIE. If mixed woodland is present then intermediate values can be

Table 4.6. Vegetation input values used in SNOMO (for the New England environment).

VARIABLE	VEGETATION TYPE		
	DECIDUOUS	MIXED	CONIFEROUS
$\sigma_f$	0.50	0.60	0.70
$\chi$	1000.00	1000.00	1000.00
$\epsilon_f$	0.97	0.975	0.98
$\alpha_f$	0.15	0.125	0.10
$z_f$	2000.00	2000.00	2000.00

used and a separate 'mixed woodland' file created. Alternatively if the woodland is predominantly one type then the input file for the dominant species is used.

#### 4.6 Discussion.

The equations and algorithms described above make various assumptions about the snowpack environment. The primary assumptions are:

- (1) That the slope, aspect, elevation and vegetation cover are homogeneous within each computational cell.
- (2) That there is no lateral movement of meltwater and heat through the snowpack and no meltwater movement via the snowpack and soil to the outflow stream.
- (3) That  $Q_g$  is zero.
- (4) That the snowpack has a one- or two-layered structure.
- (5) That all the incoming solar radiation is direct.
- (6) That the threshold temperature for the occurrence of snow or rain is  $0^{\circ}\text{C}$ .
- (7) That there is no interception by the vegetation canopy.
- (8) That snow accumulation is related simplistically to vegetation cover and elevation.

It would be possible to modify many of these assumptions for future versions of SNOMO. Some, such as assumptions (1) and (4) will remain as they are primary bases of the model design. It would be possible to modify some of the other assumptions and these possible modifications are discussed below.

SNOMO could be amended so that snowpack accumulation throughout the snow season would be modelled and so that the affect of spatially variable accumulation is modelled. This would involve a consideration of snowpack spatial accumulation, for example the effects of wind and vegetation interception, and would be based on

the existing accumulation and compacting routines.

Equations are available (Balick *et al.*, 1981a) that calculate  $Q_g$  and it would be possible to include these into a future version of SNOMO. If  $Q_g$  can be calculated then the spatial distribution of frozen ground can be modelled. This would have potential for utilization in models for civil engineering and construction purposes in addition to hydrological, geomorphological and ecological purposes.

Anderson (1976) suggests the use of a threshold temperature for snow or rain of  $0.5^{\circ}\text{C}$ . This temperature could be tested and SNOMO amended accordingly if this temperature proved more satisfactory.

The role of vegetation, at the point scale, could be improved. There is no interception routine at present, and it is possible that an alternative method to that of VEGIE, such as that used in Leaf & Brink (1973a & b) can be used with similar or improved results. The number of vegetation types modelled could be increased.

The addition of a routing algorithm would enable SNOMO to model the streamflow. This would expand the potential usage of SNOMO considerably. Available routing algorithms vary from simplistic recession algorithms (Ferguson, 1984) to physically-based distributed schemes (Bernier, 1982). The choice of routing algorithm could reflect the importance attached to the modelling of the routing of the meltwater and the resultant hydrograph. The modelling of the lateral movement of meltwater and heat through the snowpack would be more difficult.

In addition to the modification of the assumptions made in the current model additional processes could be modelled. Rain-on-frozen-snow is not currently modelled. Equations are available for this (Male & Granger, 1978). The sun-slope geometry equations (equations 4.8 - 4.11) could be used to model topographic shading. This would be facilitated by the Digital Elevation Model (DEM) developed in the existing catchment subdivision algorithm (chapter 5). The future inclusion of the modelling of additional processes

and modification of the existing assumptions would increase the potential applications of the model.

## CHAPTER 5: MODEL STRUCTURE II: SPATIAL DISTRIBUTION

### 5.1 Catchment discretization in distributed models

Four key elements can be identified in the formulation of a catchment scale distributed hydrological model. These are:

- (1) the process equations utilized
- (2) the discretization (subdivision) of the catchment
- (3) data input requirements
- (4) data output requirements

The physical equations used in the proposed model SNOMO, have been presented and discussed in chapter 4 and therefore this chapter is concerned with the discretization of the catchment which forms the basis of the spatial application of these equations.

When designing a new, or choosing an existing catchment discretization method, the implications of the discretization method for model input data requirements, data availability, output requirements, the process equations used and the underlying logic behind the use of these equations must be considered. The catchment discretization method used is important. In the current literature, for both snow and general hydrology, the method of catchment discretization has assumed less importance than the choice of process equations used and process methodology. The utility of the most sophisticated physically-based process equations will be negated to some extent if the catchment discretization routine used is too simplistic. In this case there will be a dichotomy between the scale of the data input generated by the discretization method and the scale of the process equation calculations used in the model. This is an important point and must be remembered when designing or choosing a catchment discretization method. The resulting catchment subdivisions must operate at the same scale and require the same

scale of input data as the process equations used in the model. Conversely, a discretization routine that results in a very detailed subdivision of the catchment may result in problems of input data acquisition and again may not be suitable for the process equations used.

#### 5.1.1 Consideration of catchment discretization approaches available.

Chapter 1 stated that there are at present no fully distributed physically-based models of catchment snowcover dynamics and indeed of catchment snow hydrology. Therefore the consideration of the catchment discretization approaches currently available will involve both distributed but non-snow hydrology models and non/semi-distributed snow hydrology models.

##### (1) Non-snow distributed hydrology models.

Distributed models of this type can be broadly divided into two types (Rogers, 1986):

##### (a) Models based on hillslope planes, eg. VSAS2 (Bernier, 1982)

These models are based on the subdivision of the catchment into a number of hillslope planes or elements. These elements may be regularly or irregularly shaped and are defined on the basis of topography and the channel network with additional consideration being given to soil type and vegetation variations. Solutions for each element are determined for each hillslope element in succession and may involve the use of a grid system defined within the element. The elements may cascade down to the stream, have rectangular dimensions with areas equal to the hillslopes they represent or have variable widths to represent converging and diverging hillslopes, figure 5.1.

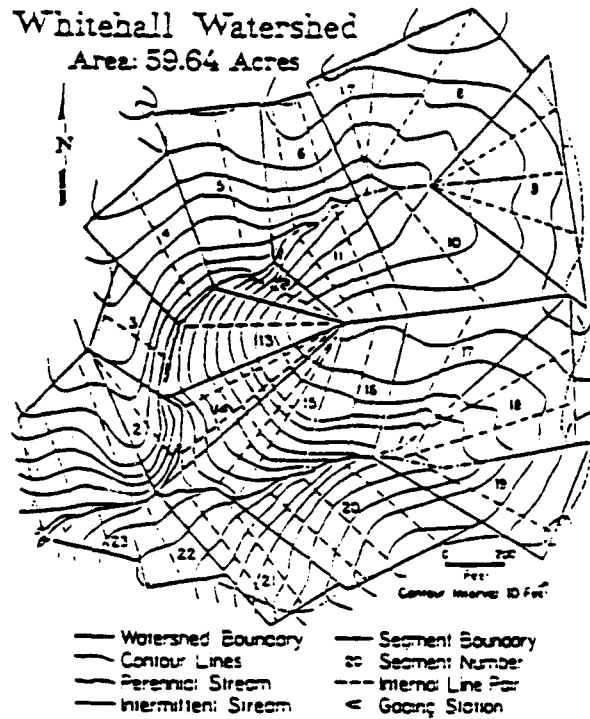


Figure 5.1. The division of a catchment using the hillslope plane method, VSAS2 (Bernier, 1982).

(b) Models based on grid systems, eg. the SHE model (Jonch-Clausen, 1979 and Beven et.al., 1980)

These models are subdivided by the use of a regular grid. The grid is superimposed upon a physiographic map of the catchment and the catchment boundary and channel network are manipulated to follow the grid lines. Associated with each grid square are characteristics of the catchment such as slope angle, vegetation and soil type. Flow calculations are undertaken sequentially for each grid square, figure 5.2.

Chapter 2 identified the factors that are important in determining the patterns of snowcover and snowdepth, namely vegetation cover, slope angle, aspect and elevation. The 2 subdivision methods above must be considered in terms of their inclusion of these four factors and therefore in the utility of the two subdivision methods for determining the patterns of snowcover and snowdepth. The grid system based model will, if the grid is of the correct resolution, allow and incorporate the spatial variability of these four factors. However, as these four factors tend to be spatially variable over small distances the grid resolution would have to be very small or each grid square would exhibit a wide range of values for each factor. Bathurst (1986) suggests a grid cell size of 1% of the catchment area or smaller. This is for applications of the SHE model. A small grid square resolution will present problems of input data availability for each grid square at the required scale. For example, if a grid size is used to match the Landsat pixel size (20x20m) then input data is required for each 20x20m grid cell. This, even in a small catchment, would generate a large input data requirement. Data such as vegetation cover and topography can be obtained from the data generated by Landsat, that is if this data is available. Data such as permeability or soil moisture content would have to be measured in the field. Ideally one measurement should be taken within each grid cell. This would however be impractical and very expensive. In practice, measurements are taken

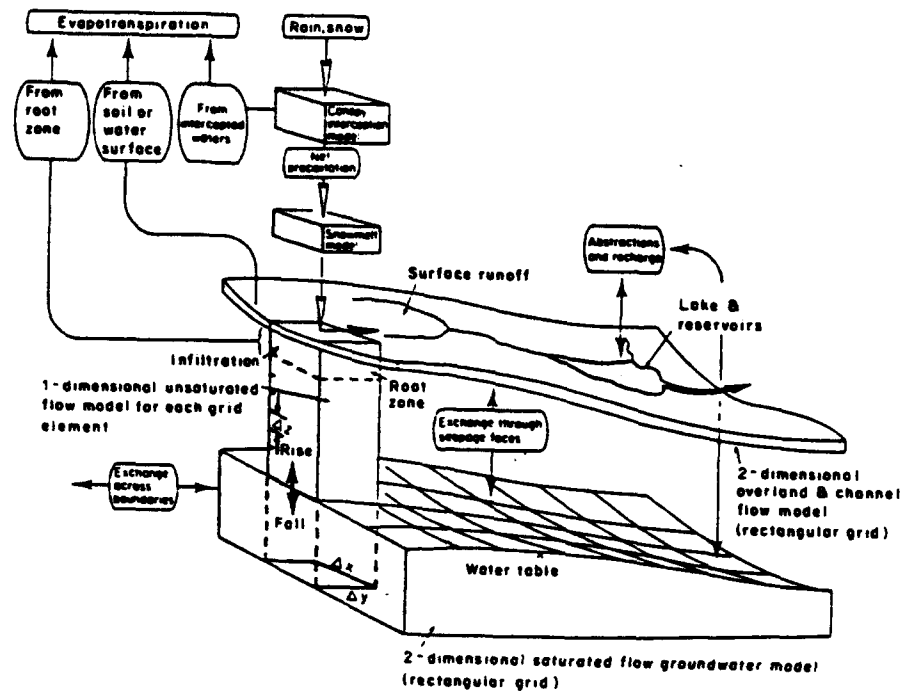


Figure 5.2. The structure of the SHE model, showing the division of a catchment using the grid method, Beven & O'Connell (1982).

that are representative of the soil types present and are considered uniform for each soil type, or one measurement is taken as representative of the whole catchment. Therefore each small grid square is receiving data which is generated at a variety of scales. The superimposition of the grid shape onto a naturally curved and irregular shape may also result in fitting problems.

A hillslope plane model is possibly more ideal than the grid system model; however there are certain limitations. The hillslope plane model places more emphasis on topography or channel network than on vegetation cover in the catchment subdivision process. The channel network is of lesser importance when considering snowcover and snowdepth distribution patterns. Problems may arise between the compatibility of the boundaries of the vegetation cover and the topographic or channel network areas. In a conflict of this type a model such as VSAS2 will choose the subdivision based on the topographic or channel network and not the vegetation cover, which would possibly produce an erroneous subdivision for the purposes required by SNOMO.

The two model types discussed above have been developed to model catchment hydrology with non-snow conditions. It would appear that a direct transferral of discretization techniques used in models of non-snow catchment hydrology to models of catchment snowcover is not applicable. A catchment discretization routine is required that does not have to result in strictly hydrologically valid elements, is more spatially flexible than the grid system and considers the four factors of slope angle, aspect, elevation and vegetation cover.

## (2) Snow hydrology models

Chapter 1 presented and discussed the snow hydrology models available today. There are no fully distributed models of snow hydrology presently available and there is therefore no direct comparison, in terms of modelling methodology, with models such as VSAS2 or the SHE model. However, there are some semi-distributed models and some examples in the snow literature of catchment

discretization on the basis of slope angle, aspect, elevation and vegetation cover. The Leaf & Brink (1973a & b) model (chapter 3) subdivides the catchment into homogeneous areas, response units, based on slope angle, aspect and forest cover composition and density. The primary output of the Leaf & Brink model is the streamflow and the subdivision of the catchment is as an aid to the generation of a correct streamflow hydrograph rather than the generation of the pattern of snowcover and snowdepth distribution.

The Leaf & Brink concept of the subdivision of the catchment into homogeneous areas that are used as spatial modelling units is important. There are several papers that substantiate this approach.

Woo & Marsh (1977 and 1978) showed that the subdivision of an arctic catchment on the basis of topography into terrain units, each with a characteristic snowdepth, enabled a much more accurate estimation of the total water equivalent available over the whole catchment, chapter 2. Buttle & McDonnell (1987) investigated various methods of modelling bare ground development due to snowmelt and divided their test catchment into homogeneous units on the basis of aspect and vegetation cover, chapter 2. Stepphun & Dyck (1974) suggest subdivision of the catchment into 'landscape classes' on the basis of vegetation cover in order to facilitate the location of snowcourse sampling points, as part of a statistical and field sampling programme to estimate true basin snowcover, chapter 2.

The four catchment subdivisions discussed above are designed to be performed manually. There are several disadvantages to the manual subdivision of a catchment:

- (1) The process is subjective and will be influenced by the operator's perceptions of the catchment.
- (2) Repetition of the results of catchment subdivision is difficult due to the subjectivity of the process, ie. different operators will produce different catchment subdivisions.
- (3) If changes occur within the catchment, eg. forest clear-cutting, there is no simple method of including these changes in the subdivision without repeating the whole process.

Most snowmelt models, if they include the spatial element, usually use a simplistic subdivision using elevation bands eg. Rango & Martinec (1982). This reflects the primary output of the models, that is streamflow, the perceived difficulty of alternative data collection eg. vegetation cover data, and the ease of incorporation of temperature or precipitation lapse rates into the models, rather than complicating the situation with the affects of vegetation or aspect on, for example, air temperatures. It can be argued that, if the model being used is a temperature index model, then a simplistic snowline-elevation model subdivision is sufficient as it will meet the requirements of the model output and does incorporate some element of discretization. However, for the proposed methodology and objectives of SNOMO this style of discretization is insufficient.

#### 5.1.2 Proposed catchment discretization.

The catchment discretization proposed for SNOMO is required to fulfil the following objectives:

- (1) to utilise subdivision criteria that are valid in describing snowcover and snowdepth distribution
- (2) to be an objective, reproducible and repeatable process
- (3) to be able to incorporate changes in catchment characteristics, such as vegetation cover changes.

In order to fulfil these objectives the following criteria will be used:

- (1) the concept of spatially homogeneous areas (cells) used as modelling units
- (2) subdivision into cells will be on the basis of slope angle, aspect, elevation and vegetation cover
- (3) a statistical clustering routine will be used to identify the homogeneous units
- (4) a GIS will be used to facilitate spatial data manipulation and

to handle the clustering routine

The use of a GIS for spatial data manipulation was mentioned in chapter 3. The following sections review briefly the components of a GIS and the current role of GIS in hydrological modelling. Two currently available models (simulating areal soil erosion and areal evapotranspiration) are then investigated in some detail as their usage of a GIS reflects the proposed usage of a GIS in SNOMO. The components required in SNOMO are then identified and the GIS used in SNOMO discussed fully.

### 5.1.3 The use of GIS in hydrology.

A GIS is a spatial data manipulation package. Burrough (1986) identifies five basic modules within a GIS (figure 5.3):

(1) Data input and verification.

This is concerned with the transformation of available data, ie. maps, field observations, aerial photographs or satellite data, into a compatible digital form.

(2) Data storage and database management.

This is concerned with the way in which data about the position linkages (topology) and attributes of geographical elements (points, lines and areas representing objects on the earth's surface) are structured and organised.

(3) Data input and presentation.

This is concerned with the ways in which the data are displayed and the results of the analysis are reported to the users.

(4) Data transformation.

This concerns the transformations needed to remove errors from the data, to bring the data up to date or to match the data to other data sets, and also the various analysis methods that are available that can be applied to the data in order to achieve answers to the questions asked of the GIS.



(5) Interaction with the user.

It is essential that the GIS be structured so that it is user-friendly and meets the requirements in terms of results that the user specifies.

The application of GIS technology to hydrology has evolved within the past twenty years from the development of digital cartographic methods and topographic representation (Doyle, 1978), to catchment delineation routines (Band, 1986) and environmental data packages (Miller, 1984), to the current usage in hydrological models. This evolution has mirrored the evolution of computer technology. The application of GIS technology to hydrological modelling has only occurred within the last few years. Table 5.1 lists and summarises some of the hydrological applications of GIS available in the literature. The literature available on snow-related applications is scarce. Two papers, one by de Roo et al. (1989) and the other by Hoshi et al. (1989) are discussed in some detail below. These two papers are examples of current GIS techniques and applications and are relevant to the GIS application to SNOMO, which is discussed subsequently.

(1) de Roo et al. (1989).

The soil erosion model ANSWERS (Areal Nonpoint Source Watershed Environment Response Simulation) is linked to a GIS in order to simulate spatial patterns of surface runoff and soil erosion. The GIS is used to provide, store, change and display data needed for the simulation model ANSWERS. ANSWERS is a quasi-physically-based model that is designed to simulate the behaviour of watersheds that have agriculture as their primary landuse, during and immediately following a rainfall event. Its primary application is in planning and the evaluation of various strategies for controlling pollution from intensively cropped areas.

A grid is superimposed on the watershed and values of the input variables (figure 5.4) are defined for each grid element or pixel. A

Table 5.1. Summary of some of the hydrological applications of GIS.

AUTHOR	SUMMARY
Bend (1986)	DEM, soils map and satellite imagery are used to subdivide the catchment into subbasin polygons. USA.
Burrough (1986)	Digital Elevation Model (DEM) and soil map used to create maps of water, oxygen and nutrient availability and erosion hazard. These then used to determine a map of suitability for growing maize. Kenya.
Moore <u>et al.</u> (1987)	Maps of elevation, rainfall, evaporation, extent of sands and gravels, extent of lakes and location and structure of river network digitised and in conjunction with gauged river flow records used to estimate mean and 85 percentile flows and catchment characteristics. N.Ireland.
Dikau (1989)	Formation of a Digital Geomorphological Relief Model (DGRM) which is an automated method of determining relief units for landform analysis. Based on a DEM. West Germany.
Ferris & Congalton (1989)	DEM and satellite ground cover and reflectance data used to estimate snowpack water volume on the Colorado River basin.
Miller (1984)	Investigation of spatial data structures for hydrological applications using DEM.
Sucksdorff <u>et al.</u> (1989)	Environmental data system consisting of digitised drainage basin divides, terrain heights, administrative borders, basin characteristics interpreted from land-use satellite images and a connection to an observation point register. Finland.

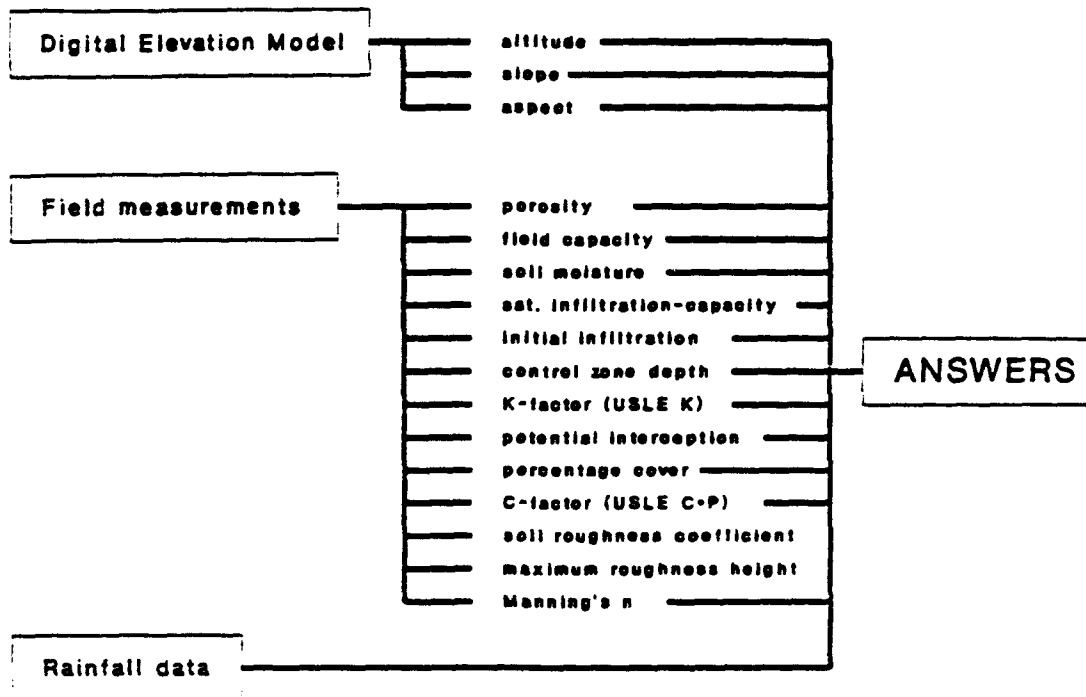


Figure 5.4. Input data required for the ANSWERS model, de Roo *et al.* (1989).

DEM is constructed by digitizing topographic maps. Within the GIS maps of elevation, slope angle, aspect, concavity/convexity and potential stream channels can be derived from the DEM.

Geostatistical interpolation techniques incorporated in the GIS are used to produce maps from point observations of, for example, soil type taken from field measurements. Where no field measurements are available the distribution of the desired input variable is derived from digitized soil or landuse maps.

ANSWERS operates at the grid-element scale. The continuity equation is used to compute the composite response of the single elements to a rainfall event. The output of up-slope elements becomes the input of downslope elements. When water and sediment reach an element with a channel they are transported to the watershed outlet, sedimentation occurs when the transport capacity is exceeded. Maps of soil erosion, sedimentation and surface runoff are produced.

Amongst several advantages of the GIS and ANSWERS are:

- (1) the incorporation of information about the spatial variability of land characteristics.
- (2) the detailed spatially displayed output of the model, useful for planners because the effectiveness of potential control measures can be evaluated.

ANSWERS was found to be very sensitive to the variables of infiltration, soil moisture content and soil roughness. Field collection and interpolation of these variables must be as accurate as possible. With insufficient data, which will be the case when many elements have to be 'filled', there is a serious risk of substantial errors occurring. A major problem is identified as the degree with which reliable location-specific estimates of the input variables can be made.

(2) Hoshi et al. (1989).

Landsat-MSS data, a DEM and meteorological data are linked together to provide input variables for a physically-based model to estimate areal evapotranspiration (ET). Landsat-MSS data is classified into landuse categories. Elevation data which is taken from the data file of the Digital National Land Information of Japan is at a different resolution from that of the Landsat-MSS data. Therefore the elevation data is interpolated and fitted to each pixel of landuse image data. Meteorological data is also required for input into the ET calculation model and this is regressed linearly with elevation to make each value at every grid point a function of elevation. ET is then calculated for every element using physically-based equations.

These two examples demonstrate the use of a GIS:

- (1) as an aid to spatial input data manipulation
- (2) in conjunction with a simulation model
- (3) to produce spatial output
- (4) to calculate using a DEM factors such as slope angle and aspect
- (5) in conjunction with satellite data which enables data to be collected from large areas, areas where data is unobtainable in conventional map form or where map information is out of date.

The GIS proposed for SNOMO will:

- (1) Handle the spatial data inputs into SNOMO and the output from SNOMO.
- (2) Derive a DEM of the catchment to be modelled using 'in-house' software developed from Roberts (1980).
- (3) Derive maps of slope angle and aspect using the DEM.
- (4) Utilise a clustering routine to derive homogeneous units (cells) that are used as the computational basis of SNOMO. The clustering routine is available on the I<sup>2</sup>S image processing system.
- (5) Generate maps of the model output using the GIMMS and ARC-INFO

data manipulation packages.

It can be seen that the GIS utilized in SNOMO consists of several software packages that are available on various machines. There is at present no package available, on one machine, that is able to do all the processes above. The transferral of data from machine to machine is time-consuming and is hindered by data incompatibility or format problems. The absence of an inclusive GIS package on one machine is a possible reason for the later development of the application of GIS technology to hydrological modelling.

The catchment discretization routine that was utilized in SNOMO is discussed below.

## 5.2 The catchment discretization routine.

The catchment discretization routine that is described below was applied to the W3 catchment, Sleepers River Research Watershed, Danville, Vermont, USA. This catchment was chosen for reasons that are outlined in chapter 6 and the characteristics of W3 are discussed in detail in chapter 6. It is sufficient to say here that the catchment has an area of 3.25 square miles (8.4km<sup>2</sup>), an elevation range of 1135-2280ft and a variable vegetation cover of clear-cut, open pasture and mixed, coniferous and deciduous forest.

The catchment discretization procedure developed is summarized in figure 5.5 and is as follows:

- (1) The topographic map, vegetation cover map and catchment mask were digitized. A DEM (photograph 2) was derived from the digitized topographic map. The method used to derive the DEM is taken from 'in-house' software developed from Roberts (1980). This algorithm converts the digitized contours into an equispaced grid of points specified by the user, and takes a series of equidistant cuts across the data in X and Y directions, forming a grid pattern. The original data is then



Photograph 2. W3 catchment: Digital Elevation Map (DEM).



Photograph 3. W3 catchment: aspect, derived from the DEM.

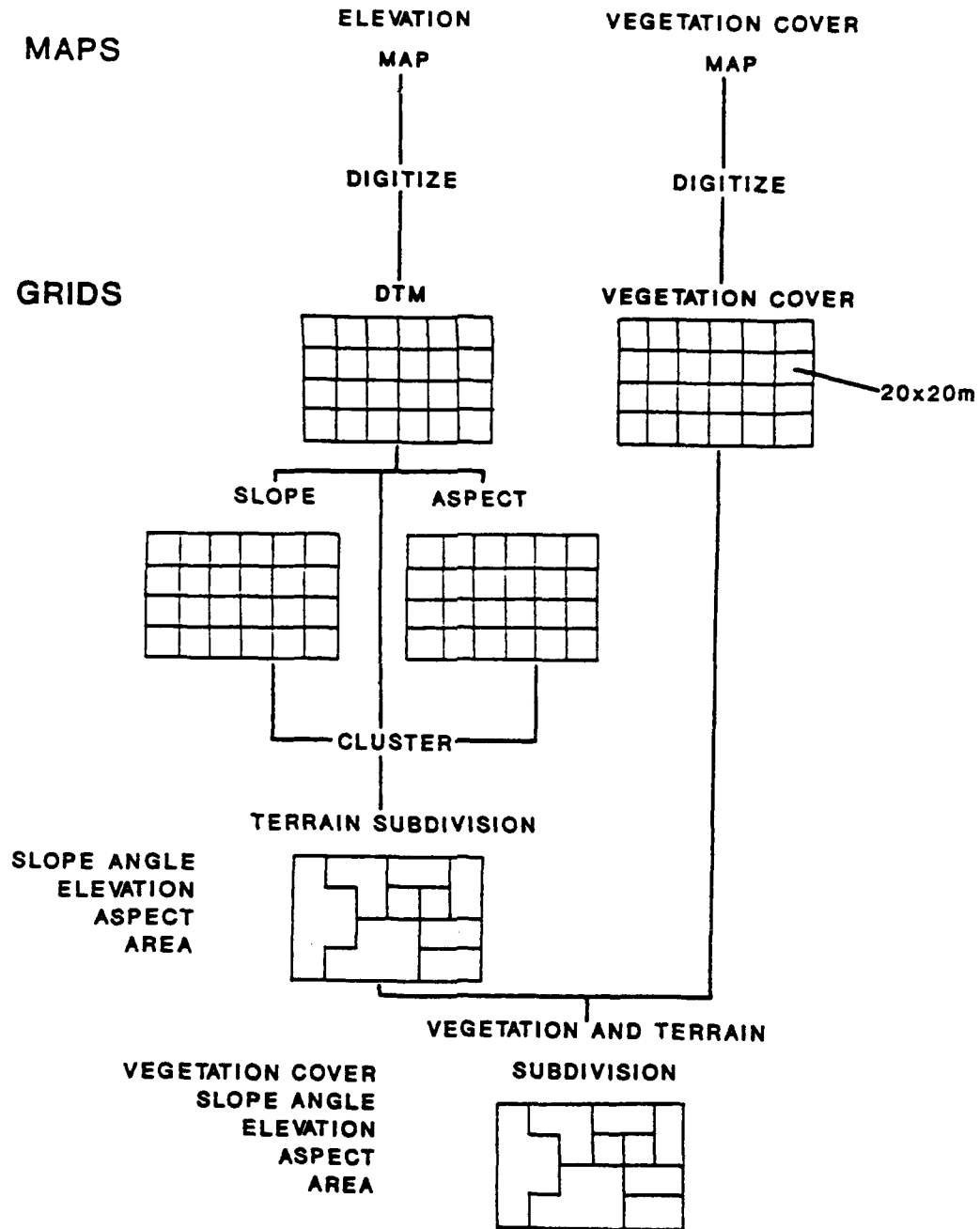


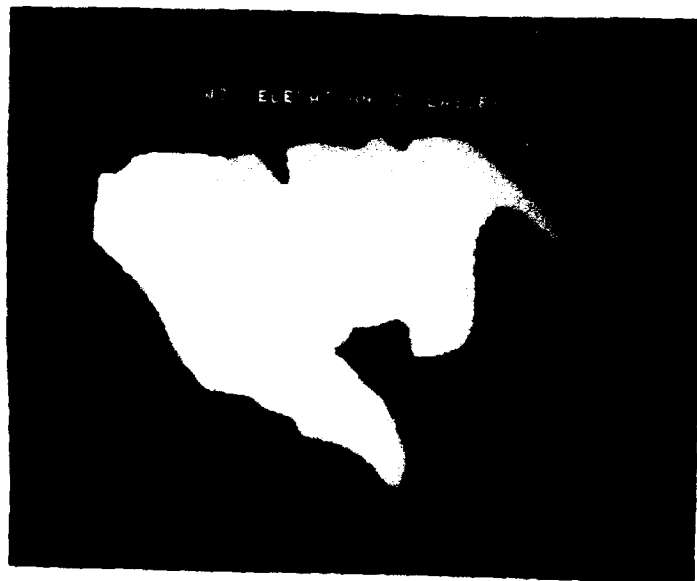
Figure 5.5. Summary of the catchment discretization procedure developed for SNOMO.

transformed to a series of points where the cuts and contours intersect. Finally, a cubic spline curve is fitted to the transformed data for interpolation of the elevation value at each grid location. Each grid cell is 20x20m. This method is thought to give a more accurate portrayal of the topography than the alternative algorithms available which only consider the surrounding data points.

- (2) Aspect and slope angle maps were derived from the DEM using 'in-house' software, Garg & Harrison, 1990, (photographs 3 and 4).
- (3) For interpretation purposes the catchment mask was superimposed upon the three maps and the maps were classified according to designated classes, photographs 5, 6 and 7. Three elevation classes were used 1135-1500ft, 1500-2000ft and 2000-2280ft. Five slope angle classes were used 0-3%, 3-8%, 8-15%, 15-25% and >25%. Eight aspect classes were used N, NE, E, SE, S, SW, W and NW. The classified maps enable the easier interpretation of the spatial distribution of the three topographic variables.
- (4) A cluster analysis was performed using software available on the I<sup>2</sup>S and using the modified aspect, elevation and slope angle data without the catchment mask. This resulted in eleven unique terrain classes (table 5.2). The mean of the slope angle (slope), aspect and elevation for each terrain class was taken as the value of that variable for that class. Table 5.2 also shows the standard deviation of each variable. There are multiple occurrences of each terrain class.
- (5) The distribution of the terrain classes was smoothed in order to eliminate edge effects, small irregularities, slivers, gaps and small data inliers and outliers (so called 'salt and pepper' effects). This smoothing of boundaries and removal of



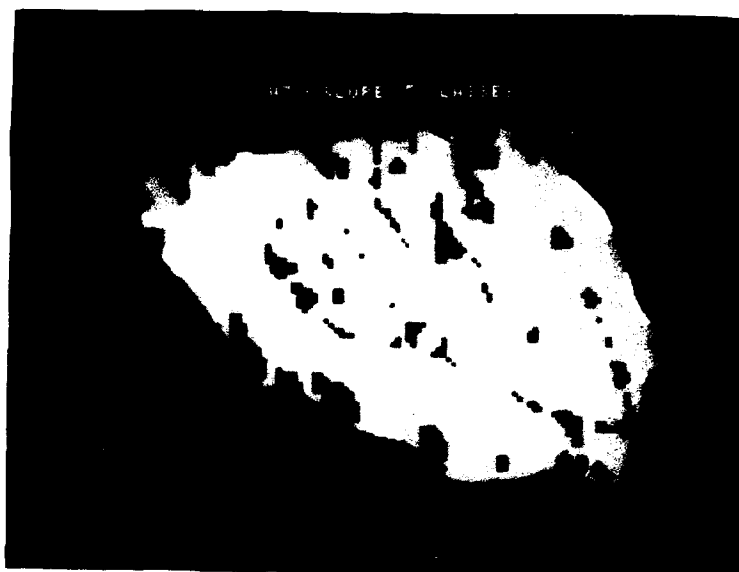
Photograph 4. W3 catchment: slope angle, derived from the DEM.  
Pixel colour decreases as slope angle increases.



Photograph 5. W3 catchment: elevation, superimposition of catchment  
mask and elevation classes.



Photograph 6. W3 catchment: aspect, superimposition of catchment mask and slope angle classes.



Photograph 7. W3 catchment, slope angle, superimposition of catchment mask and slope angle classes.

Table 5.2. Terrain classes: Means and standard deviations.

Class	Elevation	Slope	Aspect
0	1968.64	9.43	143.33
	<i>265.15</i>	<i>5.72</i>	<i>84.54</i>
1	1235.43	0.42	6.05
	<i>34.98</i>	<i>0.00</i>	<i>12.31</i>
2	1397.48	6.15	87.17
	<i>53.42</i>	<i>1.57</i>	<i>22.93</i>
3	1226.68	4.11	76.87
	<i>40.83</i>	<i>1.17</i>	<i>38.35</i>
4	1600.97	6.88	199.94
	<i>78.23</i>	<i>1.76</i>	<i>26.94</i>
5	1533.13	0.71	13.04
	<i>88.04</i>	<i>0.00</i>	<i>20.31</i>
6	1341.76	5.49	195.80
	<i>80.41</i>	<i>1.50</i>	<i>27.64</i>
7	1720.77	3.68	70.83
	<i>72.46</i>	<i>1.21</i>	<i>21.46</i>
8	1823.43	8.45	99.05
	<i>79.81</i>	<i>1.88</i>	<i>28.69</i>
9	1681.45	2.70	134.42
	<i>71.57</i>	<i>0.49</i>	<i>27.71</i>
10	1562.97	6.27	78.63
	<i>54.83</i>	<i>1.45</i>	<i>28.63</i>

Figures in italics are standard deviations.

isolated pixels resulted in the distribution over the W3 catchment of 33 terrain cells. The catchment mask was then superimposed on this distribution map (photograph 8). Terrain cell 31 is identical to that of 29 and terrain cells 32 and 33 are identical to terrain cell 24. For this reason they are omitted from all following tables concerning the terrain cells or the final cells produced by the catchment subdivision. The imposition of the catchment mask resulted in terrain cells 4, 5, 7 and 8 falling outside the boundaries of the catchment. Terrain cell 26 has an area of only one pixel (20x20m) and is therefore discounted as a separate terrain cell. Table 5.3 shows the terrain cells and their terrain class characteristics. The smoothing of the boundaries and the removal of the isolated pixels, edge effects and misclassifications has caused each terrain cell to be composed of a several terrain classes, instead of the original single unique class. However in all the terrain cells there is a majority terrain class. This is taken as representative of the terrain class of that terrain cell.

- (6) The digitized vegetation cover map (photograph 9) was then superimposed onto the terrain cell subdivisions. The result is shown in table 5.4. Each terrain cell is allocated a vegetation cover type on a majority coverage basis. The majority cover type is not as easy to identify as in the allocation of terrain class. Some terrain cells, for example cell 11, have very large secondary vegetation covers, allocation in others, for example terrain cell 30, is easy.
- (7) Table 5.5 and figure 5.6 show the end products of the catchment subdivision process. The homogeneous areas produced are called cells (as they are a combination of the terrain cell and the vegetation cover) and have a location within the catchment (figure 5.6) and attributes of area, elevation, slope angle,



Photograph 8. W3 catchment, distribution of terrain cells with catchment mask superimposed.



Photograph 9. W3 catchment, vegetation cover

Table 5.3. Terrain cells and associated terrain classes.

TERRAIN CELL	PIXELS	0	1	2	3	4	5	6	7	8	9	10
1	1152	5	0	1131	5	0	0	11	0	0	0	0
2	1375	29	0	6	2	2	0	1336	0	0	0	0
3	476	29	0	0	0	431	0	12	0	0	4	0
4	0	0	0	0	0	0	0	0	0	0	0	0
5	0	0	0	0	0	0	0	0	0	0	0	0
6	25	24	0	0	0	0	0	1	0	0	0	0
7	0	0	0	0	0	0	0	0	0	0	0	0
8	0	0	0	0	0	0	0	0	0	0	0	0
9	1333	86	8	36	1088	0	0	115	0	0	0	0
10	852	12	0	35	5	0	0	800	0	0	0	0
11	1351	13	0	1289	3	1	0	23	0	0	3	19
12	197	6	0	0	0	0	4	0	127	0	42	18
13	82	3	0	0	0	67	0	0	0	0	7	5
14	2043	62	0	39	0	29	0	5	57	17	537	1297
15	1435	128	0	8	0	1218	0	8	6	0	57	10
16	158	122	0	4	0	13	0	19	0	0	0	0
17	249	7	0	0	0	0	0	0	207	5	13	17
18	74	3	0	0	0	2	0	0	1	0	56	12
19	532	29	0	0	0	0	0	0	21	459	19	4
20	835	720	0	0	0	55	0	0	7	33	20	0
21	138	2	0	0	0	0	0	0	5	122	5	4
22	324	0	0	0	0	0	0	0	217	41	66	0
23	107	1	0	0	0	10	0	0	3	11	82	0
24	3235	15	0	47	0	78	8	0	95	14	840	2138
25	476	1	0	0	0	448	0	0	0	0	26	1
26	1	1	0	0	0	0	0	0	0	0	0	0
27	93	74	0	0	0	1	0	0	8	8	0	2
28	1035	1	0	0	0	0	0	0	958	23	25	28
29	1554	113	0	0	0	18	0	0	115	1207	101	0
30	1682	1637	0	0	0	0	0	0	0	45	0	0

Table 5.4. Terrain cells and associated vegetation cover classes.

TERRAIN CELL	PIXELS	VEGETATION COVER			
		CONIF	OP/CC	DECID	MIXED
1	1152	50	189	203	710
2	1375	18	<b>1084</b>	24	249
3	476	0	476	0	0
4	0	0	0	0	0
5	0	0	0	0	0
6	25	0	25	0	0
7	0	0	0	0	0
8	0	0	0	0	0
9	1333	46	287	0	<b>1000</b>
10	852	158	420	0	274
11	1351	62	540	0	749
12	197	0	171	26	0
13	82	0	82	0	0
14	2043	54	<b>1286</b>	609	94
15	1435	0	261	194	<b>980</b>
16	158	48	47	0	63
17	249	94	139	0	16
18	74	0	69	0	5
19	532	<b>232</b>	24	196	80
20	835	0	6	<b>639</b>	190
21	138	0	0	<b>138</b>	0
22	324	8	0	<b>316</b>	0
23	107	0	0	<b>107</b>	0
24	3235	0	<b>2341</b>	538	356
25	476	0	<b>268</b>	208	0
26	1	0	1	0	0
27	93	0	90	0	3
28	1035	0	710	325	0
29	1554	0	4	<b>1550</b>	0
30	1682	0	0	<b>1682</b>	0

Figures in bold are the dominant vegetation cover type.

**Table 5.5. Calculated catchment cells and their associated attributes**

CELL	LANDUSE TYPE	AREA (m <sup>2</sup> )	ELEVATION (ft)	SLOPE (deg)	ASPECT 1 (deg)	ASPECT 2
1	MIX	460,800	1397.48	6.15	-92.83	87.17
2	OP/CC	550,000	1341.76	5.49	+15.80	195.80
3	OP/CC	190,400	1600.97	6.88	+19.94	199.94
6	OP/CC	10,000	1968.64	9.43	-36.67	143.33
9	MIX	533,200	1226.68	4.11	-103.13	76.87
10	OP/CC	340,800	1341.76	5.49	+15.80	195.80
11	MIX	540,400	1397.48	6.15	-92.83	87.17
12	OP/CC	78,800	1720.77	3.68	-109.17	70.83
13	OP/CC	32,800	1600.97	6.88	+19.94	199.94
14	OP/CC	817,200	1562.97	6.27	-101.37	78.63
15	MIX	574,000	1600.97	6.88	+19.94	199.94
16	MIX	63,200	1968.64	9.43	-36.67	143.33
17	OP/CC	99,600	1720.77	3.68	-109.17	70.83
18	OP/CC	29,600	1681.45	2.70	-45.58	134.42
19	CONIF	212,800	1823.43	8.45	-80.95	99.05
20	DECID	334,000	1968.64	9.43	-36.67	143.33
21	DECID	55,200	1823.43	8.45	-80.95	99.05
22	DECID	129,600	1720.77	3.68	-109.17	70.83
23	DECID	42,800	1681.45	2.70	-45.58	134.42
24	OP/CC	1,294,000	1562.97	6.27	-101.37	78.63
25	OP/CC	190,400	1600.97	6.88	+19.94	199.94
27	OP/CC	37,200	1968.64	9.43	-36.67	143.33
28	OP/CC	414,000	1720.77	3.68	-109.17	70.83
29	DECID	621,600	1823.43	8.45	-80.95	99.05
30	DECID	672,800	1968.64	9.43	-36.67	143.33

Aspect 1 is the aspect in degrees from the south, 180°-north, -90°-east, +90°-west, this is the notation that SNOMO uses.

Aspect 2 is the conventional notation, north=0°, east=90° etc.

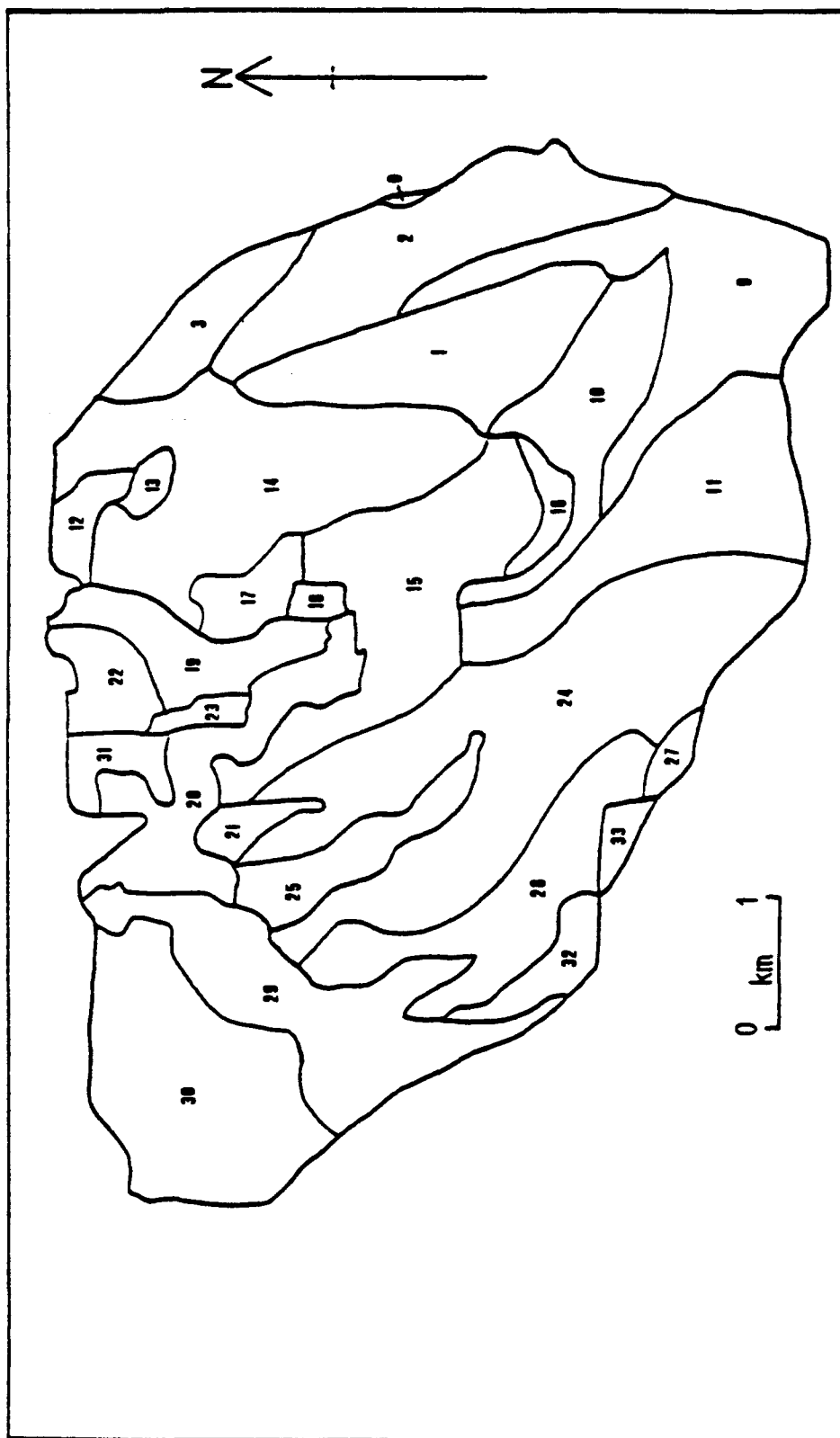


Figure 5.6. Final catchment subdivision and cell numbers.

aspect and vegetation cover. The figures for the areas of cells 24 and 29 represent the combined area of cells 24, 32 and 33, and 29 and 31. Therefore, in reality, there are 28 cells distributed around the catchment, as shown in figure 5.6.

Figure 3.3 (chapter 3) demonstrates the envisaged position of the fully integrated GIS in SNOMO. At present the remaining data inputs, that is the meteorological data and initial snowpack characteristics are not handled by the GIS but are input separately once the catchment subdivision has been completed. The GIS handles the discretization procedure described above. This procedure is responsible for the formulation of the spatial basis of the model SNOMO, calculates the input parameters slope angle and aspect and designates the input parameters of elevation and vegetation cover. The remaining input parameters are handled by SNOMO. The air temperature is affected by the designated elevation value, the initial snowdepth by the designated elevation value and vegetation cover type and the vegetation variables by the designated vegetation cover type. The remaining input variables are not affected by the discretization of the catchment. The variables describing the physical characteristics of the snow eg. albedo and thermal conductivity are spatially variable but their variability is induced by simulated changes in the snowpack structure. The meteorological inputs of precipitation, wind speed and relative humidity are not varied spatially. The values of these variables are taken from a meteorological station nearby and are assumed constant over the catchment. It is realised that this is a large assumption that could, if the meteorological station is distant from the catchment result in large errors. However, at this stage in the model development this assumption is realised and remains.

### 5.3 Discussion.

The catchment discretization method proposed for SNOMO has implications for model performance and methodology.

The mean value for slope angle, aspect and elevation is chosen as representative of each terrain class. The choice of the mean value results in a loss of the extreme values during catchment simulation. For example, very steep slope angles, where snow will either melt first or last depending upon the aspect, will be omitted. Overall, in conjunction with the omission of other extremes, this will have the effect of missing the extremes of early and late snowmelt in the catchment simulation. However, a value has to be chosen for each class and the mean appears to be the best option available. The loss of extreme values is therefore inherent in the choice of a value that is representative of a spatially varying continuum.

An examination of the cells with terrain class 0 demonstrates a problem with the output from the clustering routine that is again related to the imposition of homogeneity onto a heterogeneous surface or a continuum. Cells 6, 16, 20 and 27 have elevations (1968.64ft) that are too high to be the average elevation for their location. Also the difference in aspect between cells 15 (199.94°) and 16 (143.35°) is not apparent on the topographic map. It is only for cell 30 that the average elevation of 1968.64ft seems appropriate, however in this cell the steepest slopes of 9.43° seem inappropriate as there is a large area of flat land within cell 30.

It appears that terrain class 0 contains data that is unclassifiable i.e. data that does not fit into any of the other clusters, and can be regarded as a 'reject' class. This class contains the extremes of the data available i.e. the flattest slopes, steepest slopes and highest elevations and the data that affects the clustering routine by being at the edge of the catchment. It can be argued that there are 9 natural terrain groupings and one odd class containing the data that does not easily fit into any of these

groupings. For example, cell 30 contains the flattest slopes but the highest elevations and cells 27 and 6 are small edge cells. Class 0 has the largest standard deviations of all the terrain classes and this reflects the variety and heterogeneity of the data that is placed in this class.

The presence of a class 0, an unclassifiable class, is a product of the cluster analysis and of the attempt to impose homogeneity on a spatially varying continuum. The presence of a class 0 does not detract from the proposed catchment discretization as long as its presence is realized and noted in the interpretation of the simulation results.

The standard deviations of the terrain class variables (table 5.2) are relatively large, excluding those of terrain class 0. Slope angle varies the least within each class, elevation the most. The standard deviations available allow the variation within each class to be quantified. No such statistics are available if a manual catchment subdivision is performed.

Another problem of the proposed catchment subdivision is that of intra-cell variation. The majority (55%) vegetation class in cell 11 is mixed forest and the whole cell is therefore modelled with a mixed forest cover. However, 40% of the catchment is open/clear-cut. Open/clear-cut will melt before mixed forest and therefore by modelling the whole cell as mixed forest the melt is effectively retarded. This has implications for the streamflow hydrograph and on the visual pattern of snowcover distribution.

Intra-cell variation is implicit, again, in the artificial imposition of homogeneity on a spatially varying continuum. The reasons for the imposition of homogeneity have been stated and are considered to outweigh the disadvantages. However, it is possible with this discretization routine, where the proportions of vegetation cover within each cell are known, to devise a future method of weighting the output from each cell dependent upon the known proportions of vegetation cover types. This may be specially useful in situations such as cell 11 where over a third of the vegetation

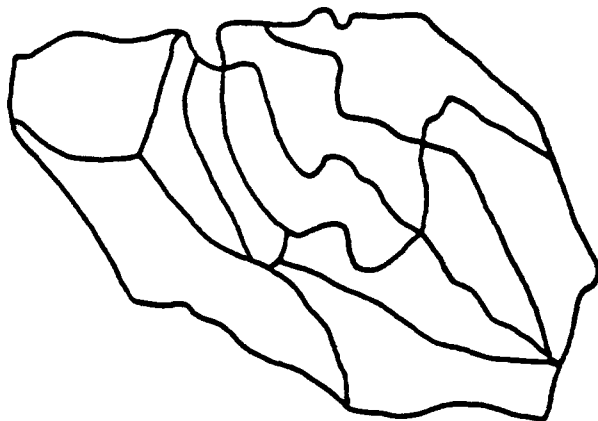
cover is of the non-dominant type. This is discussed further in chapter 10.

It is interesting to note the difference in the perception of the catchment and the homogeneous units within it and the division produced by the discretization routine. When moving around the catchment open areas are perceived as larger and become more significant than in reality. This is because they are more accessible and are easier to view, ie. they are not obscured by trees. Perception of the area, aspect or slope angle of an area of coniferous forest, for example, is very difficult from within the forest due to the dense and disorientating nature of the canopy. This difference between perception and reality was noted when looking at the aspect map (photograph 6) and then the results of clustering (figure 5.6) where cells such as 25, 10 and 2 appear to be aspect dominant. This relationship is very difficult to perceive on the ground and if a manual subdivision had been performed this relationship would have been omitted from the subdivision.

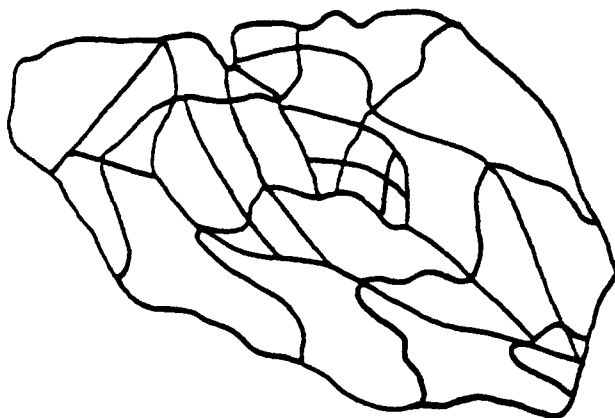
Two manual subdivisions were performed in order to compare the resultant distribution with that of the subdivision method described above. Subdivision A (figure 5.7a) followed the guide-lines given for the Leaf & Brink (1973a & b) model WATBAL, as discussed in chapter 3. Subdivision B (figure 5.7b) was conducted before the 1988 field season at W3 and by a user who was unfamiliar with the catchment. Subdivision B used only aspect and elevation as the basis of the subdivision. The use of vegetation as a subdivision criteria was considered too complicated. The predominant vegetation cover of each cell would be estimated from a vegetation cover map. Subdivision C (figure 5.7c) is that which is used in SNOMO and described above. The aim of the three subdivision methods was identical, that is to subdivide the catchment into homogeneous areas. As expected the three subdivisions exhibit a broadly similar pattern of cell distribution. There are, however, significant differences between the results of the three methods.

The number of cells generated by subdivision B is very similar

(a) WATBAL (Leaf & Brink, 1973a & b)



(b) Manual subdivision, no prior knowledge of catchment



(c) SNOMO

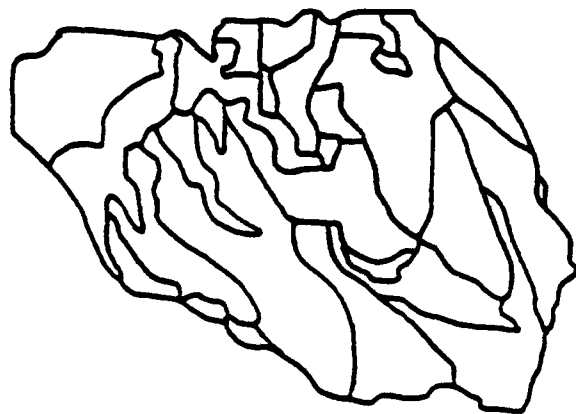


Figure 5.7. A comparison of the results of three different methods of catchment discretization.

to that of subdivision C. Whilst generating subdivision B it was difficult to reduce the number of cells to a number lower than 33. The cells of subdivision B are more hydrologically correct, they follow the direction of the slope and have a more uniform shape. This implies that subdivision B is probably more suited for the simulation of meltwater routing than for the prediction of the pattern of snowcover and snowdepth distribution. The estimation of the primary vegetation cover type for each cell in subdivision B was not attempted.

Subdivision A has many fewer cells than subdivision C. This is because of the subdivision guide-line (chapter 3) that each cell should be roughly 10% of the area of the catchment. The subdivision is primarily on the basis of aspect and elevation, vegetation cover is included but to an insufficient extent, considering that it is the usually the primary factor in the distribution of snowcover and snowdepth.

Different users will find it difficult to duplicate the subdivisions shown in figures 5.7a and 5.7b. The areas of the cells that are generated in subdivisions A and B and the primary vegetation cover type have to be calculated manually. No statistics are available to quantify subdivisions A and B. Slope angle is not really considered as a subdivision variable in subdivisions A and B and the subdivision process can be affected by the preconceptions and subjectivity of the user.

In contrast, and despite the observations made at the start of this section, which are inherent in the imposition of homogeneity on a spatially varying continuum, the advantages of the subdivision method C are:

- (1) The process is repeatable by other users.
- (2) The process is quantifiable. Statistics and a numerical breakdown are available for use in the choices that have to be made at each subdivision stage and in order to quantify the degree of homogeneity.
- (3) Amendments can be made easily. The conversion of the

vegetation cover map into digitized form and the construction of a DEM result in possible future improvements such as effects of shadowing and the easy inclusion of any changes such as clear-cutting.

- (4) The process is objective, the problems caused by user perception of the catchment are eliminated.
- (5) The process uses subdivision criteria that are responsible for the pattern of snowcover and snowdepth distribution.
- (6) The areas of the cells are calculated.
- (7) The process plots the finished cell distribution map.

## CHAPTER 6: MODEL VALIDATION I: DATA REQUIREMENTS AND FIELD DESIGN

### 6.1 Introduction.

#### 6.1.1 The validation process.

The spatial and point structure of SNOMO have been discussed in chapters 4 and 5. This chapter and chapter 7 are concerned with the validation of SNOMO. Model validation is an integral part of the process of model development (chapter 3, figure 3.1). Model validation is the process of comparing the simulated model results with observed measured results, for example, the comparison of observed and predicted outflow hydrographs. The comparison of the results demonstrates the operational and predictive validity of the model. The aims of the validation of a model can be broadly defined as:

- (1) To determine the predictive ability of the model.
- (2) To determine the robustness of the model, i.e. its predictive ability under a variety of situations.

In each case the model results are compared against observed results.

Validation is not a proof or disproof of model performance, methodology or structure, but an indicator and a check on the broad guide-lines of model performance. For example, if there is a large disparity between the simulated and the observed results then one of three conclusions can be reached:

- (1) The model structure and theory are wrong.
- (2) The model theory is correct but the model is highly sensitive to a specific variable or combination of variables.
- (3) Either the model results, the observed results or a combination of both are operating within certain accuracies and therefore the disparity between the results may be larger or smaller than

apparent.

Conclusions (1) and (2) require some modification of the model in order to decrease the disparity between the simulated and the observed results. In some cases disparities relating to specific factors, for example a rain-on-snow period, can be discerned. However, a validation does not usually indicate where the model needs to be modified. A sensitivity analysis used in conjunction with a model validation should give an insight into the reasons for the disparities between the model results and the observed results. In conclusions (1) and (2) validation will highlight a problem but will not indicate how or where modification of the model should occur in order to rectify the problem.

Conclusion (3) highlights the importance of a knowledge of the accuracy within which the model operates and the accuracy of the observed results. As Stephenson & Freeze (1974) indicate:

" an ideal validation presupposes perfect knowledge of the spatial pattern of input rates and other boundary conditions that is never attainable in practice."

As the spatial and temporal complexity of the situation that is being modelled increases the accuracy of the observed results becomes more important. In some cases model development occurs because the simulated results are very difficult to obtain, or are unobtainable, in the field or laboratory. Validation in these cases would be, by definition, difficult. In reality a combination of all three of the conclusions above can be the cause of a disparity between the observed and simulated results.

Conversely, the simulated and observed results may be very similar. This, unfortunately, does not indicate that the model is perfect. Again, as in conclusion (3) above, a knowledge of the accuracies within which the model operates and the accuracy of the observed results is important.

A small disparity between simulated and observed results may not be repeated if the model is applied to a different set of data, even if the data is similar to that used previously. Different

variable configurations may result in the improvement or decrease in the predictive ability of the model. Again, validation needs to be performed in conjunction with the exploration of the model structure and variable interrelationships, ie. a sensitivity analysis.

Validation is therefore also a test of model robustness, ie. the performance of the model under various conditions. The model is usually designed to predict behaviour within a specific environment or suite of environments (these may be limited or numerous) and therefore for a validation to be realistic it should keep within the conditions experienced within these specified environments. This does not, however, negate the validity of broadening the modelling application and validating the model in environments for which it was not designed, eg. SNOMO in the Prairie environment.

The data requirements for the operation of SNOMO have been discussed in chapter 4 (section 4.5.2). This chapter considers the validation process as conducted on SNOMO (section 6.2), the data required for both the operation and validation of SNOMO (sections 6.2 and 6.3) and the methods used to obtain this data (section 6.4). The input requirements for the operation and validation of SNOMO are identical. The validation of SNOMO does however require additional data which is used as a validation of model performance. Chapter 7 discusses the data collected in response to needs identified in this chapter and also discusses the results and implications of the validation of SNOMO.

## 6.2 Data requirements.

### 6.2.1 Operational data requirements.

The data required for the operation of SNOMO is shown in table 4.5, section 4.5.2 (chapter 4). As discussed in section 4.5.2 a lot of the operational data that is required can be obtained from the literature and from existing maps. The data that cannot be obtained

from the literature is shown in table 6.1. Daily precipitation, wind speed, maximum and minimum air temperature and relative humidity are all variables measured at a standard meteorological station. Daily cloud cover amount is less regularly observed and the value of 5 tenths is used when observations are missing. Air pressure, as stated in chapter 4, is at present not varied daily and a standard atmospheric pressure is used throughout the simulation. However, if required on a daily basis a rough estimate of atmospheric pressure could be obtained from regional weather information. Snowdepth is a measurement taken at a cold regions meteorological station either by a snowcourse, a series of snow stakes or an acoustic snowdepth sensor.

The operational data required is therefore not very extensive and, with the exception of cloud cover and type, should be that which is readily available from a standard cold regions meteorological station. The spatial variance of the input data, with the exception of air temperature (varying with elevation), is not considered by SNOMO (chapter 4). Therefore, the meteorological station that is to be used as the data input source should ideally be within the catchment that is to be modelled, or if this is impossible, it should be as close to or as representative of the conditions at the catchment as is possible. The ideal situation would be a meteorological station within each of the computational cells, this is however an impractical situation as one of the aims of SNOMO is to develop a spatial model which requires a minimum of input data (optimum complexity).

#### 6.2.2 Validation data requirements.

The maximum data that is required for the full validation of SNOMO is shown in table 6.2. This is effectively a list of all possible outputs from SNOMO. The minimum data requirements for the validation of SNOMO are the distribution and depth of the snowpack during the melt period and the snowdepth and melt volume at a point.

**Table 6.1. Remaining operational data requirements.**

Initial snowdepth  
Cloud cover type  
Air pressure

Daily: Maximum and minimum air temperature  
Precipitation  
Wind speed  
Relative humidity  
Cloud cover amount

**Table 6.2. Validation data requirements.**

Net shortwave radiation (or  $K\uparrow$ ,  $K\downarrow$ )  
Net longwave radiation (or  $L\uparrow$ ,  $L\downarrow$ )  
Sensible heat exchange  
Latent heat exchange  
Areal distribution and depth of snowpack (at least weekly)  
Snowdepth and melt volume at a point (at least weekly)  
Density of snowpack  
Surface emissivity and albedo  
Precipitation type and amount  
Snow/soil saturation  
Snow thermal diffusivity  
Snow thermal conductivity  
Snow profile temperatures  
Streamflow

This enables validation at both the point and the catchment scale. SNOMO is an energy budget model and therefore validation data allowing the comparison between the computed and observed energy exchanges, for example incoming and reflected shortwave and longwave radiation, would be informative. Indeed, the wider the range of validation data that is available the more extensive the validation can be. However, it must be remembered that SNOMO is being developed to simulate spatial snowdepth and snowcover and therefore, unless spatial data are available on, for example incoming solar radiation, the utility of concentrating on the point scale to validate the energy exchanges must be questioned. It must also be remembered that SNOMO makes specific assumptions that possibly sacrifice the accurate modelling of certain parts of the melt process in order to model the snowcover and snowdepth distribution patterns. Therefore validation data, such as snowpack temperatures, which are at the micro-scale may be of little utility in the overall validation of SNOMO, for the specific aims for which SNOMO has been designed. The validation of SNOMO will therefore examine the simulated and measured distribution and depth of the snowpack during the melt period and the snowdepth and melt volume at a point.

#### 6.2.3 Choice of initial validation catchment.

The initial validation catchment has to provide both validation and operational data for SNOMO. The minimum attributes that are required of a validation catchment for SNOMO are:

(1) Close proximity to a meteorological station.

The meteorological station is supplying, at a minimum:

- (i) Incoming and reflected shortwave radiation (daily).
- (ii) Incoming and reflected longwave radiation (daily).
- (iii) Precipitation (daily).
- (iv) Wind speed (daily).
- (v) Relative humidity (daily).

- (vi) Air temperature (daily).
  - (vii) Snowdepth (snowcourse, therefore water equivalent is measured also, weekly).
  - (viii) Point melt outflow (daily).
- (2) Snowcourse coverage of the catchment area.
  - (3) Variable cover type (at the meso-scale).
  - (4) Representativeness of a certain snow environment.
  - (5) Topographic and vegetation cover information, i.e. maps.
  - (6) If SNOMO is to be used to calculate streamflow, a gauged outflow stream is required.

The catchment used is the W3 catchment, part of the Sleepers River Research Watershed, Danville, Vermont, USA. SNOMO was validated using data from the W3 catchment for the melt periods in 1988 and 1989. Model validation is usually performed on more than one catchment or set of conditions. The application and validation of SNOMO was restricted to only one catchment, although for two years. This was primarily the result of report time constraints but is also the result of data availability constraints on other potential validation sites. The application and validation of SNOMO using data from other catchments is beyond the scope of this report and could be an extensive undertaking if SNOMO were to be applied to catchments both within and outside the New England snow environment. The catchment subdivision used was that described in chapter 5 which uses the 1989 vegetation cover map. Validation of SNOMO is required at both the point and the catchment scale. Validation of SNOMO at a point facilitates the interpretation of the spatial results and examines the predictive accuracy at the cell level which has implications for the structure and theory of the model.

6.3 Catchment description: W3. Sleepers River Research Watershed.  
Danville, Vermont, USA.

The catchment W3 is a subcatchment of the Sleepers River Research Watershed, figure 6.1, a project which was initiated in 1965 as a joint venture between NOAA and NWS. The aim of the project was to improve the data base available to snow researchers and a series of weirs and meteorological stations were established over the Research Watershed. Research at W3 is now a joint project between CRREL (U.S. Corps of Engineers Cold Regions Research and Engineering Laboratory, Hanover, New Hampshire) and UVM (University of Vermont, Burlington).

The W3 catchment is considered representative of the land use cover, soils and topographic conditions that are found in the northern areas of the New England States and southern Quebec. A more detailed description of W3 is given in Anderson et.al. (1977) and Pionke et.al. (1978).

The basin has an area of 3.25 square miles (8.4 km<sup>2</sup>) and varies in altitude from 1135 to 2280 feet above mean sea level (figures 6.2 and 6.3). Vegetation cover is predominantly forest, coniferous, deciduous and mixed with some areas of open pasture (figure 6.4). There is no arable land at W3. The main deciduous species are Birch (yellow - Betula allegheniensis, white - B. papyrifera and grey - B. populifolia), Beech (Fagus americana) and Maple (sugar - Acer saccharum and red - A. rubrum). The major coniferous species are Red Spruce (Picea rubra) and Balsam Fir (Abies balsamea).

There has been and continues to be forestry activity in certain areas of W3, mainly in the coniferous areas, which has resulted in large tracts of clear-cut. A lot of this activity occurred in the early 1980s, with the result that any new tree growth in these areas is still relatively young and light-loving shrubs, eg. Dogwood, tend to predominate.

The Waits River formation forms the underlying solid geology of

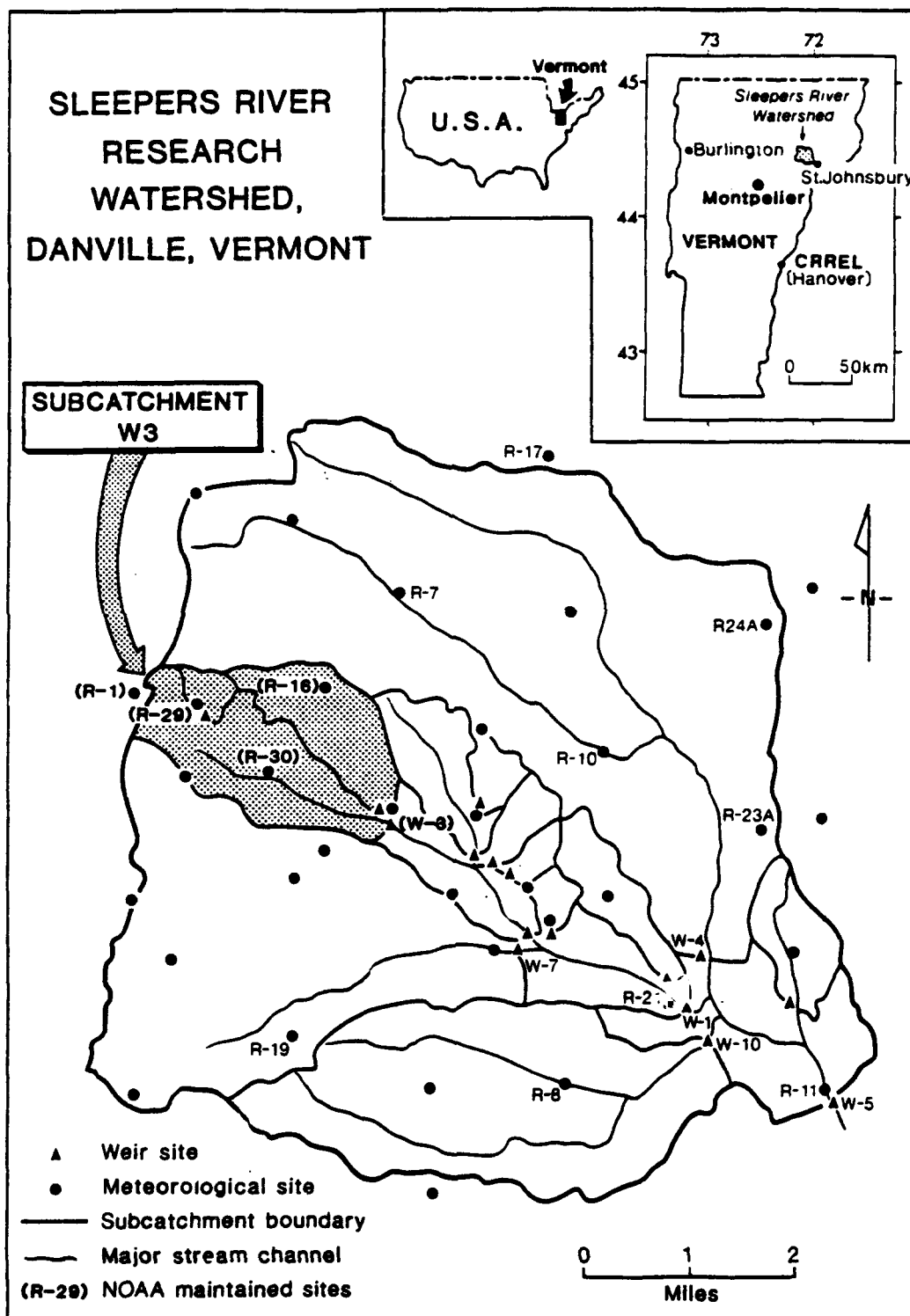


Figure 6.1. Location of the W3 catchment.

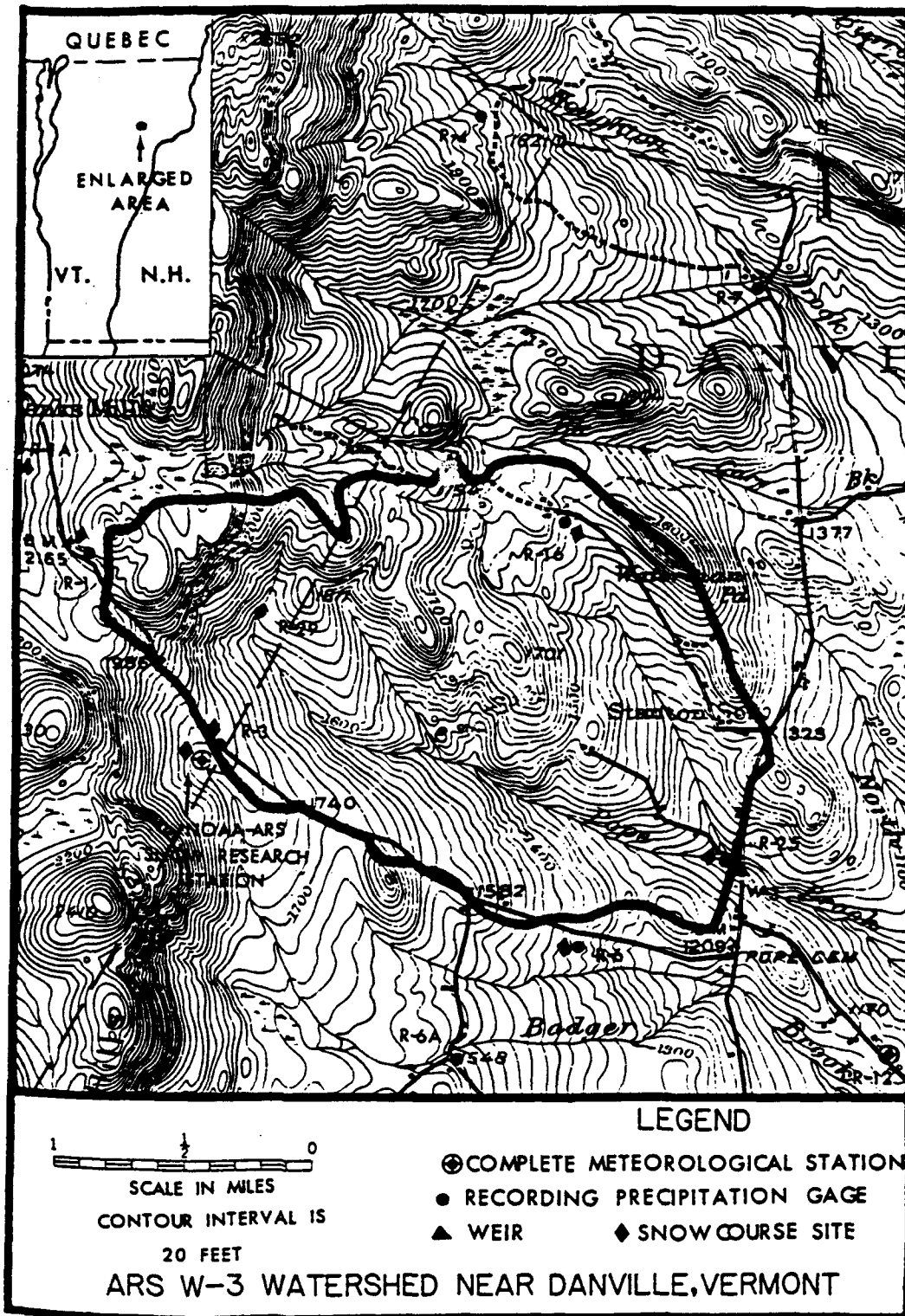


Figure 6.2. Topographic map of the W3 catchment, Anderson et al. (1977).

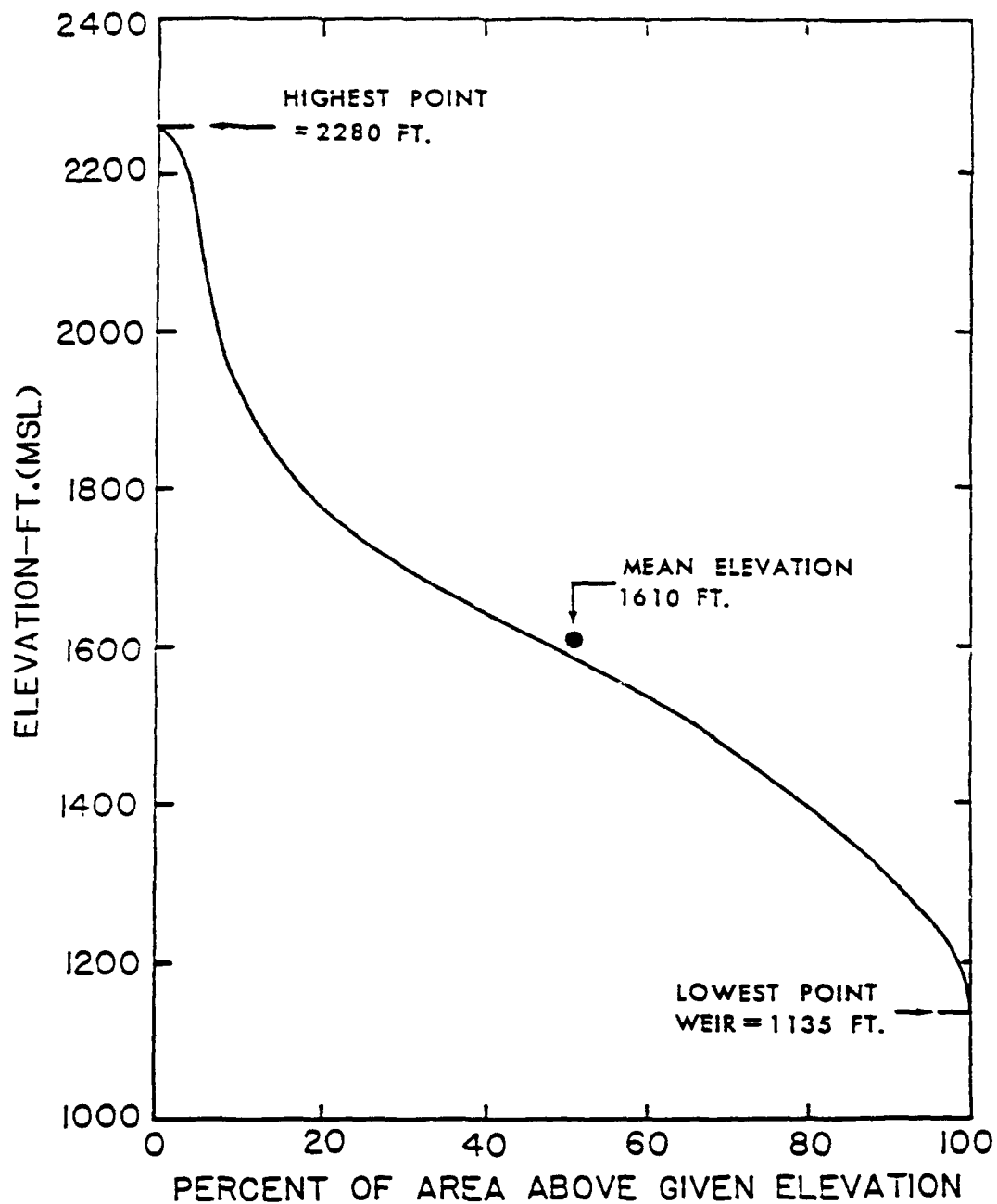


Figure 6.3. Area-elevation curve for the W3 catchment, Anderson *et al.* (1977).

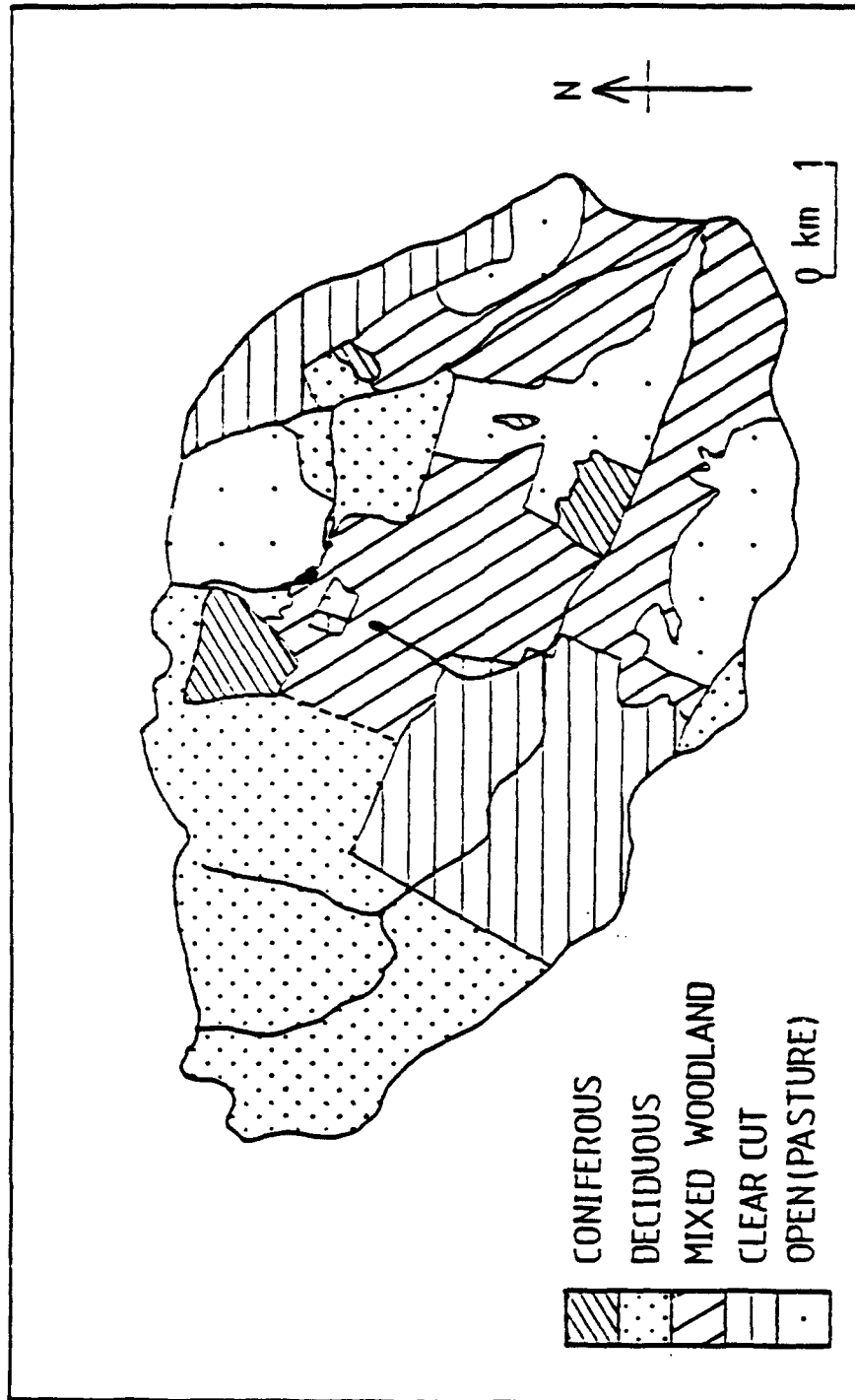


Figure 6.4. Vegetation cover, W3, 1988.

W3. The Waits River formation consists of calcareous granulites and calcareous schists (composed of quartz, calcite, muscovite and biotite), quartz-mica schist and minor micaceous quartzite. Superficial deposits are a till with a clay-silt matrix with small patches of poorly-sorted horizontally stratified (lenticular-bedded) and cross-bedded sand, pebbly sand and pebble gravel.

Soils are in general fairly shallow and are variable in depth over small areas, i.e. from zero to several inches over exposed rock outcrops to 4 to 6 feet between these outcrops. Figure 6.5 shows the distribution of soils as mapped and classified by SCS Soil Surveys 1960-64, compiled in 1969, (Pionke et.al., 1978).

Table 6.3 shows the current data available for W3 and is considered in more detail below.

- (1) Townline meteorological station (NOAA-ARS Snow Research Station, figure 6.2).

Townline has been in operation since 1968 and was established to provide an improved data base for the development and testing of physically-based models of snowmelt eg. Anderson (1976). Townline is at an elevation of 1810ft and is in a large clearing making the site effectively an open site. Table 6.4 shows the instrumentation available at Townline and the measurement errors associated with the instrumentation. In addition to the instrumentation shown in table 6.4 there is a WMO comparative study comparing different snow gauges currently in operation and an acoustic snowdepth recorder is also being tested. Anderson et.al. (1977) and Greenan & Anderson (1984) discuss the instrumentation at W3 in more detail, but it is sufficient here to state that the data measured at Townline is extensive, reliable and within known bounds of accuracy. Figure 6.6 shows the location of Townline and the areal points discussed below.

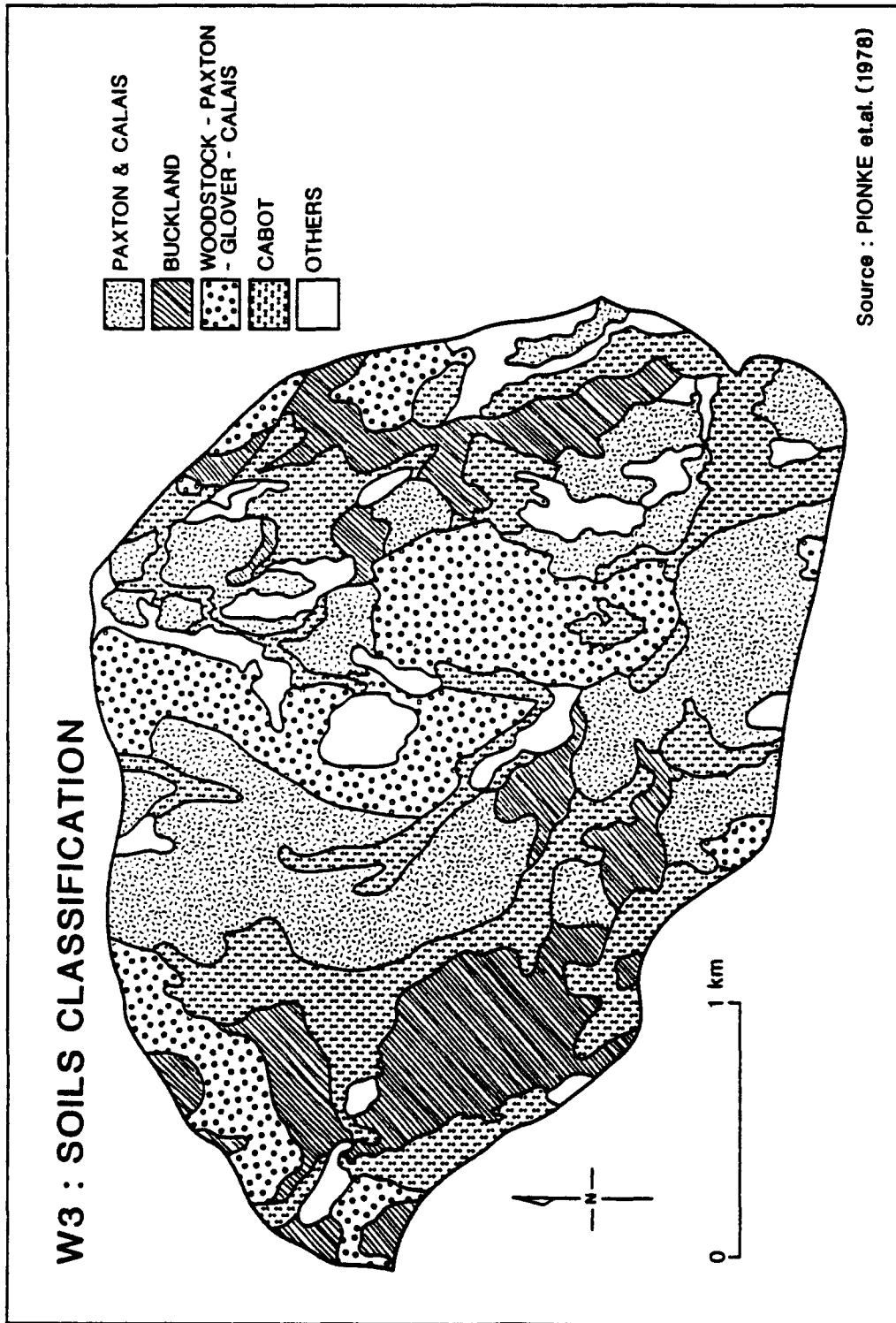


Figure 6.5. Distribution of soils, W3.

Table 6.3. Existing data coverage for W3.

**Areal: within W3**

- (1) 30 frost-tubes  
measuring: Frost depth (weekly in snow season)  
Snow depth ( " " " " )  
Water equivalent (weekly in melt season)
- (2) 2 meteorological stations  
measuring: Precipitation (continuous recorder)  
Snowcourses (weekly)
- (3) Main outflow weir and stage recorder at W-3 (Pope Brook) and tributary stage recorder and weir.
- (4) Soil, drift geology, solid geology, slope, land cover and topographic maps.

**Areal: outside W3**

- (1) Meteorological station R1A ( $\approx \frac{1}{2}$  mile from catchment boundary)  
measuring: Precipitation (continuous recorder)  
Snowcourses (weekly)

**Point data**

- (1) Main meteorological station, Townline (on catchment boundary)  
measuring: Snowdepth  
Precipitation  
Incoming and reflected shortwave and Longwave radiation  
Wind speed  
Relative humidity  
Snowcover outflow  
CRREL pit (snow density, crystal size and temperature)  
Air pressure  
General meteorological observations (cloud cover, precipitation type etc.)

Table 6.4. Summary of data available at the Townline meteorological station, Danville, Vermont.

VARIABLE	SENSOR	ACCURACY-ESTIMATED STANDARD ERROR
1. Air temperature	Platinum resistance element in ventilated radiation shield, one metre above snow surface.	1°F
2. Vapour pressure	Lithium chloride dewcell in ventilated radiation shield, one metre above snow surface.	<5% above 32°F and >10% below 0°F
3. Wind speed	Low threshold (0.7mi mph) 3-cup anemometers, one metre above snow surface.	2% or 2mph, whichever is greater (this error may be exceeded below 1mph.
4. Incoming short-wave radiation	Eppley Laboratories, Model 2 temperature compensated precision pyranometer.	2%
5. Reflected short-wave radiation	Eppley Laboratories, Model 2 temperature compensated precision pyranometer.	2%
6. Incoming long-wave radiation	Pyrgometer (hemispherical infrared radiometer) with a KRS-5 dome.	6%
7. Precipitation	Alter-shielded universal gauge, 8ft above ground.	mean catch deficiency for snow is about 15%. Based on comparison of nearby gauges, Larson 1972.
8. Snowcover water-equivalent	Snowcourse consisting of 6 sampling points. Adirondack snow tube is used.	0.3" or 3%, whichever is greater.
9. Snowcover depth	Snowcourse and snow stakes.	0.5"

(continued overleaf)

- |                       |                                                                                                         |                                                                   |
|-----------------------|---------------------------------------------------------------------------------------------------------|-------------------------------------------------------------------|
| 10. Snowcover density | Snowcourse<br>500cm <sup>3</sup> CERREL tubes inserted<br>horizontally at intervals in<br>a CERREL Pit. | 0.015 gcm <sup>-3</sup><br>0.02 gcm <sup>-3</sup>                 |
| 11. Snowcover outflow | A pair (East and West) of 10ft<br>diameter snowmelt lysimeters.                                         | Within 10% or 0.05",<br>whichever is larger,<br>on a daily basis. |

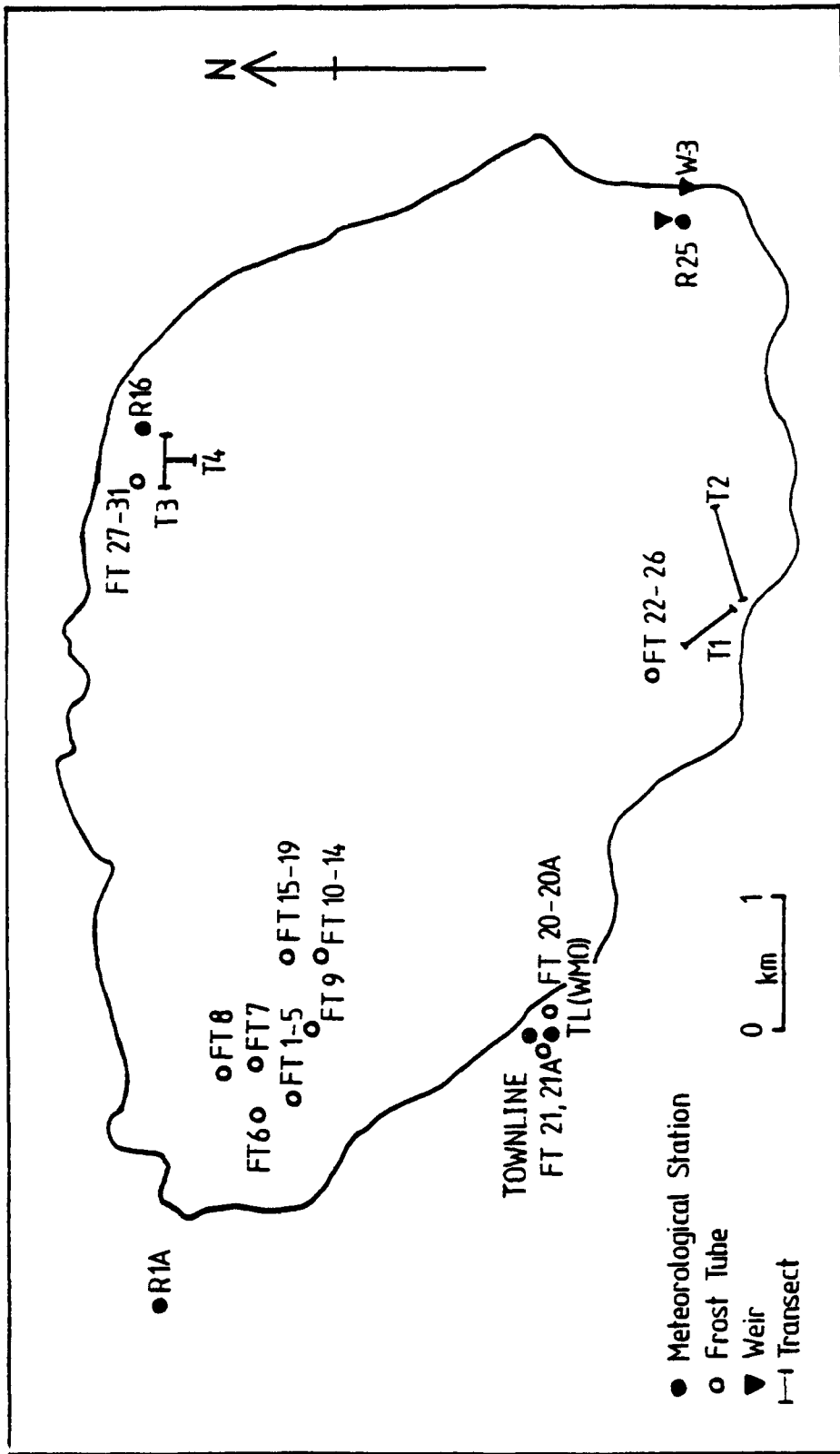


Figure 6.6. Location of frost-tube sites, meteorological stations and transect sites.

(2) Areal data.

The frost-tube programme is operated by UVM with the aim of collecting information on the spatial distribution of frozen ground and the depth to which it is frozen over W3 during the snow season. There are 30 frost-tube sites, chosen on the basis of cover type and elevation, table 6.5. The frost-tube is a section of vinyl tubing, closed at one end which is filled with a Methylene Blue dye solution (0.5 g/litre). This is inserted into a protective access tube which projects out of the ground, above the height of the expected maximum snowfall. The top of the column of Methylene Blue solution is held at the ground/air interface. The Methylene Blue solution changes colour from blue to colourless at 0°C, but does not expand or freeze itself. Therefore to measure the frost depth the vinyl tubing is removed and the change in colour is measured with a ruler. In addition to the frost depth the snowdepth is measured, using a snowtube and a snow stick, at each frost-tube site during the snow season. Snow water equivalent is also measured at the frost-tube sites during the melt period. The frost-tube data is collected weekly.

There are 3 meteorological stations R1A (elevation 2074ft), R16 (elevation 1580ft) and R25 (elevation 1140ft), that can be considered as representative of W3, in addition to Townline. Stations R16 and R25 are within the W3 boundary and station R1A is half a mile outside. Precipitation is recorded continuously, snowdepth and snow water equivalent (a snowcourse) weekly at these stations.

The topography, soils, geology and vegetation cover are all mapped for W3. The vegetation usually requires updating, as clear-cutting is at present occurring within the catchment. Streamflow in W3 is monitored using a V-notch weir and stage recorder at the outflow site, Weir 3 (W-3), and where the main tributary stream joins the Pope Brook, near to W-3.

The catchment W3 was chosen as it fulfils most of the data requirements outlined in section 6.1.3.

**Table 6.5. Frost-tube site characteristics.**

<b>Frost-tubes</b>	<b>Cover type</b>	<b>Elevation (ft)</b>
1-9	Deciduous	2000-1800
10-14	Coniferous	1820
15-19	Mixed	1820
20, 20A	Coniferous	1810
21, 21A	Open (Townline)	1810
22-26	Open (pasture)	1440
27-31	Open (pasture)	1600

(1) Operational data.

Townline provides almost all the operational data requirements (table 6.1). Cloud cover amount and type are not recorded daily but at least weekly. Therefore the value of 5 tenths is used for daily cloud cover amount when the real figure is unavailable and a constant cloud type value is used, as discussed in chapter 4. Chapter 4 also discussed the approach of SNOMO to data extrapolation from a point data source to the computational cells. Air temperature is the only input variable that is extrapolated from the point source and this varies with elevation using a lapse rate. Anderson et.al. (1977) calculated a lapse rate for W3 using data from a meteorological station R12 (now dismantled) outside W3 (figure 6.2) and Townline. A lapse rate of  $-2.6^{\circ}\text{F}/1000\text{ft}$  for maximum air temperature and  $0.6^{\circ}\text{F}/1000\text{ft}$  for minimum air temperatures was determined. However, as discussed in chapter 4 this lapse rate will not be used. Anderson et.al. (1977) concluded that despite the lapse rate because Townline is at an elevation (1810ft) only slightly higher than the mean height of the watershed (1610ft, figure 6.3) that Townline air temperatures would give a reasonable value for the average air temperatures over W3. In addition to variation with elevation air temperature varies with cover type. A short study (Anderson et.al., 1977) was conducted from Feb.- May 1974 to determine the affect of forest cover on air temperature within W3. The air temperature in a very dense grove of spruce trees located 800m SE of Townline was measured and compared with the air temperatures at Townline. The maximum temperature, on average, is 2 to 3 °F cooler and the minimum temperature 1 to 2°F warmer in the forest than in the open. The greatest differences occur when there are clear sky conditions, during overcast conditions the temperature differences are negligible. The largest measured difference in day-time temperature was 9°F cooler in the forest, for night-time temperatures, the largest difference was 6°F warmer in the forest than at the open site. The study concluded that, as dense coniferous cover only occupies a small portion of the cover of W3, that after also considering the effects of elevation, as discussed

above, the Townline air temperatures give a reasonable indication of the temperatures over the whole catchment.

The stations R1A, R16 and R25 cover almost the whole elevation range of W3 and are therefore good indicators of the elevation effects operating on precipitation within W3. Figure 6.7 shows the precipitation-elevation relationship for W3. This relationship is effectively ignored as SNOMO takes the precipitation measured at Townline as representative of that which falls over the whole catchment.

The wind speed and relative humidity are not extrapolated from the point data source and there have been no studies performed at W3 to investigate the areal variation in wind speed or relative humidity

In conclusion, therefore, W3 provides sufficient operational data for SNOMO and, in addition some of the spatial variation of the operational data is known.

(2) Validation data.

W3 provides a lot of the validation data required (table 6.2) and all of the minimum validation data requirements for SNOMO. There are however some deficiencies. The stations R1A, R16 and R25 provide snowcourse data (snowdepth and snow water equivalent) for the snow season and indicate clearly the elevation-precipitation effect. However, they are all located within small forest clearings. Previous studies at W3 (Anderson *et al.*, 1977) have indicated that small forest clearings, i.e. snowcourse sites, tend to accumulate more snow than the surrounding forest. In terms of water equivalent, maximum water equivalent in the deciduous forests was slightly less than in the open and the maximum water equivalent in dense spruce stands was 20-50% less than in the adjacent forest clearing. The small clearings usually become snow-free before the surrounding forest, even though they accumulate more than the surrounding forest. Therefore the depths obtained from snowcourse data from small forest clearings (sites R1A, R16 and R25) must be treated with caution if used as validation tools for SNOMO calculations of the adjacent forest snowdepths. Therefore snowcourses (snowdepth and snow water

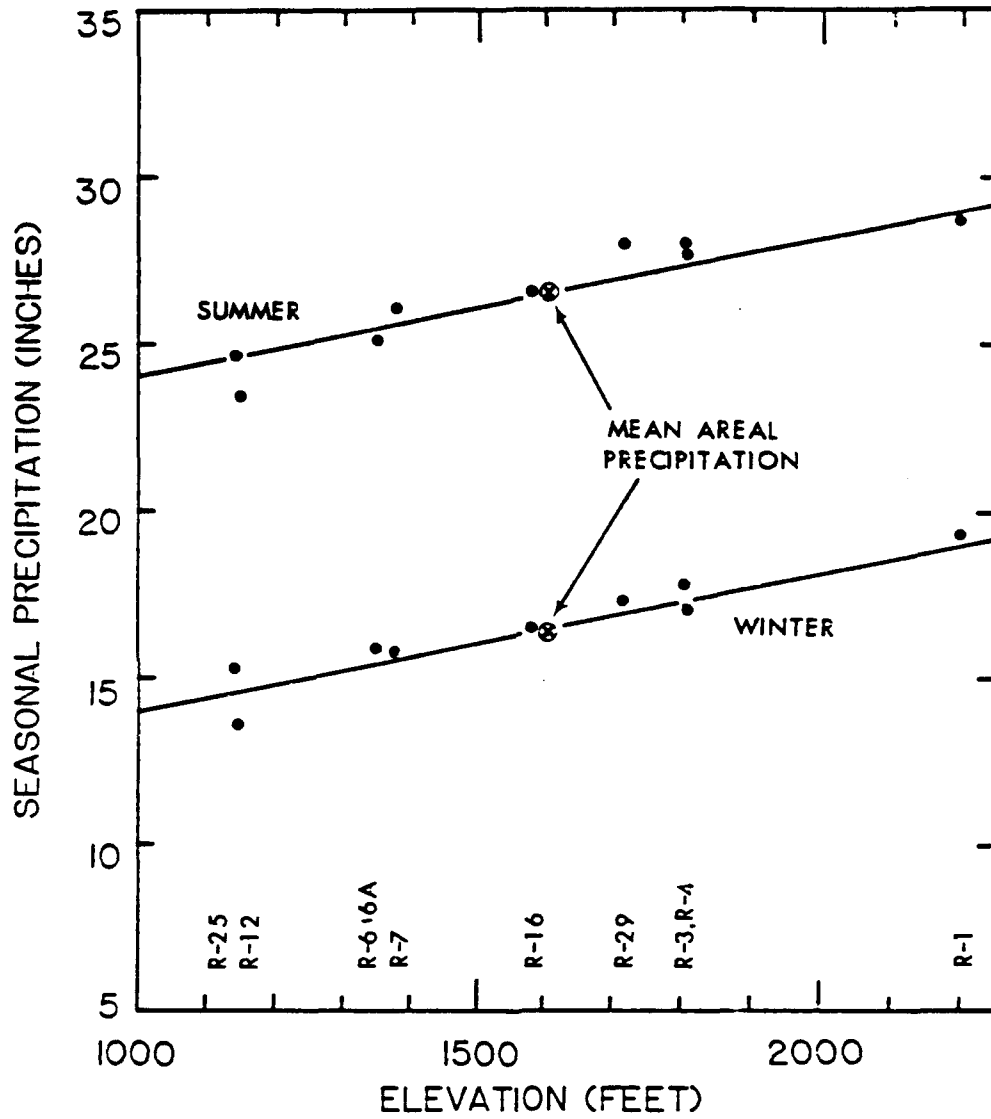


Figure 6.7. Seasonal precipitation-elevation relationships for the W3 watersheds (based on the period from 10/59 to 9/74; winter is November-March and summer is April - October). Anderson *et al.* (1977).

equivalent measurements) are required under the forest canopy. The frost-tube network does provide snowcourse data under the canopy but this is felt to be insufficient for the representation of W3.

No density of snowcourse measurements was specified in the validation data requirements, however it was decided that for validation purposes, and as the primary aim of SNOMO is the simulation of snowcover and snowdepth distribution, more snowdepth measurements were required. A field programme was devised to achieve this.

#### 6.4 Field programme.

The aim of the field programme, as stated above, was to improve the snowcover and the snowdepth distribution data that was available for the validation of SNOMO. The programme occurred over two melt seasons, 1988 and 1989. In both years a series of snowcourse sites were established in the pre-melt period during March. Additionally, in 1988 four transects were established to investigate the intra-cell variation (the micro-scale) of snowdepth and snowcover. The field programme varied slightly from 1988 and 1989 and therefore will be discussed in chronological order.

##### 6.4.1 1988 field programme.

Figure 6.8 shows the locations of the snowcourses as established in 1988, table 6.6, their characteristics. It was decided to measure both snowdepth and snow water equivalent, so as to obtain an accurate snowdepth a snowcore has to be taken (to ensure that the ground/snow interface has been reached or, conversely, to remove unfrozen soil which when coring or using a snow stake can be difficult to distinguish from snow). Once the core is taken it does not take that much extra time to weigh the core for water equivalent. Also, for water balance studies (possibly in the future) the snow

equivalent measurements) are required under the forest canopy. The frost-tube network does provide snowcourse data under the canopy but this is felt to be insufficient for the representation of W3.

No density of snowcourse measurements was specified in the validation data requirements, however it was decided that for validation purposes, and as the primary aim of SNOMO is the simulation of snowcover and snowdepth distribution, more snowdepth measurements were required. A field programme was devised to achieve this.

#### 6.4 Field programme.

The aim of the field programme, as stated above, was to improve the snowcover and the snowdepth distribution data that was available for the validation of SNOMO. The programme occurred over two melt seasons, 1988 and 1989. In both years a series of snowcourse sites were established in the pre-melt period during March. Additionally, in 1988 four transects were established to investigate the intra-cell variation (the micro-scale) of snowdepth and snowcover. The field programme varied slightly from 1988 and 1989 and therefore will be discussed in chronological order.

##### 6.4.1 1988 field programme.

Figure 6.8 shows the locations of the snowcourses as established in 1988, table 6.6, their characteristics. It was decided to measure both snowdepth and snow water equivalent, so as to obtain an accurate snowdepth a snowcore has to be taken (to ensure that the ground/snow interface has been reached or, conversely, to remove unfrozen soil which when coring or using a snow stake can be difficult to distinguish from snow). Once the core is taken it does not take that much extra time to weigh the core for water equivalent. Also, for water balance studies (possibly in the future) the snow

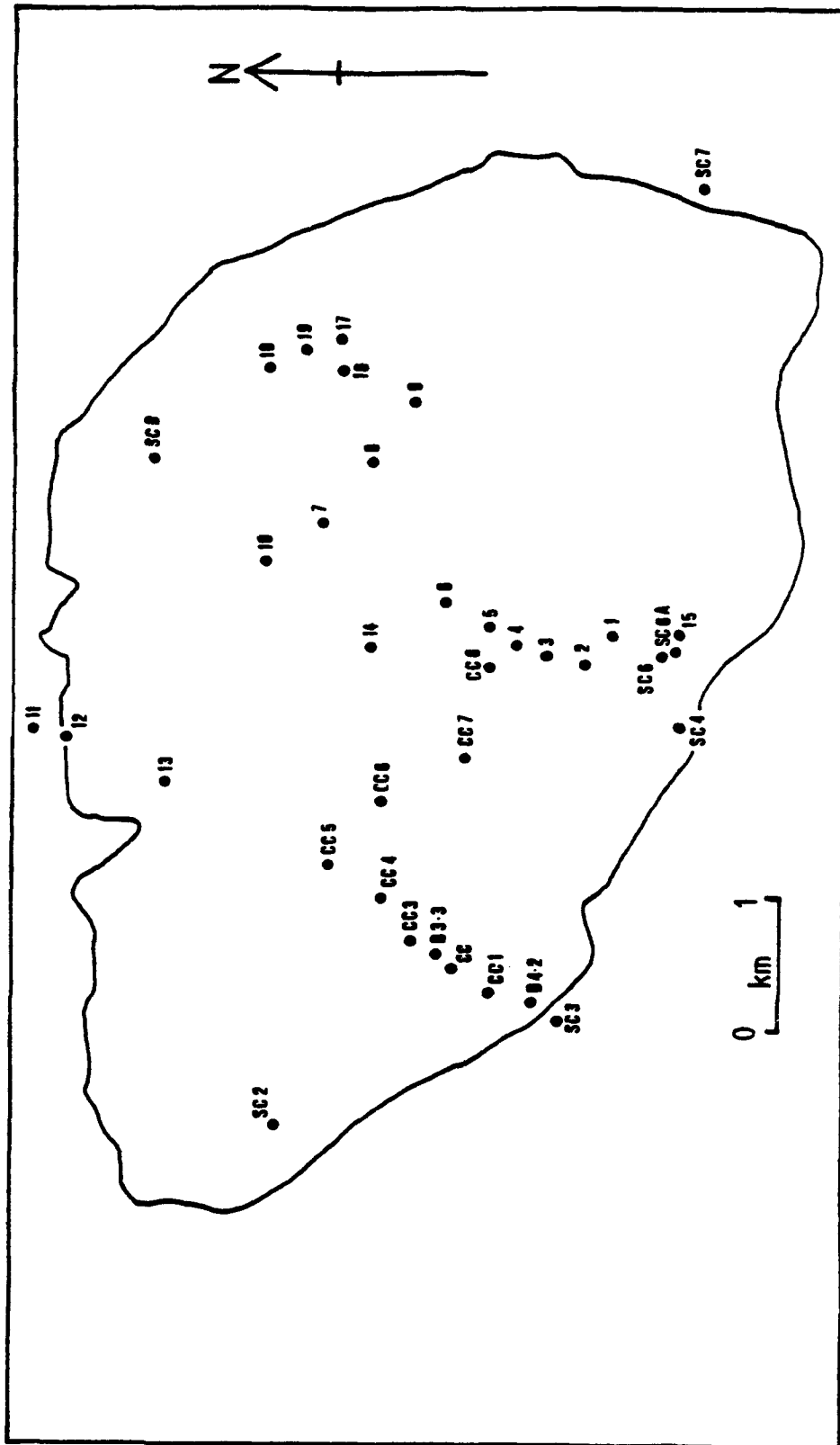


Figure 6.8. Locations of the snowcourses established in 1988 and 1989.

Table 6.6. Snowcourse locations and characteristics used in 1988 and 1989.

1988

Site	Elevation (ft)	Vegetation cover	Comments
R1A*	2074	Coniferous	clearing in forest
R16*	1580	Coniferous	" " "
R25*	1140	Mixed	" " "
Townline*	1810	Open	large grassed met. area
SC2*	2200	Deciduous	under forest canopy
SC3*	1810	Coniferous	" " "
SC4*	1640	Deciduous	" " "
SC6	1460	Open	pasture
SC6A	1460	Open	"
SC7*	1140	Coniferous	under forest canopy
SC9	1600	Open	pasture
B4.2B	1820	Deciduous	under forest canopy
B3.3	1700	Deciduous	" " "

\* used again in 1989

1989

Site	Elevation (ft)	Vegetation cover	Comments
1	1460	Coniferous	under forest canopy
2	1460	Deciduous	" " "
3	1420	Coniferous	clearing in forest
4	1440	Coniferous	under forest canopy
5	1500	Mixed	" " "
6	1600	Mixed	" " "
7	1560	Deciduous	" " "
8	1420	Deciduous	" " "
9	1400	Open	pasture

(continued overleaf)

10	1620	Open	pasture
11	1800	Deciduous	under forest canopy
12	1800	Coniferous	" " "
13	1780	Deciduous	" " "
14	1700	Coniferous	" " "
15	1440	Open	pasture
16	1340	Open	clearing in forest
17	1340	Clearcut <sup>+</sup>	cut in 1988
18	1380	Deciduous	under forest canopy
19	1380	Coniferous	" " "
20	1380	Deciduous	" " "
CC1	1800	Clearcut <sup>+</sup>	cut in 1983
CC2	1740	Clearcut <sup>+</sup>	" " "
CC3	1680	Clearcut <sup>+</sup>	" " "
CC4	1680	Clearcut <sup>+</sup>	" " "
CC5	1700	Clearcut <sup>+</sup>	" " "
CC6	1640	Clearcut <sup>+</sup>	" " "
CC7	1500	Clearcut <sup>+</sup>	" " "
CC8	1500	Clearcut <sup>+</sup>	" " "

+ clearcut modelled as 'open' in SNOMO.

water equivalent is more useful than the snowdepth and the snow density can be calculated from a known depth and water equivalent. W3 was subdivided manually, see chapter 5, and the aim of the program was to obtain a series of snowcourses representing each subdivision or as many as possible. It was hoped to be able to produce a choropleth map of W3 showing snowdepth and water equivalent at weekly intervals throughout the melt season. The snowcourse sites and the frost-tube sites were measured weekly on the same day for three weeks over the melt season with the help of extra personnel. In the intervening days certain snowcourses were measured and the transects were measured. In addition visual estimates of the ground snowcover were made from viewpoints in the catchment. Certain viewpoints enable a large area of W3 to be seen, however it is obviously not very easy to estimate snowcover in this manner in the wooded areas and more inaccessible areas. The aim was to obtain a snapshot of the snowcover and snowdepth conditions over W3 at least once a week during the melt period.

The transects were established in two open field sites, adjacent to SC6A (transects 1 and 2) and SC9 (transects 3 and 4). A bearing was taken across the field and dowels placed at 50 ft. intervals along this bearing. Snowdepths were measured at each dowel using a CRREL snow tube. Depths were measured as often as possible. The aim of the transects was to examine the micro-scale variation of snowdepth and snowcover within a computational cell, this reflects on the validity of SNOMO which uses meso-scale subdivisions as the basis of modelling.

#### 6.4.2 1989 field programme.

The aim of the 1989 field programme was again to improve the snowdepth and snowcover distribution data available to W3. Figure 6.8 shows the location of the snowcourses established in 1989. Some of the snowcourses that were used in 1988 were used again, however it was felt that a greater distribution was required, especially in the north and centre of W3. Snowcourses were therefore chosen (table 6.6) which were considered representative of a certain combination of cover type, elevation and position in the catchment, their integration with the catchment subdivision was not so important. Again the snowcourses and frost-tube sites were measured on a weekly basis, on the same day to obtain a 'snapshot' of the snowcover conditions.

The snowcourses that were established in both years were mostly under the forest canopy. Unfortunately the courses were established in March and therefore the snowpack was present. Ideally the courses should be groomed for forest debris prior to the commencement of the first snowfalls. As this was not done care had to be taken to ensure that a true snowcore was obtained. Even if this is done forest debris falls into the snowpack during winter and becomes incorporated into the snowpack making it difficult to obtain a representative snowcore. The pattern of snowcover distribution at a micro-scale under a deciduous or coniferous forest is variable. The snowdepth is usually shallower near to the tree trunk and in deciduous forests wind related deposition patterns, such as flutes, often occur. Under coniferous cover the snowcover is noticeably shallower under the branches especially if they reach down into the snow. Therefore obtaining and choosing representative snowcourses and snowcourse sites is difficult under forest cover and especially under dense coniferous cover. In addition, the snowpack under dense coniferous forest is usually dense with many ice-layers and frozen at the base, which increases the difficulty of obtaining a good snowcore.

Access to the snowcourse site is another consideration which is

important if many snowcourses need to be measured in a single day. Movement around the catchment during late spring is difficult due to muddy road conditions and soft snow and the time needed to reach each snowcourse needs to be considered. Snowcourses are time-intensive compared to the volume of data acquired. Each snowcourse consists of 5 depth and water equivalent measurements which are averaged to give one representative depth and water equivalent measurement. Therefore 5 good snowcores are required for one representative value. Under dense coniferous forest 5 good snowcores can take a long time to find. Five snowcores are taken in each snowcourse as this is the accepted standard. If one measurement is were taken the micro-scale variation in the snowdepth would cause the measurement to be unrepresentative. An average of 5 measurements from the same area will be more representative. When choosing the snowcourse locations obvious micro-topographic variations, for example slope breaks, drifts, hollows and streams were avoided.

#### 6.5 Discussion.

The results data collected by the field programmes is used and presented in the validation of SNOMO (chapter 7), however some of the implications of this data and the data that was collected but not used for validation are discussed below:

(1) Intra-cell snowcover and snowdepth distribution.

The transect data (figures 6.9, 6.10, 6.11 and 6.12) demonstrate the intra-cell snowcover distribution. The snowcover becomes patchy as was discussed briefly in chapter 2 (section 2.3). The patches relate to surrounding or underlying micro-scale features. For example, the snowdepth 6m along transect 1 is consistently shallower than the rest of the transect, specially when compared to the adjacent depth at 6.3m along the transect. The 6m sampling point was located at the top of an exposed grassy knoll and the 6.3m sampling point at a line of trees in the lee of the knoll. The wind

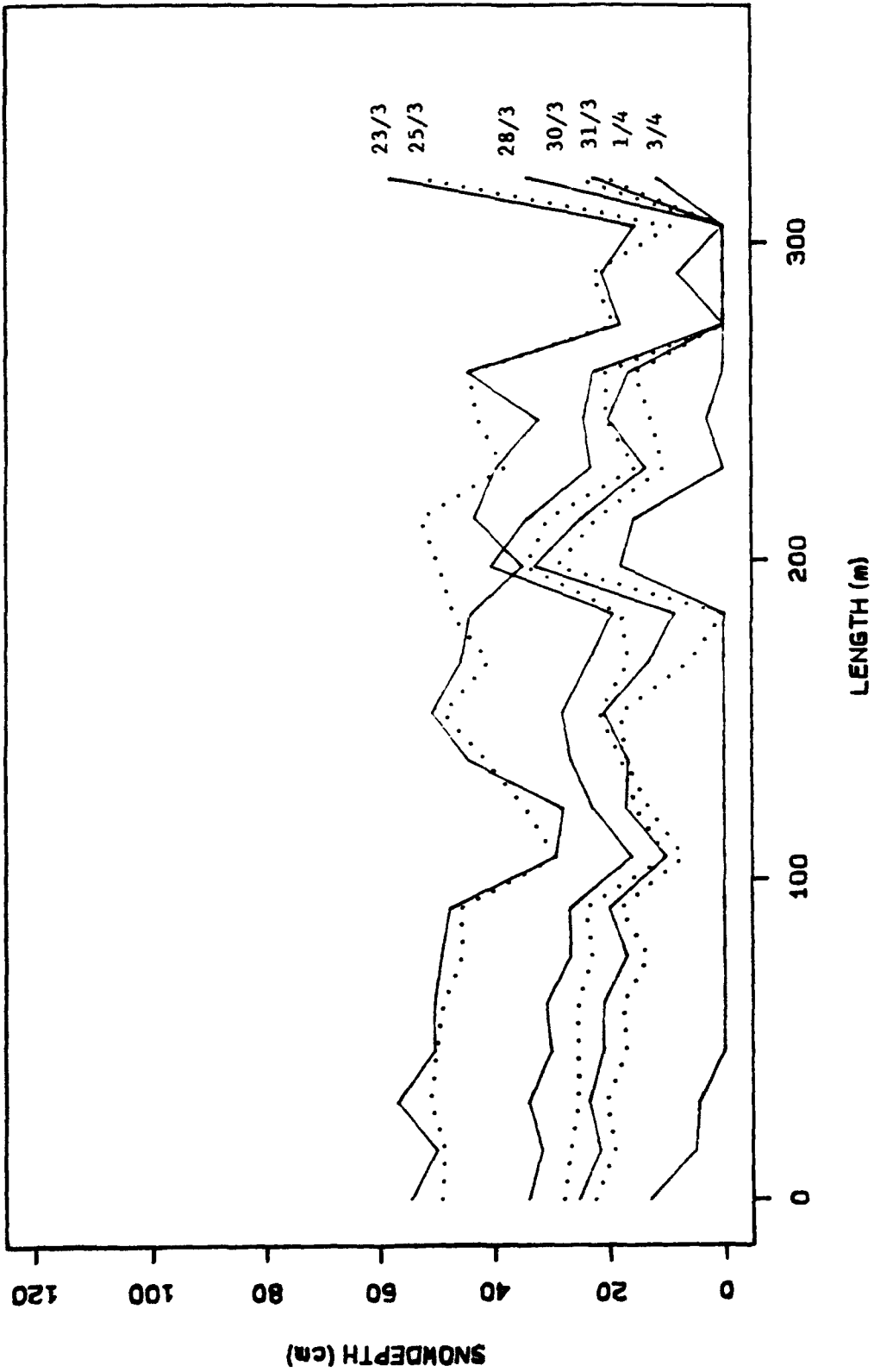


Figure 6.9. Snowdepths, transect 1, 23/3 to 3/4/88.

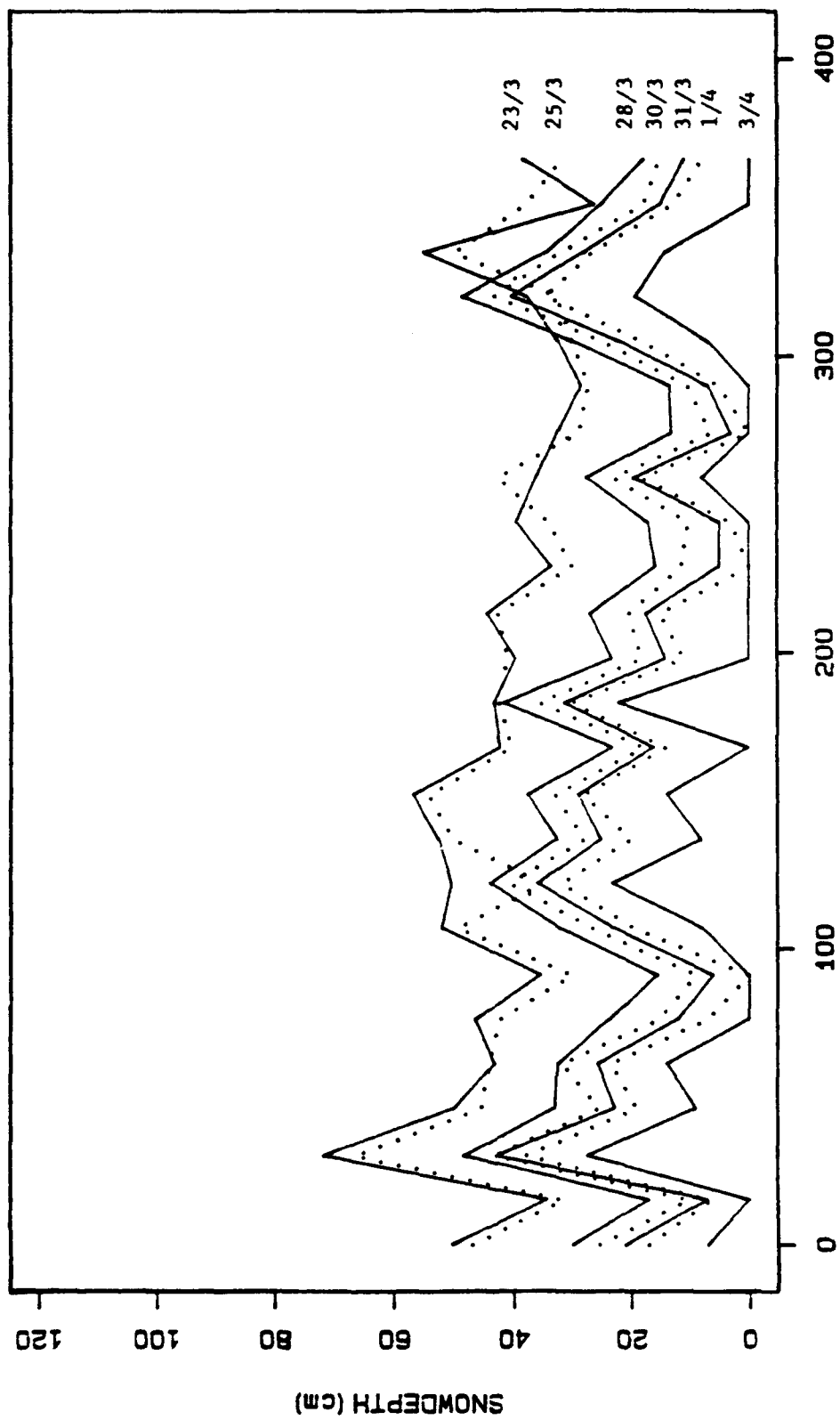


Figure 6.10. Snowdepths, transect 2, 23/3 to 3/4/88.

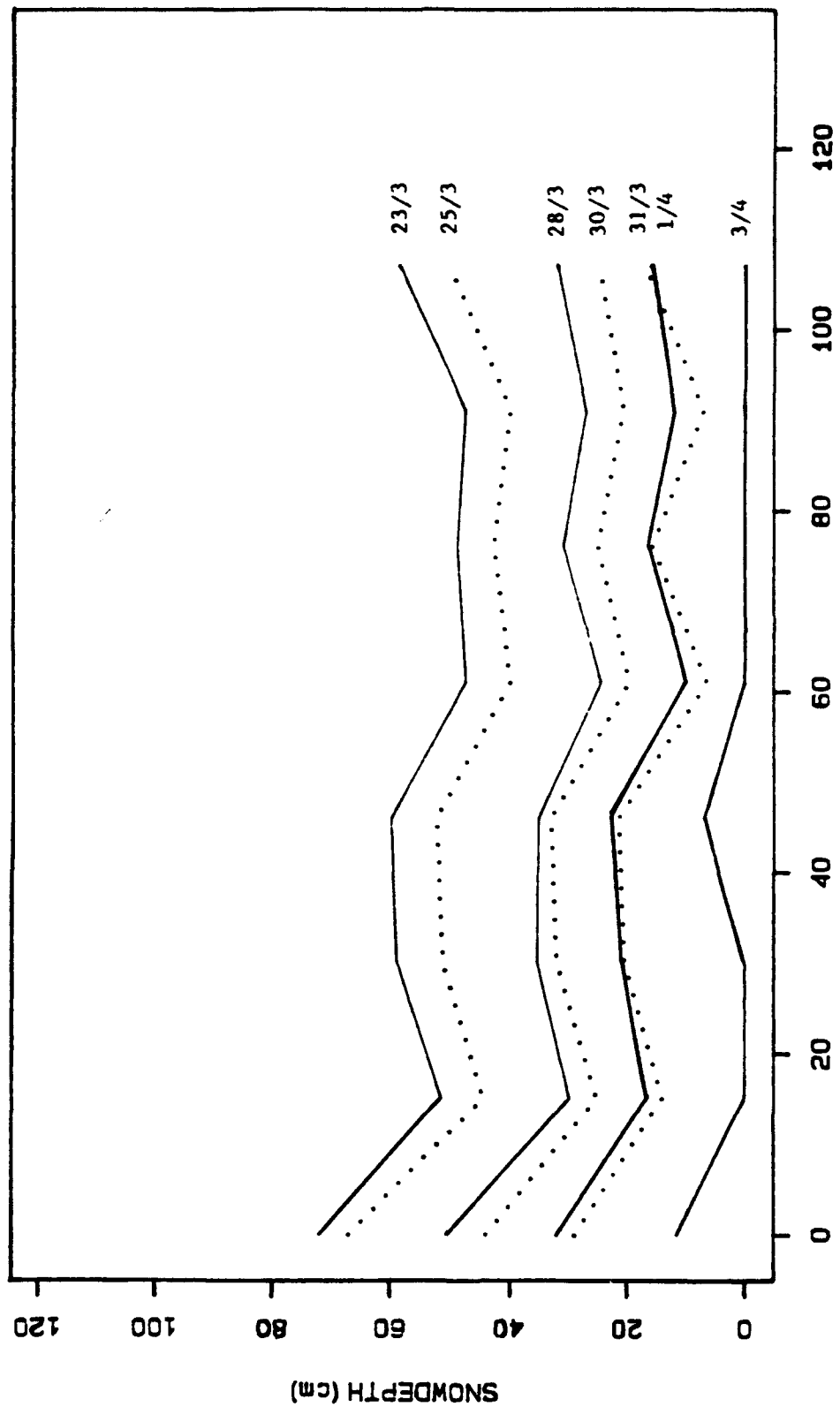


Figure 6.11. Snowdepths, transect 3, 23/3 to 3/4/88.

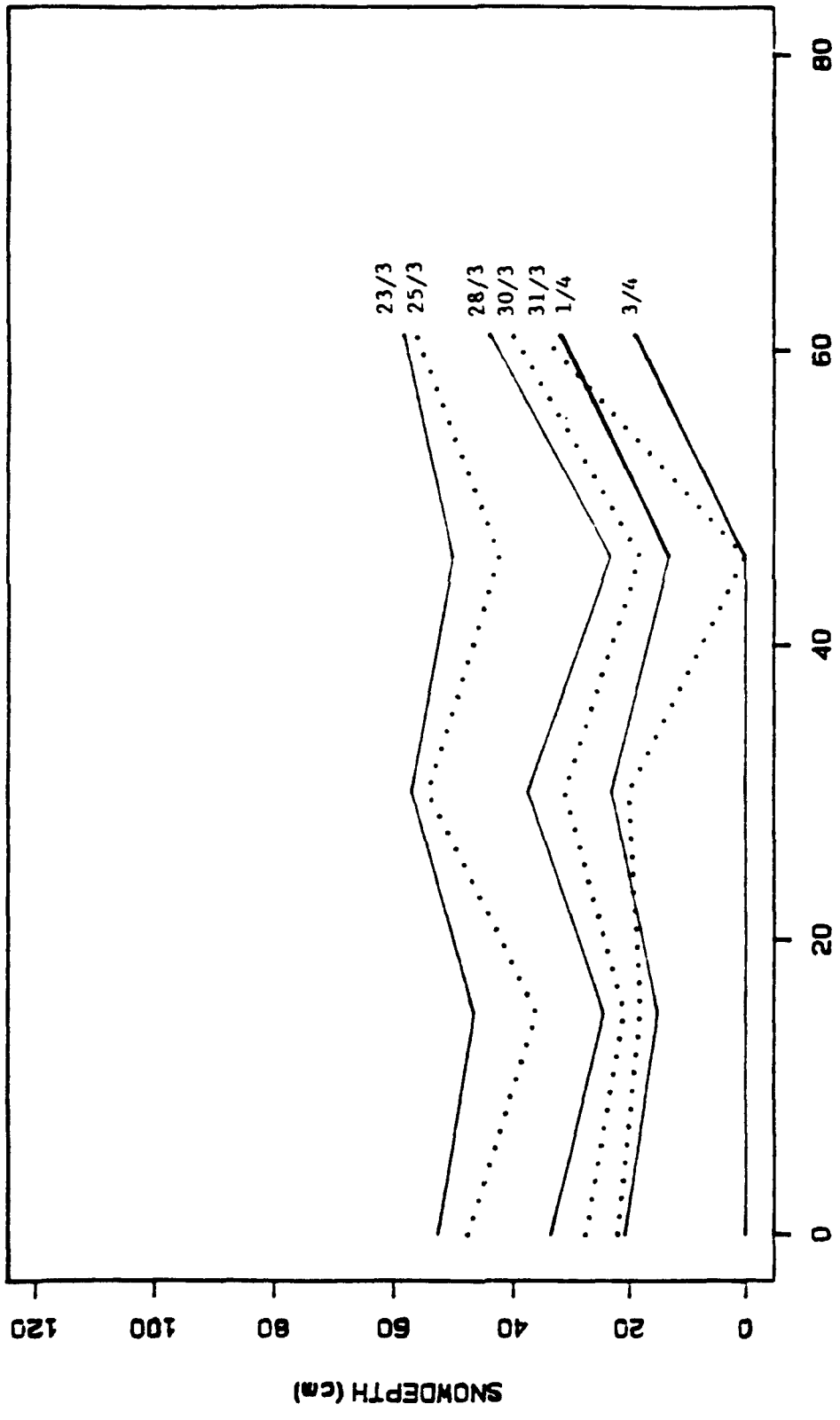


Figure 6.12. Snowdepths, transect 4, 23/3 to 3/4/88.

therefore removed the snow from the exposed 6m position and redeposited it as a drift in front of the trees at point 6.3m. Waveforms and variations in the degree of icing and in snow density can be discerned when sampling along the transects. These relate to the underlying micro-topography. Despite these topographically induced differences the rate of snowmelt seems relatively uniform (transect 3). This suggests that the snowcover patchiness is not caused by varying snowmelt rates but by varying initial snowdepths. There is evidence (Roland, 1984) for increased melting at the edge of patches, due to reflected longwave radiation from the exposed ground surface. The patchiness of a melting snowpack occurs under all cover types. SNOMO assumes a constant melt rate over each computational cell which is in accordance with the transect data, however it also assumes a constant snowcover within the cell. SNOMO cannot model, at present, the patchiness that occurs in the melting snowcover, the snowcover is present or absent (0% or 100% cover).

(2) Snowcourse location and representativeness.

The field programme has highlighted problems that occur in the collection of snowcover or snowdepth data. This data is highly spatially variable and can be highly variable temporally during the peak melt period. Total coverage of the catchment is first unnecessary as SNOMO uses the concept of homogeneous areas within the total catchment area and does not operate on a grid basis, and is secondly impossible due to problems of logistics, manpower and accessibility. Therefore, measurement site locations (snowcourse sites) must be selected that are representative of the conditions that predominate and that are taken as representative of each cell or of a group of cells. The locations must also be accessible in order that they can be reached at all times during the melt period and in order to minimize the manpower required for the data collection. A balance has to be achieved between areal coverage, data representativeness and logistics. For example, a network of snowcourse sites covering a large area is not very useful if these

sites cannot be reached in the course of one day (be this by a single person or groups of people). The ability to collect areal data on the same day, enabling a 'snapshot' of the snowcover and snowdepth distribution on that day is important. Alternative methods of collecting snowcover distribution data are the use of satellite data or aerial and ground reconnaissance and photographic evidence. These methods, with the exception of ground photography and reconnaissance, are relatively expensive and present problems in areas of coniferous forest and other areas with a dense foliage cover.

Once a site has been chosen problems may occur in obtaining a representative snowcore and snowcourse measurement due to the patchy nature of snowcover retreat. The presence of snow patches within a snowcourse creates problems when a representative snowdepth is required. If, for example, 3 out of the 5 snowcourse points were bare of snow and the remaining 2 possessed snowcover. Should the average snowdepth of all 5 points be used, or the average depth of the 2 with snow, or should the depth be zero? It is usual for the average of all 5 points to be used and this was used at W3. This method implies a total snowcover where in reality the cover is patchy. This method corresponds well with SNOMO in that until all 5 points are free of snow a total snowcover will be implied. However, even if the snowcourse is totally snow free this does not necessarily mean that the area it is representing is also totally snow-free. Ideally the snowcourse will represent a median area, melting out at the same time as most of the surrounding area, therefore over-representing the snowcover during early melt and under-representing the snowcover during late melt. These problems are inherent in the measuring of snowcover distribution and snowdepth and in obtaining representative values of these variables. These problems are realised.

### (3) Field programme design

The computer-aided catchment subdivision method described in chapter 5 can be used as an aid in the choice of the location of snowcourse sites and therefore is an aid in the design of the field programme. The 1988 and 1989 field programmes were devised without the aid of the catchment subdivision used in the operation and validation of SNOMO and that is described in chapter 5. If the establishment of a field programme to obtain representative snowcourse data is required and the location of the snowcourse sites is uncertain then the identification of unique homogeneous units is useful. A scheme such as Stepphun & Dyck (1974) is envisaged. Stepphun & Dyck (1974) suggest subdividing the catchment into homogeneous landscape units. This is done manually, and then a series of snowcourses is selected randomly within each landscape unit. Each snowcourse consisted of 36 sampling points where only snowdepth was measured using a snow stake.

To summarise, SNOMO requires both validation and operational data. This data is available at the W3 catchment and this was chosen as the initial test catchment for SNOMO. However, the catchment needed more snowcover and snowdepth distribution data than that already present. A field programme was devised for the melt periods in 1988 and 1989. The field programme has collected the data required but, in so doing, has highlighted some of the problems inherent in the modelling and measuring of snowcover and snowdepth distribution. In addition the potential utility of SNOMO and the catchment subdivision algorithm that SNOMO utilizes in formulating the field data collection programme has been identified. This is discussed in more detail in the following chapter.

## CHAPTER 7: MODEL VALIDATION II: RESULTS AND DISCUSSION

### 7.1 Introduction.

Chapter 6 discussed the procedure of model validation, the data required for the validation of SNOMO and the field programmes that were initiated for the collection of some of this data. This chapter discusses the implications of the data collected by these field programmes and the results of the validation of SNOMO. Section 7.2 examines the distribution data collected and its variability and discusses this data with relation to its use in both the point and spatial validation of SNOMO. Problems in validation data acquisition are highlighted. The validation data is then compared with the results of the SNOMO simulations (section 7.3) at both the point and catchment scales. The results of the SNOMO simulations at the point scale are investigated in detail in section 7.4. The implications of both the point and catchment scale simulation results for model and field programme design are then discussed in section 7.5.

### 7.2 Snowcover and snowdepth distribution data.

The distribution of snowcover and snowdepth is variable both temporally and spatially. This variation can be quantified and demonstrated in the field by an examination of both point snowdepths and areal patterns of snowcover and snowdepth distribution. A large amount of data was generated by the two field programmes discussed in chapter 6. The results of an examination of some of the data collected are given below. The data can be viewed in point form or in a lumped, areal manner. Areal relationships can however be determined from the point data.

### 7.2.1 Point data results.

The pattern of snowcover and snowdepth distribution can be explained by:

(1) Variation with vegetation cover.

Figures 7.1, 7.2 and 7.3 demonstrate the variation in snowdepth with vegetation cover type. Figure 7.1 demonstrates that in the pre-melt stage the largest snowdepths are found under deciduous forest cover and the smallest under the open vegetation cover type (pasture in this example). However, as the melt progresses the largest snowdepths occur under mixed and lastly coniferous vegetation cover. Snowcover disappears totally first from the open and then the deciduous forest vegetation covers. The coniferous forest cover remains with the largest snowcover when the snow has gone from the open and deciduous sites and has nearly (3cm) disappeared from the mixed forest site.

Figure 7.2 reinforces this relationship. Sites 1 and 2 are within 50m of each other and have the same slope angle, aspect and elevation. Vegetation cover is the sole factor that explains the variation in snowdepths between the two sites. Figure 7.3 demonstrates a variation in snowdepth between an open site, pasture (FT 22-26) and a clear-cut site (CC8). These two sites are not adjacent but are of roughly the same elevation, aspect and slope angle. The snowcover is shallower at the open site than at the clear-cut site. This relationship has been noted elsewhere in the catchment where bare ground has always appeared first on the pasture areas and then the clear-cut areas. SNOMO models open and clear-cut areas together and it could be argued that these areas should be modelled separately.

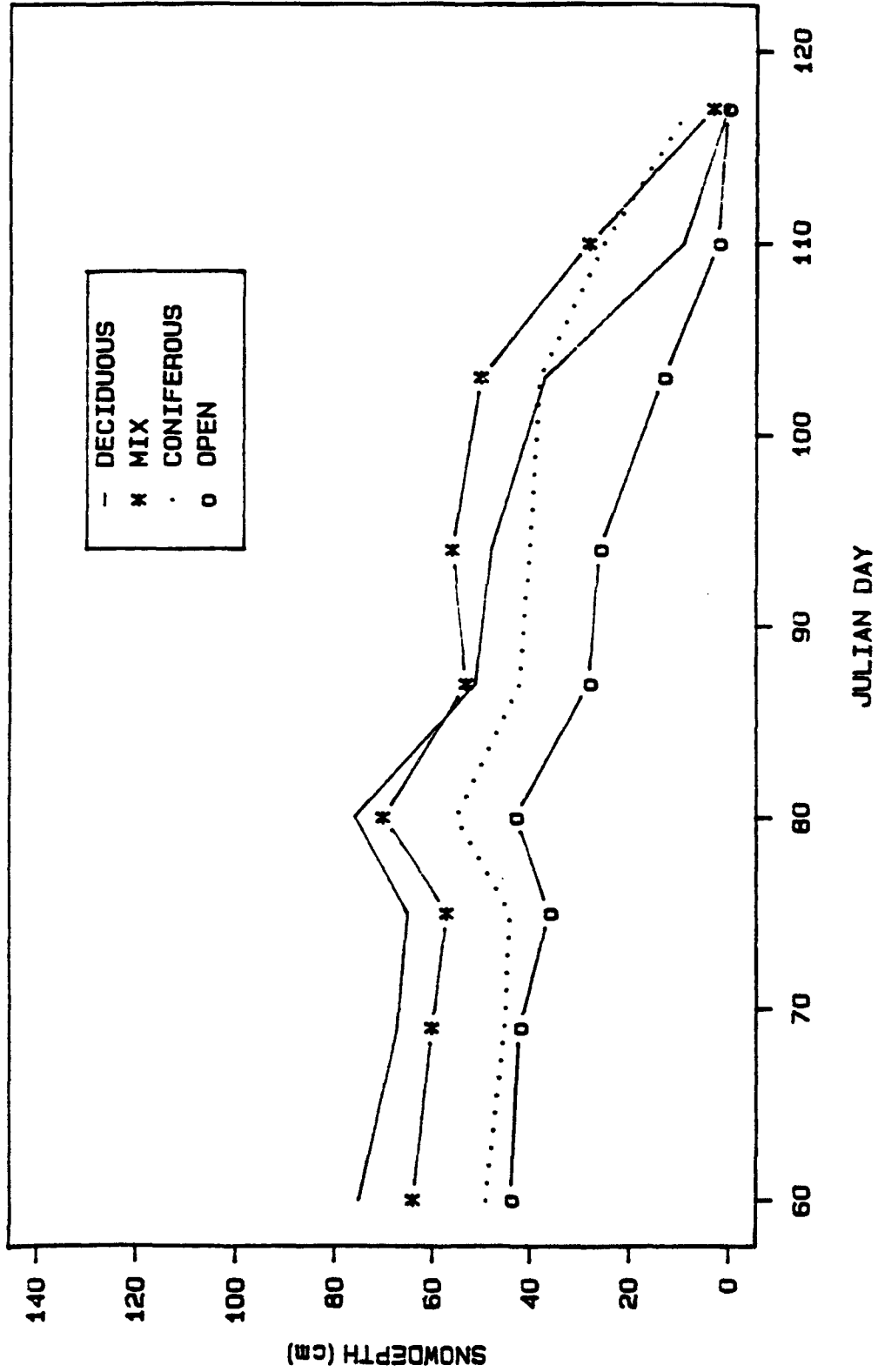


Figure 7.1. Variation in snowdepth with vegetation cover, W3, 1989.

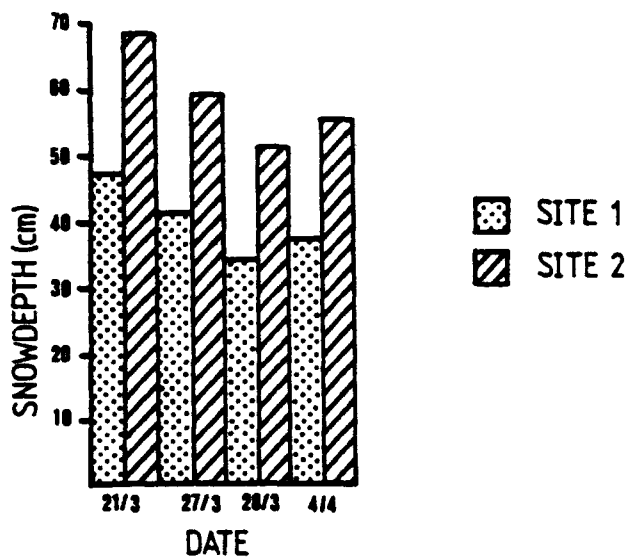


Figure 7.2. Snowdepths at snowcourse sites 1 and 2, 21/3 to 4/4/89.

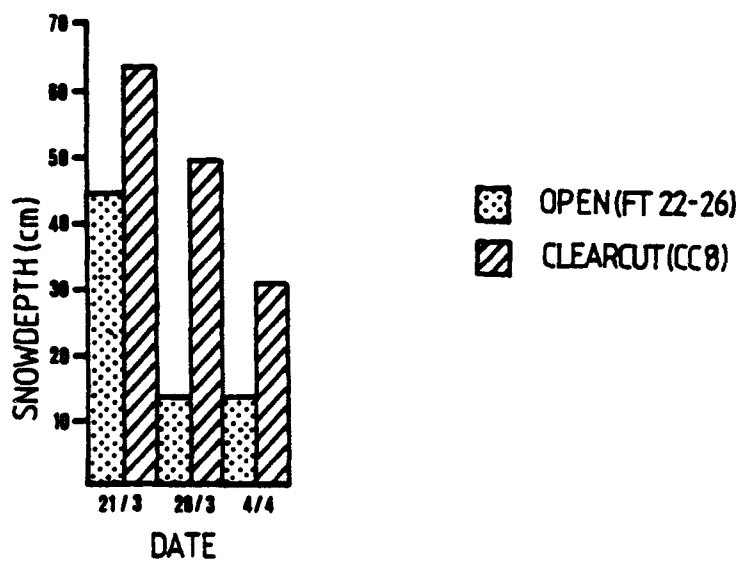


Figure 7.3. Snowdepths at frost-tubes 22-26 and clear-cut site CC8, 21/3 to 4/4/89.

(2) Variation with elevation.

Figure 7.4 shows the variation in snowdepth with elevation for the year 1988-1989. The three snowcourse sites R1A, R16 and R25, with elevations of 2074ft(632m), 1500ft(482m) and 1140ft(347m) respectively, are all small, flat clearings within mixed forest. Therefore the effects of variations in vegetation cover, slope angle and aspect are thought to be negated. The increased accumulation due to the affect of a small forest clearing (chapter 6) is assumed to be constant at each site. Figure 7.4 indicates that there is a steady increase in snowdepth with elevation, with roughly 10cm separating the low from middle and the middle from high elevations.

(3) The relative dominance of the factors affecting snowcover and snowdepth distribution.

Photographs 10 and 11 demonstrate the relative dominance of the factors influencing snowcover and snowdepth distribution. In photograph 10 snowcover is absent from the gently sloping pasture whereas the SE facing slope, covered in deciduous trees still possesses a snowcover. Here, vegetation cover is seen as the dominant factor affecting snowcover distribution. Photograph 11 shows a steep SE facing slope and a flat area at the foot of the slope, both under deciduous forest cover. The slope is devoid of snow whereas the flat area still possesses a snowcover. Here, under a uniform vegetation cover, slope angle and aspect are seen as the dominant factors affecting the distribution of snowcover.

The field data therefore appears to validate the criteria used in the spatial subdivision of the catchment, ie. slope angle, aspect, elevation and vegetation cover. At the scale of the subdivision cells the factors of vegetation cover and elevation would appear to be dominant. Slope angle and aspect appear to become important at a smaller, within uniform vegetation cover, scale. It is expected that in a situation such as a glaciated alpine valley factors such as aspect will become dominant and will reinforce and indeed be the

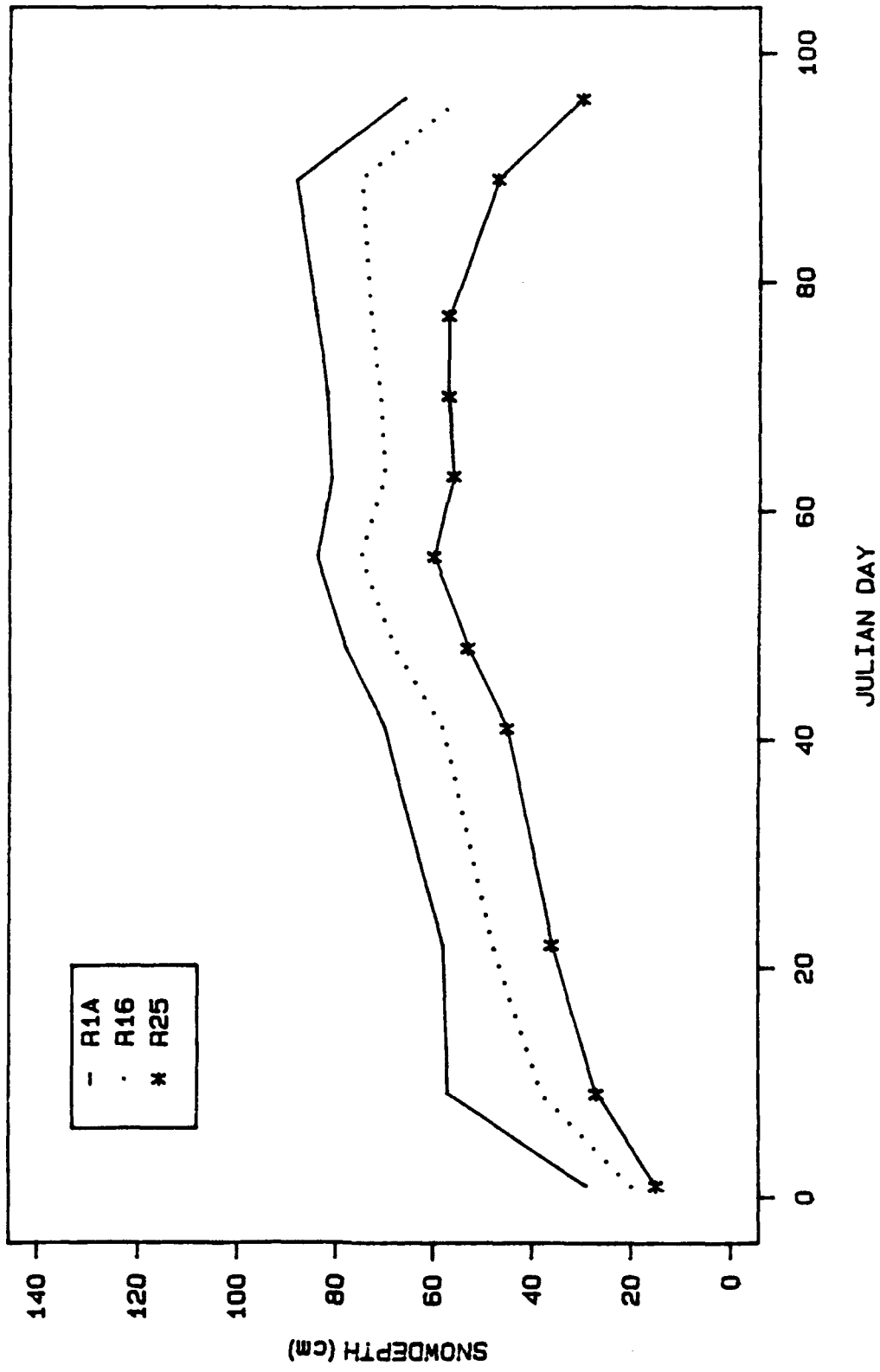


Figure 7.4. Variation in snowdepth with elevation, W3, 1989.

①



Photogra

Photograph 11. W3 catchment, 6 April 1988, slope angle and aspect control over snowcover distribution.



2

3



Photograph 10. W3 catchment, 7 April 1988, vegetation control over snowcover distribution.



cause of vegetation cover type change (Price, 1981). However, at W3 the aspect and slope angle variations are not so great and therefore these factors assume lesser importance at the cell scale.

The point data also demonstrate:

- (1) The variation of the snowcover and snowdepth at the micro-scale.

Figure 7.5 demonstrates the variation that can occur within the 5 sampling points used for a snowcourse. Figure 7.5a shows that the snowdepth at point 31 is consistently greater than that at the other 4 points and with the exception of the 21/3/89 and the 27/4/89 this discrepancy is large. The range of values of the remaining 4 points is also fairly large. The 5 values are averaged to obtain a value representative of the snowcourse. An awareness of this variation is useful when this value is used to validate SNOMO. It must be remembered that the field results used to validate SNOMO are mean values taken from a snowpack that is inherently variable at the micro-scale (the scale at which the value was measured).

The micro-variation in snowdepth is due to the accumulation pattern of the snowpack. The accumulation pattern appears to vary from year to year at this site. Figure 7.5b shows the snowdepths at the same points in 1988. In this year the range of snowdepths for the 5 points is much smaller and the four points 27,28,30 and 31 match very closely. Point 29 is the rogue point in 1988, not point 31, the depths at point 29 being consistently shallower than the remaining four points. Longer term studies would have to be made in order to determine the recurrence of the different accumulation patterns.

- (2) The patchy nature of snowcover retreat.

Photographs 12, 13 and 14 demonstrate the patchy nature of snowcover retreat. There is a gradual disappearance of snowcover not a sudden switch from 100% to 0% snowcover. The pattern of this disappearance is related to the underlying microtopography and the accumulation pattern of the snowcover. For example, bare ground

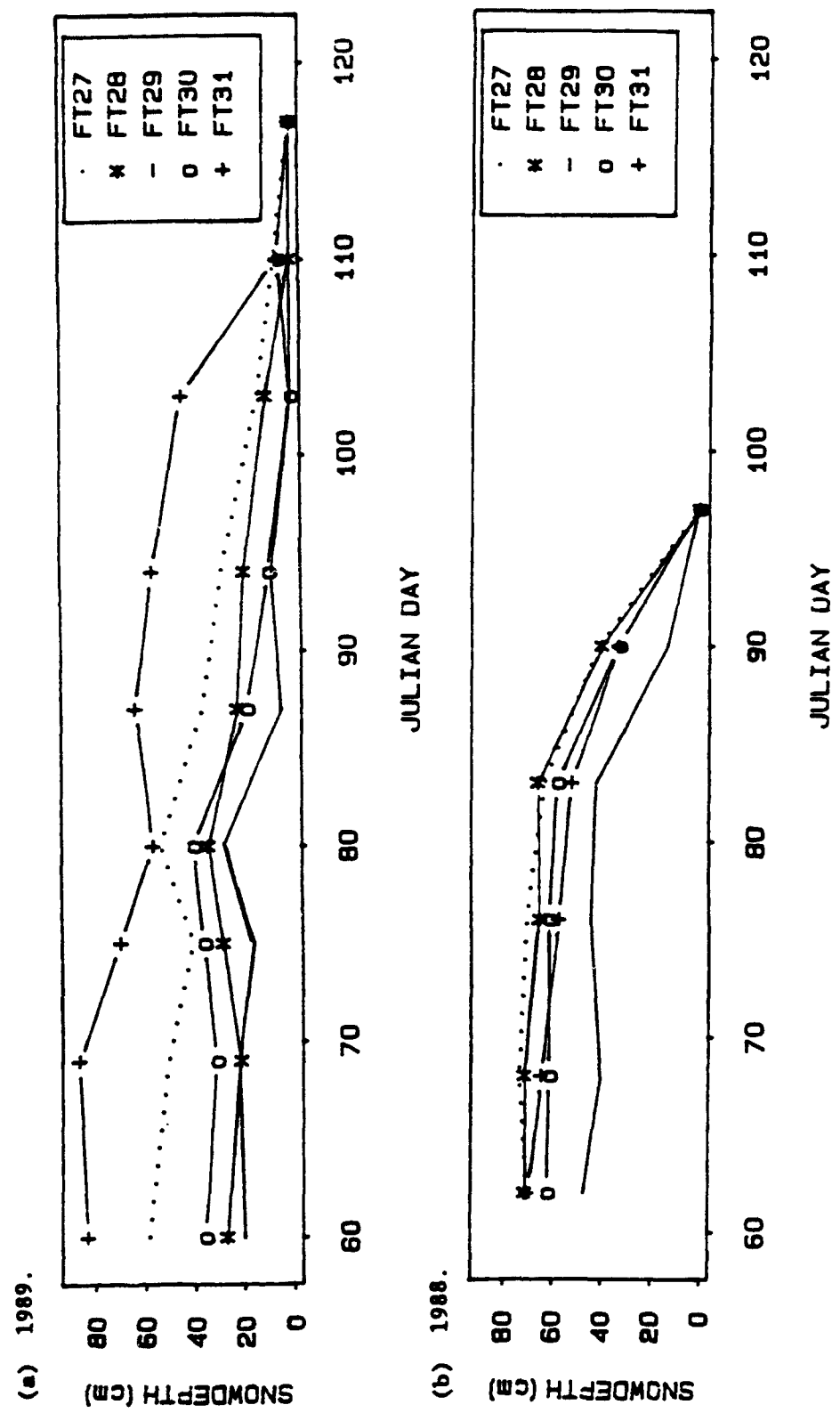


Figure 7.5. Snowdepth at 5 adjacent frost-tube sites.



Photograph 12. W3 catchment, transect 1 and SC6A. 25 March 1988.



Photograph 13. W3 catchment, transect 1 and SC6A. 31 March 1988.



Photograph 14. W3 catchment, transect 1 and SC6A, 3 April 1988.

first appears at the top of the knoll in photograph 12. This area has the shallowest snowcover due to exposure to the wind and is the most exposed to the sun. The knoll area melts out first (photograph 13) still leaving 100% cover on the surrounding, flatter areas. Finally (photograph 14), bare ground has appeared on the surrounding areas as well as the knoll, however micro-hollows on the knoll still remain snow covered and patches of snow survive in the surrounding area. These snow patches relate to the micro-topography and to areas of wind-compacted snow.

Photographs 12, 13 and 14 demonstrate the problem of scale and data collection with relation to the validation of SNOMO. The snowcourse SC6A can be seen in the left of the photographs and the photographs encompass roughly 50% of the pasture area in cell 24. At the micro-scale it can be seen that there is variation of the snowdepth at each sampling point along SC6A. This is especially noticeable in photograph 14. The snowcourse points will be represented by a mean value which is taken as representative of the open area in cell 24. However, if SC6A were positioned at the crest of the knoll, snowcover disappearance and snowdepth values would have been very different. The position of SC6A is taken as representative of the whole area within the photograph. The attributes of cell 24 are predominantly open/clear-cut but in reality clear-cut predominates, not pasture. Therefore the utility of extrapolating the snowdepths measured at SC6A to the whole of cell 24 is doubtful.

The consideration of the point snowdepth measurements in their spatial context aided the calculation of the initial snowdepth input. The snowdepth measured at the Townline meteorological station was taken as the base snowdepth from which the cell values were calculated. The cell values were calculated using the following relationships (in centimetres from the Townline snowdepth):

- (1) Cell with elevation <1500ft, -10cm
- (2) Cell with coniferous forest vegetation cover, -5cm
- (3) Cell with mixed forest vegetation cover, +5cm
- (4) Cell with deciduous forest vegetation cover, +10cm

Therefore, if the snowdepth measured at Townline was 70cm then the initial snowdepths for cells 1, 2, 22, 24, 19 and 15 would be 65, 60, 80, 70, 65 and 75 respectively. These relationships are very broadly based (they have not been examined statistically) on the point snowdepth measurements and the spatial context of these measurements. It is realised that this technique requires refinement but it is an improvement upon the use of a constant initial snowdepth that does not account for spatial accumulation differences.

#### 7.2.2 Spatial data results.

Figures 7.6, 7.7 and 7.8 show the results of the visual estimation of snowcover distribution conducted in spring 1988. The visual estimation of snowcover is effected by the perception of the catchment made by the operator conducting the estimation. Open areas, because they are easier to view and in W3 are more accessible than forested areas, become more important and dominant in the eyes of the observer. Accessibility decreases as melt progresses and makes access to dense forested areas the most difficult during the most critical time for observation. Areal snowcover estimation under dense forest cover is difficult. The patchy nature of the snowcover distribution during melt is another problem affecting the estimation process. For example, an estimation of the percentage snowcover in the area in photograph 15 is not easy. If that area were under forest (such as photograph 11) estimation would be even harder.

For the purposes of the validation of SNOMO it is considered that this method of visual estimation is subject to too many inaccuracies and problems of observer accessibility and preconceptions.

Figures 7.9, 7.10 and 7.11 show an alternative method of describing the pattern of snowcover and snowdepth distribution. However, the figures (snowdepths) are not easily interpreted unless referenced back to the vegetation cover that is present at the sites

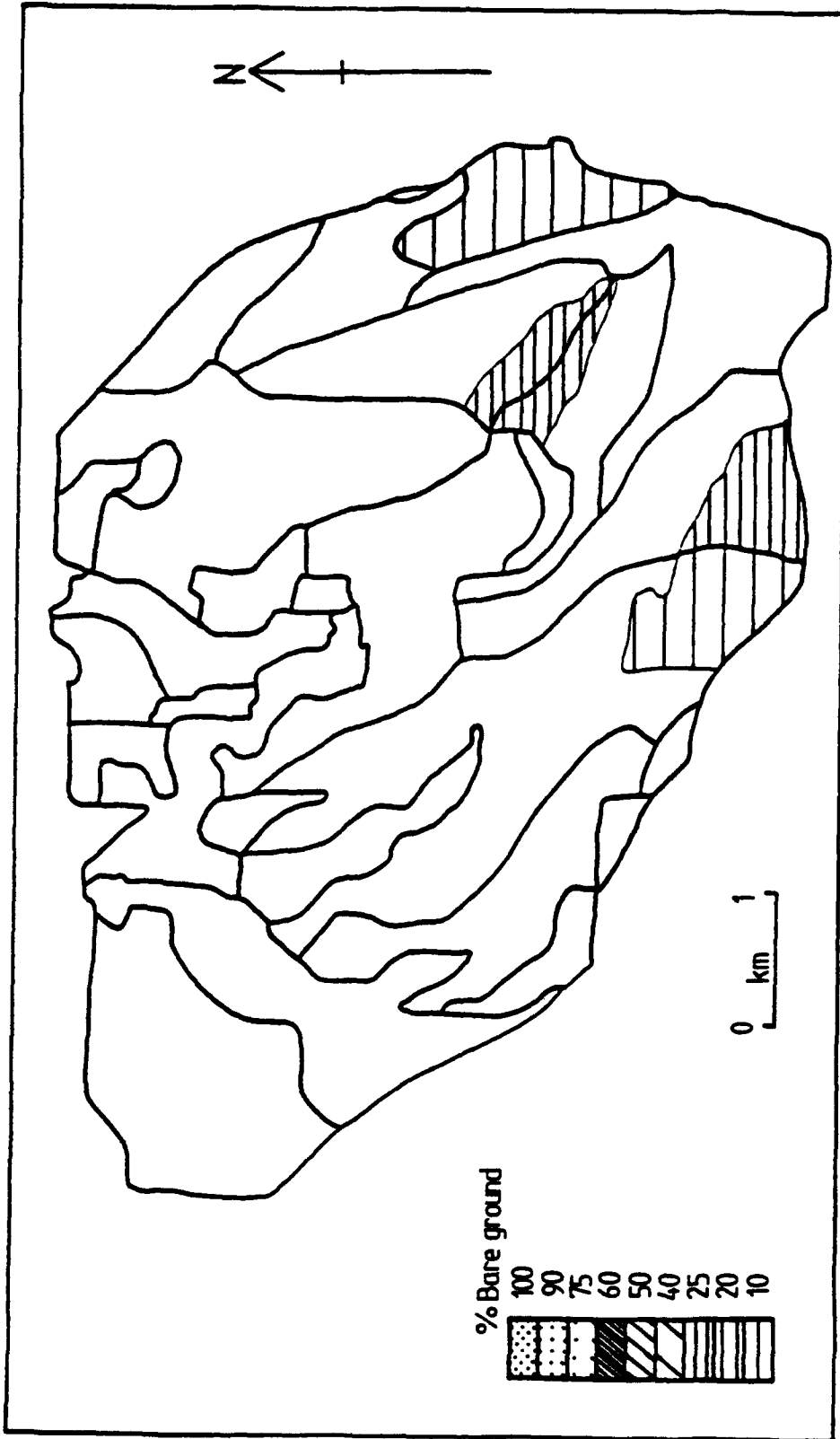


Figure 7.6. % bare ground visible, W3, 30/3/88 (Julian day 90).

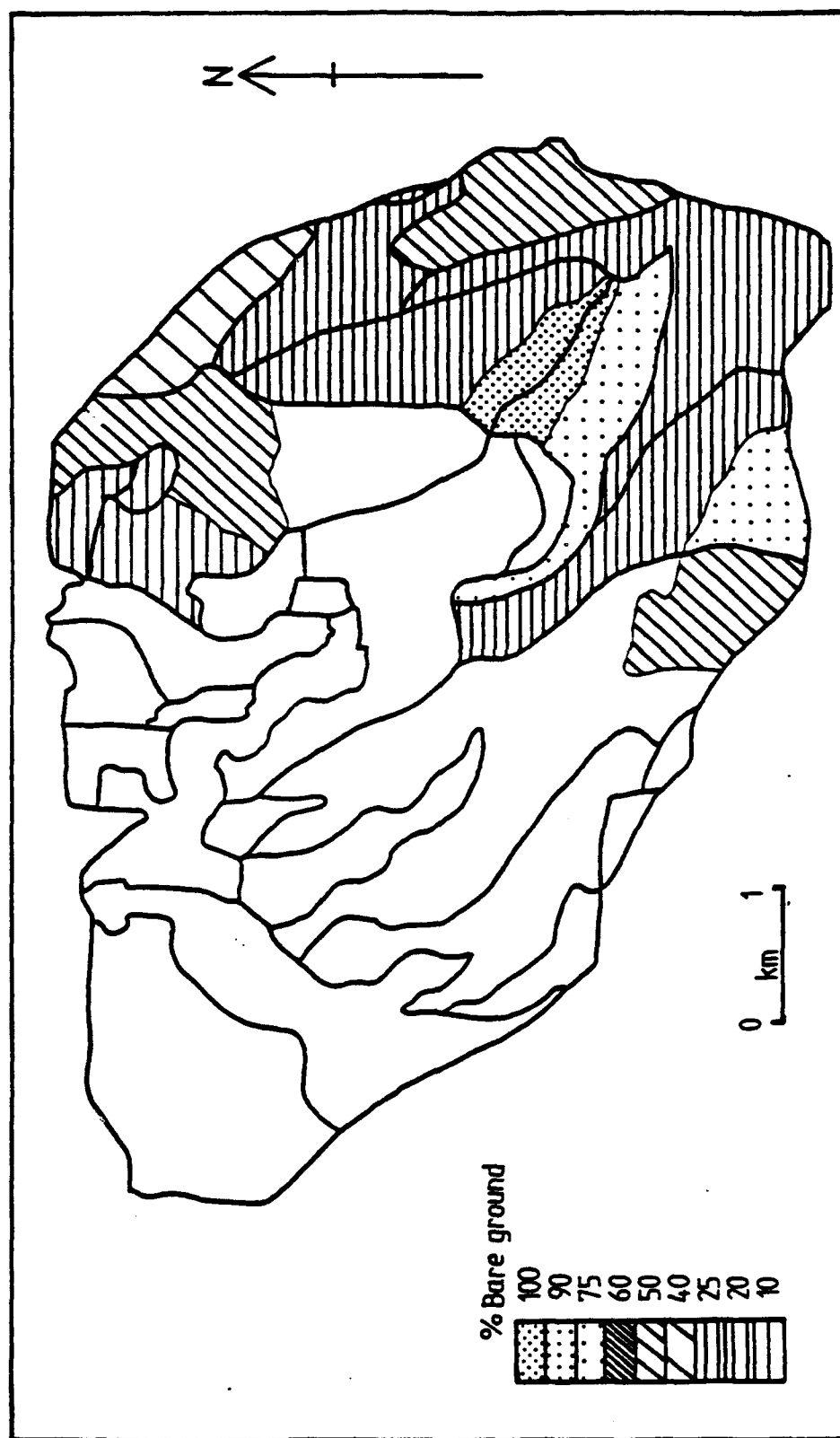


Figure 7.7. % bare ground visible, W3, 3/4/88 (Julian day 94).

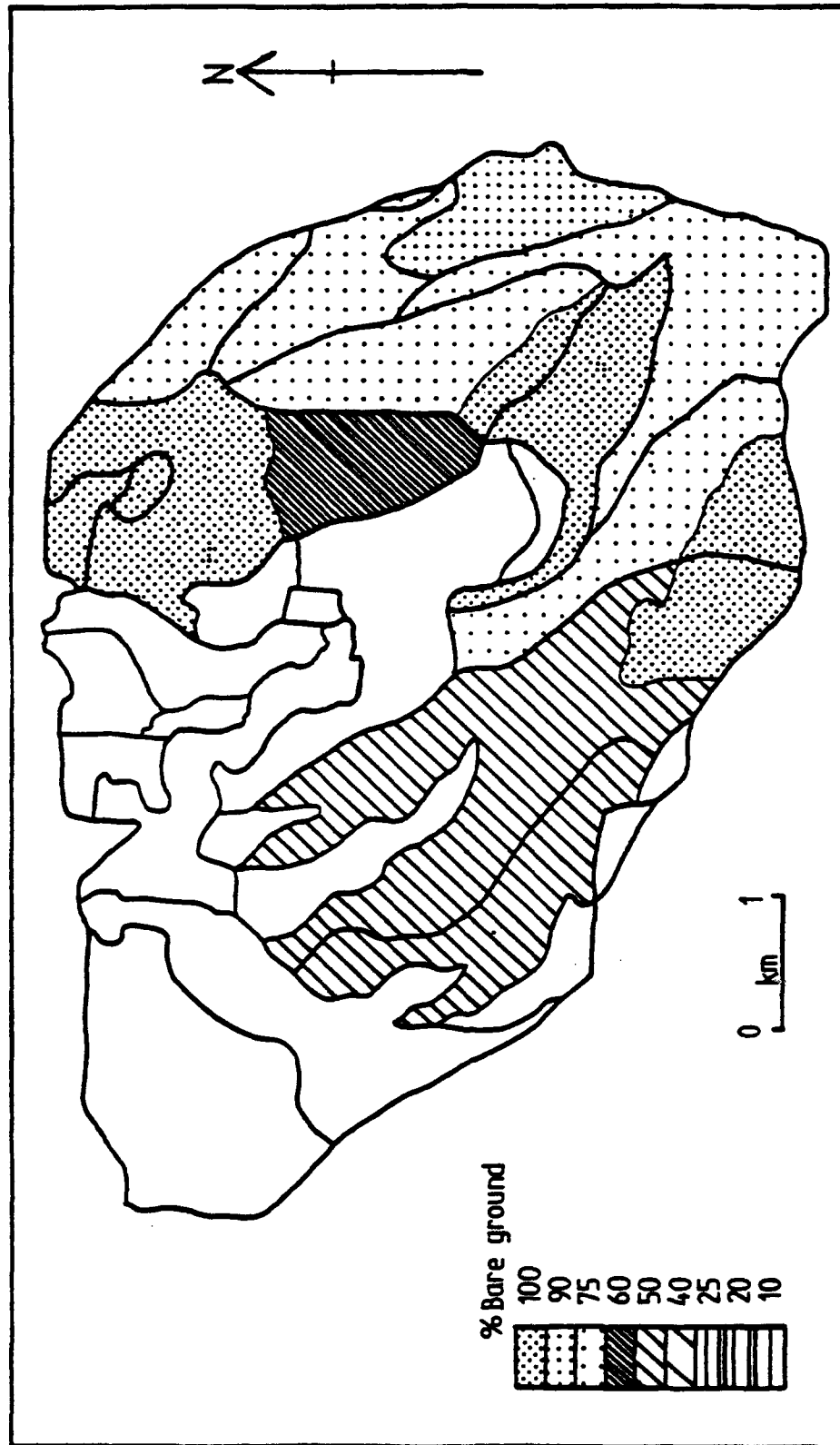


Figure 7.8. % bare ground visible, W3, 6/4/88 (Julian day 97).

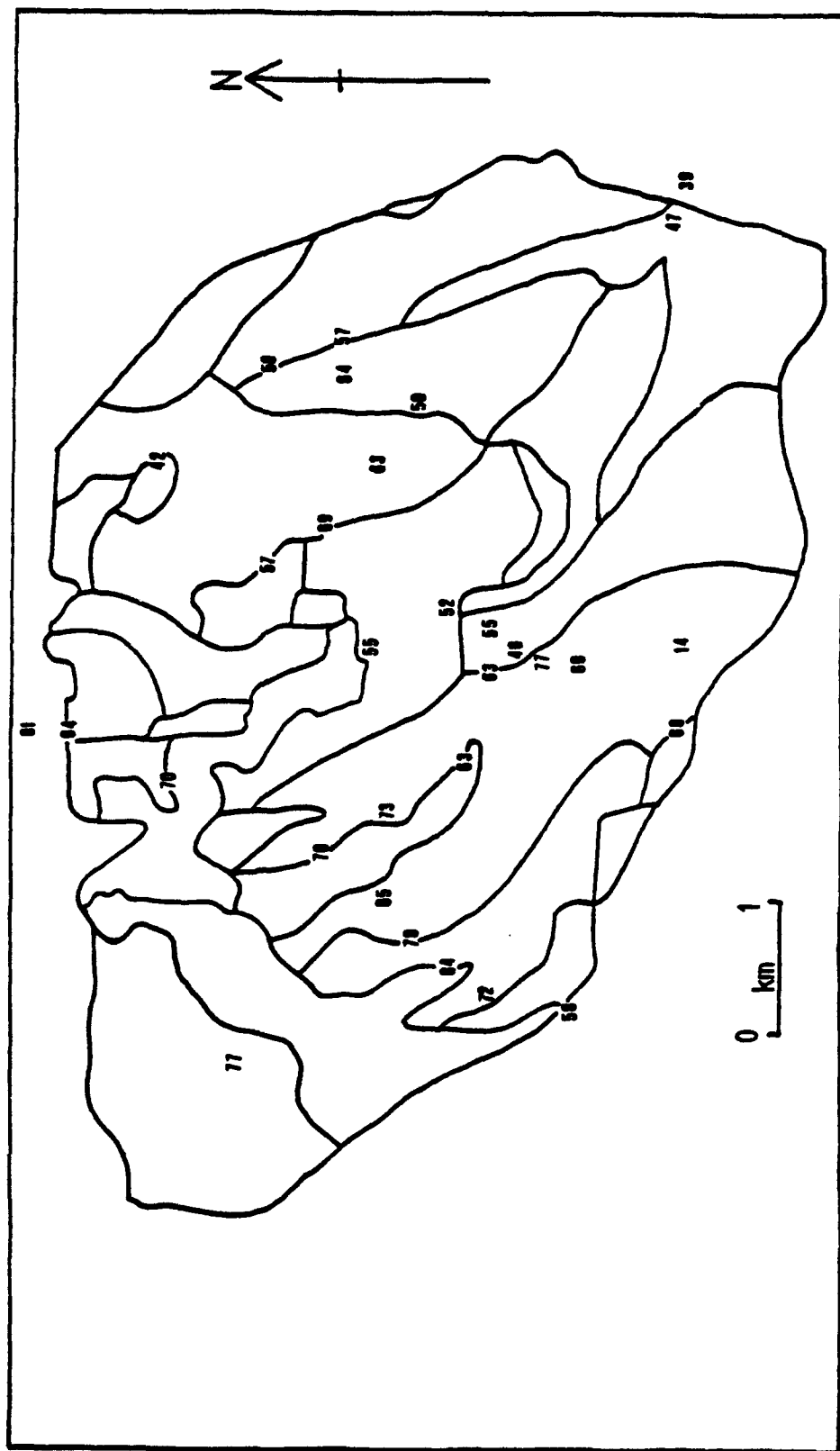


Figure 7.9. Measured snowdepths, W3, 21-23/3/89 (Julian days 80-82).

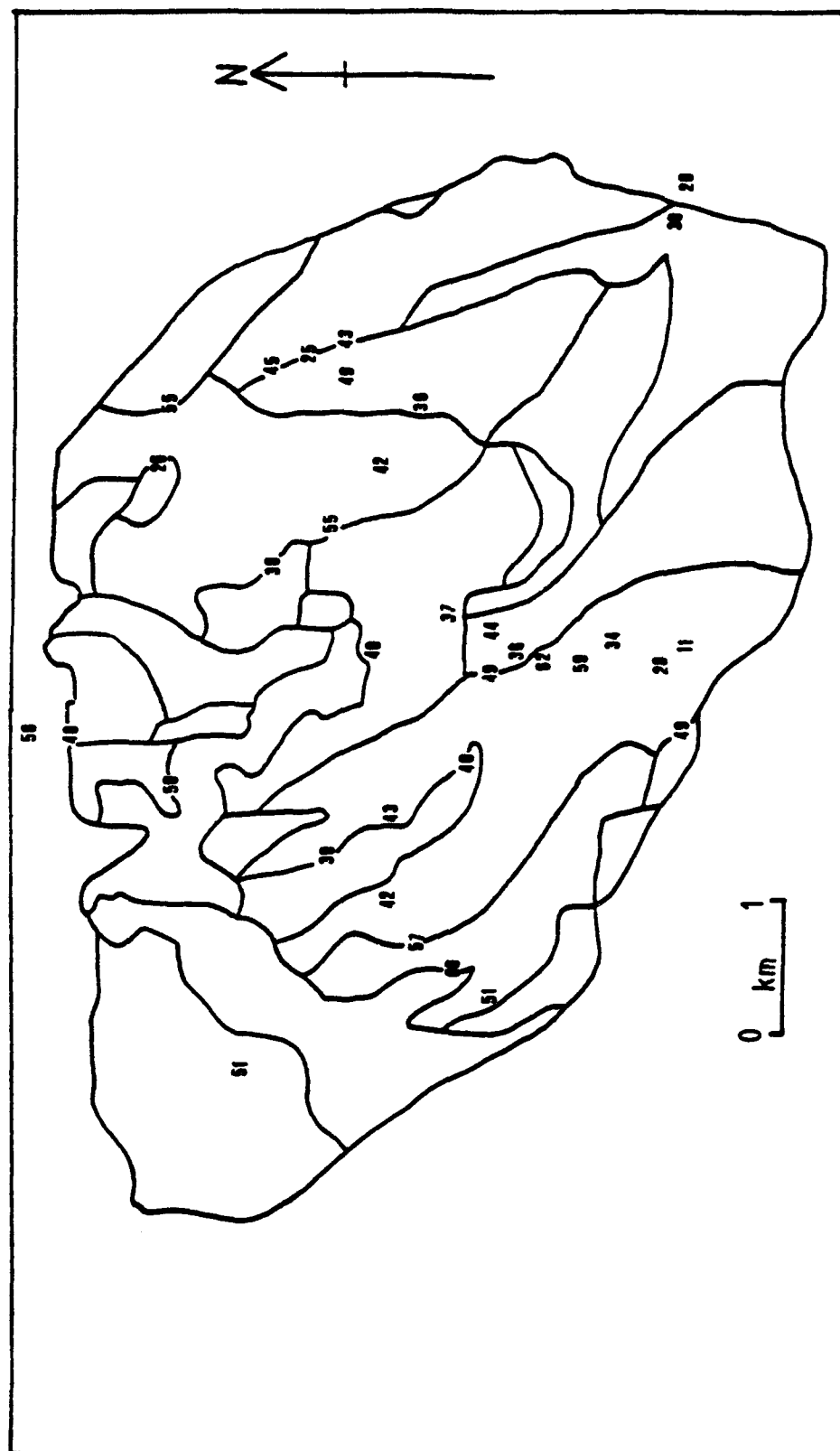


Figure 7.10. Measured snowdepths, W3, 28/3/89 (Julian day 87).

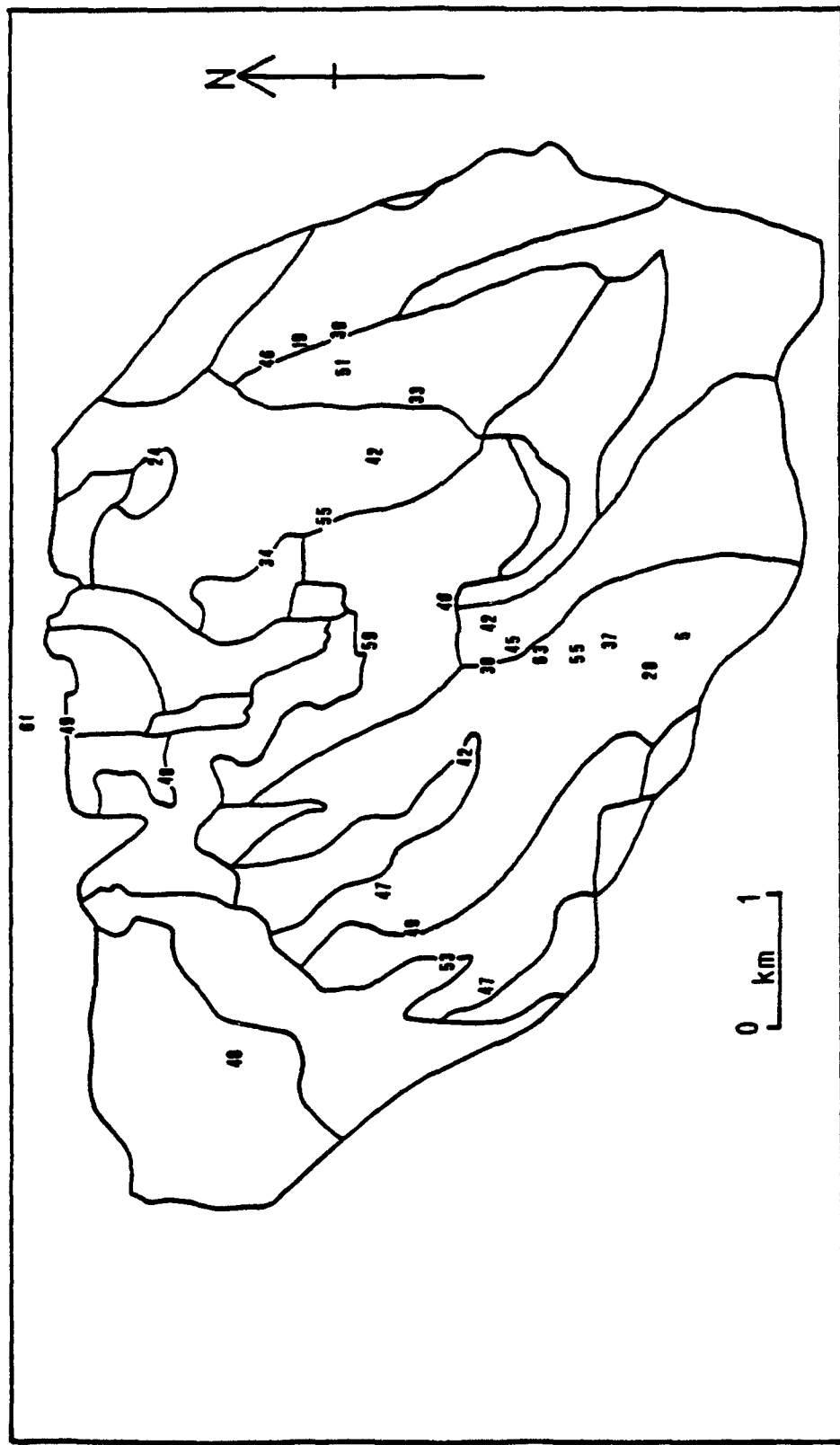


Figure 7.11. Measured snowdepths, W3, 4/4/89 (Julian day 94).

measured. A general increase in snowdepth with elevation can be discerned but this relationship is much more clearly visible using the point examples already discussed.

The utility of using these two methods of presenting the spatial data for the validation of SNOMO is questionable. Their accuracy and the absence of coverage of the whole catchment means that they cannot be used to validate SNOMO with any certainty.

The spatial and the point field results demonstrate the variability of snowcover and snowdepth over a catchment. The point data validates the catchment subdivision criteria of slope angle, aspect, elevation and vegetation cover and indicates the relative dominance of these factors at various scales. The variability of the snowcover is noted again at the various scales and this inherent variability is noted as causing difficulties in the collection of validation data and in the interpretation of validation results. The variability is seen as inherent in the process that SNOMO is modelling and therefore the problem of validation data collection is unavoidable.

### 7.3 SNOMO validation results.

#### 7.3.1 Point validation.

The point data used to validate the performance of SNOMO at a point is that collected at the Townline meteorological station and at various sites around W3. The vegetation cover type at each point site used is the same as the vegetation cover type of the cell that it is representing. It is noted that for cells 14 and 24 the validation data used is that measured on pasture rather than clear-cut, which is the predominant vegetation cover category. SNOMO treats these two vegetation cover types together and as pasture and therefore the comparison is valid. However, it must be remembered that there are differences in snowcover and snowdepth between clear-

cut and pasture. All the point data collected during the 1988 and 1989 field programmes could not unfortunately be used due to the discrepancies between the vegetation cover at the collection site and the vegetation cover designated for the cell covering that site.

Table 7.1 and figure 7.12 show the results of the point validation of SNOMO for 1988. The results are compared visually. The predictions for 1988 are encouraging and indicate that SNOMO is simulating the snowpack satisfactorily. The results for Townline (figure 7.12) are encouraging but do however show that SNOMO predicts melt slightly too quickly which results in the calculation of a melt day (first Julian day with no snowpack) that is four days earlier than that measured and predicted snowdepths that are slightly lower than those measured. Four days are considered an acceptable margin of error when the patchy nature of the snowcover disappearance and the inherent variability of the snowcover and validation data is considered. The results in table 7.1 demonstrate a variation in the calculated snowdepth with vegetation cover and again are satisfactory when compared to the measured values. In some cases in table 7.1 more than one observed value is given for comparative purposes. This is again to emphasise the variability of the snowcover and the care which must be taken when using field data to validate SNOMO.

Table 7.2 and figure 7.13 show the results of the point validation of SNOMO using 1989 data. The calculated results for 1989 do not match the observed results very well at all, except for cell 9 (table 7.2), where unfortunately the observed snowdepth record is very short (measured data is only available for 2 dates).

An investigation was conducted in order to identify the possible causes of the inaccurate 1989 snowdepth predictions and the overprediction of the melt day at Townline by SNOMO in 1988. The results of this investigation are discussed in section 7.4.

Table 7.1. Comparison between the calculated and observed snowdepths (centimetres) for points over the catchment W3, 1988.

CELL 29 Date	Deciduous Calculated	Observed	
		SC2	FT 1-9
83	72	65	73
90	61	46	49
97	23	15	13

CELL 30 Date	Deciduous Calculated	Observed	
		SC2	FT 1-9
83	68	65	73
90	55	46	49
97	12	15	13

CELL 9 Date	Mixed Calculated	Observed	
		R25	
83	60	55	
90	53	30	
97	21	0	

CELL 14 Date	Open/clearcut Calculated	Observed	
		SC9	FT 27-31
83	46	59	56
90	28	34	32
97	0	0	0

CELL 24 Date	Open/clearcut Calculated	Observed		
		SC6	SC6A	FT 22-26
83	46	47	49	58
90	28	24	21	26
97	0	0	0	2*

\* One snowpatch remains on one snowcourse point.

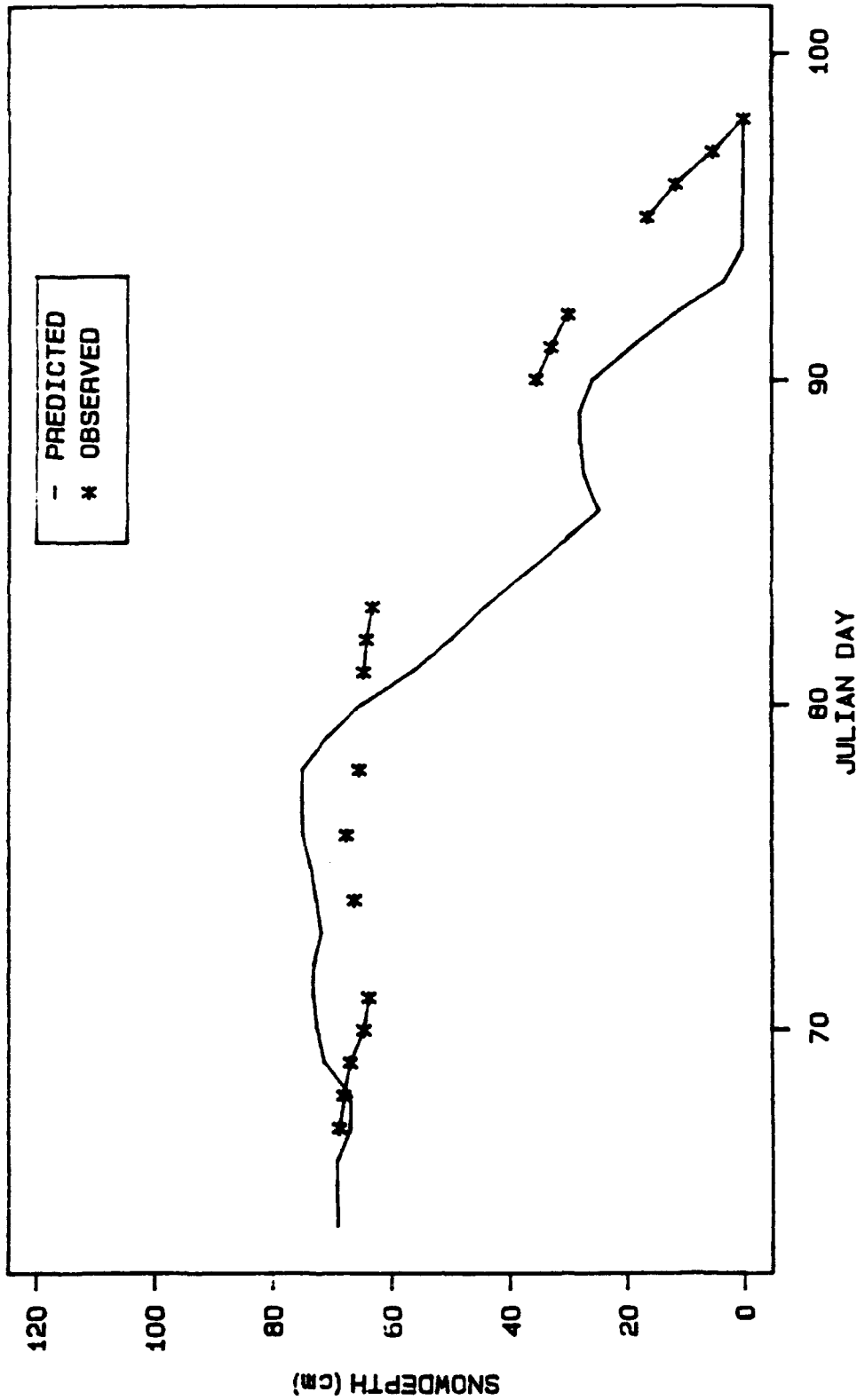


Figure 7.12. Observed and predicted snowdepths, Townline, 1988.

Table 7.2. Comparison between the calculated and observed snowdepths (centimetres) for points over the catchment W3, 1989.

CELL 29		Observed	
Date	Deciduous Calculated	Site 13	FT 1-9
80	57	70	77
87	31	50	51
94	36	48	48
103	0	NA	34
110	0	NA	9
117	0	NA	0

CELL 30		Observed
Date	Deciduous Calculated	FT 1-9
80	48	77
87	17	51
94	21	48
103	0	34
110	0	9
117	0	0

CELL 9		Observed
Date	Mixed Calculated	R25
80	51	47
87	28	30

CELL 14		Observed	
Date	Open/clearcut Calculated	Site 10	FT 27-31
80	0	57	42
87	0	38	26
94	0	34	24
103	0	NA	13
110	0	NA	4
117	0	NA	0

(continued overleaf)

CELL 24	Open/clearcut	Observed
Date	Calculated	FT 22-26
80	0	44
87	0	28
94	0	28
103	0	14
110	0	0

CELL 2	Open/clearcut	Observed
Date	Calculated	Site 17
80	0	57
87	0	43
94	0	39

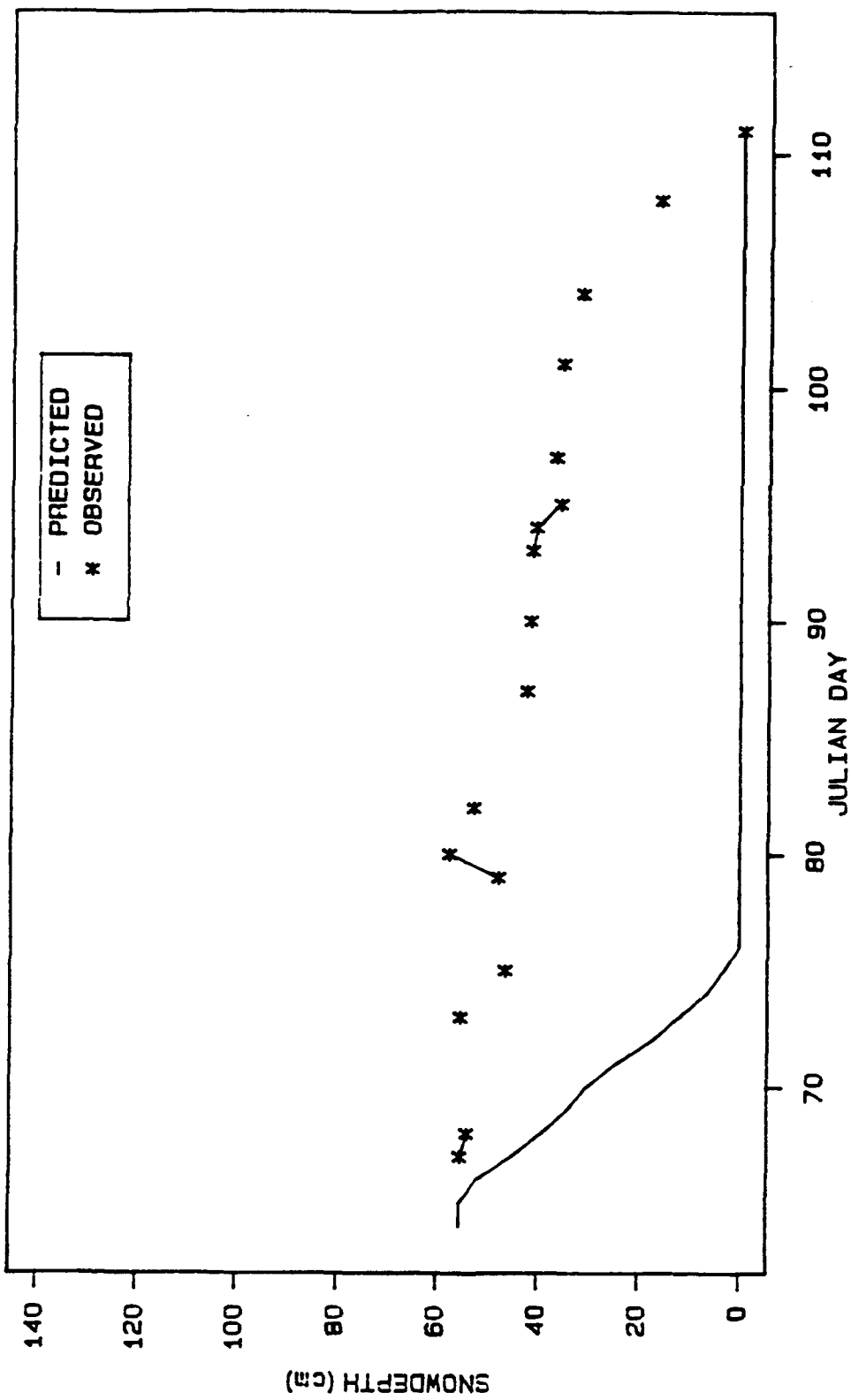


Figure 7.13. Observed and predicted snowdepths, Townline, 1989.

### 7.3.2 Spatial validation.

Tables 7.3 and 7.4 show the calculated snowdepths and melt days on selected dates for the cells within W3 for the melt periods in 1988 and 1989. Appendix BII shows the results obtained for one cell (cell 1, 1988). The results for each cell are calculated to form a table such as tables 7.3 and 7.4. Daily snowdepths have been simulated for each cell and for reasons of brevity only values for selected days have been included in tables 7.3 and 7.4. The values for the melt days (first Julian days with no snowpack) are plotted in their spatial context in figures 7.14 and 7.15, in order to obtain a visual impression of the distribution of snowcover and snowdepth at W3 as calculated by SNOMO. Unfortunately, the problems discussed in section 7.2.2 have resulted in no direct comparative data with which to validate the results shown in figures 7.14 and 7.15 against. However various spatial relationships can be discerned from both figures 7.14 and 7.15 and tables 7.3 and 7.4 and conclusions can be made about the spatial validity of SNOMO.

An analysis of tables 7.3 and 7.4 shows that the predicted spatial pattern of snowcover and snowdepth is the same in both 1988 and 1989. Tables 7.5 and 7.6 show the cells in W3 ranked in order of melt day in 1988 and 1989 with the corresponding vegetation cover and elevation. It appears from these tables that vegetation cover is the most important factor influencing the variation in predicted melt day and therefore in predicted snowcover and snowdepth distribution.

The predicted snowcover in the open/clear-cut vegetation covered areas melts earlier than that in the forested areas and predicted snowdepths are shallower, in 1988 and 1989. It is interesting to note that the 1989 results, although the dates are wrong as discussed in the point validation, exhibits the same melt day pattern as 1988 and presents the differences between the cells more clearly than in 1988. For example, in 1988 melt day variation under the open/clear-cut category occurs from between Julian days 92 to 94. In 1989 it occurs from Julian day 72 to 76 and provides a

Table 7.3. Calculated snowdepths, W3 1988.

CELL NO.	JULIAN DAY						FIRST DAY WITH NO SNOWCOVER
	64	76	83	90	97	99	
	-----Snowdepth(cm)-----						
1	69	75	60	52	20	10	101
2	59	65	30	9	0	0	92
3	69	74	40	19	0	0	93
4	NA	NA	NA	NA	NA	NA	NA
5	NA	NA	NA	NA	NA	NA	NA
6	69	75	38	17	0	0	93
7	NA	NA	NA	NA	NA	NA	NA
8	NA	NA	NA	NA	NA	NA	NA
9	69	75	60	53	21	11	101
10	59	65	30	9	0	0	92
11	69	75	60	52	20	10	101
12	69	75	46	28	0	0	94
13	69	75	40	19	0	0	93
14	69	75	46	28	0	0	94
15	79	85	68	58	24	14	101 (1)
16	79	85	67	58	23	13	101
17	69	75	46	28	0	0	94
18	69	75	43	24	0	0	94
19	64	70	58	53	28	20	101 (11)
20	84	90	68	55	12	0	99
21	84	90	72	61	23	12	101
22	84	90	73	62	27	16	101 (2)
23	84	90	71	60	21	10	101
24	69	75	46	28	0	0	94
25	69	75	40	19	0	0	93
26	NA	NA	NA	NA	NA	NA	NA
27	69	75	38	17	0	0	93
28	69	75	46	28	0	0	94
29	84	90	72	61	23	12	101
30	84	90	68	55	12	0	99

Figures in brackets refer to the depth of snow remaining in the cell on day 101.

Table 7.4. Calculated snowdepths, W3 1989.

CELL NO.	JULIAN DAY								FIRST DAY WITH NO SNOWCOVER
	64	69	75	80	87	94	100	103	
	-----Snowdepth(cm)-----								
1	53	47	41	50	27	25	2	0	101
2	43	18	0	0	0	0	0	0	72
3	53	28	0	0	0	0	0	0	74
4	NA	NA	NA	NA	NA	NA	NA	NA	NA
5	NA	NA	NA	NA	NA	NA	NA	NA	NA
6	53	27	0	0	0	0	0	0	73
7	NA	NA	NA	NA	NA	NA	NA	NA	NA
8	NA	NA	NA	NA	NA	NA	NA	NA	NA
9	53	47	35	51	28	26	3	0	101
10	43	18	0	0	0	0	0	0	72
11	53	47	35	51	27	25	2	0	101
12	53	32	2	0	0	0	0	0	76
13	53	28	0	0	0	0	0	0	74
14	53	32	2	0	0	0	0	0	76
15	63	54	38	52	27	33	7	0	102
16	63	54	27	52	26	32	6	0	102
17	53	32	2	0	0	0	0	0	76
18	53	30	0	0	0	0	0	0	75
19	48	43	34	50	32	39	21	12	105 (4)
20	68	56	35	48	17	21	0	0	97
21	68	59	43	57	31	36	7	0	102
22	68	60	46	60	35	41	12	0	103
23	68	59	41	55	28	34	3	0	101
24	53	32	2	0	0	0	0	0	76
25	53	28	0	0	0	0	0	0	74
26	NA	NA	NA	NA	NA	NA	NA	NA	NA
27	53	27	0	0	0	0	0	0	73
28	53	32	2	0	0	0	0	0	76
29	68	59	43	57	31	36	7	0	102
30	68	56	35	48	17	21	0	0	97

Figures in brackets refer to the depth of snow remaining in the cell on day 105.

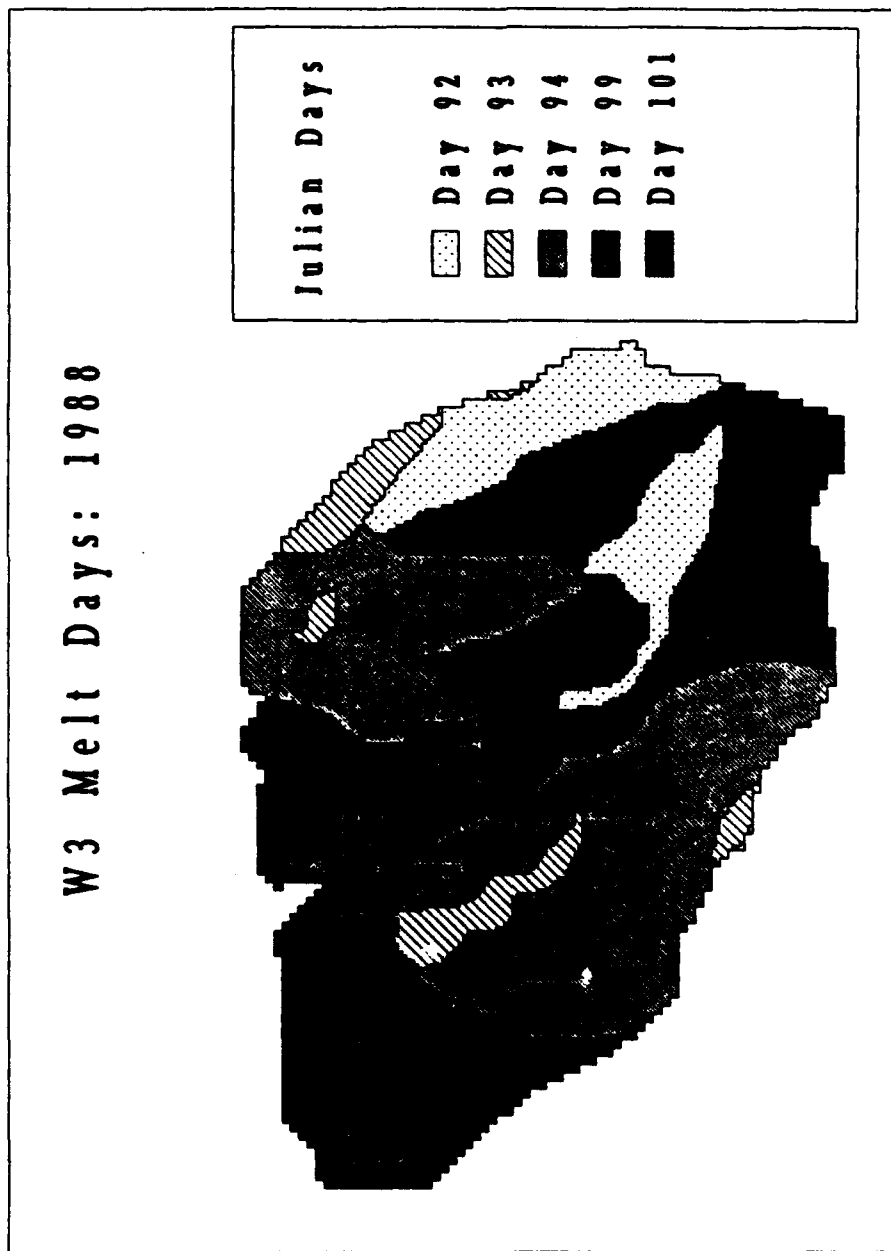


Figure 7.14. W3 melt day prediction, 1988.

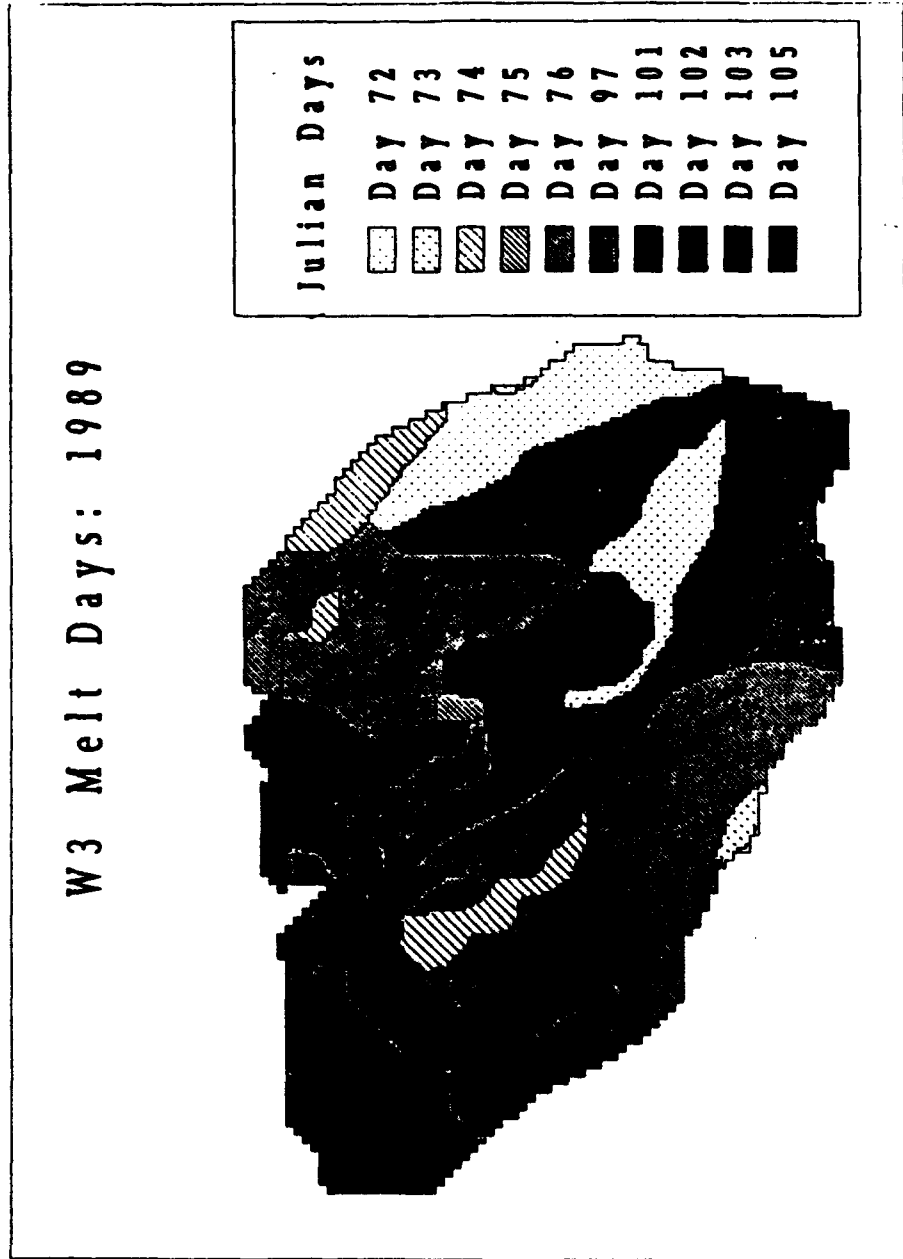


Figure 7.15. W3 melt day prediction, 1989.

Table 7.5. Results for W3 (1988) arranged in melt day order to show the cell attributes.

MELT DAY	CELL NO.	VEGETATION COVER	ELEVATION GROUP	ASPECT(°)	SLOPE ANGLE(°)
92	2, 10	OP/CC	LOW	196	5
93	3, 13, 25	OP/CC	TL	200	7
	6, 27	"	"	143	9
94	12, 17, 28	OP/CC	TL	71	4
	14, 24	"	"	79	6
	18	"	"	134	3
99	20, 30	DECID	TL	143	9
101	1, 11	MIX	LOW	87	6
	9	"	"	77	4
	16	"	TL	143	9
	21, 29	DECID	"	99	8
	23	"	"	134	3
101*	15	MIX	TL	200	7
	19	CONIF	"	99	8
	22	DECID	"	71	4

\* Snow remaining on day 101

Table 7.6. Results for W3 (1989) arranged in melt day order to show the cell attributes.

MELT DAY	CELL NO.	VEGETATION COVER	ELEVATION GROUP	ASPECT(°)	SLOPE ANGLE(°)
72	2, 10	OP/CC	LOW	196	5
73	6, 27	OP/CC	TL	143	9
74	3, 13, 25	OP/CC	TL	200	7
75	18	OP/CC	TL	134	3
76	12, 17, 28	OP/CC	TL	71	4
	14, 24	OP/CC	"	79	6
97	20, 30	DECID	TL	143	9
101	1, 11	MIX	LOW	87	6
	9	"	"	77	4
	23	DECID	TL	134	3
102	15	MIX	TL	200	7
	16	"	"	143	9
	21, 29	DECID	"	99	8
103	22	DECID	TL	71	4
105*	19	CONIF	TL	99	8

\* Snow remaining on day 105

more detailed breakdown of the melt pattern. Cells 2 and 10 are within the lowest elevation group and these melt out first. The effect of the factors of slope angle and aspect are less easy to ascertain, however there appears to be a concentration of cells with aspects of 71° and 79° that result in a melt day of 76 (1989), which possibly indicates the effect of aspect on the determination of the melt day. In both years snowcover remains at cell 19 (coniferous cover) for the longest period of time. Day 101 (1988) and 105 (1989) are the last days in April for which SNOMO can simulate due to operational data availability. In 1989 this extension of snowcover at cell 19 is more obvious as cell 19 is the only cell with a snowcover present when the simulation ends.

Therefore an analysis of the spatial results of SNOMO, even accounting for the inadequate snowdepth simulations for 1989, would appear to validate the spatial relationships used in SNOMO. Vegetation cover and elevation are seen as the dominant factors influencing snowcover and snowdepth distribution. Differences in the calculated snowdepths occur under uniform vegetation cover and elevation. This reflects the situation described in the field. The action of slope angle or aspect in these simulated areas cannot be discerned from the validation but the existence of a variation is encouraging.

That the predicted snowcover and snowdepth distribution pattern is the same in 1988 and 1989 is encouraging and again validates the choice of catchment subdivision criteria. If the snowcover and snowdepth distribution patterns had been radically different then the spatial basis of SNOMO would be questioned.

It was noted that when figures 7.14 and 7.15 were being examined the results did not match with the perception of the melt pattern over the catchment. For example, cell 11 was visualised as a cell with predominantly pasture (open/clear-cut) vegetation cover. This would result in early melt. However, mixed forest is the predominant designated vegetation cover in this cell and therefore melt is later. On first examining figures 7.14 and 7.15 the result

for cell 11 'appears' wrong and it is only when this misconception is realised that the result is accepted. This again indicates the importance of observer and operator perception in influencing both the collection of spatial validation data and the interpretation of the spatial validation results.

#### 7.4 Investigation into the point validation results.

##### 7.4.1 Introduction.

Section 7.3.1 presented the snowdepths predicted by SNOMO at various points within the W3 catchment and at the Townline meteorological station and compared these calculated snowdepths with those measured during the 1988 and 1989 field programmes. The correlation between the calculated and measured snowdepths for 1988 was considered satisfactory although the melt day at Townline was predicted 4 days too early and the predicted snowdepths were lower than those measured. The correlation between the calculated and measured snowdepths for 1989 was however much less satisfactory snowmelt occurring much faster than that measured, resulting in a discrepancy of 35 days between the observed and predicted melt days. An investigation into the reasons for the large overprediction of snowmelt in 1989 and the lesser overprediction in 1988 was conducted. The investigation was conducted using data from the Townline meteorological site as measured values of incoming and reflected shortwave radiation ( $K\downarrow$  and  $K\uparrow$ ) and incoming and reflected longwave radiation ( $L\downarrow$  and  $L\uparrow$ ), used as validation data, are available for this site.

The investigation considered two broad possible sources of error that could be the cause of the overpredictions. These are errors relating to the FORTRAN coding, the programming logic, the physical characteristics of the snowpack as modelled by SNOMO and to the calculation of the energy budget components.

(1) Errors relating to the FORTRAN coding, programming logic or to the physical characteristics of the snowpack as modelled by SNOMO.

The FORTRAN code was examined for programming errors or logic errors that would result in the overprediction of snowmelt. It was discovered that the routine to allow for the removal of snow from the snowpack due to melt was erroneous as mass was not conserved throughout the equations. A new algorithm was therefore written to allow for the conservation of mass during the melt process. In order to ensure the conservation of mass the new algorithm handled the snowpack properties in a different way from the old algorithm. Instead of using an average density value based on the proportions of new and old snow in the snowpack to calculate melt the new algorithm calculates the amount of new snow (using the density of 'new' snow) that would melt, removes this and then calculates the remaining (if any) amount of 'old' snow that would melt (using the density of 'old' snow).

The compaction routine that is used (section 4.5.1) is simplistic and is designed as an approximation of reality. Compaction is modelled as occurring on the day following a day with no snowfall. Three variations of the compaction routine were written to examine the effects on the predicted snowdepths of the extension of time before compaction and the imposition of an arbitrary compaction time that disregarded the presence or absence of previous snowfall. These variations are:

- (1) Compaction on every third day regardless of antecedent snow conditions (SNOMOII).
- (2) Compaction on every third consecutive day with no snowfall (SNOMOIII).
- (3) Compaction on every fourth consecutive day with no snowfall (SNOMOIV).

The choice of initial snowdepth may be a contributory factor to the erroneous performance of SNOMO. For example, figure 7.13 demonstrates that in 1989, due to the accelerated melting calculated

by SNOMO, the discrepancy between the simulated and the observed snowdepths is already 10cm by day 67. Possibly better results would be obtained if the model was initialised on day 67 with 55.3cm of snow rather than on day 64. SNOMO was operated using day 64 as this was the first day in March with available operational meteorological for SNOMO for both the years 1988 and 1989. SNOMO was therefore operated for both 1988 and 1989 using a start date of day 67 and with the respective known snowdepth.

(2) Errors relating to the energy budget calculation.

Overprediction could also be due to a miscalculation of the components of the energy budget calculation. Incoming and reflected shortwave radiation ( $K\downarrow$  and  $K\uparrow$ ) and incoming and reflected longwave radiation ( $L\downarrow$  and  $L\uparrow$ ) were measured at Townline and these values were compared with the values calculated by SNOMO. The causes of the possible miscalculation of  $K\downarrow$ ,  $K\uparrow$ ,  $L\downarrow$  or  $L\uparrow$ , such as the sensitivity of  $K\downarrow$  to cloud cover, were examined further if significant discrepancies occurred between the observed and calculated values of these variables. The convective and latent energy fluxes ( $Q_c$  and  $Q_e$ ) are derived from values of relative humidity, wind speed and snow/ground temperature, they are not directly measurable.  $Q_c$  cannot be calculated without knowledge of the ground/snow temperature. This measurement is not available at Townline or elsewhere at W3.  $Q_g$  is also not measured at Townline or elsewhere at W3 and the lack of ground temperature measurements does not facilitate the estimation of  $Q_g$ .  $Q_g$  is also not modelled by SNOMO (it is taken to be equal to zero). This is in order to simplify the model requirements (section 4.4).  $Q_c$ ,  $Q_e$  and  $Q_g$  are also thought to be of lesser importance in the New England snow environment, when compared to net radiation ( $Q_n$ ). This compounded with the difficulties of obtaining measured values of  $Q_c$ ,  $Q_e$  and calculated and measured values of  $Q_g$  has concentrated the initial energy budget investigation into the determination of the accuracy of the calculated values for  $K\downarrow$ ,  $K\uparrow$ ,  $L\downarrow$  and  $L\uparrow$ .

If this initial investigation and the accompanying investigation into the possible programming, logic and handling of the physical characteristics of the snowpack by SNOMO does not result in an obvious source of the erroneous simulations of snowdepths by SNOMO then the investigation of the remaining energy budget components  $Q_c$ ,  $Q_e$  and  $Q_g$  remains a possibility.

The changes made to either the SNOMO programme or to the data input file in order to conduct the investigation are discrete, the reference station being that described in section 7.3.

#### 7.4.2 Results: 1988.

##### (1) Mass conservation.

Figure 7.16 shows that the inclusion of the mass conservation algorithm does not improve the simulation of snowdepth but increases the overprediction of the melt day and increases the underprediction of snowdepth noticeably for days 87-94. No difference between the snowdepths obtained by SNOMO and the snowdepths obtained by SNOMO with the mass conservation algorithm appears until day 81. The acceleration of melt is a result of the handling of density in the mass conservation algorithm. The effect of new snowfall on the retardation of melt (by inclusion into average density as in SNOMO) is lessened by using the mass conservation algorithm. For example, days 88, 89 and 90 are days where no melt is calculated by SNOMO. This has the effect of retarding melt. Snowfall on days 87 and 88 is incorporated by SNOMO into an average density, which is less than  $0.40\text{gcm}^{-3}$  (the density of 'old' snow). The mass conservation algorithm calculates melt using the two snow layers ('new' and 'old' snow) separately. Once the 'new' snow layer has melted snow is exposed with a density of  $0.41\text{gcm}^{-3}$  instead of a lower average density. The melt rate calculated (section 4.4.3) using a density of  $0.40\text{gcm}^{-3}$  is greater than that calculated using a lower density and therefore melt is increased by using the mass conservation algorithm.

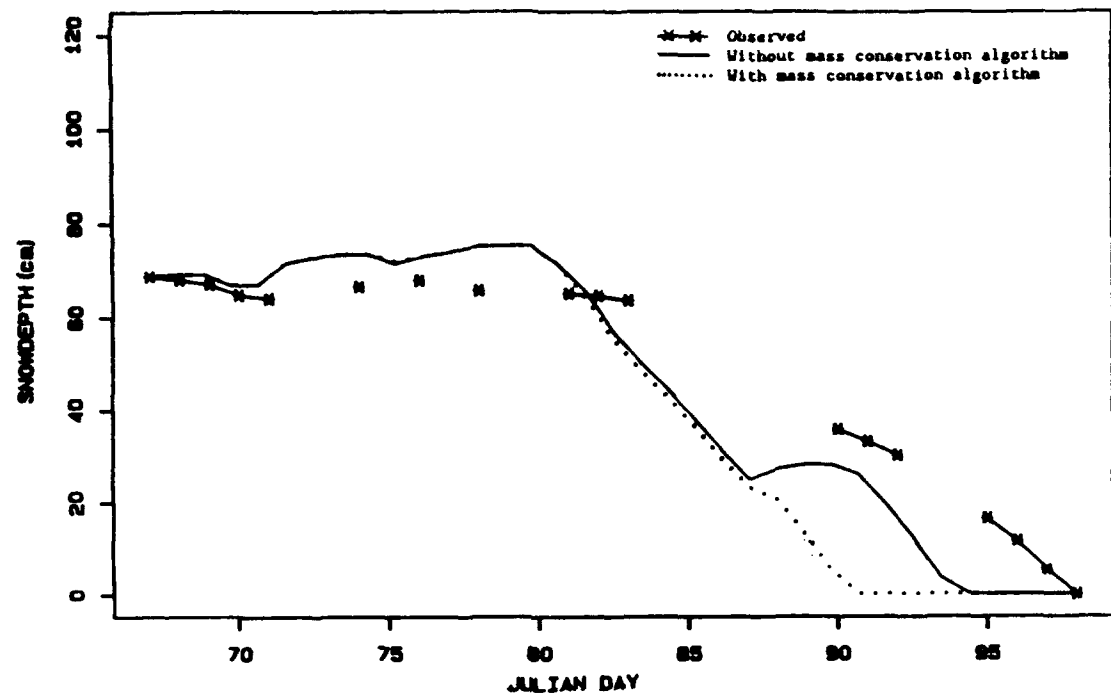


Figure 7.16. Affect of mass conservation on calculated snowdepths, 1988.

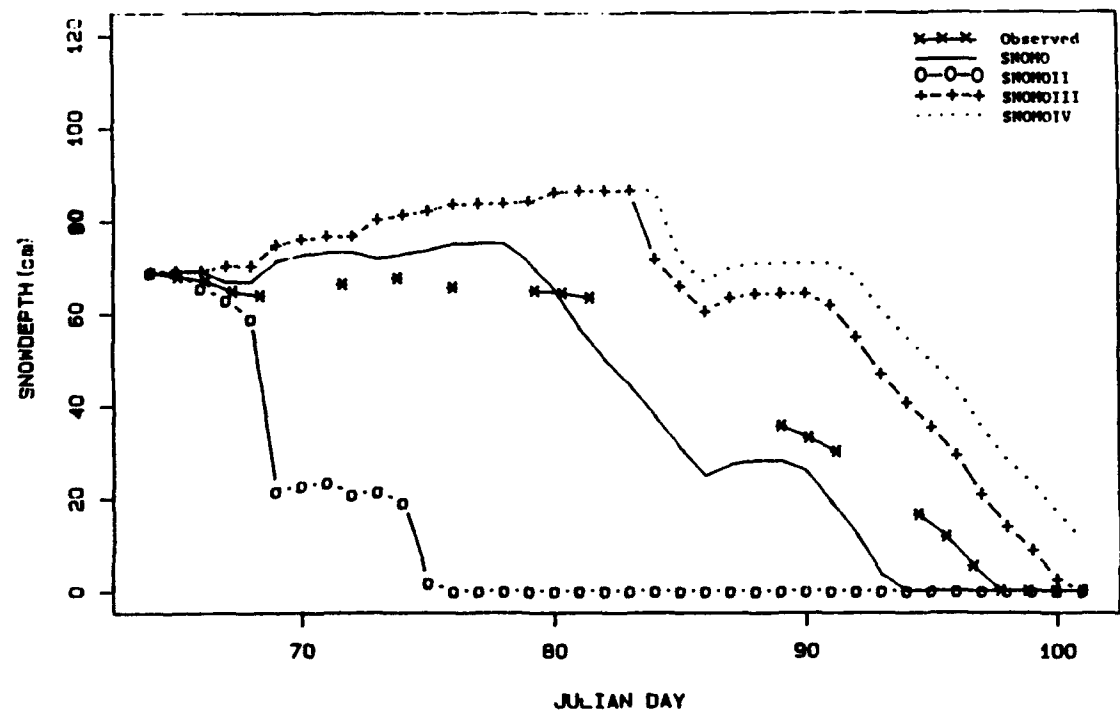


Figure 7.17. Affect of compaction on calculated snowdepths, 1988.

## (2) Compaction

Figure 7.17 compares the snowdepths calculated using SNOMO (compaction on every day after a day with no snowfall) with those calculated using compaction on every third day regardless of antecedent snow conditions (SNOMOII), every third consecutive day with no snowfall (SNOMOIII) and every fourth day with no snowfall (SNOMOIV).

These results highlight the sensitivity of SNOMO to the albedo of the snow surface and to the timing of the alteration of this albedo. Extreme values have been used (section 4.5.1) as a method of simplifying and reducing the model requirements. An 'overnight' snow surface albedo change from 0.95 to 0.40 will drastically effect the amount of radiation absorbed at that surface. The four compaction methods tested demonstrate four methods of moderating and manipulating the effects of this drastic 'overnight' albedo change. The method used by SNOMOII disregards the antecedent snow conditions. Therefore 'new' snow can be converted into 'old' snow, with an albedo of 0.40, even if the snow fell on the previous day. The retardation effect on melt of a large snowfall on the previous day would therefore be negated. This is the cause of the very rapid melt calculated by SNOMOII.

The snowdepths calculated by SNOMOIII and SNOMO envelope those measured at Townline. SNOMOIII calculates the melt 3 days too late and SNOMO calculates the melt 4 days too early. However, the compaction method used by SNOMO calculates snowdepths over the whole melt period that approximate those observed better than those calculated by SNOMOIII. SNOMOIV calculates a much deeper snowpack than that predicted by SNOMOIII or observed.

## (3) Start date.

Figure 7.18 shows the snowdepths calculated using a start date of 67 and a known snowdepth, instead of a start date of 64 and an estimated snowdepth. The accuracy of the calculated snowdepths is slightly reduced when compared to the snowdepths calculated by SNOMO. The calculated melt date is unaffected.

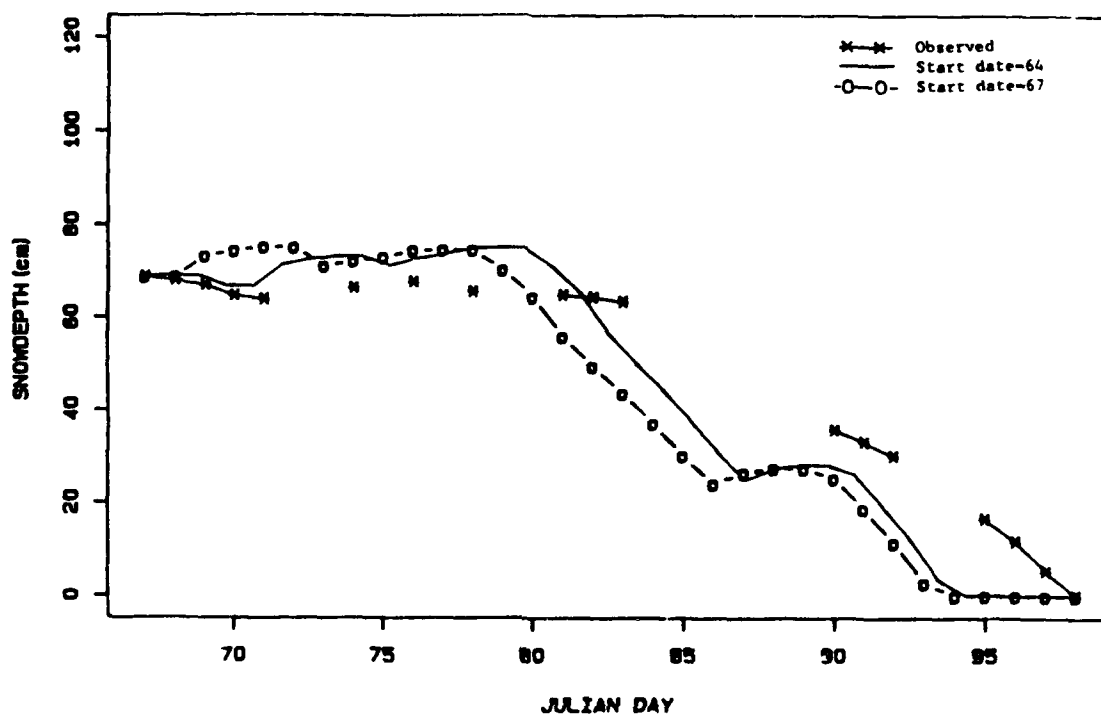


Figure 7.18. Affect of variable start date on calculated snowdepths, 1988.

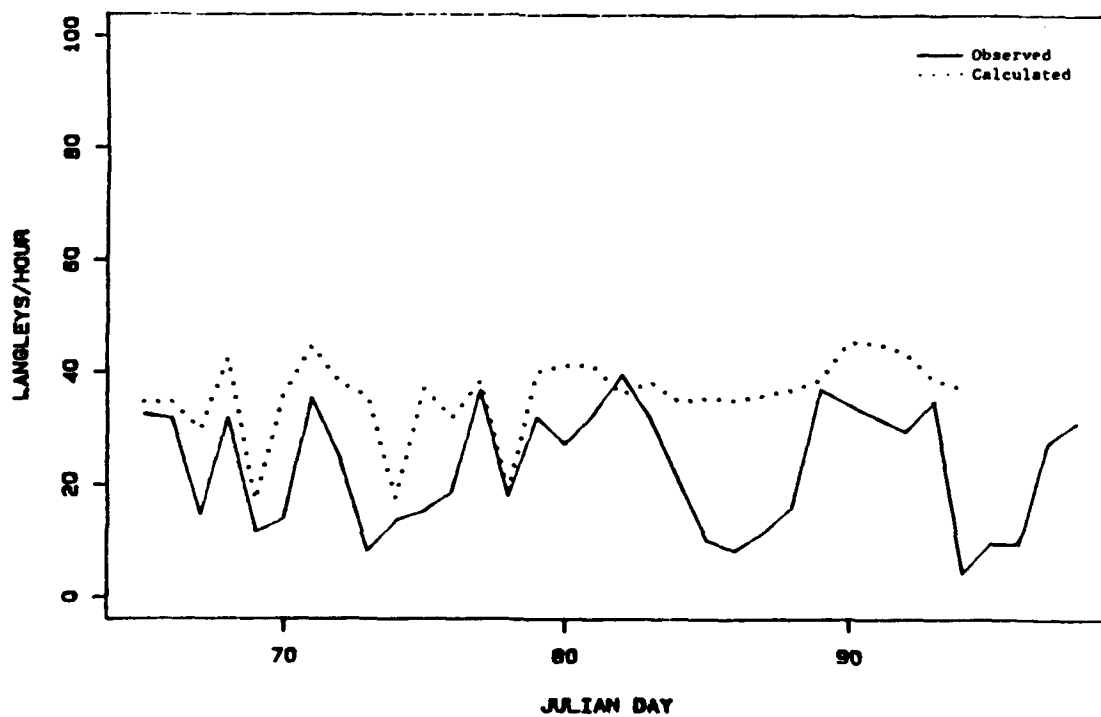


Figure 7.19. Calculated average daily  $K_t$ , Townline, 1988.

(4) Energy budget components.

Figures 7.19, 7.20, 7.21 and 7.22 show the calculated values of  $K\downarrow$ ,  $K\uparrow$ ,  $L\downarrow$  and  $L\uparrow$  respectively compared with the observed values of these variables. There is a very good correspondence between the observed and predicted values for  $L\downarrow$  and  $L\uparrow$ . The correspondence between the observed and predicted values of  $K\downarrow$  is not so good. The trend of the values is predicted satisfactorily although in general calculated values for  $K\downarrow$  are slightly higher than those observed. However, there is a large discrepancy between days 84-88. The reasons for this discrepancy were further investigated. Cloud cover can have an effect on  $K\downarrow$ , clear skies allowing more incoming shortwave radiation than cloudy skies, and as default values for the cloud cover input values were used when no observed values were available, the effect of the cloud cover variable on calculated  $K\downarrow$  and thence on the calculated snowdepths was investigated. Figure 7.23 shows the cloud cover values input into SNOMO for the melt period in 1988. Where no cloud cover values are available a default value of 5 tenths (0.5) is used. It can be seen from figure 7.23 that the cloud cover values used in the period for days 84-88 were all default values. Default values are in fact used for the period of days 82-89.

Figure 7.24 shows the snowdepths obtained by setting all the cloud cover values to 1.0 (total cover) and 0.0 (clear skies) compared with the snowdepths calculated by SNOMO (default and observed values) and the observed snowdepths. It can be seen that the snowdepths obtained by 1.0 and 0.0 cloud cover envelope those calculated by SNOMO and those observed. Snowmelt is accelerated using a cloud cover of 0.0 and retarded using a cloud cover of 1.0.

Figure 7.19 shows that the  $K\downarrow$  values calculated in the period of days 84-88 are higher than those observed. In addition days 82-89 are those where there is a marked deviation from the observed snowdepths by the snowdepths calculated using SNOMO (figure 7.12). Therefore, in order to attempt to improve the snowdepths calculated by SNOMO, the default cloud cover values for those days were changed

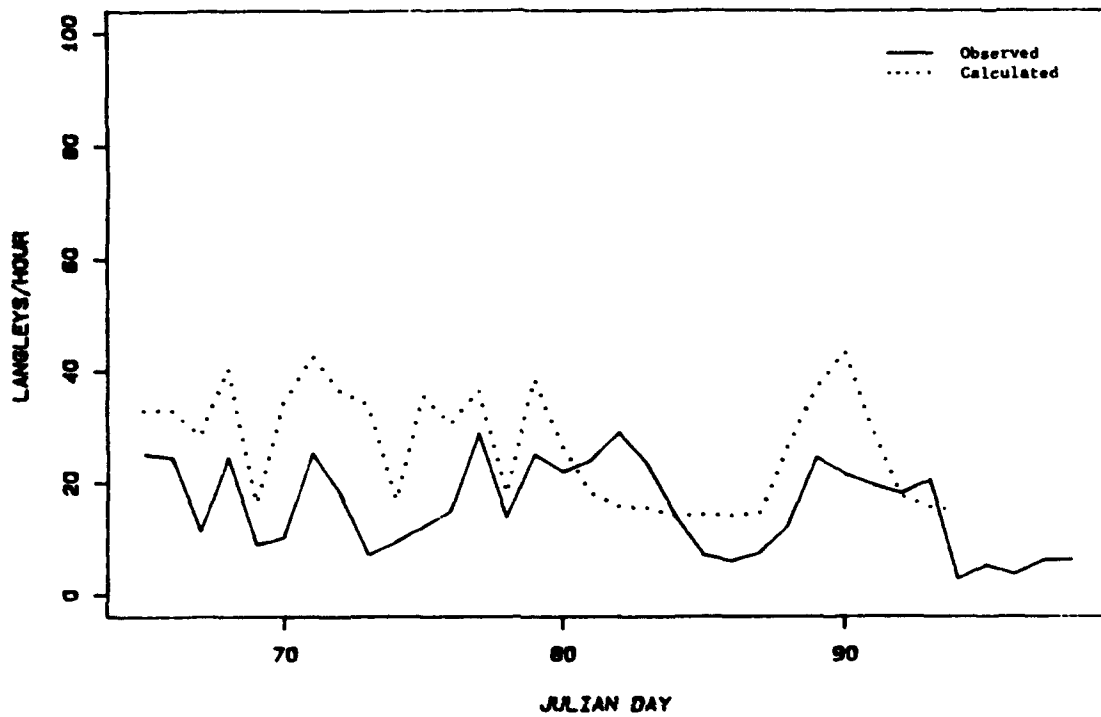


Figure 7.20. Calculated average daily  $K_t$ , Townline, 1988.

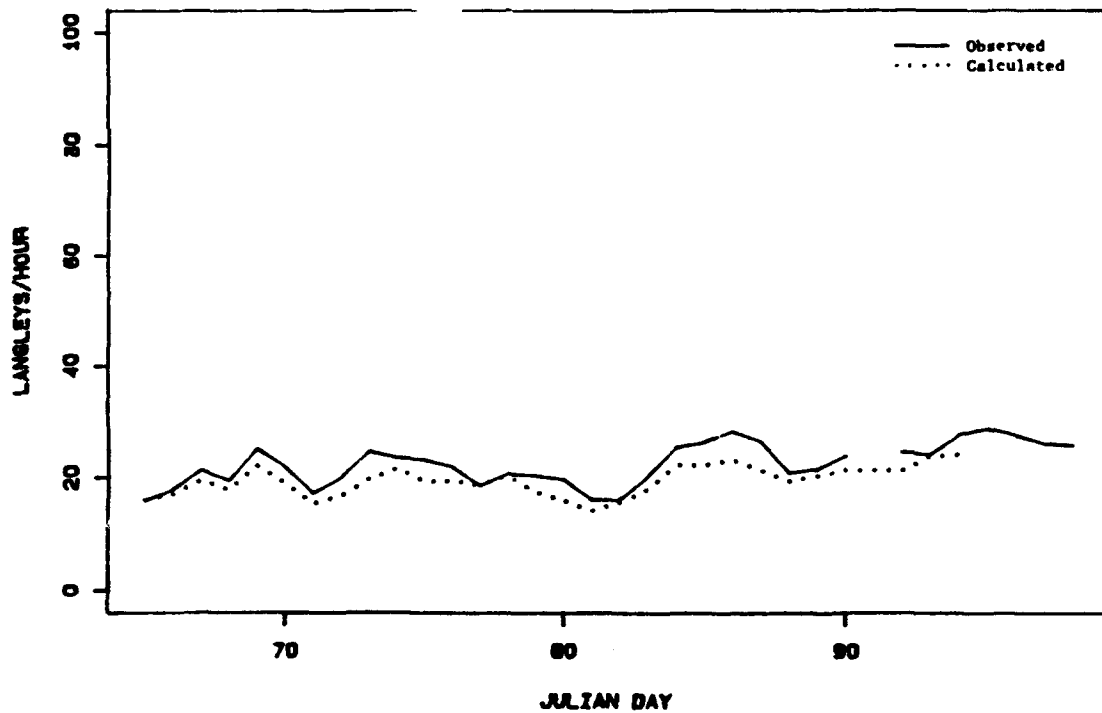


Figure 7.21. Calculated average daily  $L_t$ , Townline, 1988.

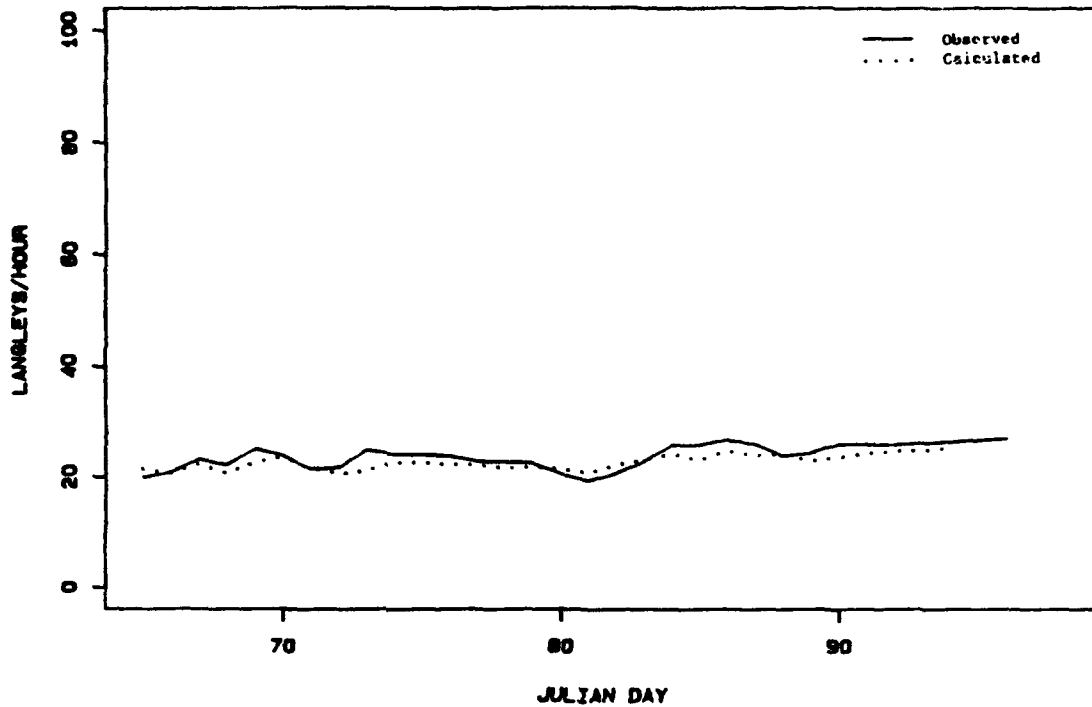


Figure 7.22. Calculated average daily Lt, Towlne, 1988.

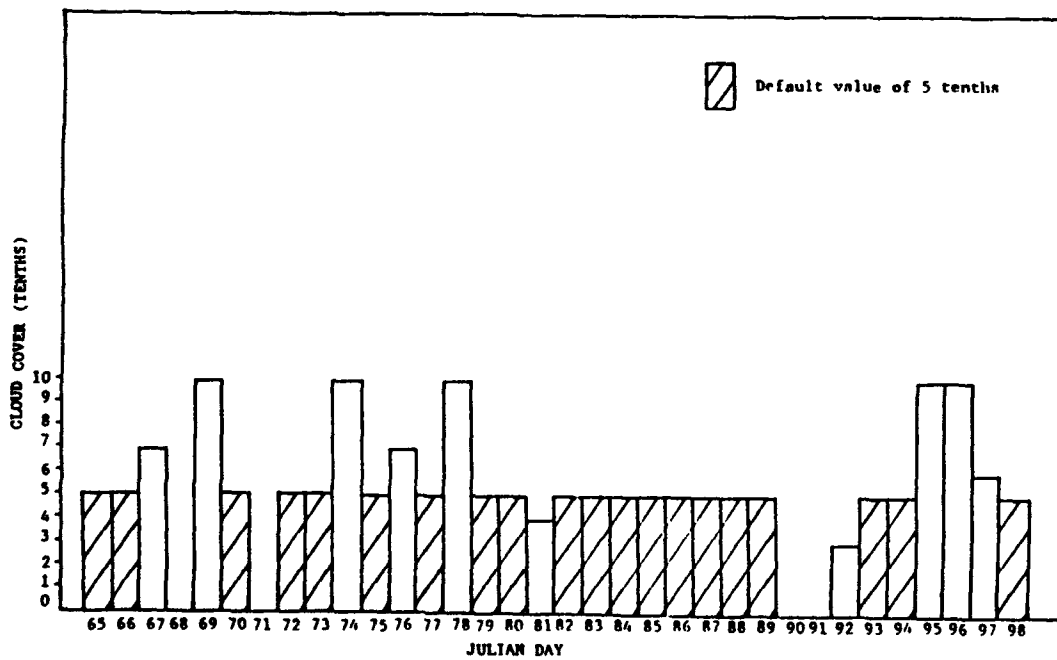


Figure 7.23. Daily input cloud cover values, 1988.

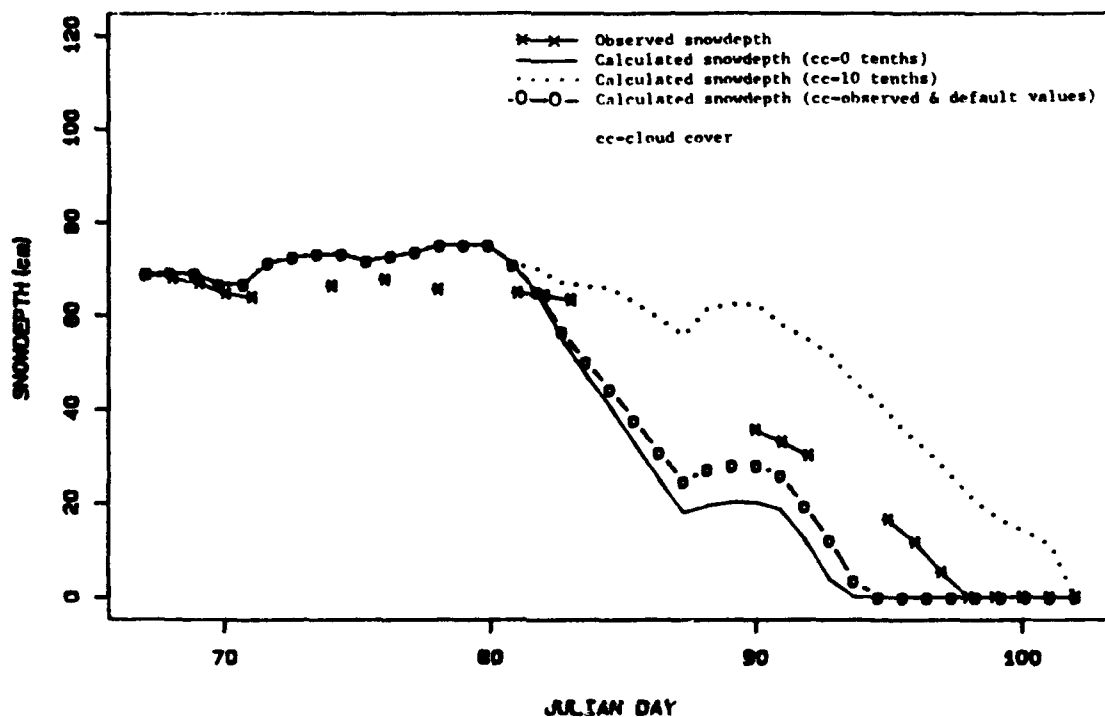


Figure 7.24. Affect of cloud cover on calculated snowdepths, 1988.

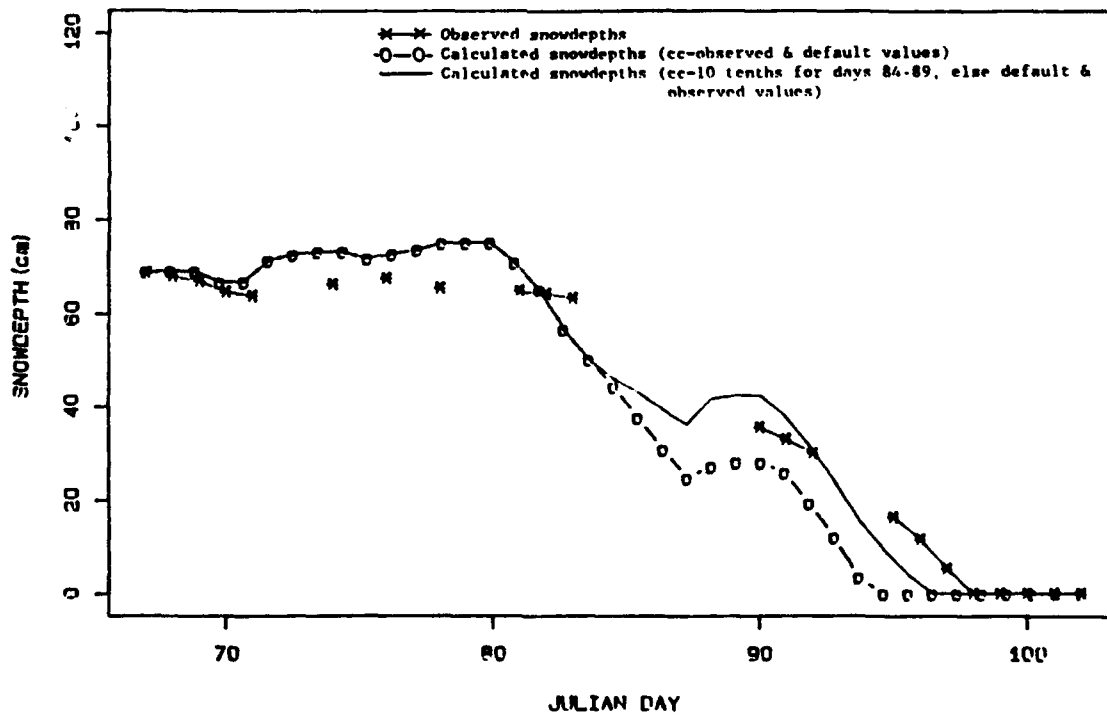


Figure 7.25. Affect of cloud cover values of 10 tenths for days 84-89 on calculated snowdepths, 1988.

from 0.5 to 1.0. The resultant snowdepths are shown in figure 7.25. The simulation of snowdepth is improved. Melt date prediction is inaccurate by 2 days, not 4, and the predicted snowdepths correlate well with the observed snowdepths and better than those calculated by SNOMO.

The accuracy of the  $K_t$  values must be considered with that of the  $K_d$  values as they are derived from these. The accuracy of the predicted  $K_t$  values when compared to the observed values is acceptable considering the discrepancies of the  $K_d$  values.

#### 7.4.3 Results: 1989.

##### (1) Mass conservation.

Figure 7.26 indicates that the addition of the mass conservation algorithm results in a negligible difference to the accuracy of the snowdepths calculated by SNOMO.

##### (2) Compaction.

Figure 7.27 shows the snowdepths calculated using the 4 different compaction methods. The result obtained using SNOMOII (compaction on every third day regardless of antecedent snow conditions) does not correlate very well at all with the measured snowdepths. Melt is drastically accelerated and there is no improvement on the snowdepths calculated using SNOMO. The snowdepths calculated using SNOMOIII and SNOMOIV improve on those calculated by SNOMO. However, melt is still accelerated (the melt day calculated by SNOMOIV is 10 days too early) and the predicted snowdepths remain considerably lower than those observed.

If these results are compared with those for 1988 (section 7.4.2, figure 7.17) it can be seen that the effect of the different compaction algorithms on the predicted snowdepths is different. In contrast to the 1988 results the snowdepths calculated by SNOMO and SNOMOII in 1989 do not envelope those measured at Townline. In addition, snowdepths are underpredicted by SNOMOIII and SNOMOIV in 1989, but overpredicted by these in 1988.

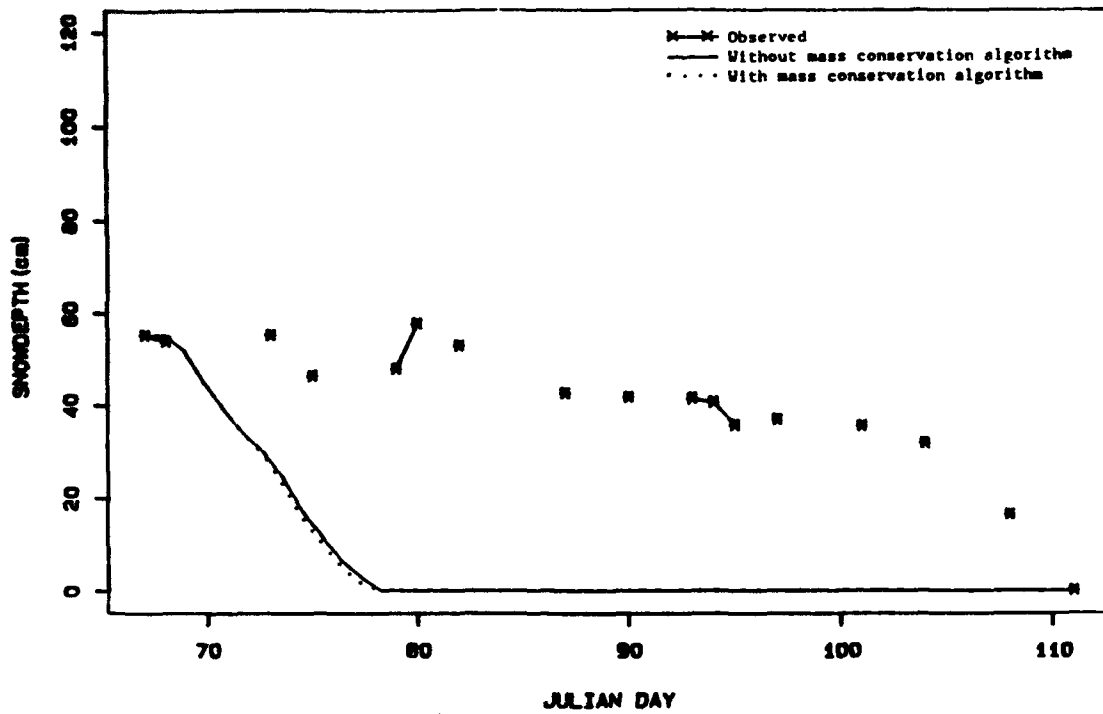


Figure 7.26. Affect of mass conservation on calculated snowdepths, 1989.

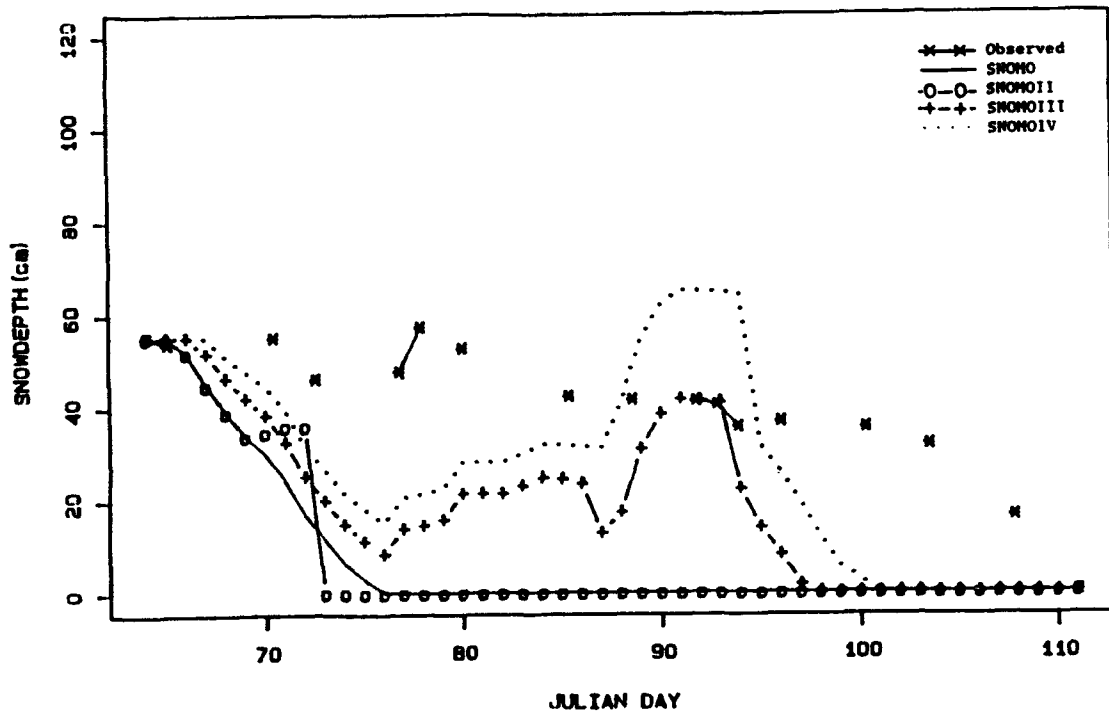


Figure 7.27. Affect of compaction on calculated snowdepths, 1989.

(3) Start date.

Figure 7.28 shows the snowdepths calculated using a start date of 67 with a known snowdepth. The snowdepths calculated are an improvement on those calculated by SNOMO but still represent a large acceleration of melt and underprediction of snowdepths.

(4) Energy budget components.

Figures 7.29, 7.30, 7.31 and 7.32 show the calculated values of  $K\downarrow$ ,  $K\uparrow$ ,  $L\downarrow$  and  $L\uparrow$  compared with the observed values of these variables. There is a very good correspondence between the observed and predicted values of  $L\downarrow$  and  $L\uparrow$ . The correspondence between the observed and predicted values of  $K\downarrow$  is not so close, but is acceptable when the use of default cloud cover values is considered (as for 1988). The cloud cover variables used are shown in figure 7.33. Figure 7.34 shows the snowdepths calculated when using constant cloud cover values of 1.0 and 0.0. The snowdepths calculated using a cloud cover value of 0.0 are identical to those calculated by SNOMO. The snowdepths calculated using a cloud cover value of 1.0 are encouraging and give the best correlation between the calculated and observed snowdepths obtained for 1989. Calculated snowdepths for 1989 do however remain underpredicted in the last third of the simulation and the melt day is 4 days too early. However the snowdepths calculated are a significant improvement on those calculated by SNOMO. The calculated values of  $K\uparrow$  are acceptable when considering the inaccuracies of the calculated values of  $K\downarrow$ .

#### 7.4.4 Discussion.

The simulations in both years were significantly improved by the manipulation of the cloud cover values input into SNOMO. None of the other variables and logic structures examined improved the simulation result as significantly. The importance of the cloud cover variable has therefore been highlighted and future field data collection programmes should be implemented with cloud cover measurement as a priority.

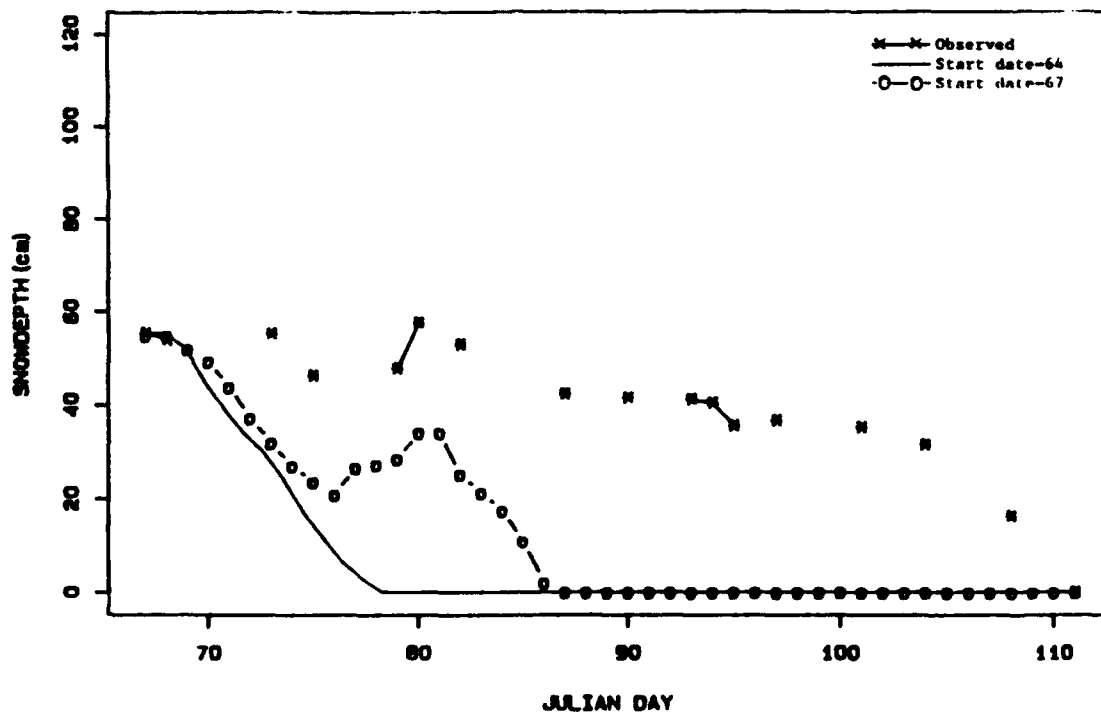


Figure 7.28. Affect of variable start date on calculated snowdepths, 1989.

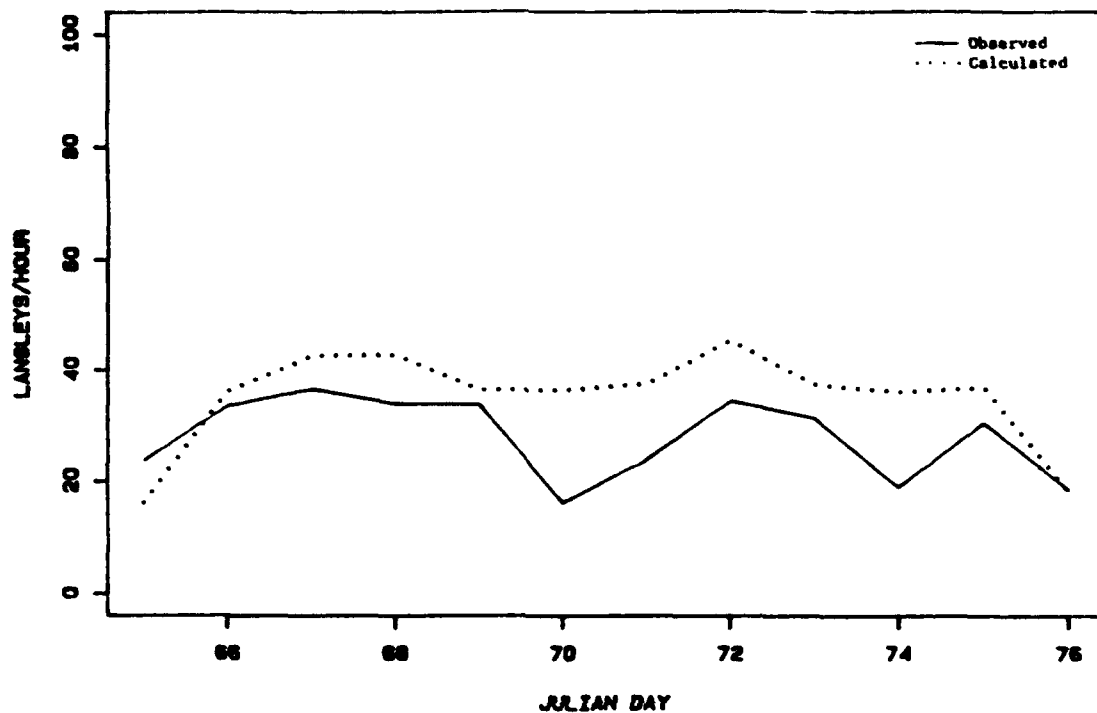


Figure 7.29. Calculated average daily  $K_t$ , Townline, 1989.

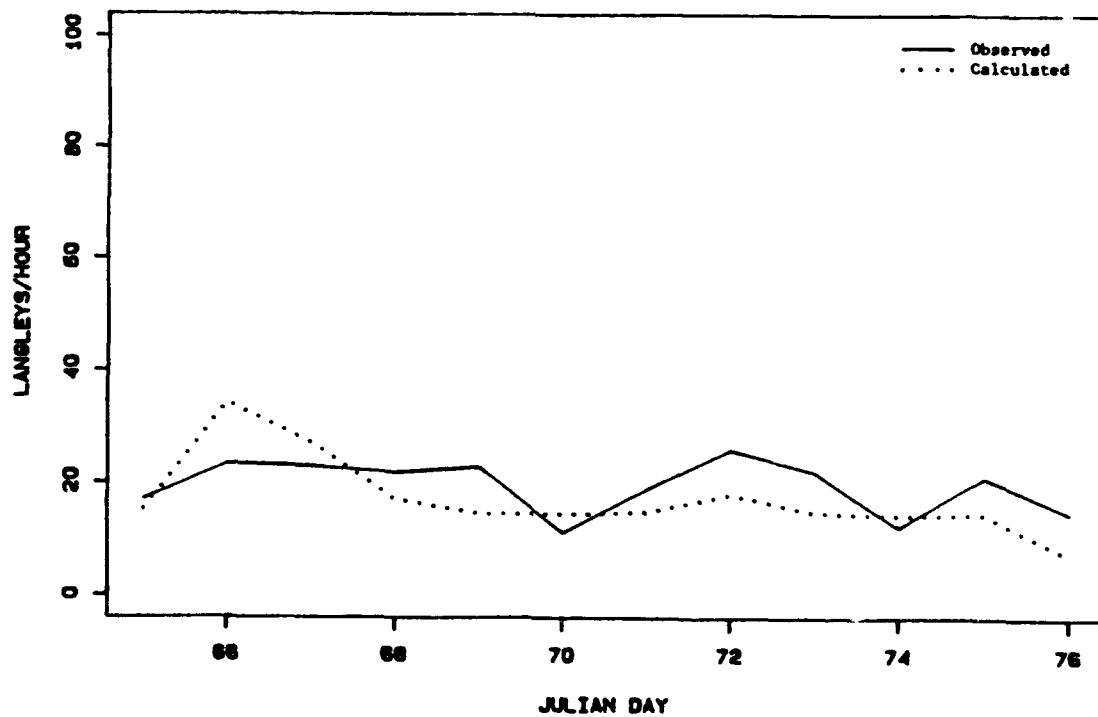


Figure 7.30. Calculated average daily  $K_t$ , Townline, 1989.

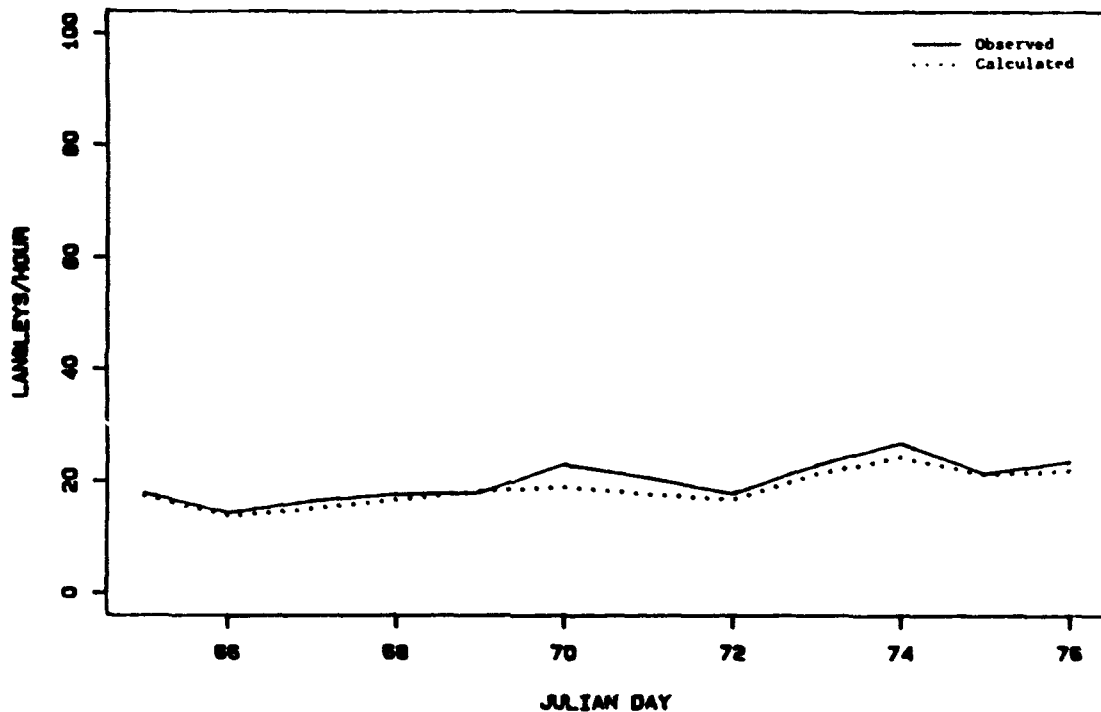


Figure 7.31. Calculated average daily Lt, Townline, 1989.

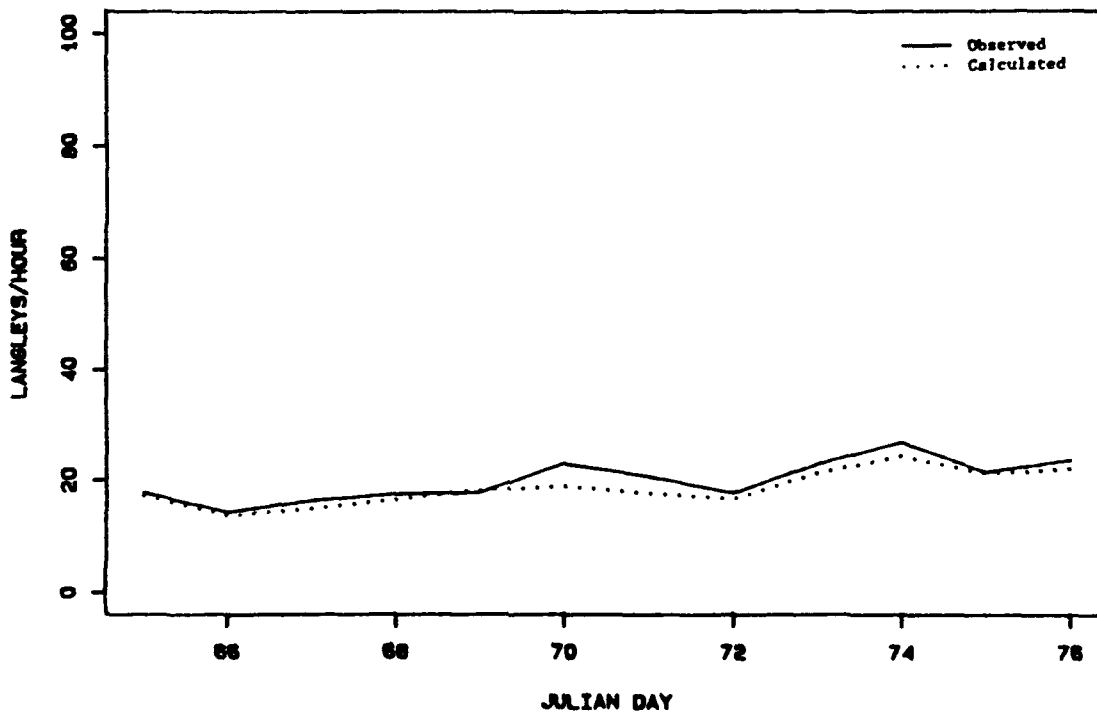


Figure 7.32. Calculated average daily Lt, Townline, 1989.

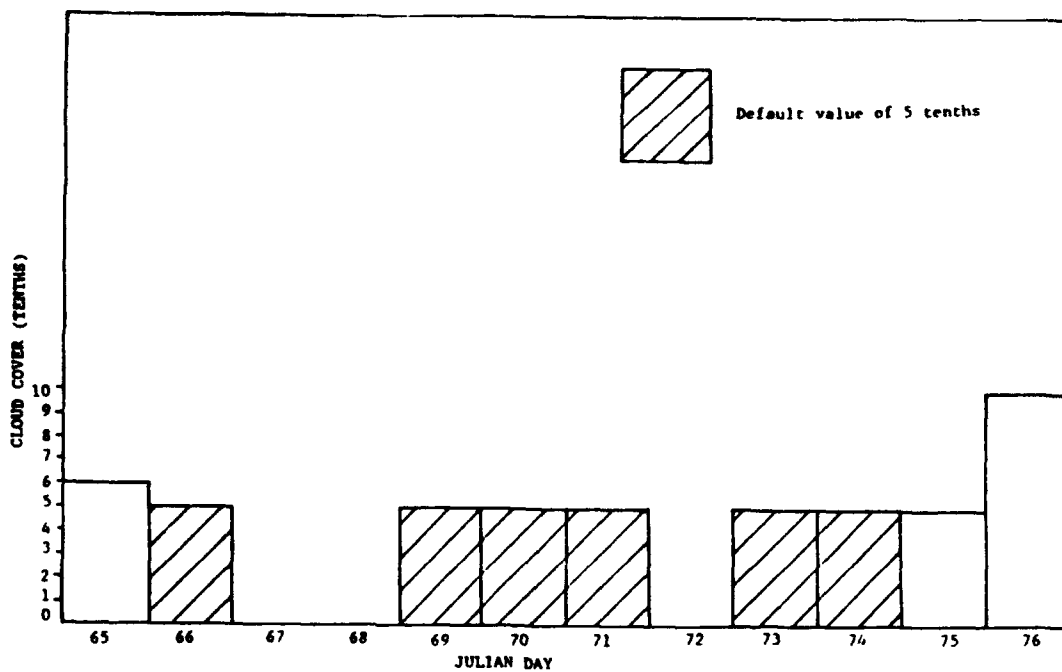


Figure 7.33. Daily input cloud cover values, 1989.

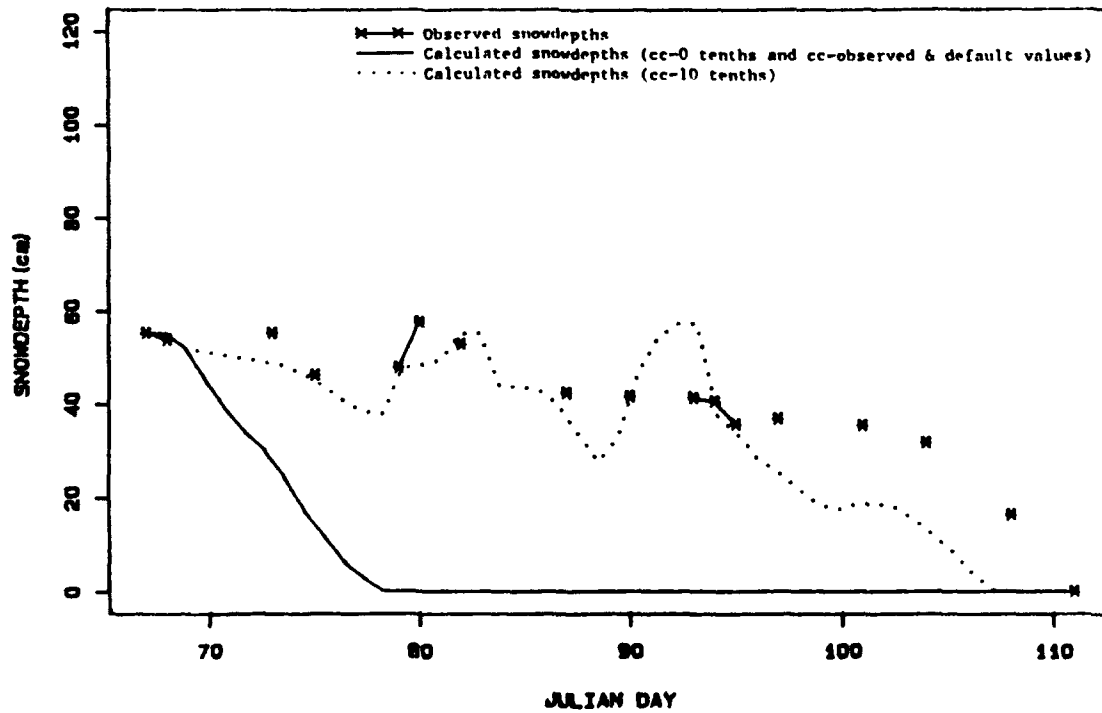


Figure 7.34. Affect of cloud cover on calculated snowdepths, 1989.

The snowdepths calculated by the manipulation of cloud cover in 1989 (cloud cover=1.0) are not as accurate as those calculated by the manipulation of cloud cover in 1988 (cloud cover on days 84-88=1.0). This may be due to reasons connected with the remaining energy budget variables. The meteorological conditions occurring during the 1988 and 1989 melt periods were very different. The 1988 melt period experienced a gradual increase in temperatures and a single melt peak. The melt period in 1989 was more prolonged due to and alternating series of warm periods during which melt occurred followed by colder periods with heavy spring snowfalls. Also the depth and occurrence of frost over the catchment was much greater than in 1988. This was due to a very cold period in early winter which, combined with an absence of snowcover, caused widespread and deep frost penetration.

The remaining energy budget variables  $Q_c$ ,  $Q_e$  and  $Q_g$  will vary in importance according to the prevailing meteorological conditions. It is possible that one or a combination of these variables is calculated less accurately in 1989 than in 1988, or becomes more prominent in 1989 than in 1988, and is therefore responsible for the less accurate calculation of the snowdepths in 1989 than in 1988. For example, the greater occurrence of frost in 1989 might indicate that  $Q_g$  is a more prominent factor in the 1989 snowpack energy budget than in that for 1988. There are unfortunately no records available for Townline or W3 with which to substantiate this contention and further investigation is therefore difficult.

### 7.5 Discussion.

The validation of SNOMO neither proves or disproves the model but provides the following points for discussion:

(1) Validation of the spatial basis of SNOMO.

Section 7.2 provided a validation of the criteria used in SNOMO to subdivide the catchment and that are used therefore as the factors responsible for the patterns of snowcover and snowdepth distribution. These factors are slope angle, aspect, elevation and vegetation cover. The relative dominance of these four factors was shown to be variable. A consideration of the spatial results of SNOMO (section 7.3.2) showed that vegetation cover and elevation were the dominant factors responsible for variations in snowcover and snowdepth as calculated by SNOMO and that some other factors that could not be identified were responsible for further variation. These results therefore suggest that SNOMO is adequately simulating the relationships in the field that are responsible for the patterns of snowcover and snowdepth distribution.

(2) Validation of the snowdepth results of SNOMO.

The point snowdepths initially calculated by SNOMO were encouraging for 1988 and unacceptable for 1989. An investigation into the reasons for the inaccurate predictions considered those due to possible inaccuracies in the programme code, the programme logic, the method used to manipulate the physical characteristics of the snowpack and the calculation of the energy budget components  $K\downarrow$ ,  $K\uparrow$ ,  $L\downarrow$  and  $L\uparrow$ . The calculation of  $K\downarrow$  and the effect of cloud cover was revealed as being most important to the accurate calculation of the snowdepths. Cloud cover values were manipulated to affect  $K\downarrow$  which resulted in a close correlation between the observed and calculated snowdepths for 1988 at Townline and an acceptable correlation for 1989. It is suggested that the remaining discrepancies between the calculated and observed snowdepths for 1989 are probably due to inaccuracies in the calculation of the remaining energy budget components  $Q_c$ ,  $Q_e$  and  $Q_g$ . This contention cannot however be investigated further due to a lack of observed values for these variables at Townline and W3. The spatial pattern of snowcover as calculated by SNOMO (despite the inaccurate predictions of depth)

validates the spatial relationships used in SNOMO.

(3) Validation problems.

The problems of validating a model such as SNOMO have been discussed. SNOMO is designed partly as an aid in the field prediction of areal snowcover. It is realised that the measurement of areal snowcover in the field is difficult. Therefore, by definition, the acquisition of areal snowcover data from the field, to validate SNOMO with, will be difficult. It was discovered that the areal data collected in both 1988 and 1989 was not very useful in the validation of the spatial results of SNOMO. The acquisition of point data can be utilised to examine spatial relationships, such as increase in snowdepth with elevation. It must be remembered however, that both point and areal data possess an inherent variability and that any data will represent an average value.

(4) The field programme.

The validation of SNOMO has demonstrated the deficiencies in the two field programmes conducted and the importance of SNOMO to future field investigations and data collections. It is suggested that the problem with the 1988 and 1989 field programmes was one of scale and perception. There is a problem with matching the scale of the subdivision cells and their attributes with the scale of the field measurements. The 1988 and 1989 measurements are too detailed and are largely unrepresentative of the cell attributes. SNOMO subdivides the catchment into 'homogeneous' areas and it is realised that these areas are not homogeneous at the micro-scale. The field programme should reflect and operate at the same level of homogeneity if possible and not concentrate, for the purposes of validation, on the detail of the catchment. Beven & O'Connell (1982) identify this problem as it relates to field-based research but it can be applied to the collection of field data for the purposes of the validation of

complex distributed models:

" It may be that field-based research should be directed towards scales at which the detailed characteristics of hydrological processes become integrated so that aggregate effects are investigated. "

The problem of the perception and accessibility of the catchment is also present. Open areas are perceived as being larger than in reality and assume an unrepresentative dominance in field collection programmes as compared to larger areas of forest. Accessibility is difficult and must be considered if data measurements are required, from sites distributed over the catchment, on the same day.

The problem of estimating total areal coverage was tackled but not solved. Several improvements for future field programmes are suggested and are a development of some of the ideas presented in chapter 6 (section 6.4):

- (1) The cell subdivision should be performed before devising the field programme.
- (2) Snowdepths should be obtained for the cells as designated by the subdivision that are representative of the cell attributes and most especially of vegetation cover. Snowdepths should also be measured for cells with a large secondary vegetation cover, for example greater than 30%.
- (3) If possible satellite or aerial photography should be used to aid the delineation of the pattern of snowcover retreat and bare-ground development.

Figure 7.35 shows the nature of the relationship between SNOMO, the catchment subdivision and the field programme. This relationship is interdependent and utilizes SNOMO as an aid to the design of the field programme. The catchment is first subdivided on the criteria of slope angle, aspect, elevation and vegetation cover. The field programme is then discussed and initiated on the basis of this subdivision and the points discussed above. Validation and

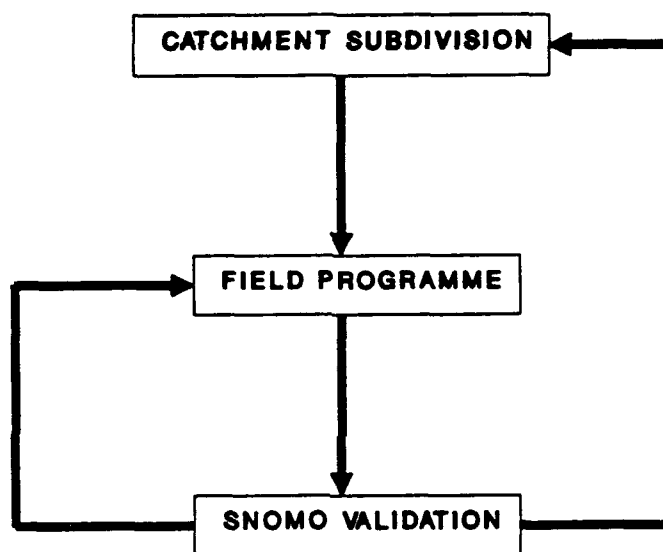


Figure 7.35. Relationship between SNOMO, the catchment subdivision and the field programme.

operational data is collected. SNOMO is then run using this operational data and subsequently validated. The results of the validation may suggest changes in the cell subdivision, for example the criteria or the scale, which will in turn affect future field programmes. Conversely, the results of the validation may suggest changes in the field programme to investigate, for example, relationships between certain variables or intra-cell variation. The validation of SNOMO and the changes this may make to the catchment subdivision and field programme all have implications for the modelling methodology and may result in the restructuring or addition of new code to SNOMO.

The model is therefore viewed as an aid in the development of a field programme and in turn the field programme will maximize the model utility and will possibly direct certain branches of the model development. This mutually dependent and beneficial relationship is important conceptually and has great potential for the improvement and expansion of SNOMO if adopted by SNOMO in the future. Unfortunately, adoption is beyond the scope of this report.

The validation of SNOMO has therefore demonstrated the utility and potential of SNOMO in:

- (1) Simulating a highly variable process (both temporally and areally) that is very difficult to quantify and measure in the field.
- (2) Revealing the interdependence between SNOMO, the catchment subdivision and the field programme.

## CHAPTER 8: MODEL SENSITIVITY ANALYSIS I: POINT SENSITIVITY

### 8.1 Sensitivity analysis.

This chapter and chapter 9 discuss the sensitivity analysis of SNOMO. A sensitivity analysis is an important and integral part of the model development strategy discussed in chapter 3. Chapter 7 has demonstrated that the interpretation of model validation would be facilitated by a sensitivity analysis on the variables that comprise SNOMO. McCuen (1973) defines the role of sensitivity analysis as:

"Sensitivity analysis is a modelling tool that, if properly used, can provide a model designer with a better understanding of the correspondence between the model and the physical processes being modelled."

Results from a sensitivity analysis have implications for the input data used in the model, the internal workings of the model and can be used as a tool for model change.

Sensitivity is defined as the rate of change in one or more factor(s) with respect to change in another or others. There are various methods of conducting a sensitivity analysis. These vary according to the methodology, that is deterministic or stochastic, that is used to determine the value of the variable parameter. Each of the methods considers the influence of a change in a parameter value on the model output. McCuen (1973), Jones (1982) and Howes (1985) consider the various classifications and methods of sensitivity analysis that are available in more detail.

#### (1) Deterministic

Two methods are available to determine the value of the variable parameter in a deterministic manner, these are factor perturbation and differentiation. Differentiation has not been used extensively because of the lack of a sufficiently well developed

mathematical framework. Factor perturbation is the most widely used method. This involves changing the variable parameter value (the factor) within known physical limits at intervals or increments that are decided by the analyst. The limits within which the factor varies can be the maximum physical limits (if known), limits relating to known field values or limits relating to a computational boundary, for example, 100% increase from a set start value. The increment size and implication is at the discretion of the analyst. For example, if slope angles are known to vary from between 0-50°, but with the majority of slopes being between 0-15° then an irregular increment such as 0, 5, 10, 15, 25, 50° is going to be of greater utility than one of +5% or +25%. The term 'deterministic sensitivity' will, henceforth, refer to the factor perturbation method.

## (2) Stochastic

The value of the variable parameter is determined in a stochastic manner. The limits of the parameter variation are set by the mean and standard deviation of the parameter and parameter values are chosen at random from a known distribution. The probability distribution that is set by the mean and standard deviation therefore gives a measure of the relative likelihood of different parameter values.

There are various numerical methods, depending on the methodology used, that are available for quantifying the degree of sensitivity of a parameter (McCuen, 1973 and Jones, 1982). The alternative is a purely visual interpretation which is more qualitative and subjective this is in some cases the easiest option and the one that is open to the least misinterpretation. In the sensitivity analysis of SNOMO a numerical method is used to aid the interpretation of the stochastic sensitivity results and the visual method is used to interpret the deterministic sensitivity results. This is due to the specific data configuration. This is explained in

more detail in section 8.2.3.

SNOMO is a complex distributed model. In order to aid the understanding of the correspondence between SNOMO and the physical processes that it models both a point and a spatial sensitivity analysis are conducted on SNOMO. This chapter discusses the sensitivity analysis of SNOMO at a point. Chapter 9 discusses the spatial sensitivity analysis of SNOMO (operating over the W3 catchment). This division enables an initial understanding of the point interactions within SNOMO (i.e. the basic model structure), without the additional complication of areal interactions and allows, in turn, a better understanding of the areal model.

## 8.2 The point sensitivity analysis of SNOMO.

Both deterministic and stochastic sensitivity analyses of SNOMO were performed at a point. The two methodologies were used to examine the sensitivity of different aspects of parameter variability in relation to the model at a point. The deterministic approach was used to:

- (1) Investigate the relative sensitivity of the different parameters with regard to implications for field program design and model design.
- (2) Determine the presence of any 'sensitivity thresholds' above or below which model performance would increase, decrease or fluctuate significantly.
- (3) Determine if the observed field relationships between parameters were replicated in the model.

The stochastic approach was used to investigate the affect of the field variability of the input data. This assumes that the values input into SNOMO have an error associated with them which reflects the accuracy of the instruments with which they were measured and the natural variability of the parameter.

The point sensitivity analysis was therefore performed:

- (1) To obtain a more detailed knowledge of the correspondence between the point model and the processes being modelled prior to conducting an analysis of the areal model.
- (2) To investigate the relative sensitivity of certain model parameters and the implications of this on model and field design.
- (3) To determine the affect of natural field variability and measurement error on model performance.

### 8.3 Deterministic point sensitivity analysis.

#### 8.3.1 Introduction.

A deterministic sensitivity analysis was performed, for the operation of SNOMO at a point, on six groups of input data parameters, table 8.1. These are considered below in more detail:

##### (1) Slope angle and aspect.

It was decided that as in the areal situation which was to be analysed subsequently (chapter 9) there were very few actual slopes over 30°, and in the cell subdivision all slopes were between 0-10°, that to model slopes over 30° was not necessary. Initially the east facing slope situation was modelled. However this was found to be identical to that of the west and therefore it is only necessary to analyse one of the two. The results for slopes with a west aspect can therefore be taken as identical to slopes with an east aspect. The 0° slope situation, with no aspect, was also modelled.

##### (2) Elevation.

The lapse rate used was from Hendrick & DeAngelis (1976), (chapter 4).

**Table 8.1. Parameters and values used in the deterministic point sensitivity analysis of SNOMO.**

**(1) Slope angle and aspect (degrees)**

North	5, 10, 15, 20, 25, 30° slope
South	" " " " " " "
West	" " " " " " "
0° slope	

**(2) Elevation**

Elevation bands used (ft):	3500-4000
	3000-3500
	2500-3000
	2000-2500
	1500-2000
	1000-1500
	500-1000
	0-500

Lapse rate used: -2°F/1000ft, maximum daily temperature  
 -1°F/1000ft, minimum daily temperature

**(3) Snow albedo (decimal)**

New snow	0.75, 0.80, 0.85, 0.90, 0.95
Old snow	0.40, 0.475, 0.55, 0.625, 0.70

**(4) Snow emissivity (decimal)**

New snow	0.82, 0.8625, 0.905, 0.945, 0.99
Old snow	0.82, 0.8625, 0.905, 0.945, 0.99

**(5) Initial snow temperature (°C)**

Surface temperature	0.0, -0.2, -0.4, -0.6, -0.8, -1.0
Base temperature	-1.0, -2.0, -4.0, -6.0, -8.0, -10.0

(continued overleaf)

(6) Vegetation parameters (decimal)

- (a) Vegetation density,  $\sigma_f$   
0.60, 0.695, 0.79, 0.885, 0.98
- (b) Vegetation albedo,  $\alpha_f$   
0.05, 0.075, 0.10, 0.125, 0.15
- (c) Vegetation emissivity,  $\epsilon_f$   
0.97, 0.975, 0.98, 0.985, 0.99
- (d)  $\alpha_f = \alpha_{sn}(\text{new})$   
0.75, 0.80, 0.85, 0.90, 0.95

(3) Snow albedo.

The limits (0.75-0.95 and 0.40-0.70) were obtained from the literature (chapter 4) and the increments were equal to an increase of 25% of the difference between the limits.

(4) Snow emissivity.

The limits (0.82-0.99) were obtained from Oke (1987) and the increments were equal to an increase of 25% of the difference between the limits.

(5) Initial snow temperature.

The initial snow temperatures were varied at almost constant increments from the initial snow temperatures of 0.0 and -1.0°C for the open, mixed and deciduous situation and -1.0 and -10.0°C for the coniferous situation (chapter 4).

(6) Vegetation parameters.

The increments of all four parameters are equal to an increase of 25% of the difference between the limits. The limits of the vegetation density ( $\sigma_f$ ) are from table 4.6 (chapter 4) and cover a range of coniferous and deciduous species. The limits of the vegetation albedo ( $\alpha_f$ ) and emissivity ( $\epsilon_f$ ) are taken from Oke (1987). The snow albedo vegetation parameter refers to the situation where snow is lying on the canopy. The snow is assumed to be new snow and the new snow albedo value is substituted for the vegetation value. The limits are therefore the same as the ground snow albedo (0.75 - 0.95), but the situation is different.

Each of the parameters above was analysed using SNOMO with the 'open' vegetation option (i.e. the VEGIE subroutine is inactive) and SNOMO with the 'coniferous' vegetation option (i.e. the VEGIE subroutine is active). The 'coniferous' option was used as this represents the extreme condition and values for 'mixed' and 'deciduous' forest would lie between the 'open' and 'coniferous' values (chapter 4).

The choice of parameters used in the analysis was based on a variety of reasons. Firstly, to perform an analysis on all the

parameters involved in SNOMO would have been a large undertaking occupying a considerable amount of time. Also a logical structured analysis focusing on less parameters is likely to be more useful in determining parameter interactions than a blanket 'analyse-everything' approach. Therefore the parameters have to be selected. The aim of SNOMO is to model areal snowcover and snowdepth and to aid this the model is subdivided into areal units (cells) depending upon slope angle, aspect, elevation and vegetation cover. It is therefore logical to analyse these four basic parameters (slope angle, aspect, elevation and vegetation cover) as they are an important part of the structure and theory of SNOMO. The remaining parameters were ranked in order of supposed importance to the model structure and their expected influence on model results. The parameters at the top of the ranking were analysed. This may appear slightly tautological, but for the reasons mentioned above not all the parameters could be analysed and once the parameters at the top of the ranking have been analysed selected parameters below these can be analysed, their selection being based upon the results of the top ranking analysis. Balick *et al.* (1981a) conducted a sensitivity analysis of the model TSTM. This is the original, daily, point energy budget model from which SNOMO was developed (chapter 4) and therefore there are many differences between SNOMO and TSTM. However, the results of their analysis (table 8.2) are another aid in the determination of the parameter relationships in SNOMO.

The data file used in the sensitivity analysis (both deterministic and stochastic) was for a 5° west-facing slope with/without coniferous vegetation cover, within the elevation band of the Townline meteorological station, W3. Input data was available until Julian day 152 which enabled SNOMO to operate, if necessary, until Julian day 150. Julian day 150 is equivalent to the 29<sup>th</sup> or 30<sup>th</sup> May and this was considered a sufficient time period for SNOMO to model. The data file used was a modified version of the 1988 validation data file. The 1988 data ceases on day 101. It was expected that the sensitivity analysis would result in simulations

Table 8.2. Relative sensitivity of TSTM parameters, Balick *et al.* (1981a).

Very sensitive	Moderately sensitive	Very insensitive
Air temperature	Relative humidity	Air pressure
Solar absorption	Shelter height	Cloud type (types 1, 2)
Thermal emissivity	Wind speed	Thermal diffusivity
Initial temperature profile	Cloud cover (types 3, 4)	Time step
Saturation	Cloud type: group to group (1, 2) (3, 4, 5) (6, 7, 8)	24-hr repetitions
Top layer heat conductivity		

extending well over day 101 and therefore this data file was amended from day 101 using data for the year 1974 (Anderson *et al.*, 1977). Data from 1974 were chosen because the snowmelt situation and air temperatures up to day 101 resembled the situation at W3 in 1988 fairly closely. The results obtained by the point sensitivity analysis are not compared with the actual 1988 results and therefore the artificiality of the point sensitivity data file is irrelevant. The sensitivity analysis in chapter 9 is to be performed at W3, Vermont and therefore the latitude of W3 and the meteorological data used in the input file were all taken from W3 and the Townline meteorological station.

### 8.3.2 Results.

The results of the point deterministic sensitivity analysis of SNOMO are shown in tables 8.3, 8.4, 8.5, 8.6, and 8.7. In all the tables the figures in brackets indicate the result for SNOMO with the activated VEGIE subroutine. The results are given in table form with the Julian date of the first day with no snowpack being used as the result index. The first day with no snowpack will be known as the 'melt day'.

### 8.3.3 Discussion.

Most deterministic sensitivity analyses compare the model results, for example an outflow hydrograph, with an observed output. The degree of sensitivity of the parameter being analysed is often determined numerically using a statistical procedure such as the Root-Mean-Squares method. This is however impossible in the case of the sensitivity analysis of SNOMO due to the nature of the input data. Figure 8.1, drawn from table 8.7 demonstrates this problem. The melt days increase fairly steadily with the increase in the old snow albedo values. However the last value, 0.70, has a melt day of 137 compared to that of 113 which is the previous value. Therefore

Table 8.3. Deterministic point sensitivity analysis: Melt date results for slope and aspect.

SLOPE ANGLE (degrees)	ASPECT		
	North	West	South
5	101 (113)	99 (111)	98 (109)
10	103 (119)	99 (111)	97 (108)
15	106 (121)	99 (111)	92 (106)
20	111 (134)	100 (112)	91 (106)
25	119 (137)	100 (112)	91 (105)
30	132 (142)	100 (113)	91 (105)
Zero degree slope, no aspect	99 (112)		

Figures in brackets refer to the results obtained with the activated VEGIE routine.

Table 8.4. Deterministic point sensitivity analysis: Melt date results for elevation.

ELEVATION (ft)	MELT DATE
3500-4000	100 (131)
3000-3500	100 (121)
2500-3000	100 (120)
2000-2500	100 (114)
1500-2000	99 (111)
1000-1500	99 (110)
500-1000	98 (109)
0-500	98 (108)

Figures in brackets refer to the results obtained with the activated VEGIE routine.

Table 8.5. Deterministic point sensitivity analysis: Melt date results for initial snow temperature.

INITIAL SNOW TEMPERATURE		MELT DATE
Surface	Base	
0.0	-1.0	99 (111)
-0.2	-2.0	99 (111)
-0.4	-4.0	99 (111)
-0.6	-6.0	99 (111)
-0.8	-8.0	99 (111)
-1.0	-10.0	99 (111)

Figures in brackets refer to the results obtained with the activated VEGIE routine.

Table 8.6. Deterministic point sensitivity analysis: Melt date results for vegetation parameters.

PARAMETER	% INCREASE BETWEEN LIMITING VALUES				
	0	25	50	75	100
Snow albedo	112	112	112	113	114
Vegetation density	106	110	120	140	150
Vegetation albedo	111	111	111	111	111
Vegetation emissivity	111	111	111	111	111

Table 8.7. Deterministic point sensitivity analysis: Melt date results for snow albedo and emissivity.

% INCREASE BETWEEN LIMITING VALUES	VARIABLE			
	New snow albedo	Old snow albedo	New snow emissivity	Old snow emissivity
0	99 (111)	99 (111)	92 (92)	92 (101)
25	99 (111)	103 (119)	92 (97)	100 (103)
50	99 (111)	107 (134)	92 (98)	100 (107)
75	99 (111)	113 (142)	92 (100)	101 (112)
100	99 (111)	137 (150)	92 (102)	101 (121)

Figures in brackets refer to the results obtained with the activated VEGIE routine.

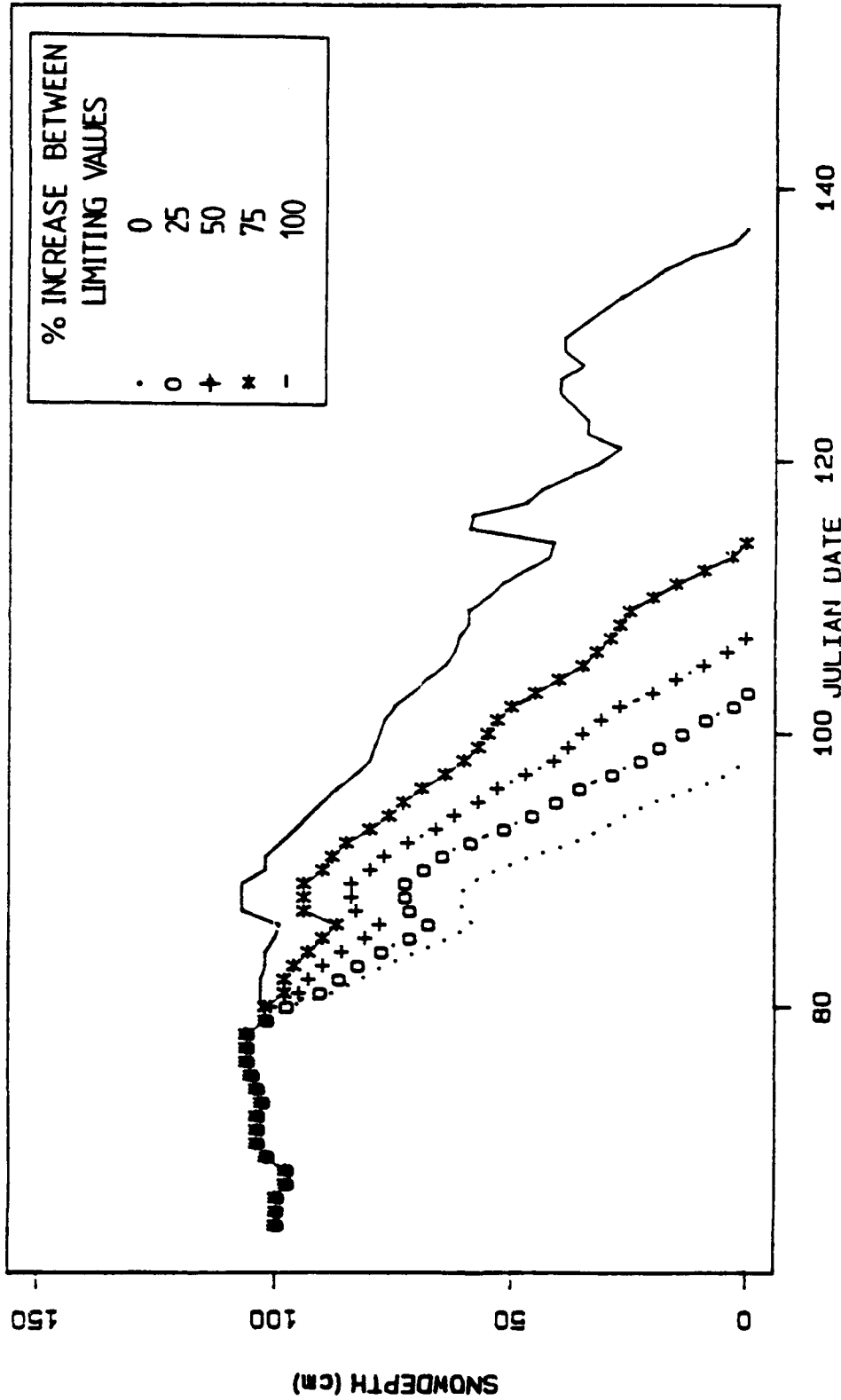


Figure 8.1.1. Affect of variation of the snow albedo on snowdepth.

it would appear that SNOMO is more sensitive to old snow albedo values of 0.70 than it is to values of 0.625 and lower. A sensitivity threshold could be surmised. However, if figure 8.1 is examined more closely it is seen that there is a snowfall on days 115 and 116 and days 122-128. These two snowfalls extend the duration of the snowpack by increasing the amount of snow available for melt. The 0.625 value for the old snow albedo melts out before this snowfall, the 0.70 value does not. It is this additional snowfall that causes the apparent increase in sensitivity of the old snow albedo. A statistical comparative test would not allow for this situation with the result that the interpretation of the results would be complicated. It is for this reason that a purely visual analysis was made.

The results are summarized in table 8.8. The categories 'very sensitive', 'moderately sensitive' and 'very insensitive' were obtained by examining the results up to day 115 and comparing the number of increments taken to reach day 115, the less increments the greater the sensitivity. Those parameters which displayed no variation were placed in the 'very insensitive' category. Those exhibiting a little were placed in the 'moderately sensitive' category and the remainder in the 'very sensitive' category. It is realised that this subdivision is somewhat subjective but it is presented as the best available in the circumstances. Closer examination of tables 8.3-8.7 reveals that the sensitivity of SNOMO varies depending on the VEGIE subroutine. For example SNOMO is very sensitive to elevation with the activated VEGIE subroutine and moderately sensitive without (table 8.8). As SNOMO will be tested in an areal situation where VEGIE will be both active and inactive the elevation parameter is designated the higher sensitivity of 'very sensitive'. A similar process was applied to the new snow emissivity parameter.

Table 8.8 reinforces the model areal subdivision based on aspect, slope angle, elevation and vegetation cover. Vegetation density, snow albedo and snow emissivity are also found to be

**Table 8.8. Deterministic point sensitivity analysis: Results summary.**

<b>Very sensitive</b>	<b>Moderately sensitive</b>	<b>Very insensitive</b>
Aspect	Vegetation albedo - snow albedo	New snow albedo
Slope angle	New snow emissivity	Initial snow temperature
Vegetation density		Vegetation albedo
Old snow emissivity		Vegetation emissivity
Old snow albedo		
Elevation		

important parameters. The sensitivity of SNOMO to the albedo and emissivity are not unexpected given table 8.2 and the energy budget basis of SNOMO.

SNOMO is more sensitive to the emissivity and the albedo of old snow than that of new snow. This is due to the modelling routine which allows only one day to elapse after snowfall before conversion to old snow, and to the modelling of the melt period where, by definition, old snow will be exposed more often than new and the incidence of snowfall will decrease. Old snow is therefore more prevalent (due to the modelling structure and the process being modelled) and therefore will have a greater influence on SNOMO than new snow.

SNOMO is very sensitive to slope angle and aspect. The retardation of melt on north-facing slopes with increase in slope angle is greater than the acceleration of melt with increase in slope angle on south-facing slopes. This can be partly explained by the later snowfall and variation in meteorological conditions that are available when the melt is retarded. The meteorological conditions are fixed when melt is accelerated. The west- and east-facing slopes are relatively insensitive to increase in slope angle when compared to the north- and south-facing slopes.

The sensitivity analysis subjected SNOMO to a wider range of conditions than would be experienced in reality (at the W3 catchment). For example, the elevation range at W3 is 1135-2280ft and not 0-4000ft. However, by exposing SNOMO to a wider range of conditions, some of which would not be experienced at W3, the robustness, in addition to the sensitivity, of SNOMO is demonstrated.

The deterministic sensitivity analysis has other implications for model design and field program design and these will be discussed in general after the stochastic point sensitivity analysis.

#### 8.4 Stochastic point sensitivity analysis.

##### 8.4.1 Introduction.

The parameters that were subjected to the stochastic point sensitivity analysis and their associated measurement error or natural variability (mean and standard deviation) are shown in table 8.9.

The standard deviations were calculated using either the known measurement errors, by manipulating the means, or from distribution data available in the literature. This was because of a lack of sufficient measured data relating to the parameters from which the measurement error or natural variability could be calculated. The original daily input values were taken as the means for the wind speed, relative humidity, air temperature, initial snowdepth and snow albedo. The standard deviation for these parameters was calculated by using the known percentage error to calculate the limits within which 95% of the parameter variation occurs. The known error for the precipitation parameter is a deficiency of 15% and therefore the mean was calculated from the input value (the input value is deficient by 15%). The standard deviation was calculated in the same manner as the previous parameters, using an error of  $\pm 5\%$  around the calculated mean. The  $\pm 5\%$  error was set by the operator, as a possible error value for precipitation. The mean and standard deviation for the emissivity values were taken from Price & Petzold (1984). The mean and standard deviation for the thermal diffusivity and thermal conductivity parameters were calculated using old and new snow values as means and setting one of the upper distribution limits to equal the median between the two means. This enables the lower distribution limit to be calculated and the two limits were set to describe 95% of the variation. The standard deviation was then calculated from this distribution. Once the distributions of the parameters were calculated values for the parameters were selected from the probability distributions at random.

Table 8.9. Stochastic point sensitivity parameters and associated measurement errors or probability distributions.

PARAMETER	MEASUREMENT ERROR	NATURAL VARIABILITY	
		Mean	Standard Deviation
Wind speed	+2% or $\pm 0.2$ mph, whichever greater	NA	NA
Relative humidity	$\pm 5\%$	NA	NA
Air temperature	$\pm 1^\circ\text{F}$	NA	NA
Precipitation	15% deficiency	NA	NA
Snow albedo	$\pm 2\%$	NA	NA
Initial snowdepth	$\pm 0.5''$	NA	NA
Snow emissivity			
New snow	NA	0.99	0.012
Old snow	NA	0.94	0.012
Thermal conductivity			
New snow	NA	0.03	0.01
Old snow	NA	0.08	0.01
Thermal diffusivity			
New snow	NA	0.06	0.046
Old snow	NA	0.24	0.046

Again, the parameters were chosen by a system of ranking and choice of those that would be expected to be the most important. Wind speed, air temperature, relative humidity, precipitation and initial snowdepth are all inputs into SNOMO that originate from actual field measurements, not from the literature and, as such, the measurement error that is associated with them could have an important influence on the model results. These parameters also vary naturally and it is assumed that the measurement error accounts for this natural variability.

The deterministic sensitivity of SNOMO demonstrated that SNOMO was very sensitive to the snow albedo and snow emissivity. Therefore, the sensitivity of SNOMO to the natural variability of these parameters (the albedo variability is assumed to be equivalent to the radiometer error, even though the albedo value used in SNOMO is literature based) should be investigated.

Where applicable the sensitivity analysis of the parameter was subdivided, for example the air temperature parameter was analysed by varying the maximum air temperature first, then the minimum and finally both. In reality SNOMO operates with both the maximum and the minimum varying. However, by subdividing the parameter a more detailed investigation of the sensitivity is possible. The stochastic variability of SNOMO was examined for 20 runs of SNOMO for each parameter. Twenty runs was considered a large enough sample to be representative.

In contrast to the deterministic sensitivity analysis the stochastic sensitivity results could be examined using the coefficient of variation, CV, which is a numerical technique for the quantification of sensitivity. CV is expressed as a percentage relating to the mean and standard deviation of the results, equation 8.1.

$$CV = \frac{\sigma}{\bar{x}} \times 100\% \quad (8.1)$$

where,

CV coefficient of variation.

$\sigma$  standard deviation.

$\bar{x}$  mean.

It was possible to use CV as the results did not vary as greatly as with the deterministic sensitivity analysis and the problem of additional snowfall being misinterpreted as increased sensitivity did not occur. In fact, it occurred only once and in this case two CV values were calculated, one relating to the CV value calculated with the distorted result (n=20) and one without (n=19). Again, as with the deterministic sensitivity analysis, SNOMO was examined with both an active and inactive VEGIE subroutine.

#### 8.4.2 Results.

The results of the stochastic point sensitivity analysis of SNOMO are shown in table 8.10. The stochastic sensitivity results can be divided into degrees of relative sensitivity (table 8.11), as in the deterministic sensitivity analysis. Table 8.11 only considers the 'both' cases of subdivided variables, because this is the situation when SNOMO is operating normally. SNOMO is most sensitive to the snow emissivity. The CV value of 1.17% relates to a four day variation in the melt day, whereas the CV value of 2.16% relates to an eleven day variation in the melt day. The remaining CV values relate to 3 and 2 day variations in the melt date. If the CV=2.16% value is discounted, for the reasons mentioned in section 8.3.1, then the largest CV value represents a variation of four days. Therefore most of the variation is small, between 1 to 3 days, with the exception of the snow emissivity under a forest canopy, here the sensitivity is greater than four days but in reality is less than

Table 8.10. Stochastic point sensitivity analysis results.

PARAMETER	CV (%), n=20	
<b>Albedo</b>		
New snow	0.00	(0.00)
Old snow	0.00	(0.27)
Both	0.44	(0.45)
<b>Emissivity</b>		
New snow	0.00	(0.00)
Old snow	0.36	(0.64)
Both	0.61	(2.16, 1.17*)
<b>Thermal conductivity</b>		
New snow	0.00	(0.00)
Old snow	0.00	(0.00)
Both	0.00	(0.43)
<b>Thermal diffusivity</b>		
New snow	0.00	(0.00)
Old snow	0.00	(0.00)
Both	0.00	(0.45)
<b>Air temperature</b>		
Maximum	0.00	(0.00)
Minimum	0.20	(0.00)
Both	0.00	(0.00)
<b>Initial snowdepth</b>	0.00	(0.00)
<b>Precipitation</b>	0.00	(0.00)
<b>Relative humidity</b>	0.00	(0.00)
<b>Wind speed</b>	0.00	(0.00)

\* n=19

Figures in brackets refer to the results obtained with the activated VEGIE routine.

**Table 8.11. Stochastic point sensitivity analysis: Results summary.**

<b>Very sensitive</b>	<b>Moderately sensitive</b>	<b>Very insensitive</b>
Snow emissivity	Snow albedo	Initial snowdepth
	Thermal conductivity	Precipitation
	Thermal diffusivity	Relative humidity
		Wind speed
		Air temperature

eleven.

SNOMO is insensitive to initial snowdepth, precipitation, relative humidity and wind speed. It must be noted that, as with the deterministic sensitivity the melt days may be equal and therefore no sensitivity is registered, but the snowdepth remaining on the day before the melt day is always slightly different. This indicates that SNOMO is affected by the parameter change but not to the degree that results in a change in melt date.

There appears to be an interaction between some of the parameters that varies between their single option and the corresponding 'both' option. For example, the snow emissivity and snow albedo parameters both have lower CV values for their 'old' options than their 'both' options. Why is the CV value increased when the constituent old and new CV values are zero or much lower? Conversely the CV value for the minimum air temperature parameter is 0.20% and that for both maximum and minimum air temperature zero. These results could be due to unknown interactions within SNOMO, this is the most likely explanation of variability of the snow emissivity and snow albedo parameters. Alternatively, they are due to the random selection of the parameter values from the probability distribution, this is a more likely explanation of the variability of the air temperature parameter.

Again, the old snow albedo and emissivity are more sensitive than those for the new snow and SNOMO with the activated VEGIE option appears to be more sensitive than with the inactive VEGIE subroutine.

## 8.5 Discussion.

The point sensitivity analysis of SNOMO was performed for the reasons outlined in section 8.2. The results discussed in sections 8.3.3 and 8.4.2 have resulted in a more detailed knowledge of the operation of SNOMO and the interactions between parameters.

The deterministic sensitivity analysis has demonstrated that

the model emphasis on the areal subdivision by aspect, slope angle, elevation and vegetation cover was correct. This supports the relationships observed in the field, where slope angle, aspect, elevation and vegetation cover appear to be responsible for the variation in snowcover and snowdepth. It has also indicated that the parameters of snow albedo, snow emissivity and vegetation density are important. The values of these three parameters are, at present, taken from the literature. Vegetation density is highly variable spatially and therefore the utility of conducting a field programme to collect a representative vegetation density is debatable. The program would have to collect large volumes of data to result in a representative average value. Vegetation density is not easy to measure and the improved representativeness of a measured average value is probably not going to be that much greater than for a value taken from the literature. A similar argument can be applied to the snow albedo and snow emissivity parameters. It must be remembered that the sensitivity analysis was conducted between the physical limits of many of the parameters. Therefore many of the parameter values used will not be utilised in reality during a usual SNOMO run.

The stochastic sensitivity demonstrated the importance of field variability and measurement error on the model results and indicated that the melt date can be modelled to within slightly more than four days.

The sensitivity analysis could have been improved and would have been easier to interpret had the data set used not contained a late spring snowfall. However, this demonstrated the caution necessary when interpreting the results and is another aspect of the complex snow processes that are being modelled. Both the deterministic and the stochastic sensitivity analyses demonstrated the sensitivity of SNOMO to various parameters and reinforced the theory and structure of SNOMO.

## CHAPTER 9: MODEL SENSITIVITY ANALYSIS II: SPATIAL SENSITIVITY

### 9.1 Introduction.

Chapter 8 identified sensitivity analysis as an important and integral part of model development. The sensitivity analysis of SNOMO which is used as an aid in the understanding of SNOMO and the processes that SNOMO models is divided into a point sensitivity analysis (chapter 8) and a spatial sensitivity analysis (this chapter). The primary aim of SNOMO is the prediction of the spatial pattern of snowcover and snowdepth distribution (chapter 1) and therefore the spatial sensitivity analysis of SNOMO is vital in order to facilitate a better understanding of the model.

The spatial sensitivity analysis of SNOMO is a means of examining the complex relationships operating between variables at the catchment scale and of exhibiting the robustness of SNOMO and its utility as a research tool for examining the result of potential management scenarios. In the spatial sensitivity analysis, each variable is assigned its original value in each cell, except for one which is systematically altered in all cells across the catchment. In some cases the alteration is achieved by simply adding or subtracting a single value eg. elevation; in others it involves changing the character of the variable eg. from coniferous to deciduous vegetation cover. The response in terms of the distribution of snowcover and the melt day is then examined. For example, the interaction between vegetation cover type and the existing increase in elevation over the catchment can be examined, ie. it is possible that open areas at higher elevations within the catchment will melt at the same rate as coniferous areas at lower elevations within the catchment. Some of the scenarios that can be used to examine SNOMO using method are physically possible, for example, vegetation cover change (clear-cutting and planting). In contrast some of the scenarios are physically impossible, for

example, elevation and aspect changes. However these scenarios are useful as they provide further insights into the relationships operating between variables at the catchment scale and examine the response of the model to a series of conditions which, although unrepresentative of that particular catchment, are within the range of conditions that could be experienced within that snow environment.

The point sensitivity analysis is used as a basis from which the spatial sensitivity analysis can begin and is necessary as a means of identifying and simplifying some of the processes and interactions that occur within SNOMO, before the consideration of the more complex spatial processes and interactions. The deterministic and stochastic point sensitivity analyses showed that SNOMO is very sensitive to the variables slope angle, aspect, elevation, vegetation density, snow emissivity and old snow albedo (tables 8.8 and 8.11, chapter 8). In addition SNOMO was moderately sensitive to the vegetation albedo when this equalled the snow albedo and to the emissivity of new snow. It would therefore appear to be logical to examine the spatial sensitivity of SNOMO to these variables. However the spatial sensitivity of SNOMO would also have to consider the combinations of the four vegetation cover types that the computational cells could possess and the affects of changing air temperature, precipitation, relative humidity and wind speed over the catchment. Table 9.1 demonstrates the calculation of the number of potential variable combinations that would be required in order to conduct a spatial sensitivity analysis on the variables discussed above for the 28 cells of the W3 catchment. If 5 values of each variable, except for aspect and vegetation cover type, are used (they are chosen deterministically within realistic limits) the total number of potential variable combinations is approximately 1575! This is a huge number. If only one value for each variable is used the total number of potential variable combinations is approximately 325!, this is also a huge number.

Clearly an analysis using all the potential variable combinations is impractical and a selection to reduce the number of

Table 9.1. Calculation of the number of potential variable combinations for the spatial sensitivity analysis of SNOMO.

VARIABLE	NO. OF VARIABLE VALUES
Slope angle	5
Aspect	4
Elevation	5
Vegetation density	5
Old snow emissivity	5
New snow emissivity	5
Old snow albedo	5
Vegetation albedo	
-snow albedo	5
Vegetation cover types	4
Air temperature	5
Precipitation	5
Relative humidity	5
Wind speed	5
Number of cells	25

Number of potential variable combinations:

$$[(11 \times 5) + (2 \times 4)] \times 25! = 1575!$$

If the number of variable values is restricted to 1 then the number of potential variable combinations is:

$$(13 \times 25)! = 325!$$

combinations has to be made. Table 9.2 shows the variables chosen in the spatial sensitivity analysis of SNOMO and their values. The point sensitivity analysis of SNOMO indicated that SNOMO was very sensitive to the variables slope angle, aspect, elevation and vegetation cover. These four variables are also the criteria used for the subdivision of the catchment into computational cells and field results have shown their importance in determining snowdepth and snowcover distribution (chapters 5, 6 and 7). In order to limit the number of analyses only three aspects (North, South and East) were tested as the results for west aspects would be the same as those for east aspects, one elevation and one slope angle value were used. The choice of the elevation and slope angle value used was arbitrary. The number of vegetation combinations was also limited. The uniform vegetation cover types coniferous and open were chosen as these types represent the extremes of the vegetation cover types. This reasoning also applied to the choice of coniferous and open vegetation types and the half and half vegetation configuration. The choice of deciduous and coniferous vegetation types in this situation represented the extremes of the forest cover types. Initial snowdepth was also chosen as a sensitivity variable although the point sensitivity analysis had shown SNOMO to be insensitive to this variable. It was thought that SNOMO might be more sensitive to this variable spatially than at a point. Again this variable was limited to one value, the value for the initial snowdepth at the meteorological station (69cm). Each variable was changed in turn whilst the others remained constant. Again, the number of potential analyses was limited by avoiding the changing of the combinations of the variables.

The very large number of potential variable combinations demonstrates the complexity of SNOMO and the spatial sensitivity of SNOMO. Interpretation of the results of the spatial sensitivity analysis is correspondingly complex, even if using a drastically reduced number of variable combinations. Sensitivity analyses usually involve a statistical analysis or quantitative description of

**Table 9.2. Variables used in the spatial sensitivity analysis of SNOMO.**

(1)	SLOPE ANGLE	+10°
(2)	ASPECT	+90° +180° +270°
(3)	ELEVATION	+2000ft, therefore: 3500-4000ft (Townline) 3000-3500ft (lower than Townline)
(4)	INITIAL SNOWDEPTH	69.0cm
(5)	VEGETATION COVER:	
	5.1	Uniform coniferous
	5.2	Uniform open/clear-cut
	5.3	Bottom ½ catchment coniferous, top ½ deciduous
	5.4	Bottom ½ catchment deciduous, top ½ coniferous
	5.5	Bottom ½ catchment coniferous, top ½ open/clear-cut
	5.6	Bottom ½ catchment open/clear-cut, top ½ coniferous.

Cell numbers 1, 2, 6, 9, 10 and 11 comprise the bottom ½ of the catchment.

the relationships identified by the analysis. However, the complex nature of this spatial sensitivity analysis and the number of analyses involved has resulted in a qualitative and descriptive approach to the consideration of the results of the analysis.

The spatial sensitivity analysis was performed using data for the W3 catchment, March-April 1988. In order to avoid the problem of the late snowfall discussed in chapter 8 the datafile used was that used in chapter 7 for the validation of SNOMO. This therefore allowed direct comparison of the spatial sensitivity analysis results with the actual results for the 1988 melt. Unfortunately however this meant that the simulation had to cease on Julian day 101. If snow remained on day 101 the depth was recorded. As demonstrated in chapter 6 the deepest snowpack does not necessarily melt out last due to the affect of vegetation cover. However once depths of 10-20cm are reached the date of complete melt is usually related to snowdepth and this can be examined in conjunction with the vegetation cover. The datafile used in the point sensitivity analysis was an extended version of the datafile used in chapter 7 and therefore, until day 101, the point sensitivity analysis results are directly comparable to the spatial sensitivity analysis results. Use of the 'true' data file also allows direct comparison with the 1988 results which is useful for the examination of the affects of management practices such as clear-cutting.

The spatial sensitivity analysis was used to:

- (1) Determine the sensitivity of SNOMO to the spatial input parameters slope angle, aspect, elevation, vegetation cover and initial snowdepth.
- (2) Identify areas of potential model improvement.

## 9.2 Spatial sensitivity results.

The results of the spatial sensitivity analysis are presented in map and table form. A table was produced for the results of each variable showing the order in which the cells melted out, the first to melt being at the top. In each of the tables it must be remembered that cell 29 gives the same result as cell 31 and cell 24 gives the same result as cells 32 and 33. Therefore only the results for cells 29 and 24 are shown in the tables. It must also be remembered that cells 4, 5, 7, 8 and 26 are outside the catchment mask and are therefore omitted from the tables. The validation result for 1988 (figure 9.1) is presented as this is the constant that the results of the sensitivity analysis are compared against. The computational cells are also divided into groups based on their aspect, elevation and vegetation cover (table 9.3). This is as an aid in the interpretation of the results of the analysis. The 1988 vegetation cover map (figure 9.2) is also included as an aid in the interpretation of the results. The results of the analysis are difficult to interpret as the situation they represent is complex. Therefore the results for each variable or group of variables will be discussed individually. Section 9.3 will discuss the implications of all the results of the analysis together.

### 9.2.1 Initial snowdepth (figure 9.3, table 9.4).

The affect of vegetation cover becomes very apparent when a constant initial snowdepth is applied to all the cells in the catchment. Table 9.4 shows this clearly with the open/clear-cut, deciduous, mixed and coniferous vegetation cover melting out in that order. Aspect appears to differentiate between the mixed vegetation cells (cells 1,9,11,15 and 16). Cells 1, 9 and 11 are at lower elevations than 15 and 16 and might therefore be expected to melt first. However, cells 15 and 16 melt on Julian day 100 and cells 1, 9 and 11 on day 101. Cells 15 and 16 have aspects of 200° and 143°

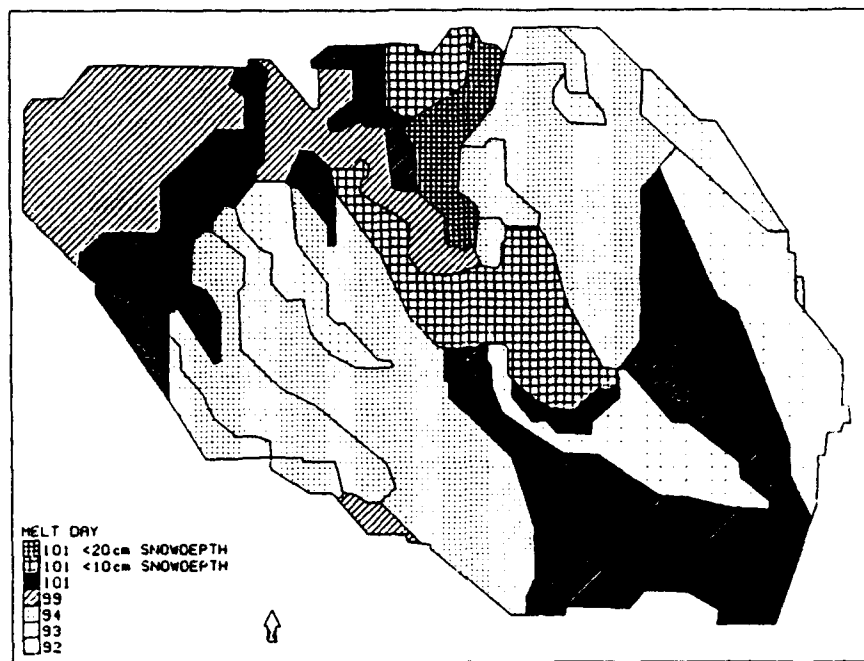


Figure 9.1. 1988 validation result.

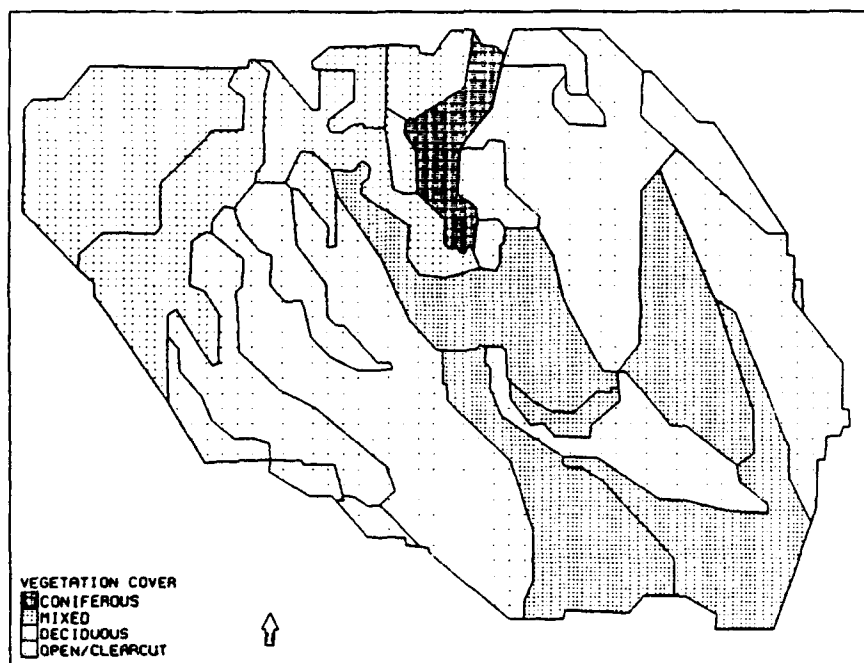


Figure 9.2. Vegetation cover, W3, 1988.

**Table 9.3. Distribution of cells in figure 9.1 on the basis of aspect, elevation and vegetation cover.**

**(1) ASPECT**

Aspect		Slope angle	Cell numbers
(1)	(2)		
71°	-109	4	12, 17, 22, 28
77°	-10	4	9
79°	-101	6	14, 24
87°	-93	6	1, 11
99°	-81	8	19, 21, 29
134°	-46	3	18, 23
143°	-37	9	6, 16, 20, 27, 30
196°	+16	5	2, 10
200°	+20	7	3, 13, 15, 25

Aspect 1 refers to the standard aspect notation, aspect 2 to the system used by SNOMO and TSTM (chapter 4).

**(2) ELEVATION**

Lower than Townline	1, 2, 9, 10, 11
Townline	3, 6, 12, 13, 14, 15, 16, 17, 18, 19, 20, 21, 22, 23, 24, 25, 27, 28, 29, 30

**(3) VEGETATION**

Open/clear-cut	2, 3, 6, 10, 12, 13, 14, 17, 18, 24, 25, 27, 28
Deciduous	20, 21, 22, 23, 29, 30
Mixed	1, 9, 11, 15, 16
Coniferous	19

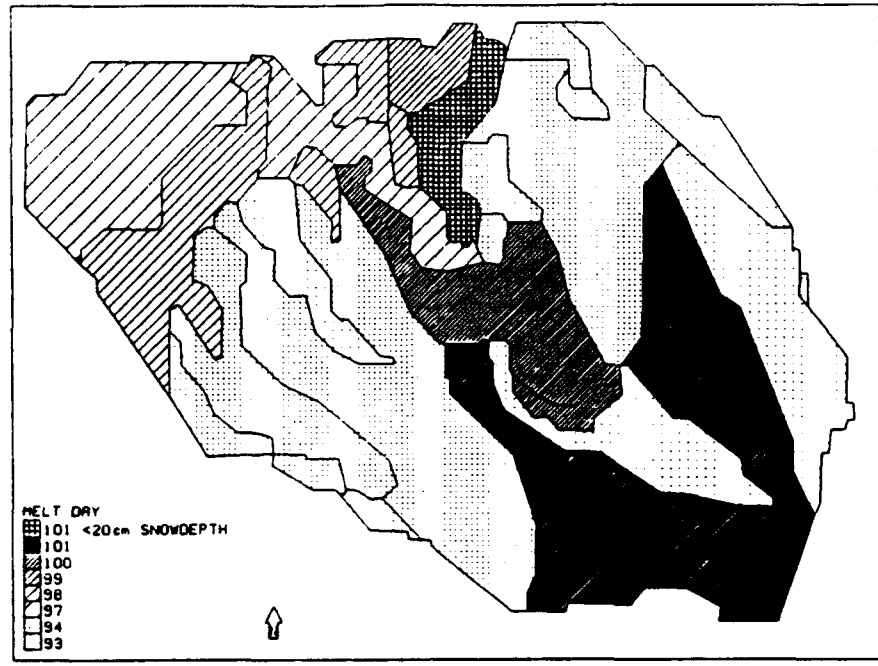


Figure 9.3. Spatial sensitivity analysis results: Initial snowdepth.

Table 9.4. Cells arranged in order of melt, for figure 9.3.

Melt day	Cells	Vegetation cover
93	2, 3, 6, 10, 13, 25, 27	op/cc.
94	12, 14, 17, 18, 24, 28	op/cc.
97	20, 30	decid.
98	21, 23, 29	decid.
99	22	decid.
100	15, 16	mix.
101	1, 9, 11	mix.
101<20cm	19	conif.

respectively whereas cells 1,9 and 11 have aspects of 77° and 87°. It appears therefore that aspect masks the affect of elevation, but is subordinate to vegetation cover in determining the pattern of snowcover and snowdepth distribution. Overall the period over which melt occurs is not significantly altered by the application of a constant initial snowdepth.

#### 9.2.2 Elevation change (figure 9.4, table 9.5).

The affect of changing the elevation was unexpected. An increase in elevation of 2000ft was expected to retard the melt date in every cell. However, cells 2,3,6,10,13,18,25 and 27 experienced an acceleration of melt by four days. Cells 15,19 and 22 were not affected by the elevation change and the remainder of the cells were retarded as expected. It is not understood why this occurred and it is suggested that further investigation into the spatial sensitivity of SNOMO to the elevation variable be conducted, this is however beyond the scope of this report. Overall the affect of a change in elevation was to prolong the period over which melt occurred.

#### 9.2.3 Slope angle (figure 9.5, table 9.6).

The affect of the increase in slope angle is difficult to quantify. The melt in cells 2,3,6,10,13,15,16,18,20,23,25 and 30 was accelerated, that in cells 19,21 and 29 did not change and that in the remaining cells (1,9,11,12,14,17,22,24 and 28) retarded. The influence of aspect is discernible when the affect on the melt day is examined. The cells where melt was retarded vary in aspect from 71°-87°, those where no change occurred have an aspect of 99° and those where melt was accelerated vary from 134°-200°. This is expected as melt will be retarded on steeper northerly-facing slopes and accelerated on steeper southerly-facing slopes. The affect of aspect is therefore enhanced by increasing the slope angle. Again, in order to investigate this relationship properly the slope angle needs to be

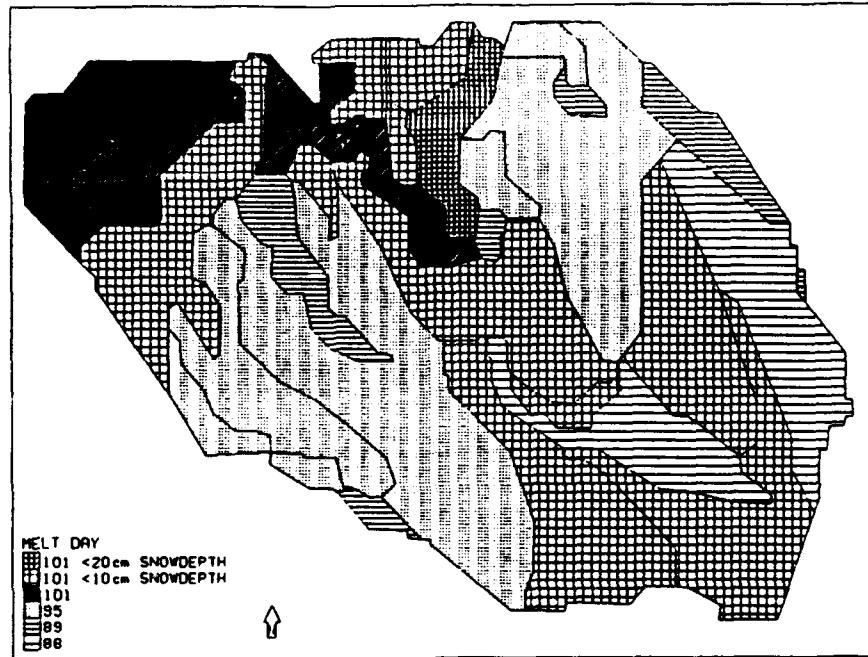


Figure 9.4. Spatial sensitivity analysis results: Elevation change.

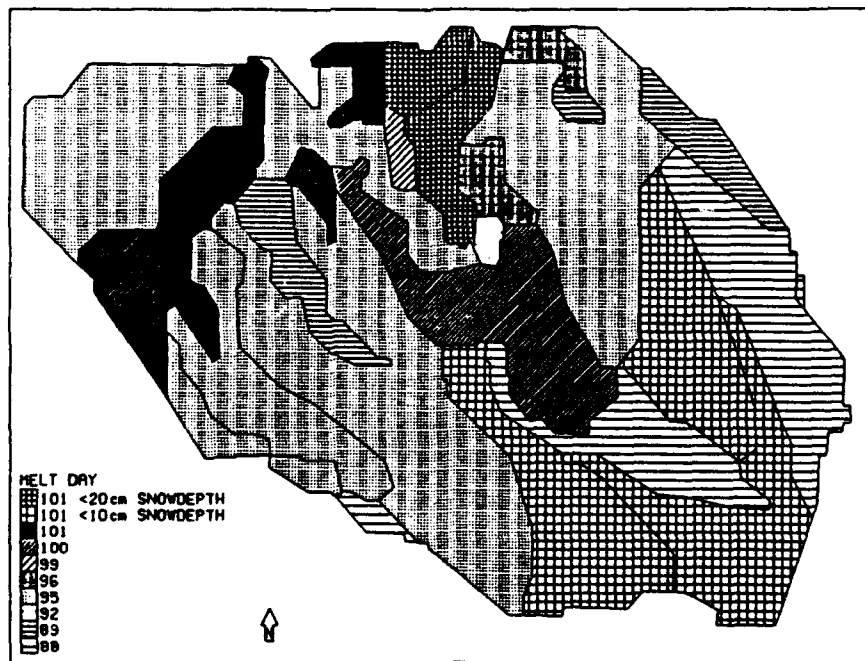


Figure 9.5. Spatial sensitivity analysis results: Slope angle.

Table 9.5. Cells arranged in order of melt, for figure 9.4.

Melt day	Cells	Vegetation cover
88	2, 10	op/cc.
89	3, 6, 13, 18, 25, 27	op/cc.
95	12, 14, 17, 24, 28	op/cc.
101	20, 30	decid.
101<10cm	1, 9, 11, 15, 16, 21, 22, 23, 29	decid, mix.
101<20cm	19	conif.

Table 9.6. Cells arranged in order of melt, for figure 9.5.

Melt day	Cells	Vegetation cover
88	2, 6, 10, 27	op/cc.
89	3, 13, 25	op/cc.
92	18	op/cc.
95	14, 20, 24, 28, 30	op/cc., decid.
96	12, 17	op/cc.
99	23	decid.
100	15, 16	mix.
101	21, 29	decid.
101<10cm	1, 9, 11	mix.
101<20cm	19, 22	decid., mix.

varied within reasonable limits, as in the point sensitivity analysis. However, this is beyond the scope of this report. The affect of slope angle might be easier to distinguish if the vegetation cover were kept constant and the slope angle varied. Overall the affect of increasing the slope angle was to extent the period over which melt occurred.

#### 9.2.4 Aspect (figures 9.6, 9.7, and 9.8, tables 9.7, 9.8 and 9.9).

The model response to a change in aspect appears to be correct. For example, originally cells 1 and 11 have an aspect of 87° (almost due east). These cells are rotated through 90° to produce aspects of 87°(East), 177°(South), 267°(West) and 357°(North), the melt days corresponding to these aspects are 101, 99, 101 and 101 with <20cm snow remaining respectively. Melt is therefore accelerated when south-facing and retarded when north-facing and is identical when east and west-facing. Cells 2 and 10 are much less strongly orientated north-south. These cells experience aspects of 196°, 286°, 16° and 106° and melt out on days 92, 93, 94, and 92 respectively. Here the same result (day 92) is achieved for aspects of 196° and 106°. However, the general affect of changing the aspect remains the same. Overall the affect of vegetation remains dominant especially the open/clear-cut vegetation cover option. The variation in aspect did not significantly affect the period over which melt occurred.

#### 9.2.5 Vegetation cover.

##### 9.2.5.1 Uniform vegetation cover, coniferous (figure 9.9, table 9.10).

The affect of aspect and elevation is clearly seen when the vegetation over the whole catchment is coniferous. Cells 2 and 10 melt first as they have a low elevation and a southerly aspect (196°). Cells 1, 11 and 9 are the next to melt and they have

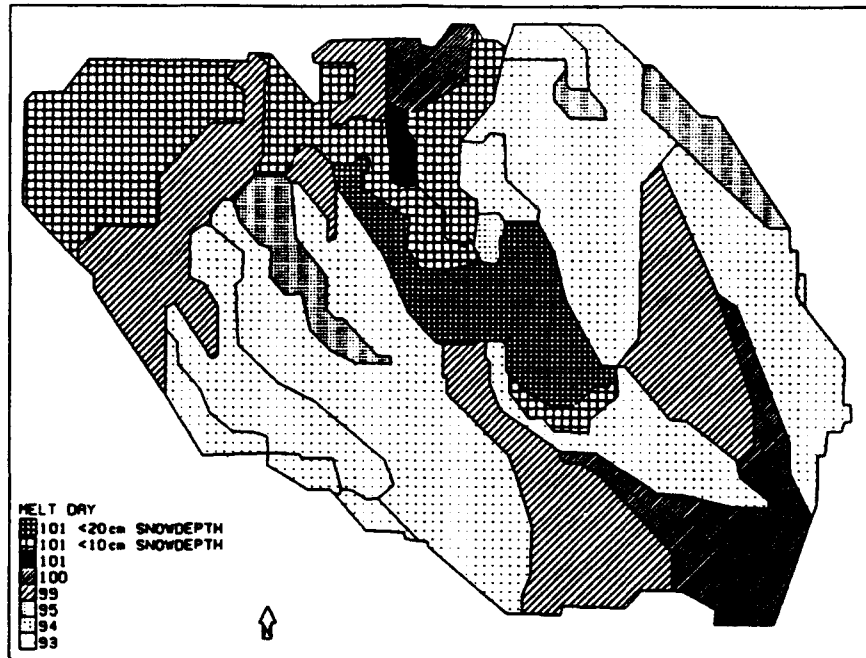


Figure 9.6. Spatial sensitivity analysis results: +90° aspect.

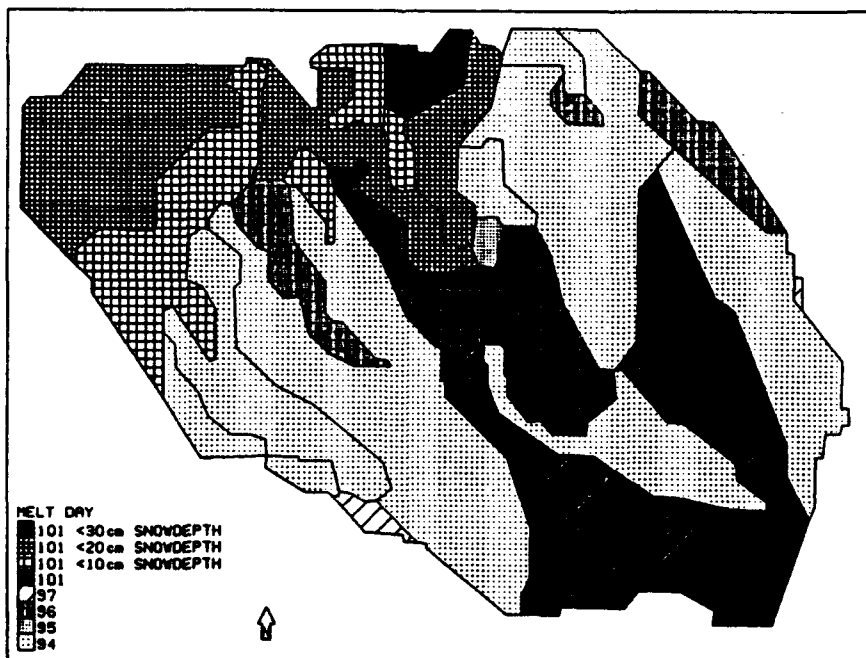


Figure 9.7. Spatial sensitivity analysis results: +180° aspect.

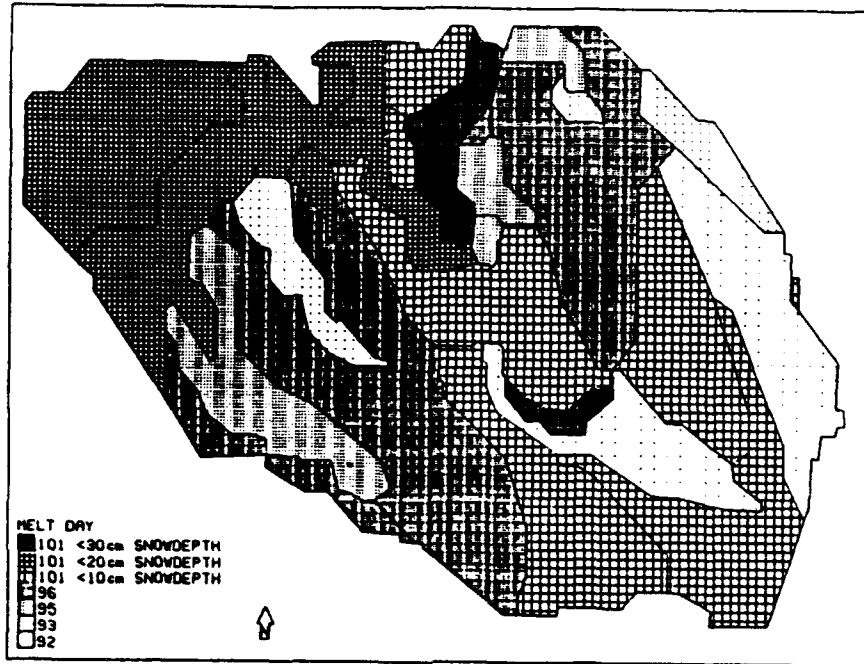


Figure 9.8. Spatial sensitivity analysis results: +270° aspect.

Table 9.7. Cells arranged in order of melt, for figure 9.6.

Melt day	Cells
93	2, 10, 12, 14, 17, 24, 27, 28
94	18
95	3, 13, 25
99	21, 29
100	9, 20, 22, 30
101	23
101<10cm	16, 19
101<20cm	15

Table 9.8. Cells arranged in order of melt, for figure 9.7.

Melt day	Cells
94	2, 10, 12, 14, 17, 24, 28
95	18
96	3, 13, 25
97	6, 27
101	1, 9, 11, 22
101<10cm	21, 29
101<20cm	19, 20, 30
101<30cm	15, 16

Table 9.9. Cells arranged in order of melt, for figure 9.8.

Melt day	Cells
92	2, 10
93	3, 13, 25
95	6, 12, 17, 18
96	14, 24, 27
101<10cm	1, 9, 11, 15, 22, 23
101<20cm	20, 21, 29, 30
101<30cm	16, 19

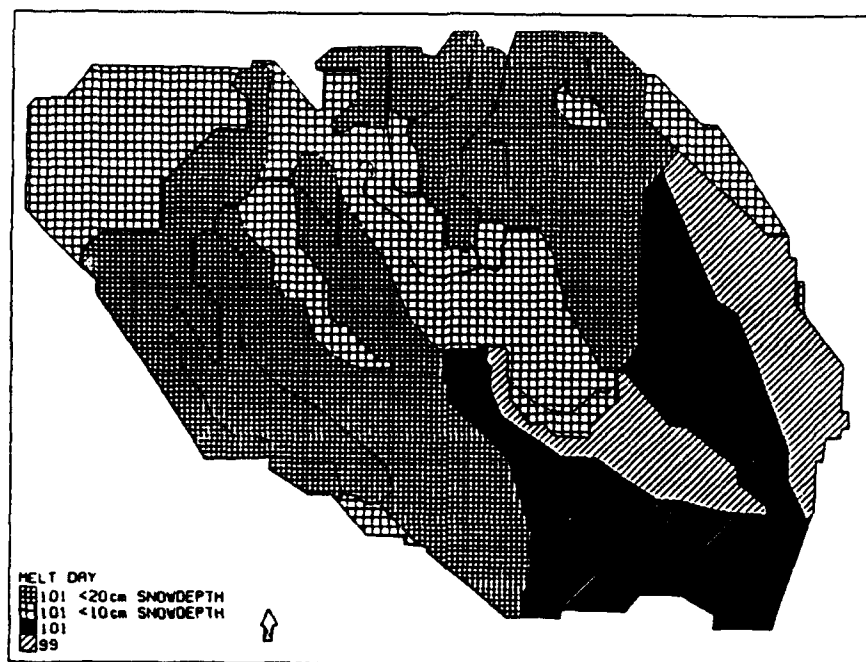


Figure 9.9. Spatial sensitivity analysis results: uniform vegetation cover, coniferous.

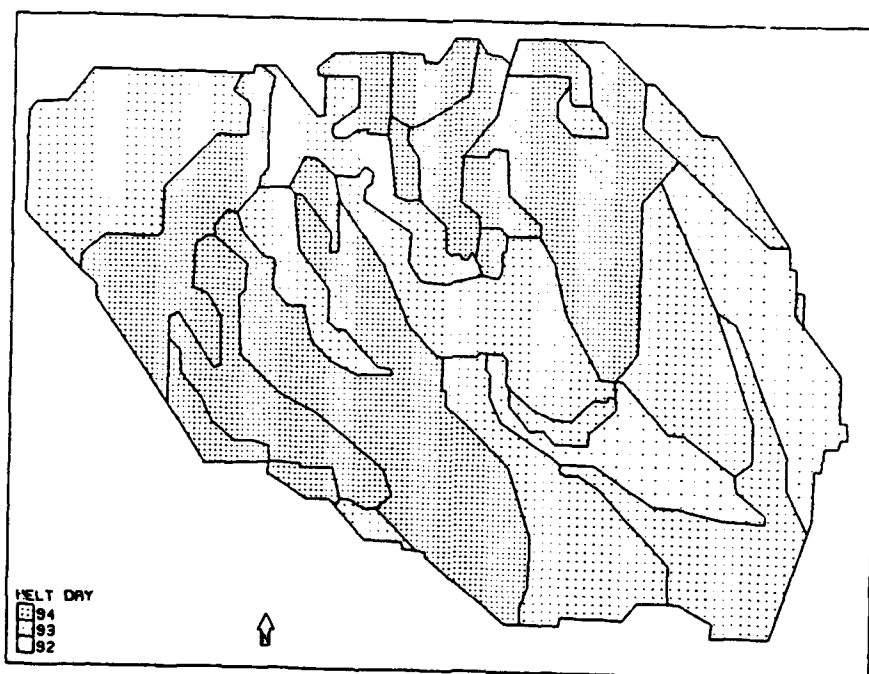


Figure 9.10. Spatial sensitivity analysis results: uniform vegetation cover, open.

**Table 9.10. Cells arranged in order of melt for figure 9.9.**

Melt day	Cells
99	2, 10
101	1, 9, 11
101<10cm	3, 6, 13, 15, 16, 18, 20, 23, 25, 27, 30
101<20cm	12, 14, 17, 19, 21, 22, 24, 28, 29

**Table 9.11. Cells arranged in order of melt, for figure 9.10.**

Melt day	Cells
92	2, 10
93	1, 3, 6, 9, 11, 13, 15, 16, 20, 25, 27, 30
94	12, 14, 17, 18, 19, 21, 22, 23, 24, 28, 29

easterly aspects but low elevations. The cells with less than 10cm of snow remaining on day 101 all have southerly aspects (134°-200°) whereas those cells with less than 20cm of snow remaining on day 101 have aspects ranging from 71°-99°. Overall the melt period is compressed but retarded. The compression is partly due to the inability to model beyond day 101 due to the data file. The overall retardation of melt is as expected, as snow has been observed to melt later under coniferous cover.

#### 9.2.5.2 Uniform vegetation cover, open (figure 9.10, table 9.11).

The affect of aspect and elevation is again apparent, although to a lesser degree, when the catchment vegetation cover is uniformly open/clear-cut (this will be referred to as 'open' for the remainder of this chapter). As in figure 9.9 cells 2 and 10 are the first to melt. This is explained by their aspect (196°) and low elevation. However, in contrast to figure 9.9 cells 1, 9 and 11 are not separately identifiable. However the majority of the cells that melt on day 93 have aspects of 143°-200° and those that do not are cells 1, 9 and 11, which have a low elevation. Overall the melt period is compressed and accelerated. The acceleration of melt is as expected, as snow has been observed to melt earlier in the open rather than in the forested environment.

The slight difference in the pattern of snowcover and snowdepth distribution discussed above, apart from the retardation or acceleration of melt, possibly reflects the relative dominance of the two vegetation types. Under the open cover type vegetation seems to be more dominant, in that it masks the affect of aspect and elevation. Under coniferous cover the affect of aspect and elevation is more visible. Further studies into the affects of varying the vegetation cover type uniformly would have to be made, in addition to varying the vegetation cover variables over the whole catchment, before any real conclusions could be drawn. Unfortunately, this is not within the scope of this report.

9.2.5.3 Vegetation cover configurations (figures 9.11, 9.12, 9.13 and 9.14, tables 9.12, 9.13, 9.14 and 9.15).

(1) Configuration 1 (top ½ catchment deciduous, bottom ½ coniferous) and configuration 2 (top ½ catchment coniferous, bottom ½ deciduous)

The response to vegetation configuration 1 is unexpected. It appears that aspect is as important as vegetation type in determining the snowcover and snowdepth distribution. For example, cells 2, 10, 20, 27 and 30 melt on day 99. Cells 2 and 10 have a coniferous cover but an aspect of 196° (south). Cells 20, 27 and 30 have a deciduous cover and an aspect of 143° (SE-SSE). Melt is usually retarded under coniferous cover when compared to other cover types. However, it appears in this case that the influence of aspect is such that this retardation is negated and that the usual distinctions that can be made between the melt patterns under coniferous and deciduous vegetation cover are not possible. As the aspects of the cells with coniferous cover become less southerly the influence of aspect diminishes and vegetation cover and elevation become the dominant factors influencing the pattern of snowcover and snowdepth distribution. The influence of elevation must not be discounted. The combination of elevation and coniferous vegetation cover results in an initial snowdepth value -15cm of that measured at Townline. This combination will therefore result in a shallow initial snowpack and, because there is simply less snow to melt, melt may appear to be accelerated. The variable interrelationships are complex.

The response to vegetation configuration 2 was as expected. The cells that were designated deciduous cover (lower ½ of the catchment) melted first followed by the cells with a coniferous cover. Within these two vegetation cover determined groups the affect of aspect was apparent. Within the deciduous cover group cells 2 and 10 have a 196° aspect, cell 6 a 143° aspect and cells 1, 9 and 11 aspects of 87° and 77°. For the coniferous cover group those cells with less than 10cm of snow remaining had aspects of 134°, 143° and 200° and those with less than 20cm of snow remaining had aspects of 71°, 79° and 99°.

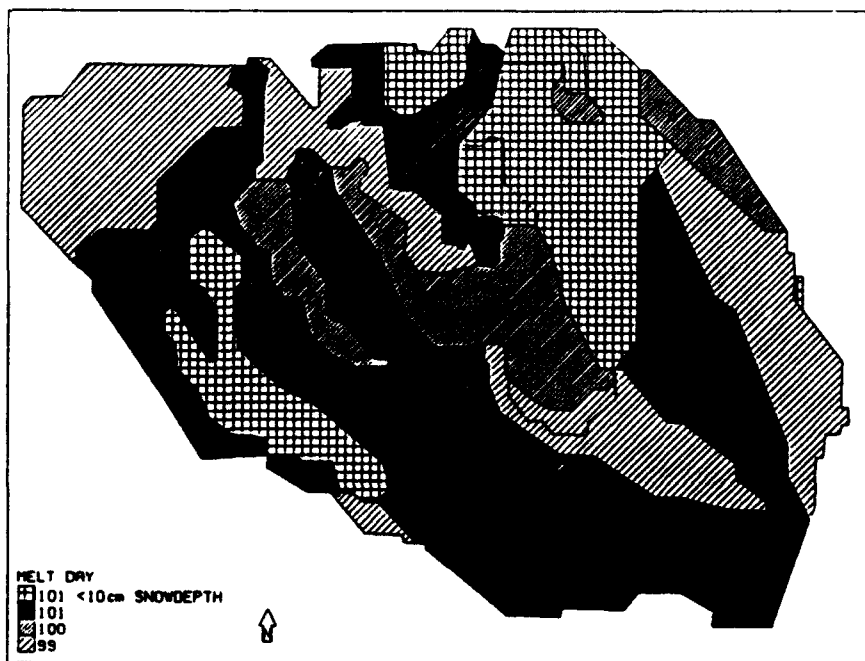


Figure 9.11. Spatial sensitivity analysis results: vegetation configuration 1.

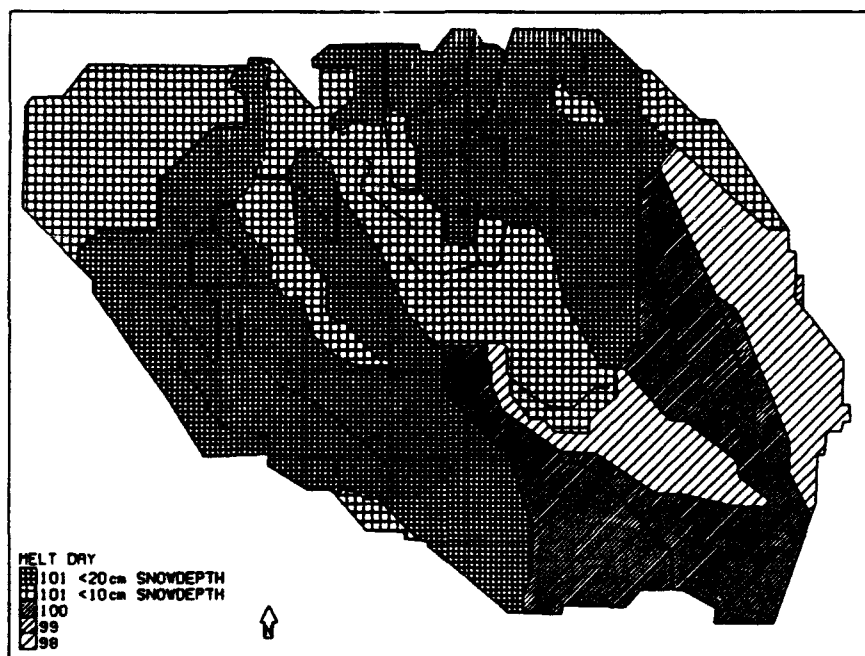


Figure 9.12. Spatial sensitivity analysis results: vegetation configuration 2.

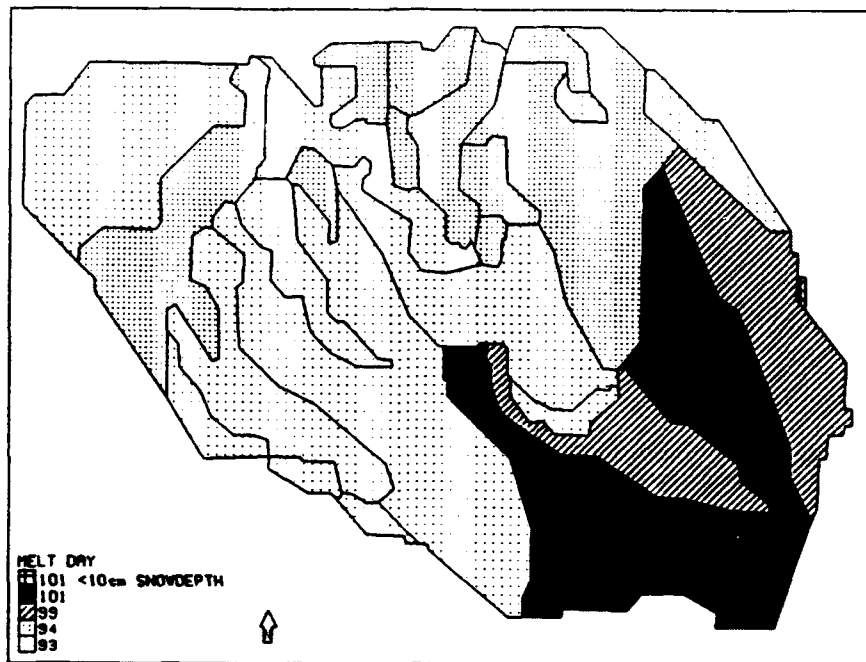


Figure 9.13. Spatial sensitivity analysis results: vegetation configuration 3.

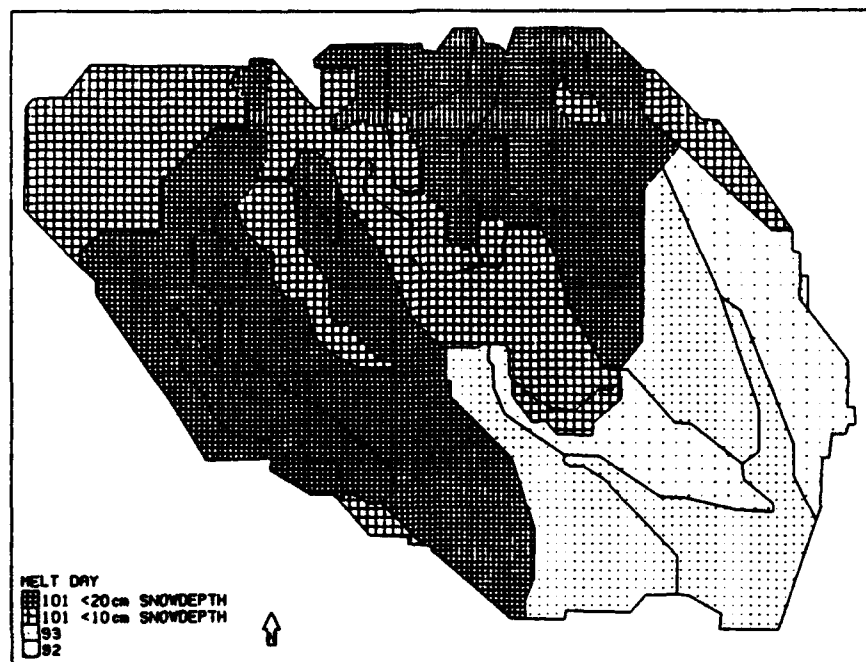


Figure 9.14. Spatial sensitivity analysis results: vegetation configuration 4.

Table 9.12. Cells arranged in order of melt, for figure 9.11.

Melt day	Cells
99	2, 10, 20, 27, 30
100	3, 13, 15, 16, 25
101	1, 9, 11, 19, 21, 23, 24, 29
101<10cm	6, 12, 14, 17, 22, 28

Table 9.13. Cells arranged in order of melt, for figure 9.12.

Melt day	Cells
98	2, 10
99	6
100	1, 9, 11
101<10cm	3, 13, 15, 16, 18, 20, 23, 25, 27, 30
101<20cm	12, 14, 17, 19, 21, 22, 24, 28, 29

Table 9.14. Cells arranged in order of melt, for figure 9.13.

Melt day	Cells
93	3, 13, 15, 16, 20, 24, 25, 27, 28, 30
94	12, 14, 17, 18, 19, 21, 22, 23, 29
99	2, 10
101	1, 9, 11
101<10cm	6

Table 9.15. Cells arranged in order of melt, for figure 9.14.

Melt day	Cells
92	2, 10
93	1, 6, 9, 11
101<10cm	3, 13, 15, 16, 18, 20, 23, 25, 27, 30
101<20cm	12, 14, 17, 19, 21, 22, 24, 28, 29

To summarize, in configuration 1 aspect appears to be dominant or equal to the affect of coniferous vegetation, especially if south-facing, but the affect of elevation in conjunction with vegetation on the initial snowdepth must not be discounted. In configuration 2 vegetation is the dominant factor affecting the pattern of snowdepth and snowcover distribution although the affect of aspect and elevation can be seen operating within the vegetation divisions.

(2) Configuration 3 (top  $\frac{1}{2}$  catchment open, bottom  $\frac{1}{2}$  coniferous) and configuration 4 (top  $\frac{1}{2}$  catchment coniferous, bottom  $\frac{1}{2}$  open).

The response to both configurations was as expected. In both cases the cells with the open vegetation cover melted first. The response to configuration 3 is interesting because this is the only variable permutation of those analysed which has not resulted in cells 2 and 10 being the or amongst the first cells to melt. This is in contrast with configuration 1 and suggests that the open vegetation cover type is more successful than the coniferous vegetation type in masking the affects of aspect. The order in which the cells with the open vegetation cover melt in response to configuration 3 does not appear to be related too strongly with aspect. Cells with aspects of 200°, 143°, 79° and 71° melt on day 93, those with aspects of 134°, 99° and 71° on day 94. The influence of aspect and elevation is apparent in the melt day separation of the cells with coniferous cover.

The response to configuration 4 was as expected. Those cells with an open vegetation cover melted earliest, those with a coniferous vegetation cover later. The four simple vegetation configurations discussed above and the two uniform vegetation cover examples illustrate the complexity of the situation that SNOMO is modelling and the difficulty of results interpretation. These examples are, as stated, only a very small number of the many permutations available.

### 9.3 Discussion.

The discussion of the spatial sensitivity of SNOMO is concerned with the specific results that have been derived from the spatial sensitivity analysis and with the problem of conducting a spatial sensitivity analysis on a model such as SNOMO. The results of the sensitivity analysis of SNOMO have highlighted the following points:

- (1) The relative dominance of aspect, elevation and vegetation cover in the determination of snowcover and snowdepth distribution.

The relative dominance of aspect, elevation and vegetation cover has been discussed individually for each variable permutation (section 9.2). In general vegetation cover is the dominant factor affecting the distribution of snowcover and snowdepth. This is demonstrated when the variation in cover type over the catchment is removed. This causes a shortening of the period over which melt occurs. Variation in snowcover and snowdepth distribution still occurs but is much less. Variation in snowcover and snowdepth distribution within each cover type is due to elevation and aspect. The open vegetation cover type appears to have a dominant affect over the remaining cover types and the elevation and aspect. This is demonstrated by vegetation configuration 3 (discussed in detail above) where cells 2 and 10, which melt first or are among the first to melt in every other parameter permutation analysed, are not among the first to melt.

- (2) The elevation response.

The response of SNOMO to an increase in elevation was unexpected and suggests further investigation of the model structure and further sensitivity analyses using different elevation changes.

- (3) The utility of SNOMO in catchment management studies.

The vegetation configurations 3 and 4 can be viewed as prototype clear-cutting scenarios. The results from vegetation configurations

3 and 4 demonstrate that SNOMO is sensitive to changes in vegetation cover. If these changes are due to forest management practices then SNOMO has the potential for use as a forest management tool. In addition the affects of landuse changes due to, for example, resort development or real estate development could also be modelled. However, further validation of SNOMO and sensitivity analyses relating to clear-cutting and landuse changes would have to be made before valid and qualified forest management predictions could be made.

(4) Further spatial sensitivity analysis.

The choice of parameters selected for the spatial sensitivity analysis of SNOMO was explained in section 9.1. Having conducted the spatial sensitivity analysis on these parameters further parameter combinations are suggested:

- (a) Potential forest management scenarios.
- (b) Deterministic variation of elevation and slope angle within realistic values.
- (c) Deterministic variation of slope angle, elevation and aspect under a uniform vegetation cover.
- (d) The uniform vegetation cover types of deciduous and mixed forest.
- (e) Variation of the vegetation configurations in the same half and half manner as before, although with deciduous and open and mixed and open cover types.

The results of these analyses can then be used to determine if other analyses on factors such as precipitation or snow albedo need to be performed. These are proposed spatial sensitivity analysis parameter permutations that have arisen from the analysis of the results of the current spatial sensitivity analysis. They are beyond the scope of, but result from, this report.

The spatial sensitivity analysis of SNOMO has identified difficulties in conducting a spatial sensitivity analysis on a model

such as SNOMO. The large number of potential variable combinations available necessitates a reduction in the number of variable combinations analysed. The choice of variables analysed is based on existing knowledge of the model and variable interrelationships but as the situation is so complex it is probable that some important variables or variable combinations are omitted. The interpretation of the analysis results is also difficult. Usual statistical and quantitative interpretation techniques are unsuited for this type of analysis due to the number and complexity of the interrelationships and variables. The difficulty of achieving a spatial sensitivity analysis for a model such as SNOMO, that is a physically-based model with spatial output, could be interpreted as a limiting factor in the development of models of this type. It is possible that an alternative approach should be devised for the spatial sensitivity analysis of models such as SNOMO. An approach that uses quantitative methods other than statistics in order to identify and quantify variable and spatial relationships. It is not suggested here what this approach would specifically comprise but is suggested as an indication of the possible future direction that the analysis and treatment of models of this type might take.

However, the spatial sensitivity analysis performed on SNOMO does provide results and from these it is possible to gain an insight into some of the internal relationships and variable interactions that operate within the model.

The spatial sensitivity analysis of SNOMO has demonstrated some of the complexity of the interactions that SNOMO makes in order to simulate the snowcover and snowdepth distribution. This mirrors the situation in the field, which is itself complex and difficult to identify (chapter 6). The spatial sensitivity analysis has posed almost as many questions as it has provided answers and has suggested the need for further spatial sensitivity analyses and possibly the need for a new approach to spatial sensitivity analysis for models such as SNOMO. This report contends that this situation is

unavoidable when considering the spatial sensitivity analysis of a distributed physically-based model such as SNOMO that is modelling a situation that is as spatially variable and complex as the pattern of snowcover and snowdepth distribution.

## CHAPTER 10: GENERAL AND SPECIFIC MODELLING ISSUES ARISING FROM THE MODEL DEVELOPMENT

This chapter considers the issues that have arisen from the development of SNOMO as outlined in chapter 3 (figure 3.1), the stages of which have been discussed in the preceding chapters. At the current stage of model development (chapter 10) the question must be asked "have the modelling objective and aims been fulfilled?". In addition several future modifications to SNOMO and implications of SNOMO are proposed that arise from the current model development.

The development of SNOMO has also highlighted several general conceptual points that relate to models such as SNOMO, that is physically-based models that simulate processes that are highly variable both temporally and spatially. These issues arising from the development of SNOMO are discussed below.

### 10.1 Specific model development issues.

#### 10.1.1 Fulfilment of modelling objective and aims.

This report contends that a satisfactory model of snowcover dynamics, SNOMO, has been developed. SNOMO is able to:

- (1) Model the spatial and temporal variations of hydrological, meteorological and energy budget parameters in a cold regions watershed.
- (2) Simulate the spatial pattern of snowcover throughout the melt season.
- (3) Simulate the impact of landuse change on cold regions watershed hydrology.

This report also provides the model code and an operational

manual.

The originality of the modelling design arises from the design requirements which are themselves dictated by the modelling objective. The model objective and aims result in an original catchment subdivision method and an original methodology and structure that is a balance between the complex and the simple, but physically-based wherever possible. The fulfilment of the modelling objective and aims does not however signal the end of the model development process.

#### 10.1.2 Suggested future modifications to SNOMO.

The discussions at the end of chapters 4, 6, 7, 8 and 9 contain suggestions for future model improvement and modification. These modifications are beyond the scope of this report due to time constraints but are included in this discussion as they emphasise the continued development of SNOMO and are themselves part of the continuum of model development. The most important of the suggested modifications to SNOMO are summarised below:

(1) The inclusion of meltwater routing.

This would enable streamflow to be predicted thereby increasing the utility of SNOMO. This would also enable SNOMO to be evaluated against snowmelt models which have streamflow as their primary output and would therefore increase the number of models that SNOMO can be evaluated against dramatically. A simple recession relationship can be used to model the routing or a more complex physically-based scheme such as VSAS2 or the SHE model (discussed in chapter 5) can be used. The use of a scheme such as VSAS2 or the SHE model would require a catchment subdivision method that is different from that which is used for the calculation of the pattern of snowcover and snowdepth distribution and snowmelt volume. The presence of a digitized topographic map and a GIS to handle the spatial data would facilitate the calculation of a catchment subdivision for routing

purposes. A method would have to be devised to transfer the snowmelt calculated using SNOMO to the routing catchment subdivisions where it would be used as an input into the routing process. The use of a physically-based scheme to route the snowmelt should be designed to operate within the design criteria and objectives of SNOMO, that is to use physically-based equations wherever possible but to keep a balance between complexity and simplicity. The prediction of streamflow would allow, with the addition of a snow accumulation routine, the simulation of streamflow throughout the year. This, again, increases the utility of SNOMO.

(2) The inclusion of a snow accumulation routine.

This would enable the modelling of the snowpack throughout the winter and the spring and would negate the necessity for the use of an initial snowdepth input. The accumulation routine would also solve the problem that exists at present where SNOMO stops modelling in spring due to predicted total snow disappearance and therefore misses heavy spring snowfalls that could occur during the following days. The accumulation routine would have to allow for the affect of wind redistribution of the snow. A possible method for achieving this would be to weight each computational cell using a wind factor. The wind factor would be determined primarily by the vegetation type of the cell and would be multiplied by the snowfall precipitation.

(3) The inclusion of the calculation of  $Q_g$

The inclusion of the calculation of the heat flux across the ground/snow interface ( $Q_g$ ) would enable the depth of frost under the snowpack to be calculated and the energy budget of the snowpack to be calculated more accurately, this would be useful for agriculture. In environments such as the Prairies  $Q_g$  is more important than the situation in, for example, Vermont. Therefore the inclusion of the calculation of  $Q_g$  expands the number of potential application environments of SNOMO. The calculation of  $Q_g$  would be aided by the simulation of the accumulation of the snowpack. The calculation of

$Q_g$  is also useful for the prediction of the behaviour of road surfaces (metalled or unmetalled) during the melt period. This has potential implications for transport planning and logistics.

(4) The inclusion of shadowing effects.

The inclusion of a routine to calculate the affect and extent of shadowing on the pattern of snowcover and snowdepth distribution would enable the snowpack energy budget to be calculated more accurately. The number of environments that SNOMO can be applied to are also extended, in that more accurate results should be obtained in areas with strong aspect-induced melt patterns (eg. alpine valleys).

(5) A revised field programme.

A revised field programme with a strong emphasis on the use of SNOMO as an aid in the formulation of the field programme is suggested in chapter 7. Guide-lines for the formulation of future field programmes have been discussed and it is suggested here that these be applied to future field programmes. The wider implications of the field programme-model design relationship are discussed in section 10.2.

These suggested modifications enhance the utility of SNOMO and increase the knowledge of the interrelationships between the variables operating within SNOMO.

### 10.1.3 Suggested future modelling strategies.

The discussions at the end of chapters 5, 6, 7, 8 and 9 also contain suggestions for future modelling strategies, that is the major investigation of part of the model structure or of certain stages in the model development. These are summarized below:

(1) Further sensitivity analysis and implementation of current sensitivity analysis suggestions.

Certain variable combinations for future point and spatial analysis were suggested in chapters 8 and 9. The relationship of SNOMO to certain variables requires further examination, this was identified as a result of the sensitivity analyses that have already been conducted.

(2) Additional validation.

In order to fully validate SNOMO further applications of SNOMO should be made. Only one application of SNOMO has been made at present, that discussed in chapter 7 on the W3 catchment, Danville, Vermont. This reflects the overall emphasis of the report. The modelling development strategy has been outlined in figure 3.1 (chapter 3). Roughly 70% of the report time has been devoted to the formulation of the research question, the model design and the translation of that design into an operational model. The remaining 30% of the report time has been devoted to the validation and sensitivity analysis of the model, and to the field data collection. Applications of SNOMO and hence validations of SNOMO are required for catchments similar to W3 such as Hubbard Brook (New Hampshire) or Lac Laflamme (Quebec, Canada) and catchments experiencing more diverse snow environments such as the Canadian boreal forest (Schaefferville), the Prairie, the Alpine or High Mountain (Rockies) and the Pacific Northwest environments. SNOMO is based on the energy budget of the snowpack and is not calibrated therefore it is expected that the transition between snow environments should be easier than, for example, the Leaf & Brink (1973a & b) model, WATBAL. It is envisaged that the transition of SNOMO to environments that are less spatially diverse and more climatically stable than the Northeastern USA, for example the Alpine/High mountain environment (Rockies) should be relatively simple.

(3) The investigation of intra-cell snowcover and snowdepth distribution patterns.

The structure and energy budget basis of SNOMO allows the future investigation of micro-scale snowcover and snowdepth distribution patterns, ie. those within a computational cell. Detailed mapping and field survey would enable the subdivision of the computational cell into micro-cells using the micro variation of aspect, slope angle, and vegetation cover as the subdivision criteria. Elevation would not be an important factor in determining the pattern of snowcover and snowdepth distribution at this scale. Intra-cell variation can then be investigated. The results from such an investigation may be important to SNOMO at the catchment-scale and may be incorporated into SNOMO by developing a means of realistically representing the patchy nature of snowcover retreat.

(4) Examination of the spatial basis of SNOMO.

The spatial basis of SNOMO can be examined by using a grid as an alternative to the present spatial basis of SNOMO. The use of a grid must be considered in terms of the spatial scale of the input data required and the availability of this data. Various combinations of groups of grid cells can be tested to find the most ideal combination of grid cells and the result obtained using this ideal combination tested against the 'homogeneous areas' concept that is used at present.

## 10.2 General model development issues.

The development of SNOMO has identified several general conceptual points that have implications in the context of the wider modelling arena and specially with reference to complex physically-based models such as SNOMO. These general conceptual points are discussed below.

### 10.2.1 Validation problems.

The complete validation of models such as SNOMO is difficult because of problems of:

(1) Data availability.

The validation data required for models such as SNOMO is often not readily available. This is because models such as SNOMO are simulating processes that are complex both areally and temporally, such as the pattern of snowcover and snowdepth distribution. These models should be validated using data that is as representative as possible to the process that the model is simulating. For example, it is insufficient to validate SNOMO using the more readily available streamflow hydrograph data, data describing the pattern of snowcover and snowdepth distribution should be used. The more complex data that is required is usually not readily available.

(2) Data representativeness.

The nature of the validation data also causes problems of data representativeness, both of the field situation and when used as a validation variable. The problems of obtaining a representative snowdepth value have been discussed (chapters 6 and 7). When a model such as SNOMO is validated the calculated results (that exist within certain accuracy limits) are compared with the measured results (that are taken as representative of the field situation). The comparison of two fixed values that in reality represent a value within certain limits could result in the misinterpretation of the validity of SNOMO.

The problem of model validation forces a more qualitative and descriptive model validation than is traditionally acceptable. This possibly suggests that a new validation method should be formulated for models of this type so that the validation, even though it is qualitative, remains structured and replicable.

If model validation is to be comprehensive then validation must occur on more than one catchment (chapter 6). The model environment-

design relationship will result in model modification if validation is attempted for environments other than those for which the model was designed. In the adaptation of the model for these environments parameterization and calibration must be avoided wherever possible (chapter 7).

#### 10.2.2 Sensitivity analysis problems.

The general problems that were experienced during the sensitivity analysis of SNOMO can be applied in general to models of this type. The problems were most apparent in the spatial sensitivity analysis of SNOMO (chapter 9). The nature of the model and the process that is simulated resulted in a qualitative and descriptive spatial sensitivity analysis. Traditional statistical methods would have been inoperable. In addition, the very large number of potential variable combinations for analysis forced a reduction in the number of analyses and therefore a subjective choice of variables for the analysis had to be made. This resulted in a possible incomplete analysis of the model. Even with a limited number of variables the interpretation of the spatial sensitivity results is difficult due to the complex nature of the interactions that SNOMO models. It is suggested that a different method of spatial sensitivity analysis be formulated for models such as SNOMO.

#### 10.2.3 Field programme-model relationship.

The relationship between the model and the design of the field programme to collect validation and operational data and in order to further understand the processes occurring in the environment has been fully discussed in chapter 7. The relationship between the field programme and the model is an important conceptual point and demonstrates the future utility and potential of SNOMO.

#### 10.2.4 The development of multi-model, catchment management models.

The inclusion of the Leaf & Brink (1973a & b) model, WATBAL, within a catchment management model, MMARM, was discussed in chapter 3 and was proposed as a possible future modelling development for SNOMO. SNOMO is a physically-based model and therefore has a large potential for use by hydrologists, environmental chemists, agriculturalists, ecologists, planners and engineers. SNOMO could be linked with, for example, a forest growth model, an insect pest model or a forest chemistry model. Figure 10.1 shows a scheme for the inclusion of SNOMO into a catchment eco/hydro-system model. The GIS holds and manipulates the basic spatial data and the climatic data inputs. Changes to, for example, vegetation cover can be easily incorporated into this structure. Two primary models exist, one to simulate the pattern of snowcover and snowdepth distribution and calculate snowmelt volume (SNOMO) and the other to calculate runoff (either using a variable source area or grid spatial approach). The spatial bases of these two models are therefore different but are derived from the same base data held in the GIS. The results from the primary models enable the utilisation of the secondary modelling units. These are additional ecosystem models such as forest chemistry and erosion models. These models use some or all of the outputs generated by the primary model units. In some cases they are modifications of the primary model units, others are separate models. The spatial basis of these models is either that of the primary model units or a separate original basis. Again, the GIS enables the storage and modification of spatial data and as long as point continuity is adhered to the changing of the spatial basis is not important.

Outputs from the proposed management model would occur at each modelling stage or when the operator requires. The management model would be designed to be user-friendly and menu-driven. A choice of models and options would be offered at each stage in the modelling process. This model choice was mentioned in chapter 3. For

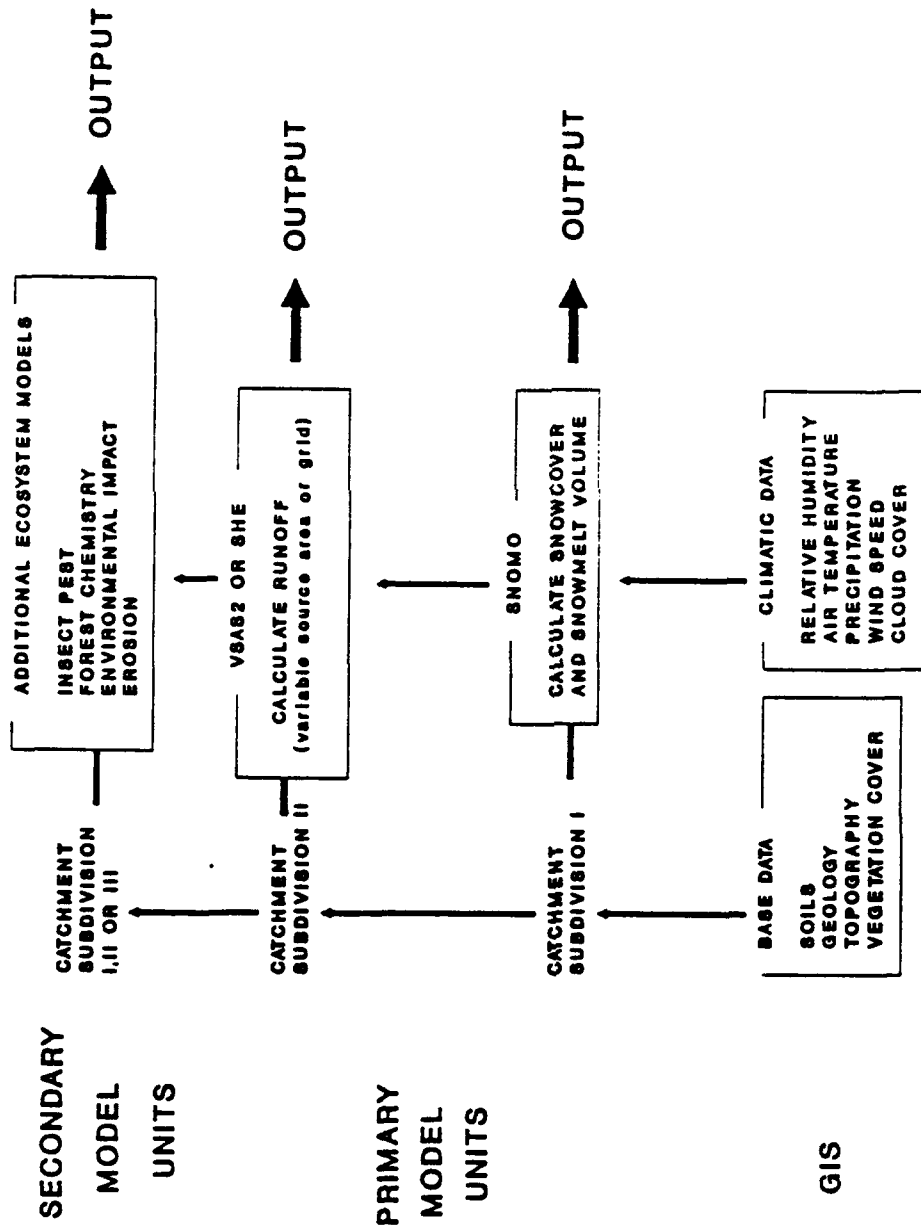


Figure 10.1. The inclusion of SNOMO into a catchment eco/hydro-system model.

instance, the choice of a grid or variable source area method is offered for the calculation of runoff. Model selection can be determined by the operator and model operation can be halted when required. For example, if the operator was only interested in the pattern of snowcover and snowdepth distribution then the management model would halt after the calculation of this and would not continue to calculate runoff. Conversely, if summer runoff were required SNOMO would not be activated.

SNOMO could also be developed to utilise satellite data input. This has already been achieved with an index snowmelt model (Ferris & Congalton, 1989) but a physically-based model has many more potential uses. In addition the pattern of snowcover and snowdepth distribution that is calculated by SNOMO can be used as ground truth data for satellite snow observations. This may have great potential use in satellite derived estimates of total catchment snowcover and water equivalent which are used in many irrigation, water resource and river management schemes. The satellite data input could also be incorporated into a management model structure.

The inclusion of SNOMO into a management model structure and the utilization of satellite data are envisaged as an additional future modelling objective and not a current modelling objective. The possibility of this development of SNOMO demonstrates the utility and potential of SNOMO.

The development of multi-model catchment management models has been described in detail for SNOMO. This form of model development can be applied to models similar to SNOMO.

### 10.3 Discussion.

A central theme can be observed linking all the chapters of this report together. It is that the complexity of the situation that SNOMO is modelling, i.e. snowcover dynamics, is reflected by the complexity of the variable relationships within SNOMO. It is hoped

that the complexity of SNOMO mirrors that of snowcover dynamics in the environment. However, ascertaining whether this is true is not an easy task and results in some of the points discussed above.

SNOMO is a complex model developed to simulate a complex situation. Simple models can be used to simulate complex situations, but they will give less of an insight into the situation that they are modelling and will not perform as well when subjected to abnormal or changeable conditions. Simple models are of less utility, other than that for which they were designed, than complex models. There are more unforeseen benefits ('spin-offs') with a complex model. To counter this the complexity of a distributed physically-based hydrological model such as SNOMO means that model validation, data collection and representation, and sensitivity analysis are difficult. However, these difficulties are not insurmountable and, in the case of the field data collection, are solved in part by the model. These difficulties do not outweigh the advantages of a more complex physically realistic model but are inherent in the nature of the model and the situation that is being modelled.

This report has presented and discussed the development of a model of snowcover dynamics, SNOMO. This model is a distributed physically-based model that is able to simulate the pattern of snowcover and snowdepth distribution, the variation in snowpack properties and the volume of meltwater generated by melt over a catchment throughout the melt period. Difficulties in the model development process are primarily a function of the complexity of the process being modelled. These difficulties are addressed and are outweighed by the modelling advantages and potential of SNOMO.

## BIBLIOGRAPHY

- Ambach, W. (1974). The influence of cloudiness on the radiation balance of a snow surface with high albedo. J. of Glaciology, 13(67), 73-84.
- Anderson, E.A. (1968). Development and testing of snow pack energy balance equations. Water Resour. Res., 4(1), 19-37.
- Anderson, E.A. (1973). National Weather Service River Forecast System - Snow Accumulation and Ablation Model. NOAA Technical Memorandum NWS HYDRO-17, US Dept. Commerce, National Oceanic and Atmospheric Admin. National Weather Service.
- Anderson, E.A. (1976). A Point Energy and Mass Balance Model of a Snow Cover. NOAA Technical Report NWS 19, US Dept. of Commerce, Silver Spring, MD, 150pp.
- Anderson, E.A. (1978). Streamflow simulation models for use on snow covered watersheds. In: Proc. Modeling of Snow Cover Runoff. (eds. S.C.Colbeck & M.Ray), US Army CRREL, Hanover, New Hampshire, 336-350.
- Anderson, E.A., Whipkey, R.Z., Greenan, H.J. & Machell, C.T. (1977). NOAA-ARS Cooperative Snow Research Project - Watershed Hydro-Climatology and Data for Water Years 1960-1974, US Dept. of Commerce, Silver Spring, MD, 304pp.
- Anderson, M.G. & Sambles, K.M. (1988). A review of the basis of geomorphological modelling. In: Modelling geomorphological systems. (ed. M.G.Anderson), John Wiley & Sons Ltd., 1-32.
- Balick, L.K., Link, L.E.Jr., Scoggins, R.K., & Solomon, J.L. (1981a). Thermal Modelling of Terrain Surface Elements. Technical Report EL-81-2 prepared by the Environmental Laboratory, Waterways Experiment Station, in collaboration with Mississippi State University, for the US Army Engineer Waterways Experiment Station, CE, Vicksberg, Miss.
- Balick, L.K., Scoggins, R.K. & Link, L.E.Jr. (1981b). Inclusion of a simple vegetation layer in terrain surface temperature models for thermal infrared (IR) signature prediction, Miscellaneous Paper EL-81-4, US Army Engineer Waterways Experiment Station, CE, Vicksberg, Miss.
- Band, L.E. (1986). Topographic partition of watersheds with Digital Elevation Models. Water Resour. Res., 22(1), 15-24.
- Bathurst, J.C. (1986). Sensitivity analysis of the Systeme Hydrologique Europeen for an upland catchment. J. of Hydrol., 87, 103-123.

- Bergen, J.D. (1975). A possible relation of albedo to the density and grain size of natural snow cover. Water Resour. Res., 11(5), 745-746.
- Bernier, P.Y. (1982). VSAS2: A revised source area simulator for small forested basins. Unpub. PhD thesis, Univ. of Georgia.
- Berris, S.N. & Harr, R.D. (1987). Comparative snow accumulation and melt during rainfall in forested and clear-cut plots in the Western Cascades of Oregon. Water Resour. Res., 23(1), 135-142.
- Beven, K.J. & O'Connell, P.E. (1982). On the role of distributed models in hydrology. Inst of Hydrology Report 81, Wallingford, UK.
- Beven, K.J., Warren, R. & Zaoui, J. (1980). SHE: towards a methodology for physically-based distributed forecasting in hydrology. In: Hydrological Forecasting, IAHS Publ. No. 129, 133-137.
- Brugnot, G & Pochat, R. (1981). Numerical simulation study of avalanches. J. of Glaciology, 27(95), 77-88.
- Burrough, P.A. (1986). Principles of geographic information systems for land resources assessment (Monographs on soil and resources survey No. 12), Oxford Univ. Press, New York, 194pp.
- Buttle, J.M. & McDonnell, J.J. (1987). Modelling the areal depletion of snowcover in a forested catchment. J. of Hydrol., 90, 43-60.
- Colbeck, S.C. (1974). The capillary effects on water percolation in homogeneous snow. J. of Glaciology, 13(67), 85-97.
- Colbeck, S.C. (1977). Thermodynamic deformation of wet snow. In: Proc. 34th Ann. Eastern Snow Conf. (Belleville, Ontario), 130-146.
- Deardorff, J.W. (1978). Efficient prediction of ground surface temperature and moisture with inclusion of a layer of vegetation. J. of Geophysical Res., 83, 1889-1902.
- De La Casinère, A.C. (1974). Heat exchange over a melting snow surface. J. of Glaciology, 13(67), 55-72.
- Dewalle, D. & Meiman, J. (1971). Energy exchange and late season snowmelt in a small opening in Colorado subalpine forest. Water Resour. Res., 7(1), 184-188.

- Dewalle, D.R., Parrott, H.A. & Peters, J.G. (1977). Effect of clearcutting deciduous forest on radiation exchange and snowmelt in Pennsylvania. In: Proc. 34th Ann Eastern Snow Conf. (Belleville, Ontario), 105-117.
- Dikau, R. (1989). The application of a digital relief model to landform analysis in geomorphology. In: Three dimensional applications in Geographical Information Systems (ed. J.Raper), Taylor & Francis, London, 51-77.
- Doyle, F.J. (1978). Digital Terrain Models: An Overview. Photogrammetric Engineering and Remote Sensing, 44(12), 1481-1485
- Dunne, T. & Black, R.D. (1971). Runoff processes during snowmelt. Water Resour. Res., 7(5), 1160-1172.
- Dunne, T., Price, A.G. & Colbeck, S.C. (1976). The generation of runoff from subarctic snowpacks. Water Resour. Res., 12(4), 677-685.
- Everett, K.R. & Ostendorf, B. (1988). Hydrology and geochemistry of a small drainage basin in upland tundra, northern Alaska. In: Proc. 5th Int. Permafrost Conf. (Trondheim, Norway), 574-580.
- Ferguson, R.I. (1984). Magnitude and modelling of snowmelt runoff in the Cairngorm Mountains, Scotland. Hydrol. Sci. J., 29(1), 49-62.
- Ferguson, R.I. & Morris, E.M. (1987). Snowmelt modelling in the Cairngorms, N.E. Scotland. Trans. Royal Soc. Edinburgh: Earth Sci., 78, 261-267.
- Ferris, J.S. & Congalton, R.G. (1989). Satellite and Geographic Information System Estimates of Colorado River Basin Snowpack. Photogrammetric Engineering and Remote Sensing, 55(11), 1629-1635.
- Frank, E.C. & Lee, R. (1966). Potential solar beam irradiation on slopes: tables for 30° to 50° latitude. US. Forest Serv. Res. Paper RM-18, Rocky Mt. Forest & Range Exp. Stn., Fort Collins, Colorado, 116pp.
- Garg, P.K. & Harrison, A.R. (1990). Quantitative representation of land-surface morphology from digital elevation models. Proc. 4th Int. Symp. on Spatial Data Handling, Zurich, 1990, in press.
- Garstka, W.U., Love, L.D., Goodell, B.C. & Bertle, F.A. (1958). Factors affecting snowmelt and streamflow, US. Dept. Interior, Bureau of Reclamation, US. Dept. of Agric., Forest Service, 189pp.

- Geiger, R. (1965). The climate near the ground, Harvard Univ. Press, Cambridge, Mass. 611pp.
- Golding, D.L. (1978). Calculated snowpack evaporation during Chinooks along the Eastern slopes of the Rocky Mountains in Alberta. J. Appl. Met., 17, 1647-1651
- Goodison, B.E., Louie, P.Y.T. & Metcalfe, J.R. (1986). Investigations of snowmelt acidic shock potential in south central Ontario, Canada, In: Proc. Symp. on Modelling Snowmelt-Induced Processes (Budapest, Hungary), IAHS Publ. No.155, 297-310.
- Granberg, H.B. (1988). A forest shading model using bit-mapped graphics. Agricultural & Forest Met., 43, 225-234.
- Granger, R.J. & Male, D.H. (1978). Melting of a Prairie Snowpack. J. Appl. Met., 17, 1833-1842.
- Gray, D.M. & Male, D.H. (1981). Handbook of Snow, Pergamon Press, Oxford, 776pp.
- Greenan, H.J. & Anderson, E.A. (1984). A snowmelt lysimeter for research applications. Proc. 41st Ann. Eastern Snow Conf. (Washington D.C.), 209-218.
- Hamelin, L.E. & Cook, F.A. (1967). Le périglaciaire par l'image - Illustrated glossary of periglacial phenomena Les presses de l'université Laval, Québec.
- Harr, R.D. (1986). Effects of clearcutting on Rain-on-Snow runoff in Western Oregon: A new look at old studies. Water Resour. Res., 22(7), 1095-1100.
- Hendrick, R.L. & DeAngelis, .J. (1976). Seasonal snow accumulation, melt and water input - A New England model. J. Appl. Met., 15(7), 717-727.
- Hendrick, R.L., Filgate, B.D. & Adams, W.P. (1971). Application of environmental analysis to watershed snowmelt. J. Appl. Met., 10(3), 418-429.
- Hendrie, L.K. & Price, A.G. (1978). Energy balance and melt in a deciduous forest. In: Proc. Modeling Snow Cover Runoff, (eds. S.C. Colbeck & M. Ray), US. Army CRREL, Hanover, New Hampshire., 101-124.
- Hoshi, T. Uchida, S. & Kotoda, K. (1989). Development of a system to estimate evapotranspiration over complex terrain using Landsat MSS, elevation and meteorological data. Hydrol. Sci. J., 34(6), 635-649.

- Howes, S. (1985). A mathematical hydrological model for the ungauged catchment, Unpub. PhD. thesis, Univ. of Bristol, 404pp.
- The Independent (1989). Rethinking the politics of plenty, The Independent, Saturday 28th Jan.
- Jonch-Clausen, T. (1979). Système Hydrologique Européen: a short description. SHE Report 1, Danish Hydraulics Institute, Horsholm, Denmark.
- Jones, D.A. (1982). Various approaches to the sensitivity analysis of SHE: a Discussion. SHE Report No. 20, Inst. of Hydrology, Wallingford, pp10.
- Jordan, R., O'Brien, H. & Bates, R. (1986). Thermal measurements in snow. In: Proc. of Snow Symp. 5, CRREL Special Report 86-15, 1, US. Army CRREL, Hanover, New Hampshire, 183-193.
- Kelly, R.J., Morland, L.W. & Morris, E.M. (1986). A three phase mixture model for melting snow. In: Modelling snowmelt-induced processes (Proc. Budapest Symp., July 1986), IAHS Publ. No. 155, 17-26.
- Kuchment, L.S., Demidov, V.N. & Motovilov, Yu.G. (1986). A physically-based model of the formation of snowmelt and rainfall-runoff. In: Modelling snowmelt-induced processes (Proc. Budapest Symp., July 1986), IAHS Publ. No. 155, 27-36.
- Kuusisto, E. (1978). Optimal complexity of a point snowmelt model. In: Proc. Modeling Snow Cover Runoff (eds. S.C.Colbeck & M.Ray), US. Army CRREL, Hanover, New Hampshire, 205-209.
- Kuusisto, E. (1986). The energy balance of a melting snow cover in different environments. In: Modelling snowmelt-induced processes (Proc. Budapest Symp., July 1986), IAHS Publ.No. 155, 37-45.
- Kuz'min, P.P. (1961). Protsess tavaniva shezhnogo pokrova, Gridometeorologicheskoe Izdatel'stvo, Leningrad. (English translation: "Melting of Snow Cover". Isreal program for scientific translations, Jerusalem, 1972, 290pp).
- Lafleur, P. & Adams, P. (1986). The effect of subarctic woodland vegetation on the radiation balance of a melting snow cover. Arch. Met. Geophy. Bioclim., Ser. A34, 297-310.
- Landsberger, S., Davies, T.D., Tranter, M., Abrahams, P.W. & Drake, J.J. (1989). The solute and particulate chemistry of background versus a polluted, black snowfall on the Cairngorm Mountains, Scotland. Atmospheric Environment, 23(2), 395-401.

- Langham, E.J. (1981). Physics and properties of snowcover. In: Handbook of Snow (eds. D.M.Gray & D.H.Male), Pergamon Press, Oxford, 275-337.
- Leaf, C.F. & Brink, G.E. (1973a). Computer simulation of snowmelt within a Colorado Subalpine Watershed. USDA Forest Serv. Res. Pap. RM-99, Rocky Mt. Forest and Range Exp. Stn., Fort Collins, Colorado, 22pp.
- Leaf, C.F. & Brink, G.E. (1973b). Hydrologic simulation model of Colorado Subalpine Forest. USDA Forest Serv. Res. Pap. RM-107, Rocky Mt. Forest and Range Exp. Stn., Fort Collins, Colorado, 23pp.
- Leavesley, G.H. (1989). Problems of snowmelt runoff modelling for a variety of physiographic and climatic conditions. Hydrol. Sci. J., 34(6), 617-634.
- Male, D.H. & Granger, R.J. (1978). Energy mass fluxes at the snow surface in a Prairie environment. In: Proc. Modeling Snow Cover Runoff (eds. S.C.Colbeck & M.Ray), US. Army CRREL, Hanover, New Hampshire, 101-124.
- Male, D.H. & Gray, D.M. (1975). Problems in developing a physically based snowmelt model. Can. J. Civ. Eng., 2, 474-488
- Male, D.H. & Gray, D.M. (1981). Snowcover ablation and runoff. In: Handbook of Snow, (eds. D.M.Gray, & D.H.Male), Pergamon Press, Oxford, 360-436.
- Martinec, J. & Rango, A. (1986). Parameter values for snowmelt runoff modelling. J. of Hydrol., 84, 197-219.
- McCuen, R.H. (1973). The role of sensitivity analysis in hydrologic modeling. J. of Hydrol., 18, 37-53.
- McKay, G.A. & Gray, D.M. (1981). The distribution of snowcover. In: Handbook of Snow, (eds. D.M.Gray & D.H.Male), Pergamon Press, Oxford, 153-191.
- Miller, S.W. (1984). A spatial data structure for hydrologic applications. Proc. Int. Symp. on spatial data handling, Vol 1, Zurich, Switzerland, 267-288.
- Moore, R. & Owens, I. (1984). Controls of advective snowmelt in a maritime alpine basin. J. Climate Appl. Met., 23, 135-142.
- Moore, R.V., Morris, D.G. & Bonvoisin, N.J. (1987). Digital mapping as an aid to hydrological analysis. In: Proc. National Hydrology Symp. (Hull, Sept. 1987), British Hydrological Soc., 31.1-31.13.

- Morris, E.M. (1985). Snow and Ice. In: Hydrological Forecasting (eds. M.G.Anderson & T.Burt), J.Wiley & Sons Ltd., 153-182.
- Morris, E.M. (1987). Modelling of water flow through snowpacks. In: Seasonal Snowcovers: Physics, Chemistry, Hydrology (eds. H.G.Jones & W.J.Orville-Thomas), D.Reidel Pub. Company, 179-208.
- Motovilov, Yu.G. (1986). A model of snowcover formation and snowcover processes. In: Modelling snowmelt-induced processes (Proc. Budapest Symp., July 1986), IAHS Publ. No. 155, 47-57.
- Moussavi, M, Wyseure, G & Feyen, J. (1989). Estimation of melt rate in seasonally snow-covered mountainous areas. Hydrol. Sci. J., 34(3), 249-263.
- Obled, C. & Harder, H. (1978). A review of snowmelt in the mountain environment. Proc. Modeling of Snow Cover Runoff (eds. S.C.Colbeck & M.R.Ray), Wiley & Sons Ltd., 153-182.
- Obled, C. & Rosse, B. (1977). Mathematical models of a melting snowpack at an index plot. J. of Hydrol., 32, 139-163.
- Ohmura, A. (1982). Climate and energy balance on the arctic tundra. J. Climatol., 2, 65-84.
- Oke, T.R. (1978). Boundary Layer Climates 1st ed., Methuen & Co. Ltd., London.
- Oke, T.R. (1987). Boundary Layer Climates 2nd ed., Methuen & Co. Ltd., London.
- Olyphant, G.A. (1986). The components of incoming radiation within a mid-latitude alpine watershed during the snowmelt season. Arctic & Alpine Res., 18(2), 163-169.
- O'Neill, A.D.J. & Gray, D.M. (1972). Spatial and temporal variations of the albedo of Prairie snowpacks. In: The role of snow and ice in hydrology (Proc. Banff Symp., Sept. 1972), IAHS Publ. No. 107, 1, 176-186.
- Pangburn, T. (1987). Documentation of the Cold Regions Modification to the MILHY (Military Hydrology) Model. Unpub. US. Army CRREL Report, Hanover, New Hampshire.
- Perla, R. & Glenne, B. (1981). Skiing. In: Handbook of Snow (eds. D.M.Gray & D.H.Male), Pergamon press, Oxford, 709-740.

- Pionke, H.B., Bahleda, K. & Chamberlain, B.J. (1978). Data directory, data and data collection site characteristics for the Sleepers River Watershed, N. Danville, Vermont. Northeast Watershed Research Centre, USDA-SEA-FR, 111 Research Building A, University Park, Pennsylvania 16802.
- Powers, D.J., Colback, S.C. & O'Neill, K. (1985). Thermal convection in snow. CRREL Report 85-9, US. Army CRREL, Hanover, New Hampshire, 70pp.
- Price, A.G. (1977). Runoff processes in a subarctic area. McGill Sub-Arctic Res. Paper No. 29, Climatological Res. Series No. 10., June 1977, 106pp.
- Price, A.G. (1988). Prediction of snowmelt rates in a deciduous forest. J. of Hydrol., 101, 145-157.
- Price, A.G. & Dunne, T. (1976). Energy balance computations of snowmelt in a subarctic area. Water Resour. Res., 12(4), 686-694.
- Price, A.G. and Petzold, D.E. (1984). Surface emissivities in a boreal forest during snowmelt. Arctic and Alpine Research, 16(1), 45-51.
- Price, L.W. (1981). Mountains and Man, Univ. of California Press, London.
- de Quervain, M.R. (1972). Snow structure, heat and mass flux through snow, In: The Role of Snow and Ice in Hydrology (Proc. Banff Symp., Sept. 1972), IAHS Publ. No. 107, Vol. 1, 203-226
- Rachner, M. & Matthäus, H. (1986). Project SNOW: operational estimation of snowcover development in the mountains of the German Democratic Republic. In: Modelling snowmelt-induced processes (Proc. Budapest Symp., July 1986), IAHS Publ. No. 155, 71-82.
- Rango, A. (1988). Progress in developing an operational snowmelt-runoff forecast model with Remote Sensing input. Nordic Hydrology, 19, 65-76.
- Rango, A. & Martinec, J. (1982). Snow accumulation derived from modified depletion curves of snow coverage. In: Hydrological Aspects of Alpine and High Mountain Areas (Proc. Exeter Symp., July 1982), IAHS Publ. No. 138, 83-90.
- Rau, R.G. & Herrmann, A. (1982). Variations in the properties of Alpine snow-cover stores. In: Hydrological Aspects of Alpine and High Mountain Areas (Proc. Exeter Symp., July 1982), IAHS Publ. No. 138, 91-100.

- Reiners, W.A., Hollinger, D.Y. & Lang, G.E. (1984). Temperature and evapotranspiration gradients of the White Mountains, New Hampshire, USA. Arctic & Alpine Res., 16, 31-36.
- Roberge, J. & Plamondon, A.P. (1987). Snowmelt runoff pathways in a boreal forest hillslope, the role of pipe throughflow. J. of Hydrol., 95, 39-54.
- Roberge, J., Stein, J. & Plamondon, A. (1988). Evaluation d'un modèle de fonte nivale en forêt boréale (Evaluation of a snowmelt model in a boreal forest environment). J. of Hydrol., 97, 161-179.
- Roberts, P.A. (1980). Computer-based techniques for converting a contour map into an equispaced grid of points. Technical Report TR 80110, Royal Aircraft Establishment, Farnborough, UK.
- Rogers, C.C.M. (1986). Future development of distributed hydrological models with reference to the Institute of Hydrology Distributed Model Unpub. PhD. thesis, Univ. of Bristol, pp462.
- Roland, E. (1984). Increased snow melting due to longwave radiation from snowfree ground. The role of snow and ice in Northern basin hydrology, Proc. Fifth Northern Research Basins symp., 5.117-5.125.
- de Roo, A.P.J., Hazelhoff, L. & Burrough, P.A. (1989). Soil erosion modelling using 'ANSWERS' and geographical information systems. Earth Surface Processes and Landforms, 14, 517-532.
- Sellers, W.D. (1965). Physical Climatology University of Chicago, Ill.
- Simons, P. (1988). Apres ski le deluge. New Scientist, 14th Jan. 1988, 1595, 49-52.
- Sosedko, M.N. & Kochelaba, E.I. (1986). Modelling snowmelt-induced processes in a mountain river basin given standard hydrometeorological data. In: Modelling snowmelt-induced processes (Proc. Budapest Symp., July 1986), IAHS Publ. No. 155, 83-91.
- Stephenson, G.R. & Freeze, R.A. (1974). Mathematical simulations of subsurface flow contributions to snowmelt runoff, Reynolds Creek Watershed, Idaho. Water Resour. Res., 10(2), 284-298.
- Steppuhn, H. & Dyck, G.E. (1974). Estimating true basin snowcover. Proc. Symp. on Advanced Concepts and Techniques in the Study of Snow and Ice Resources, Nat. Acad. Sci. Wash. D.C., 314-328.

- Sucksdorff, Y., Lemmela, R. & Keisteri, T. (1989). The environmental Geographic Information System in Finland. New Directions for Surface Water Modeling (Proc. Baltimore Symp., May 1989), IAHS Publ. No. 181., 427-434.
- Swanson, R.H. (1972). Small openings in poplar forest increase snow accumulation. In: The role of snow and ice in hydrology (Proc. Banff Symp., July 1972), IAHS Publ. No. 107, Vol. 2, 1382-1389.
- Swift, L.W.Jr. (1976). Algorithm for solar radiation on mountain slopes. Water Resour. Res., 12(1), 106-112.
- Treidl, R. (1970). A case study of warm air advection over a melting snow surface. Boundary Layer Met., 1, 155-168.
- US. Army Corps of Engineers (1956). Snow Hydrology U.S. Army Corps of Engineers, Portland, Oregon, 437pp.
- US. Army Corps of Engineers (1960). Runoff from snowmelt. EM 1110-2-1406, US. Army Corps of Engineers, 59pp.
- USFS. (1980). An Approach to Water Resources Evaluation of Non-point Silvicultural Sources (A Procedural Handbook). EPA-600/8-80-012, US. Forest Serv., Dept. Agric., 173pp.
- Vehviläinen, B. (1986). Modelling and forecasting snowmelt floods for operational forecasting in Finland. In: Modelling snowmelt-induced processes (Proc. Budapest Symp., July 1986), IAHS Publ. No. 155, 235-246.
- Weller, G. & Holmgren, B. (1974). The microclimates of the arctic tundra. J. Appl. Met., 13, 854-862.
- Wendler, G. & Ishikawa, N. (1974). The effect of slope exposure and mountain screening on the solar radiation of McCall glacier, Alaska: a contribution to the International Hydrological Decade. J. of Glaciology, 13(68), 213-226.
- Wilson, R.G. & Petzold, D.E. (1973). A solar radiation model for sub-arctic woodlands. J. Appl. Met., 12, 1259-1266.
- Woo, M-K. & Marsh, P. (1977). Determination of snow storage for small eastern High Arctic basins. In: Proc. of the 34th Ann. Eastern Snow Conf. (Belleville, Ontario), 147-162.
- Woo, M-K. & Marsh, P. (1978). Analysis of error in the determination of snow storage for small High Arctic basins. J. Appl. Met., 17, 1537-1541.
- Woo, M-K. & Steer, P. (1986). Monte Carlo simulation of snow depth in a forest., Water Resour. Res., 22(6), 864-868.

**APPENDIX A**

Derivation of energy budget terms used in VEGIE, from Balick et.al.  
(1981b).

The notation used below is that of Balick et al. (1981b) and direct referral to this paper is therefore possible. Some of the terms and variables referred to within chapters 1, 2 and 4 are expressed using different symbols and therefore a list of VEGIE symbols and their interpretation is included for reference at the end of the list of equations. Units for the equations are not given in Balick et al. (1981b) but it can be seen from the original computer code that the calculations are performed in the c.g.s. system, with the energy fluxes calculated in  $\text{cal cm}^{-2} \text{min}^{-1}$  and temperatures in degrees Kelvin.

### FOLIAGE

1. The foliage energy budget is calculated by:

$$F_f = \sigma_f [(1 - \alpha_f)S] + \epsilon_f R_{s\downarrow} + R_n - H_f - E_f \quad (\text{A1})$$

1.1.  $R_n$  is calculated by:

$$R_n = R_1 - R_2 \quad (\text{A2})$$

where,

$$R_1 = (\epsilon_f \epsilon_g / \epsilon_1) \sigma T_g^4 \quad (\text{A3})$$

$$R_2 = [(\epsilon_1 + \epsilon_g) / \epsilon_1] \epsilon_f \sigma T_f^4 \quad (\text{A4})$$

where,

$$\epsilon_1 = \epsilon_f + \epsilon_g - \epsilon_f \epsilon_g \quad (\text{A5})$$

1.2.  $H_f$  is calculated by:

$$H_f = -\rho_{af} C_p k^2 z^2 \overline{\Delta U \Delta \theta} / \overline{\Delta z \Delta z} \quad (\text{A6})$$

where,

$$\rho_{af} = 0.348P / [(T_a + T_f) / 2] \quad (\text{A7})$$

$$\Delta U = U_a - U_{af} \quad (\text{A8})$$

where,

$$U_{af} = 0.83 \sigma_f U_a / CH_h + (1 - \sigma_f) U_a \quad (\text{A9})$$

where,

$$CH_h = k^2 / (\ln[(z_a - z_d)/z_o])^2 \quad (A10)$$

where,

$$z_d = 0.701 \times z_f^{0.979} \quad (A11)$$

$$z_o = 0.131 \times z_f^{0.997} \quad (A12)$$

$$\Delta z = z_a$$

$$\Delta \theta = \theta(T_a) - \theta(T_f) - \theta(T_a - T_f) \quad (A13)$$

where,

$$\theta(T) = T(1000/P)^{0.286} \quad (A14)$$

1.3.  $E_f$  is calculated by:

$$E_f = (\rho_{af} C_p / 0.66) [e_s(T_f) - e(T_a)] / (r_a + r_c) \quad (A15)$$

where,

$$e_s(T_f) = 6.108 \exp[17.269(T_f - 273.16)/(T_f - 35.8)] \quad (A16)$$

$$e(T_a) = e_s(T_a) / RH \quad (A17)$$

$$r_a = (\ln[(z_a - z_d)/z_o] \tau)^2 / (k^2 U_a) \quad (A18)$$

where,

$$\tau = c_1 (1 - c_2 Ri)^{c_3} \quad (A19)$$

where,

$$c_2 = 1.0, c_1 = 5.0, c_3 = 2.0 \text{ if } Ri > 0$$

$$c_2 = 1.175, c_1 = 15.0, c_3 = 0.75 \text{ if } Ri \leq 0$$

$$Ri = (g / [\theta(T_a) + \theta(T_f)] / 2) [(\Delta \theta / \Delta z) / (\Delta u / \Delta z)^2] \quad (A20)$$

If  $Ri \geq 0.2$ ,  $Ri$  set equal to 0.199.

$$r_c = \chi r_s / LAI \quad (A21)$$

$$r_s = (0.05 + 0.0021 S)^{-1} \quad (A22)$$

$$LAI = 7 \sigma_f \quad (A23)$$

GROUND

2. The ground energy budget is calculated by:

$$F_g = (1-\sigma_f)[(1-\alpha_g)S] + R_{g\downarrow} - R_{g\uparrow} - H_g - E_g - G \quad (A24)$$

2.1  $R_{g\downarrow}$  is calculated by:

$$R_{g\downarrow} = (1-\sigma_f)R_{s\downarrow} + \sigma_f[\epsilon_f\sigma T_f^4 + (1-\epsilon_f)\epsilon_g\sigma T_g^4]/\epsilon_1 \quad (A25)$$

2.2  $R_{g\uparrow}$  is calculated by:

$$R_{g\uparrow} = (1-\sigma_f) [\epsilon_g\sigma T_g^4 + (1-\epsilon_g)R_{s\downarrow}] + \sigma_f[\epsilon_g\sigma T_g^4 + (1-\epsilon_g)\epsilon_f\sigma T_f^4]\epsilon_1 \quad (A26)$$

2.3  $H_g$  is calculated by:

$$H_g = \rho_{ag}CpCH_gU_{af}(T_g - T_{af}) \quad (A27)$$

where,

$$\rho_{ag} = 0.348P/T_{af} \quad (A28)$$

where,

$$T_{af} = (1-\sigma_f)T_a + \sigma(0.3T_a + 0.6T_f + 0.1T_g) \quad (A29)$$

$$CH_g = (1-\sigma_f)CH_o + \sigma_fCH_h \quad (A30)$$

where,

$$CH_o = k^2/\ln(z_a/z_o)^2 \quad (A31)$$

2.4  $E_g$  is calculated by:

$$E_g = \rho_{ag}CH_gU_{af}L(q_g - q_{af}) \quad (A32)$$

where,

$$q_g = Wq_s(T_g) + (1-W)q_{af} \quad (A33)$$

where,

$$q_s(T_f) = 0.622/[P/e_s(T_f) - 0.378] \quad (A34)$$

$$q_{af} = (1-\sigma_f)q(T_a) + \sigma_f[0.3q(T_a) + 0.6q_f + 0.1q_g] \quad (A35)$$

where,

$$q(T_a) = 0.622/[P/e(T_a)-0.378] \quad (A36)$$

$$q_f = r''q_s(T_f) + (1-r'')q_{af} \quad (A37)$$

where,

$$r'' = r_a/(r_s + r_a) \quad (A38)$$

2.5. G is calculated by:

$$G = -K(T_x - T_g)/Z_x \quad (A39)$$

#### LIST OF SYMBOLS.

Roman capital letters.

$CH_g$	heat transfer coefficient between $CH_o$ and $CH_h$ .
$CH_h$	heat transfer coefficient for ground with complete cover.
$CH_o$	heat transfer coefficient for ground with no cover.
$C_p$	specific heat of dry air at constant pressure.
$E_f$	latent heat loss to atmosphere from foliage.
$E_g$	latent heat loss to atmosphere from ground.
$G$	conduction of heat in top soil (snow) layer.
$H_f$	foliage sensible heat flux with atmosphere.
$H_g$	foliage sensible heat flux with atmosphere.
$K$	heat conductivity of the soil (snow).
$L$	latent heat of evaporation, temperature dependent.
$LAI$	leaf area index.
$P$	air pressure.
$R_{g\downarrow}$	downward longwave radiation flux at the ground surface.
$R_{g\uparrow}$	upward directed longwave radiation flux at the ground surface.
$RH$	relative humidity.
$Ri$	Richardson's Number.

$R_n$	combined net thermal IR term for interaction between foliage, ground and their loss to the sky.
$R_{s\downarrow}$	incoming longwave radiation from sky ( $L\downarrow$ ).
$S$	incoming solar radiation from sky ( $K\downarrow$ ).
$T_a$	air temperature at instrument height.
$T_{af}$	temperature of the air within foliage layer.
$T_f$	foliage air temperature.
$T_g$	ground surface temperature.
$T_x$	temperature at first grid point below surface.
$U_a$	wind speed at instrument height.
$U_{af}$	wind speed within foliage layer.
$W$	relative saturation of ground near surface with respect to field capacity (0-1.0).
$Z_x$	distance from surface to first grid point, $T_x$ .

Roman small letters.

$c_1, c_2, c_3$	coefficients dependent on Ri for value.
$g$	acceleration due to gravity.
$k$	von Karman's constant.
$q$	specific humidity.
$q_{af}$	specific humidity of air within foliage layer.
$q_f$	specific humidity of air at top of foliage.
$q_g$	specific humidity of air at ground surface.
$q_s$	saturated specific humidity.
$r_a$	atmospheric resistance.
$r_c$	canopy resistance to water vapour diffusion.
$r_s$	stomatal resistance.
$r''$	fraction of potential evaporation rate from foliage.
$z_a$	instrument height above ground.
$z_d$	zero displacement height.
$z_f$	foliage height.
$z_o$	roughness length.

## Greek letters.

$\alpha_f$	foliage albedo.
$\alpha_g$	ground albedo.
$\epsilon_f$	foliage emissivity.
$\epsilon_g$	ground emissivity.
$\theta$	potential temperature.
$\rho_{af}$	density of air within foliage layer.
$\rho_{ag}$	density of air near ground surface.
$\sigma$	Stefan-Boltzmann constant.
$\sigma_f$	foliage cover fraction.
$r$	correction factor for stability.
$x$	state of vegetation.

## Basic subscripts.

a,f,g	air (at instrument height), foliage, ground (in the SNOMO application of VEGIE the 'ground' is modelled as a snowpack)
af	air within foliage layer.
ag	air near ground surface.